Ground-Water-Quality Assessment of the Central Oklahoma Aquifer, Oklahoma: Geochemical and Geohydrologic Investigations

United States
Geological
Survey
Open-File Report
92–642

Ground-Water-Quality Assessment of the Central Oklahoma Aquifer, Oklahoma: Geochemical and Geohydrologic Investigations

By David L. Parkhurst, Scott Christenson, and George N. Breit

U.S. GEOLOGICAL SURVEY OPEN-FILE REPORT 92–642

Oklahoma City, Oklahoma

U.S. DEPARTMENT OF THE INTERIOR
BRUCE BABBITT, Secretary

U.S. GEOLOGICAL SURVEY
DALLAS L. PECK, Director

UNITED STATES GOVERNMENT PRINTING OFFICE: 1993

For additional information write to:

District Chief
U.S. Geological Survey
Water Resources Division
202 NW 66th Street, Building 7
Oklahoma City, OK 73116

Copies of this report can be purchased from:

Books and Open-File Reports Section
U.S. Geological Survey
Federal Center, Box 25425
Denver, CO 80225

CONTENTS

FIGURES

TABLES

CONVERSION FACTORS, VERTICAL DATUM, AND ABBREVIATED WATER-QUALITY UNITS

Multiply	By	To obtain
foot (ft)	0.3048	meter
foot per day (ft/d)	0.3048	meter per day
foot per mile (ft/mi)	0.1894	meter per kilometer
foot squared per day (ft^2/d)	0.09290	meter squared per day
cubic foot per second (ft^3/s)	0.02832	cubic meter per second
gallon (gal)	3.785	liter
gallon per day (gal/d)	0.003785	cubic meter per day
gallon per minute (gal/min)	0.06309	liter per second
gallon per minute per foot [(gal/min)/ft]	0.2070	liter per second per meter
inch (in)	2.540	centimeter
inch per year (in/yr)	25.40	millimeter per year
mile (mi)	1.609	kilometer
square mile (mi^2)	2.590	square kilometer

Temperature in degree Fahrenheit (°F) can be converted to degree Celsius (°C) as follows:

$$°C = (°F - 32)/1.8$$

Temperature in degree Celsius (°C) can be converted to degree Fahrenheit (°F) as follows:

$$°F = 1.8\ °C + 32$$

The following terms and abbreviations are also used in this report:

centimeter (cm)
kilometer (km)
microgram per liter (µg/L)
micrometer (µm)
milliequivalent (meq)
milliequivalent per liter (meq/L)
milligram per liter (mg/L)
milliliters per liter (mL/L)
millimole per liter (mmol/L)
percent modern carbon (pmc)
picocuries per liter (pCi/L)

Sea level: In this report "sea level" refers to the National Geodetic Vertical Datum of 1929 (NGVD of 1929)—a geodetic datum derived from a general adjustment of the first-order level nets of both the United States and Canada, formerly called Seal Level Datum of 1929.

GROUND-WATER-QUALITY ASSESSMENT OF THE CENTRAL OKLAHOMA AQUIFER, OKLAHOMA: GEOCHEMICAL AND GEOHYDROLOGIC INVESTIGATIONS

By David L. Parkhurst, Scott Christenson, *and* George N. Breit

Abstract

The National Water-Quality Assessment pilot project for the Central Oklahoma aquifer examined the chemical and isotopic composition of ground water, the abundances and textures of minerals in core samples, and water levels and hydraulic properties in the flow system to identify geochemical reactions occurring in the aquifer and rates and directions of ground-water flow. The aquifer underlies 3,000 square miles of central Oklahoma and consists of Permian red beds, including parts of the Permian Garber Sandstone, Wellington Formation, and Chase, Council Grove, and Admire Groups, and Quaternary alluvium and terrace deposits.

In the part of the Garber Sandstone and Wellington Formation that is not confined by the Permian Hennessey Group, calcium, magnesium, and bicarbonate are the dominant ions in ground water; in the confined part of the Garber Sandstone and Wellington Formation and in the Chase, Council Grove, and Admire Groups, sodium and bicarbonate are the dominant ions in ground water. Nearly all of the Central Oklahoma aquifer has an oxic or post-oxic environment as indicated by the large dissolved concentrations of oxygen, nitrate, arsenic(V), chromium(VI), selenium(VI), vanadium, and uranium. Sulfidic and methanic environments are virtually absent.

Petrographic textures indicate dolomite, calcite, sodic plagioclase, potassium feldspars, chlorite, rock fragments, and micas are dissolving, and iron oxides, manganese oxides, kaolinite, and quartz are precipitating. Variations in the quantity of exchangeable sodium in clays indicate that cation exchange is occurring within the aquifer. Gypsum may dissolve locally within the aquifer, as indicated by ground water with large concentrations of sulfate, but gypsum was not observed in core samples. Rainwater is not a major source for most elements in ground water, but evapotranspiration could cause rainwater to be a significant source of potassium, sulfate, phosphate and nitrogen species. Brines derived from seawater are the most likely source of bromide and chloride in the aquifer.

The dominant reaction in recharge is the uptake of carbon dioxide gas from the unsaturated zone (about 2.0 to 4.0 millimoles per liter) and the dissolution of dolomite (about 0.3 to 1.0 millimoles per liter). This reaction generates calcium, magnesium, and bicarbonate water composition. If dolomite does not dissolve to equilibrium, pH values range from 6.0 to 7.3; if dolomite dissolves to equilibrium, pH values are about 7.5. By the time recharge enters the deeper flow system, all ground water is saturated or supersaturated with dolomite and calcite.

After carbonate-mineral equilibration has occurred, cation exchange of calcium and magnesium for sodium is the dominant geochemical reaction, which occurs to a substantial extent only in parts of the aquifer. Mass transfers of cation exchange greater than 2.0 millimoles per liter occur in the confined part of the Garber Sandstone and Wellington Formation and in parts of the Chase, Council Grove, and Admire Groups. Associated with cation exchange is dissolution of small quantities of dolomite, calcite, biotite, chlorite, plagioclase, or potassium feldspar, which produces pH values that range from 8.6 to 9.1.

Large tritium concentrations indicate ground-water ages of less than about 40 years for most samples of recharge. Carbon-14 ages for samples from the unconfined aquifer generally are less than 10,000 years. Carbon-14 ages of ground

water in the confined part of the aquifer range from about 10,000 to 30,000 years or older. These ages produce a time trend in deuterium values that qualitatively is consistent with the timing of the transition from the last glacial maximum to the present interglacial period.

The most transmissive geologic units in the Central Oklahoma aquifer are the Garber Sandstone and Wellington Formation and the alluvium and terrace deposits; the Chase, Council Grove, and Admire Groups are less transmissive on the basis of available specific-capacity data. The transmissivities of the Permian geologic units depend largely on the percentage of sandstone; the percentage is greatest in the central part of the aquifer and decreases in all directions from this central part. Because of large mudstone and siltstone contents, the Hennessey Group and the Vanoss Formation are assumed to be confining units above and below the aquifer. The Cimarron and Canadian Rivers are defined to be the northern and southern extent of the aquifer because of decreases in transmissivity beyond the rivers and because there is no indication of ground-water underflow at these rivers. The eastern boundary of the aquifer is the limit of the outcrop of the Chase, Council Grove, and Admire Groups. The presence of brines in the western part of the study unit and below the aquifer indicate the extent of the freshwater flow system in these directions.

Regional ground-water flow is west to east; the Deep Fork is a major discharge area for the regional flow system. Local flow systems are present within the unconfined part of the study unit. Most streams are gaining streams, and very few losing streams are evident.

Median values of aquifer properties were estimated as follows: recharge to the saturated zone, 1.6 inches per year; evapotranspiration of water that never reaches the saturated zone, 25 to 30 inches per year; porosity, 0.22; storage coefficient, 0.0002; transmissivity, 260 to 450 feet squared per day; horizontal hydraulic conductivity, 4.5 feet per day; and the ratio of horizontal to vertical hydraulic conductivity, 10,000. Reported ground-water withdrawals peaked in 1985 at 13,900 million gallons but had decreased to 7,860 million gallons by 1989. Unreported domestic withdrawals were estimated to be 1,685 million gallons in 1980.

The flow system in the aquifer can be considered to have three major components: (1) A shallow, local flow system in the unconfined part of the aquifer, (2) a deep, regional flow system in the unconfined part of the aquifer, and (3) a deep, regional flow system in the confined part of the aquifer. In the shallow, local flow system, water flows relatively quickly along short flowlines from the point of recharge to the point of discharge at the nearest stream. Many water samples from shallow wells contain large concentrations of tritium, which indicate ground-water ages of less than 40 years. In the deep, regional flow system in the unconfined part of the aquifer, water takes more time to flow along longer flowlines than in the shallow, local flow system. Much of the water in this flow system is recharged along ridges that correspond to ground-water divides between drainage basins. Transit times for water recharging the aquifer along ridges is greater than 5,000 years, computed using a numerical flow model in conjunction with a particle-tracking model. The deep, regional flow system in the confined part of the Garber Sandstone and Wellington Formation is recharged from a small part of the outcrop area of the Garber Sandstone. From the recharge area, water flows west under the confining unit to discharge to streams as far away as the Cimarron River. Flowpaths are relatively long, as much as 50 miles. The transit times in this flow system range from thousands to tens of thousands of years.

The long-term hydrogeochemical process occurring in the Central Oklahoma aquifer is removal of unstable minerals, including dolomite, calcite, biotite, chlorite, and feldspars, and the replacement of exchangeable sodium on clays with calcium and magnesium. Over geologic time, the flux of water through the rapidly moving, local flow system has been sufficient to remove most of the dolomite, calcite, and exchangeable sodium. In places, chlorite and feldspars have been removed. In the deep, regional flow system of the unconfined part of the Garber Sandstone and Wellington Formation, the flux of water has been sufficient to remove most of the exchangeable sodium, but carbonate minerals remain sufficiently abundant to maintain dolomite and calcite equilibrium. In the confined part of the Garber Sandstone and Wellington Formation and in the less transmis-

sive parts of the unconfined aquifer, including the Chase, Council Grove, and Admire Groups, ground-water flow is slowest, and the flux of water and extent of reaction have been insufficient to remove either the carbonate minerals or the exchangeable sodium on clays.

INTRODUCTION

Beginning in 1986, the Congress annually has appropriated funds for the U.S. Geological Survey to conduct a National Water-Quality Assessment (NAWQA) Program. The long-term goals of the Program are to:

1. Provide a nationally consistent description of current water-quality conditions for a large part of the Nation's water resources;
2. Define long-term trends (or lack of trends) in water quality; and
3. Identify, describe, and explain, as possible, the major factors that affect the observed water-quality conditions and trends.

This information, which is being obtained on a continuing basis, will provide water managers, policy makers, and the public an improved scientific basis for evaluating the effectiveness of water-quality management programs and for predicting the likely effects of contemplated changes in land- and water-management practices. A description of the concepts for a NAWQA Program is provided by Hirsch, Alley, and Wilber (1988).

Initially, seven project areas were selected as pilot studies to test and refine the assessment concept. The Central Oklahoma aquifer was selected for study in the pilot NAWQA Program because it is a major source of water supplies in central Oklahoma and because it has several known or suspected water-quality problems. These problems include arsenic, chromium, and selenium concentrations in excess of public drinking-water standards established by the U.S. Environmental Protection Agency; large gross alpha particle activity; contamination by synthetic organic compounds; and contamination by oil-field brines and drilling fluids. The aquifer also was chosen for study because it underlies large urban areas, and the effects of an urban environment on regional ground-water quality have not been studied extensively.

The objectives of the Central Oklahoma aquifer project are to: (1) Investigate regional ground-water quality throughout the aquifer, emphasizing the occurrence and distribution of potentially toxic substances, including trace elements, organic compounds, and radioactive constituents; (2) describe the relation of ground-water quality to hydrogeologic and other pertinent factors; and (3) provide a general description of the location, nature, and causes of selected water-quality problems within the study unit (Christenson and Parkhurst, 1987).

The Central Oklahoma aquifer project has four major components (Christenson and Parkhurst, 1987). The first component is the compilation and analysis of available information. The second component is geochemical and geohydrologic investigations of the aquifer flow system. The third component is a regional water-quality sampling for a variety of inorganic, organic, and radioactive constituents that will produce a set of data consistent with the other ground-water pilot projects. The fourth component is targeted water-quality sampling that will address, in more detail, some of the major water-quality problems in the aquifer.

The second component of the project, the geochemical and geohydrologic investigations of the aquifer flow system, is needed to provide background information for the water-quality assessment. The fate and movement of chemical constituents in ground water depend on the ground-water flow system and the geochemical environment of the aquifer. This report is one of two primary products of the geochemical and geohydrologic investigations. The other report, "Hydrogeologic maps of the Central Oklahoma aquifer, Oklahoma," by Christenson, Morton, and Mesander (1992), presents large-scale maps of the major hydrogeologic features of the Central Oklahoma aquifer.

Purpose and Scope

This report provides a comprehensive description of the major elements of the geochemistry and geohydrology of the Central Oklahoma aquifer. The report describes the geohydrologic units that are part of the aquifer; the mineralogy of the geologic units; the geochemical reactions that affect the major-ion composition of water in the aquifer; recharge; discharge; hydraulic properties; flowlines; and the age of ground water. Most of the discussion is directed toward the Permian bedrock geologic units in the study area, and only a brief discussion of the Quaternary alluvium and terrace deposits is included. The scope of the work included petrographic analysis of core material, measurements of water levels and stream flows, sampling wells for a large variety of chemical constituents, analyses of aquifer tests, age dating of ground water, numerical flow modeling, and geochemical modeling.

Acknowledgments

The authors are indebted to many people throughout the study area for their cooperation and assistance in obtaining information concerning wells, ground-water withdrawals, use of water, and other pertinent data. Many individuals from municipal water departments and individual well owners provided information and allowed field personnel from the U.S. Geological Survey to measure water levels and collect water samples from their wells.

Thirteen Federal, State, and local governmental agencies met on a regular basis to ensure that the scientific information produced by the Central Oklahoma NAWQA study was relevant to local and regional interests. This group formed a committee known as the Central Oklahoma aquifer NAWQA Liaison Committee. The Liaison Committee includes the Association of Central Oklahoma Governments, the Directorate of Environmental Management from Tinker Air Force Base, the Environmental and Ground Water Institute at the University of Oklahoma, Oklahoma Corporation Commission, Oklahoma Department of Agriculture, Oklahoma Department of Pollution Control, Oklahoma Geological Survey, Oklahoma State Department of Health, Oklahoma Water Resources Board, U.S. Army Corps of Engineers, U.S. Bureau of Reclamation, U.S. Environmental Protection Agency, and the University Center for Water Research at Oklahoma State University. The assistance and guidance of this group is gratefully acknowledged.

During the geochemical and geohydrologic investigation, the Oklahoma Water Resources Board provided drillers' logs and water-use information. The authors also would like to thank Engineering Enterprises, Inc., in Norman, Oklahoma, and especially Michael Gates, for allowing access to reports and geophysical logs that are the property of Engineering Enterprises, Inc.

DESCRIPTION OF THE STUDY UNIT

The Central Oklahoma aquifer underlies about 3,000 square miles (mi^2) of central Oklahoma (fig. 1), where the aquifer is used extensively for municipal, industrial, commercial, and domestic water supplies. Most of the usable ground water within the aquifer is in the Garber Sandstone and the Wellington Formation. Substantial quantities of usable ground water also are present in the Chase, Council Grove, and Admire Groups, which underlie the Garber Sandstone and Wellington Formation, and in alluvium and terrace deposits, which are associated with the major streams in the study unit.

Location and Physiography

The Central Oklahoma aquifer underlies all or parts of Cleveland, Logan, Lincoln, Oklahoma, Payne, and Pottawatomie Counties (fig. 2). The eastern part of the study unit is characterized by low hills and has relief of 30 to 200 feet (ft). The western part of the study unit is characterized by a gently rolling grass-covered plain and has relief of less than 100 ft. Elevations within the study unit generally are higher in the west than in the east. The highest altitude is about 1,300 ft above sea level in the western part of the study unit along the drainage divide between the Canadian and North Canadian Rivers; the lowest altitudes are about 800 ft above sea level along the Cimarron River and Deep Fork, in the northeastern part of the study unit.

The major streams in the study unit are the Cimarron River, the Deep Fork, the North Canadian River, the Little River, and the Canadian River (fig. 2). These streams, which flow from west to east across the study unit, have formed broad, flat alluvial valleys. The Little River is a tributary to the Canadian River, and the Deep Fork is a tributary to the North Canadian River. The headwaters of the Little River and the Deep Fork are within the study unit.

The average annual temperature in the study unit is about 16°C. The average annual precipitation is approximately 33 inches (in.), most of which falls from April through October.

Definition of the Central Oklahoma Aquifer

The Central Oklahoma aquifer consists of those geologic units that yield substantial volumes of water to wells from the extensive, continuous ground-water flow system in all or parts of Cleveland, Lincoln, Logan, Oklahoma, Payne, and Pottawatomie Counties. Ground water in this flow system originates as recharge from precipitation and circulates in alluvium and terrace deposits along major streams; in the Garber Sandstone and Wellington Formation; and in the Chase, Council Grove, and Admire Groups. Because most deep wells in central Oklahoma are completed in the Garber Sandstone and the Wellington Formation, the Central Oklahoma aquifer commonly has been referred to as the "Garber-Wellington aquifer," but this terminology is imprecise because: (1) The Garber Sandstone and Wellington Formation are not an aquifer outside of central Oklahoma because of a decrease in transmissivity; and (2) the water in the underlying Chase, Council Grove, and Admire Groups, and in the overlying alluvium and terrace deposits, is part of the same flow system. Therefore, the term "Central Oklahoma aquifer" is

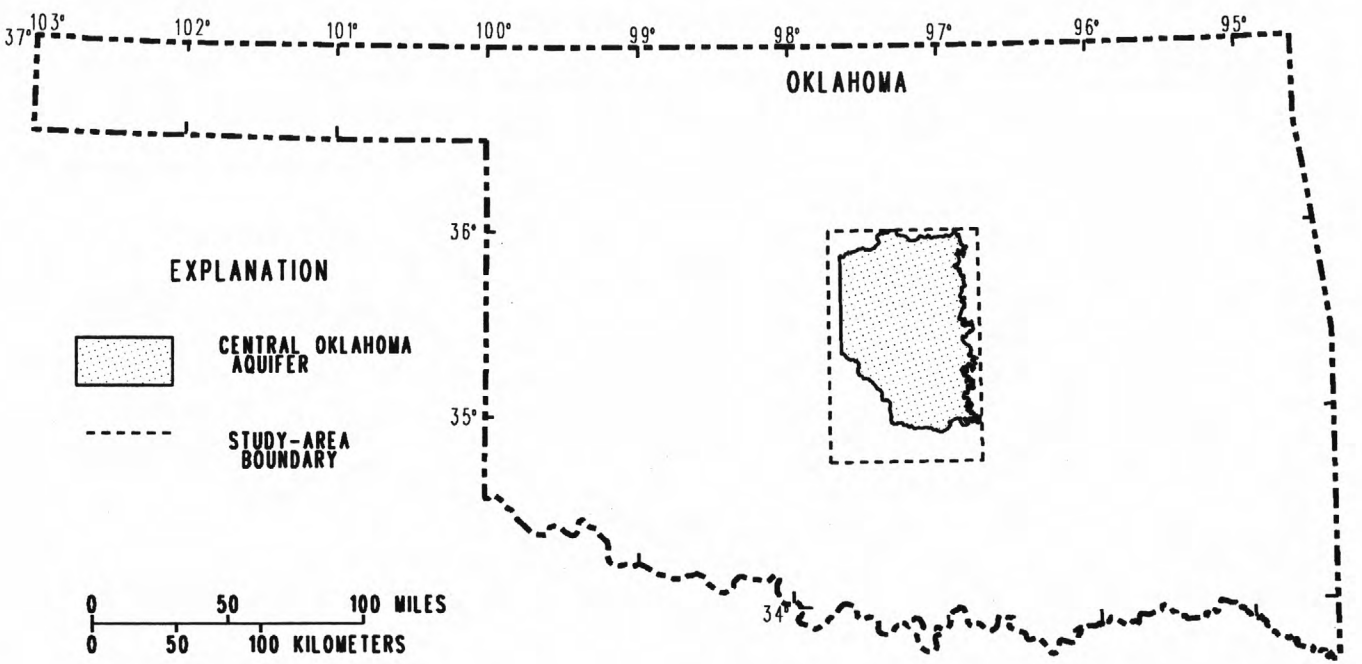

Figure 1. Location of the Central Oklahoma aquifer and the study area.

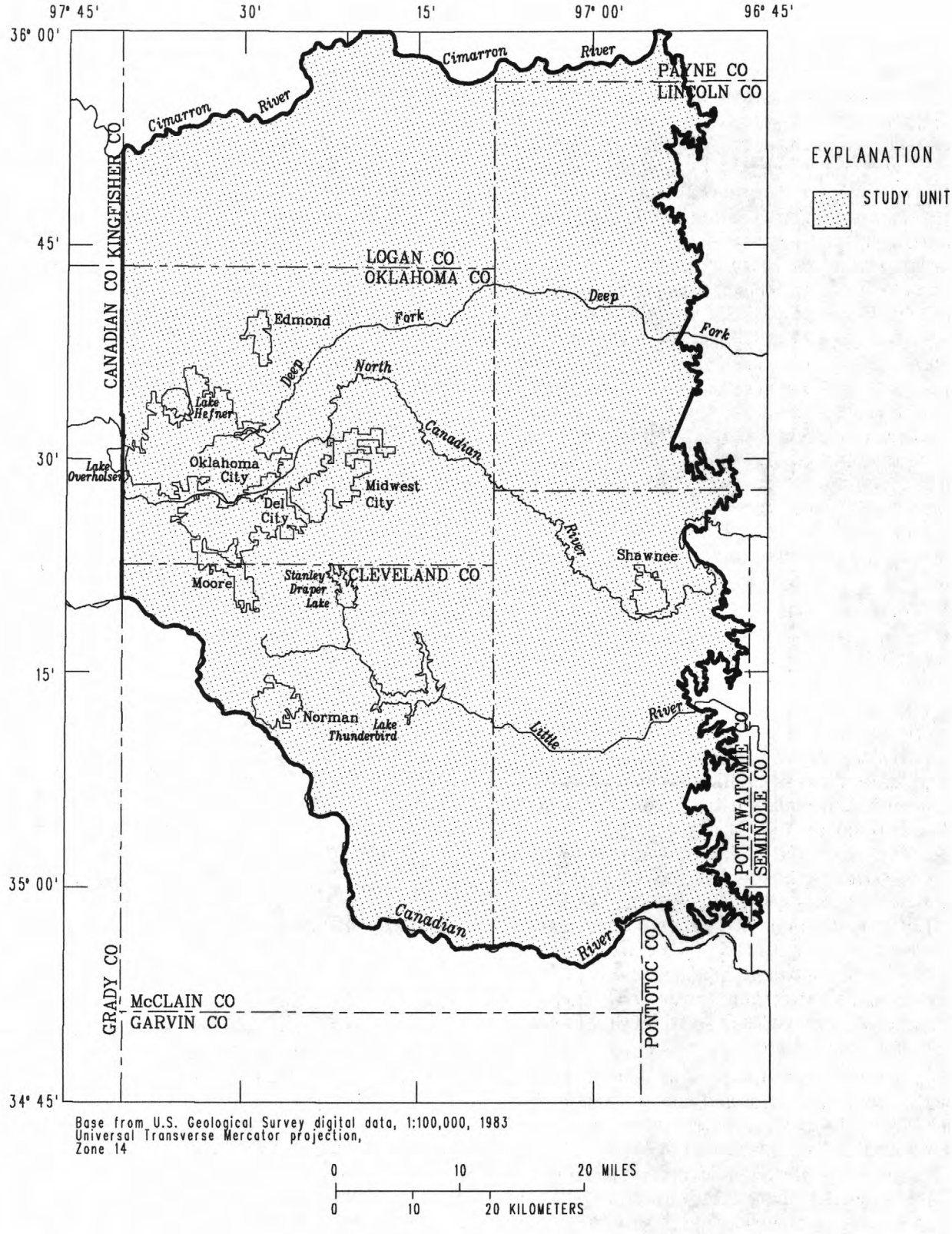

Figure 2. Major geographic features of the study unit.

preferred. A map of the surficial geology overlying the Central Oklahoma aquifer is shown in figure 3.

The transmissivities of the Garber Sandstone, Wellington Formation, and Chase, Council Grove, and Admire Groups decrease to the north and south to the point where these geologic units no longer yield substantial quantities of water to wells. Ideally, well yields would define the limit of the Central Oklahoma aquifer. Unfortunately, data are insufficient to define the limits of the aquifer on the basis of well yields. Therefore, the limits of the Central Oklahoma aquifer are defined by hydrologic inferences. The Cimarron River was defined to be the northern boundary of the aquifer because (1) the Garber Sandstone, Wellington Formation, and Chase, Council Grove, and Admire Groups are less transmissive north of the river; (2) few (if any) large-capacity wells are completed in these geologic units north of the river; and (3) it is believed that the river is a hydrologic boundary to ground-water flow, and little or no ground water flows from one side of the river to the other. The Canadian River was defined to be the southern boundary of the aquifer, for similar reasons.

The eastern boundary of the aquifer was defined to be the eastern limit of the outcrop of the Chase, Council Grove, and Admire Groups. These groups are underlain by the Vanoss Formation, which has a smaller transmissivity and confines the flow system to the overlying units. The western boundary of the study unit is considered to be where freshwater circulation in the aquifer becomes negligible. An increase in dissolved-solids concentration in the western part of the study unit is thought to indicate a decrease in the circulation of ground water. A dissolved-solids concentration of 5,000 milligrams per liter (mg/L), selected to be consistent with the work of Hart (1966), was established as the indicator of an increase in dissolved solids and a decrease in circulation. Therefore, the western boundary of the study unit is defined by the increase in dissolved solids to 5,000 mg/L that occurs at approximately the Oklahoma-Canadian/Kingfisher-Logan County line (Hart, 1966).

The lower boundary of the aquifer is considered to be the lower limit of ground water containing less than 5,000 mg/L dissolved solids. Hart (1966) referred to this lower limit as the "base of fresh ground water," and this term is retained in this report. The altitude of the base of fresh ground water is shown in figure 4. The base of the fresh ground water is deepest in south-central Oklahoma County, where the depth from land surface to the base of fresh ground water is about 1,000 ft. To the north, south, and east, the base of the fresh ground water slopes upward gradually, until it is only about 100 ft below land surface at the boundaries of the aquifer. To the west, the base of fresh ground water rises gradually to approximately the Oklahoma-Canadian/Logan-Kingfisher County line. At that line, the depth to the base of fresh ground water decreases abruptly from about 800 ft to about 200 ft.

The western third of the aquifer is confined, where the Garber Sandstone is overlain by the Hennessey Group. The eastern two-thirds of the aquifer is considered to be unconfined, where the Garber Sandstone, Wellington Formation, or Chase, Council Grove, and Admire Groups are exposed at the surface. Because of the presence of siltstones and mudstones, water deep in the aquifer may be confined, even in the eastern part of the aquifer. However, for this report use of the term "confined" refers to that part of the aquifer underlying the Hennessey Group.

Two terms are used in this report to describe the limit of the study in relation to the Central Oklahoma aquifer, "study area" and "study unit." The term "study area" is used to describe the area on the earth's surface bounded by 34°45′ and 36° north latitude, and 96°45′ and 97°45′ west longitude. The term "study unit" is used to define the volume of earth between the upper limit of the zone of saturation and the base of fresh ground water, bounded by the extent of the Central Oklahoma aquifer (fig. 1). The study area is larger than the study unit because the geochemistry and geohydrology of the Central Oklahoma aquifer are affected by geologic units adjacent to the aquifer; thus, data were collected beyond the limits of the study unit. Note that the study unit contains a large volume of Hennessey Group and a small volume of both the El Reno Group and the Vanoss Formation, none of which are considered to be part of the Central Oklahoma aquifer.

Description of Geohydrologic Units

The Central Oklahoma aquifer consists of both Quaternary alluvium and terrace deposits and Permian geologic units. In central Oklahoma, it is difficult to study ground water in geologic units of either age without studying the other, because ground water that flows through the Permian geologic units discharges through the Quaternary geologic units, and many wells are completed in both geologic units. However, much of the discussion in this report is directed toward the flow system in the Permian units because ground water in the alluvium and terrace deposits volumetrically is a small fraction of the Permian units, the flow system in the alluvium and terrace deposits is relatively simple (as compared to that in the Permian units), and the alluvium and terrace deposits have been studied previously.

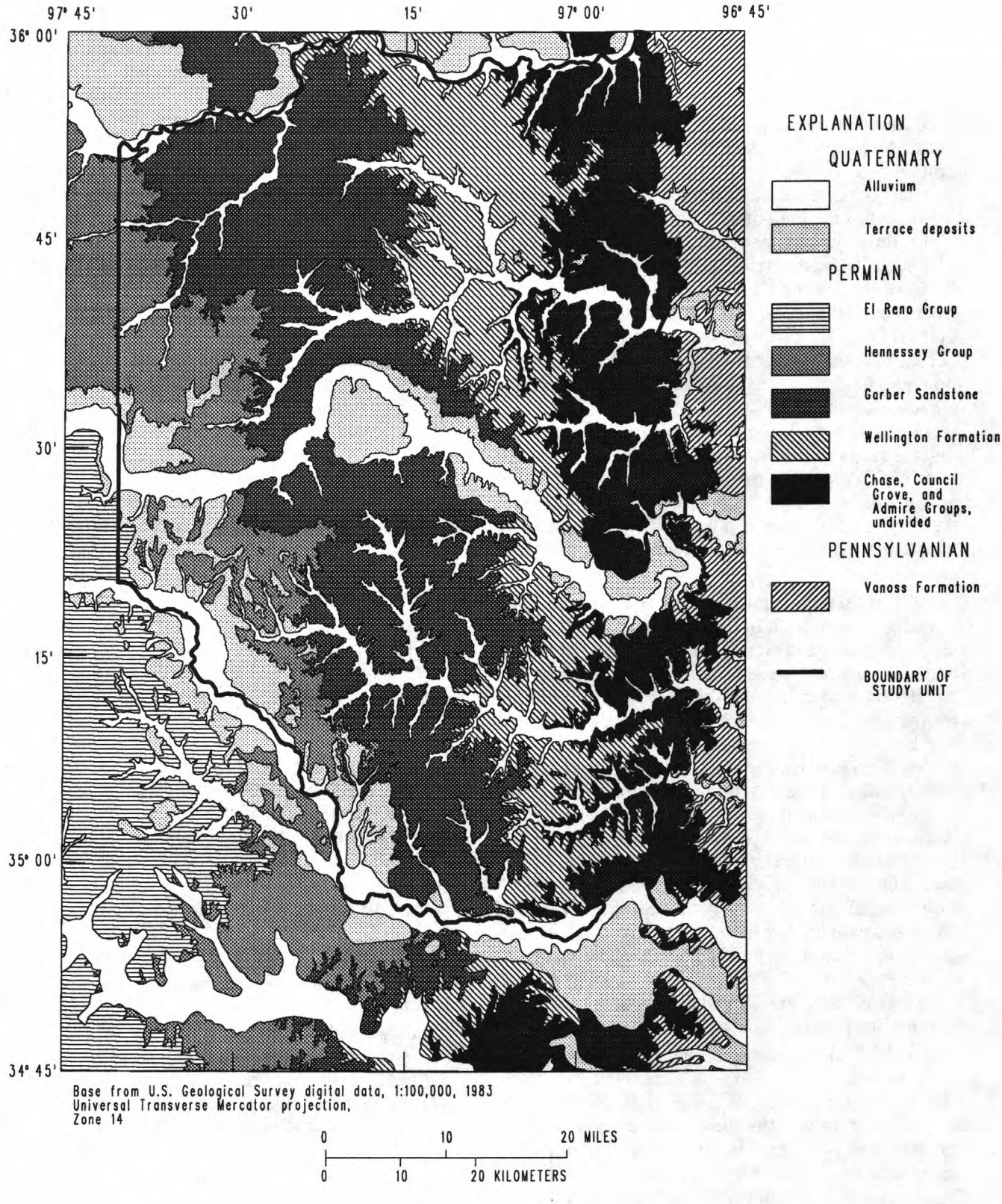

Figure 3. Geologic map of central Oklahoma.

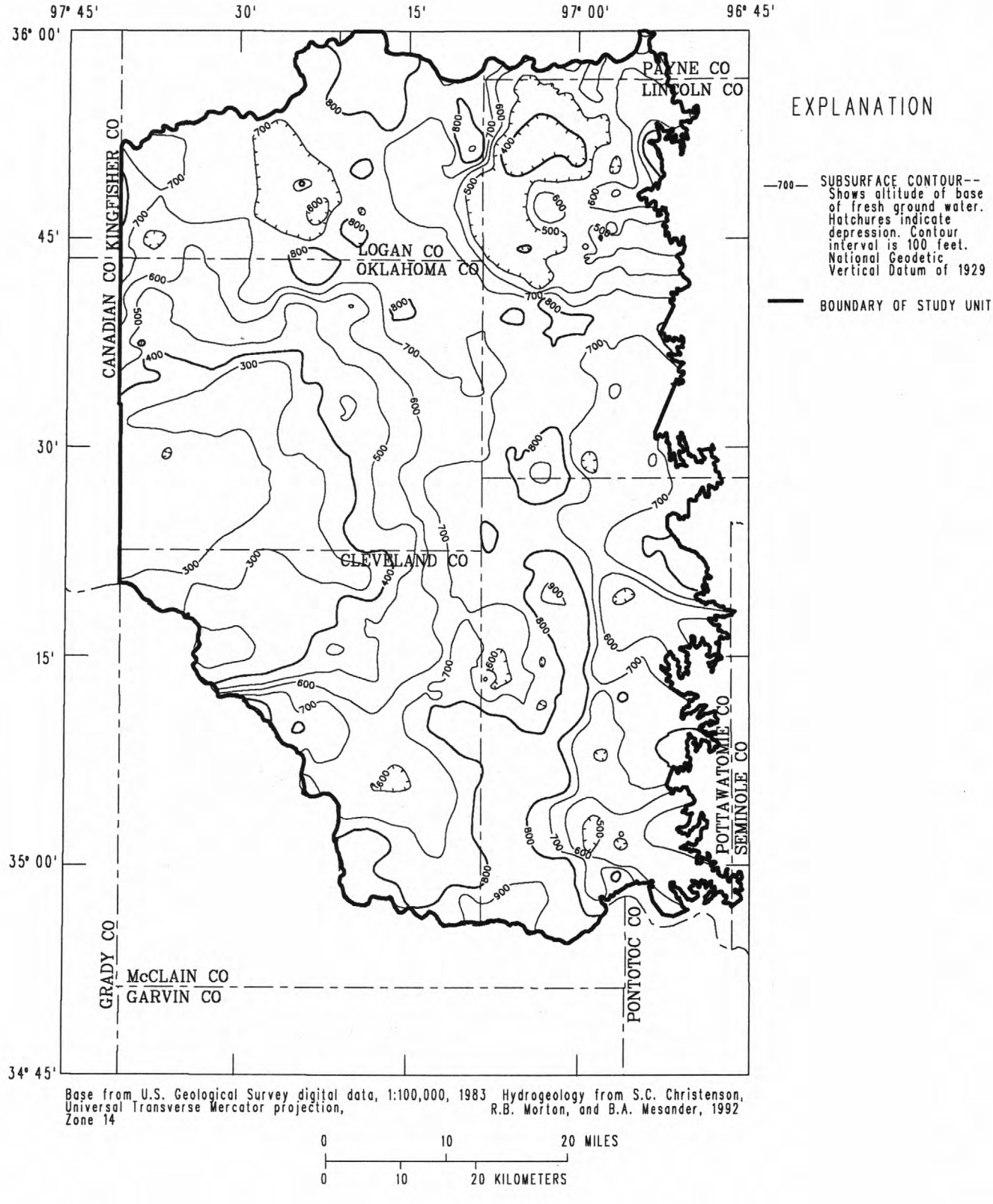

Figure 4. Altitude of the base of fresh ground water.

Quaternary Geologic Units

The Quaternary geologic units consist of alluvium and terrace deposits that occur along streams in the study unit. The hydrogeology of some of the alluvium and terrace deposits has been described previously in Bingham and Moore (1975), Case (1973), Christenson (1983), and Havens (1989). For this report, the alluvium and terrace deposits are discussed only in general terms, and there is no detailed analysis of the ground-water flow system or geochemistry.

Alluvium

Alluvium deposited by streams is the youngest geologic unit in the study unit. The alluvium constantly is being eroded, transported, and deposited by streams. Alluvium is present along most of the perennial streams in the study unit. The most extensive alluvium is present along the North Canadian and Canadian Rivers, where it is as much as 3 miles (mi) wide. The alluvium consists of lenticular beds of unconsolidated clay, silt, sand, and gravel. The thickness of the alluvium ranges from 0 to about 100 ft. Where the alluvium is thickest and contains beds of gravel, wells yield as much as 700 gallons per minute (gal/min) (Bingham and Moore, 1975).

Terrace deposits

Terrace deposits associated with streams in the study unit are older alluvial deposits that occur where erosion has deepened the stream valleys and left the terrace deposits topographically above the present-day alluvium. In the study unit, terrace deposits occur along the Deep Fork, Canadian, and North Canadian Rivers, and are as much as 8 mi wide. Outside of the study unit, terrace deposits occur along the Cimarron and Little Rivers, but none are mapped along these streams within the study unit. Like the alluvium, the terrace deposits consist of lenticular beds of unconsolidated clay, silt, sand, and gravel. Thickness of the terrace deposits in the study unit ranges from 0 to 100 ft. Wells completed in the most productive terrace deposits may yield up to 300 gal/min (Bingham and Moore, 1975).

Permian Geologic Units

Beneath the alluvium and terrace deposits are consolidated geologic units of Permian age. These strata generally are red or reddish-brown in color, and thus generally are referred to as "red beds." The structural geology of these Permian units is very simple. No faults are mapped on the surface in the geologic maps included in Bingham and Moore (1975) or Hart (1974). The regional dip is to the west at about 50 ft/mi. The simple structural geology can be seen in the geohydrologic section shown in figure 5.

El Reno Group

The youngest consolidated geologic unit in the study unit is the El Reno Group. The El Reno Group consists of red-brown fine-grained sandstone with some mudstone conglomerates and shales. The El Reno Group generally yields sufficient water for domestic and stock wells. The El Reno Group is not considered to be part of the Central Oklahoma aquifer because it is separated from the aquifer by the Hennessey Group, which is a confining layer. The El Reno Group is discussed further in this report because a small outcrop of the El Reno Group exists within the study unit.

Hennessey Group

Stratigraphically below the El Reno Group are rocks of the Hennessey Group. The Hennessey Group is present in the western one-third of the study unit, but has been removed by erosion in the eastern two-thirds. The Hennessey Group consists of reddish-brown shales and mudstones, with a few thin beds of very fine-grained sandstone. Because the Hennessey Group is composed mainly of shale and mudstone, transmissivity is low and, thus, the Hennessey is a confining unit. Even though the transmissivity is low, a few small-yield wells, for domestic and stock use, are completed in the Hennessey Group. The Hennessey Group is not considered to be part of the Central Oklahoma aquifer but is discussed in this report because it confines the Central Oklahoma aquifer and crops out within the study unit. A map of the altitude of the base of the Hennessey Group is shown in figure 6.

Garber Sandstone and Wellington Formation

Stratigraphically below the Hennessey Group are the Garber Sandstone and the Wellington Formation. In central Oklahoma, the Garber Sandstone and the Wellington Formation have similar lithologies. These units consist of lenticular beds of fine-grained, cross-bedded sandstone interbedded with siltstone and mudstone. The sand grains are predominantly quartz, and the sandstone is friable. These units were deposited in a fluvial-deltaic sedimentary environment, and the lithologic variability is very large, even over short distances. In the central part of the study unit, the lithology of the Garber Sandstone is predominantly sandstone. However, away from the central part of the study unit,

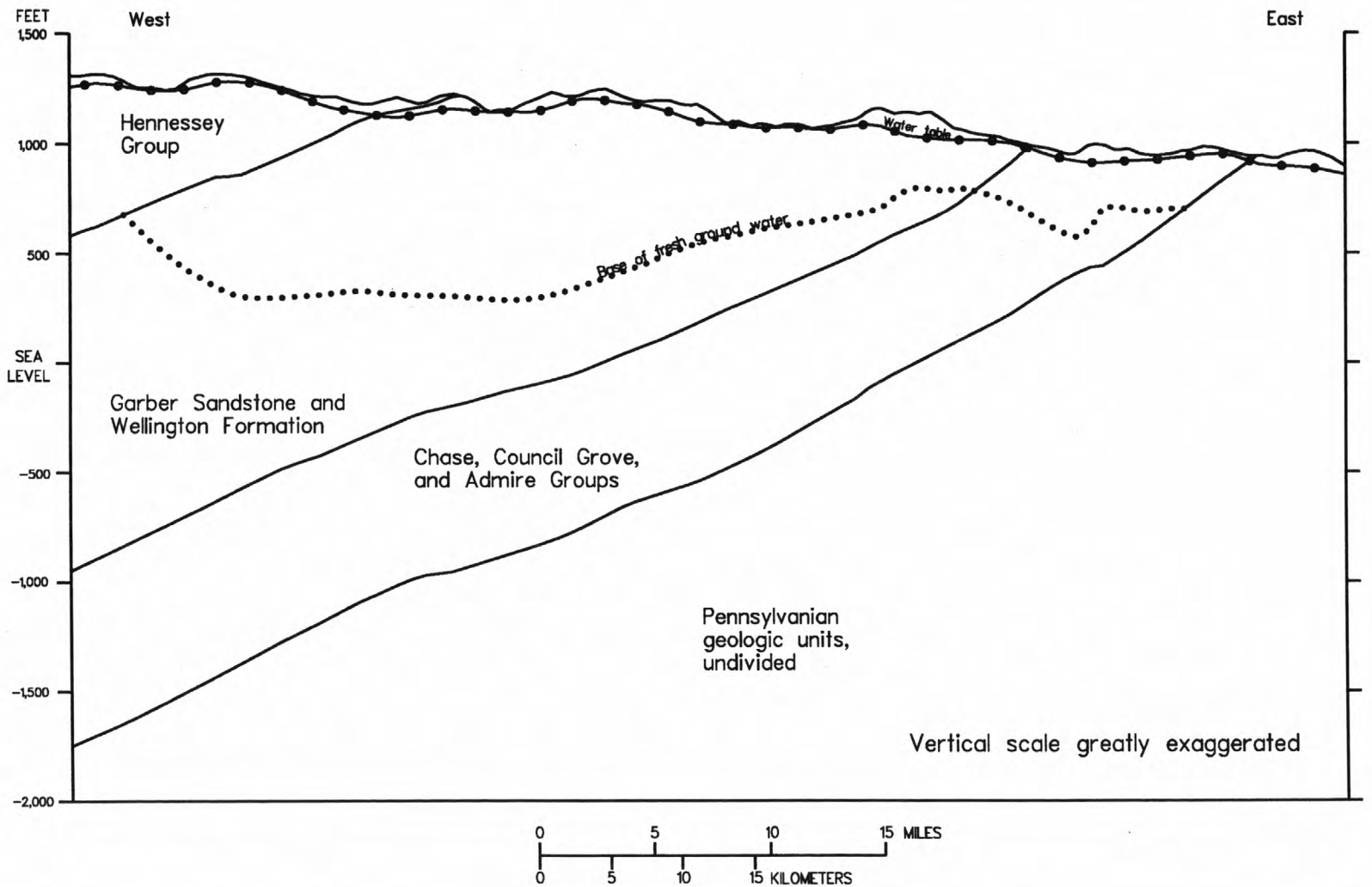

Figure 5. Geohydrologic section along latitude 35°30′.

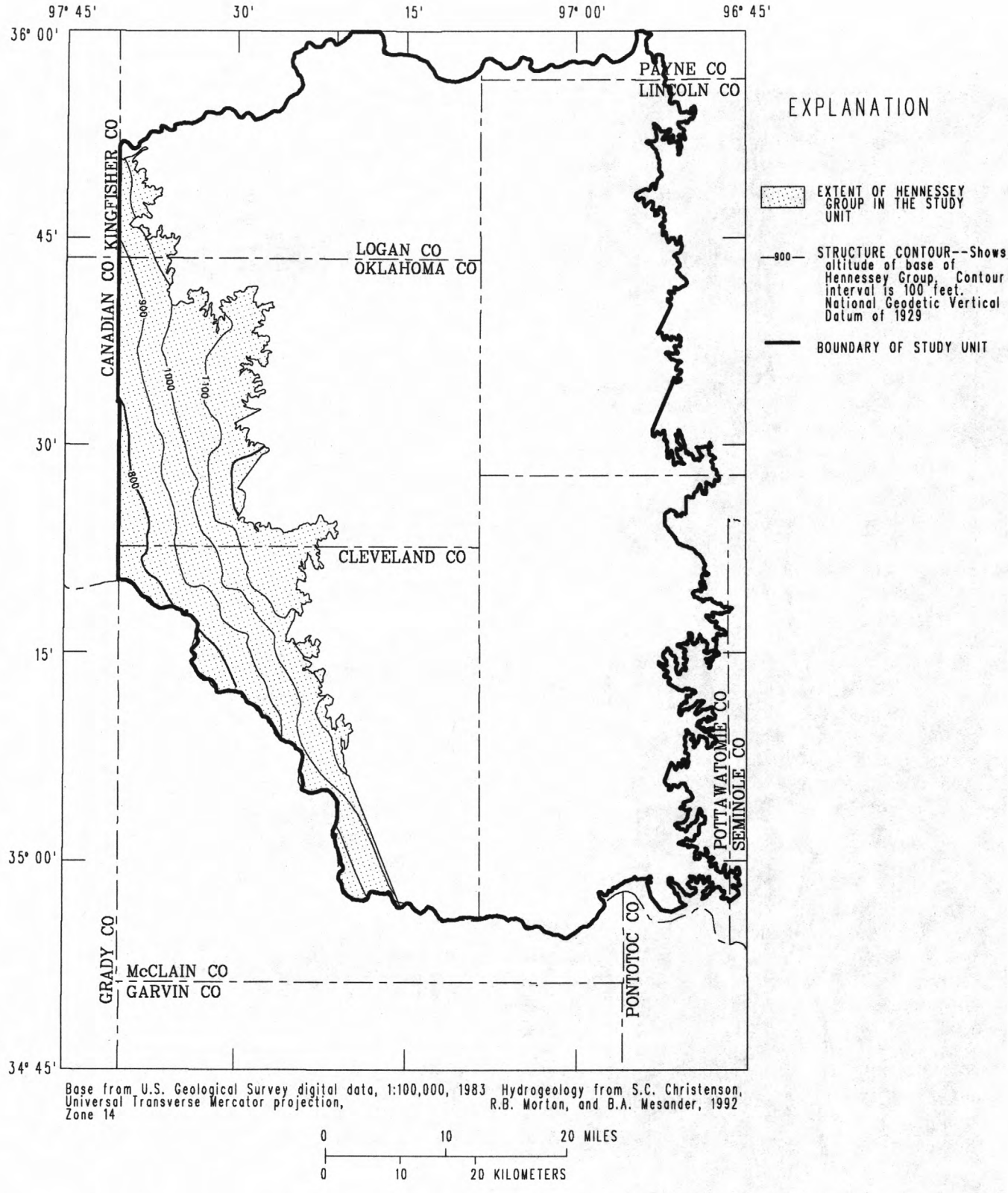

Figure 6. Altitude of the base of the Hennessey Group.

the Garber Sandstone becomes more of a mixture of sandstones, siltstones, and mudstones, and is difficult to distinguish from the underlying Wellington Formation. Therefore, these two geologic units are treated as a single hydrologic unit in this report.

In southwestern Oklahoma County, a few wells completed in the Garber Sandstone and Wellington Formation intercept more than 70 percent sandstone (R.A. Funkhouser, U.S. Geological Survey, written commun., 1990). Sandstone percentage was calculated by summing the thickness of sandstone lithologies intercepted in a well and dividing by the total well depth. Sandstone percentage decreases in all directions from southwest Oklahoma County. Sandstone percentage is about 40 percent at the eastern limit of the Wellington Formation and at the Cimarron and Canadian Rivers. Median sandstone percentage in the Garber Sandstone and Wellington Formation is about 60 percent.

The Garber Sandstone and Wellington Formation are at the surface in the central part of the study unit, but have been removed by erosion in the east. Where a full section of the Garber Sandstone and Wellington Formation is present in wells examined for this study, their combined thickness ranges from 1,165 to 1,600 ft, and has a median thickness of 1,510 ft (Christenson, Morton, and Mesander, 1992). A map of the base of the Wellington Formation is shown in figure 7.

A few wells completed in the Garber Sandstone and Wellington Formation yield as much as 600 gal/min, but because the sandstone is fine grained, yields generally range from 200 to 400 gal/min, in wells designed for maximum yield.

Chase, Council Grove, and Admire Groups

Stratigraphically below the Wellington Formation are the Permian Chase, Council Grove, and Admire Groups (undivided in this report). Bingham and Moore (1975) referred to the Chase, Council Grove, and Admire Groups as the "Oscar Group," and assigned it to the Pennsylvanian System. Although data from Bingham and Moore (1975) are cited frequently, the term "Oscar Group" is not used in this report. Lindberg (1987) refers to these geologic units as the Permian Chase, Council Grove, and Admire Groups. This terminology follows the usage of the U.S. Geological Survey and is used in this report.

Where complete sections are present in wells examined for this study, the combined thickness of these groups ranges from 570 to 940 ft with a median thickness of 745 ft (Christenson, Morton, and Mesander, 1992). In surface exposures in the eastern part of the study unit, these groups have similar lithologies, consisting of beds of fine-grained, cross-bedded sandstone, shale, and thin limestone. Median sandstone percentage in the freshwater section is 26 percent. A map of the base of these groups is shown in figure 8.

In the central part of the study unit, wells are completed in the Wellington Formation and in one or more of the underlying Chase, Council Grove, and Admire Groups. East of the outcrop of the Wellington Formation, wells that are completed only in the Chase, Council Grove, and Admire Groups generally yield 10 to 100 gal/min; a few wells yield as much as 120 gal/min.

Pennsylvanian Geologic Unit

Vanoss Formation

The Vanoss Formation is the only Pennsylvanian geologic unit in the study unit and is the oldest geologic unit considered in this report. The Vanoss Formation underlies the Chase, Council Grove, and Admire Groups and occurs along the eastern boundary of the study unit. The Vanoss Formation consists mainly of shale and a few thin, fine-grained sandstone beds. The Vanoss Formation generally does not yield substantial volumes of water to wells and is considered to be a confining layer. The Vanoss Formation is not considered to be part of the Central Oklahoma aquifer but is discussed in this report because it confines the Central Oklahoma aquifer.

GEOCHEMISTRY

The chemical evolution of ground water is due to geochemical reactions between water and the minerals and gases within the unsaturated and saturated zones of the aquifer. The purpose of the geochemical investigation is to identify these geochemical reactions and to quantify the extent to which they occur. The evidence used to investigate the geochemical reactions is obtained by petrographic examination of the aquifer material and analysis of the chemical and isotopic composition of ground-water samples. The ultimate descriptions of the geochemical reactions are mass-balance models that quantitatively account for the chemical and isotopic evolution of ground water and are consistent with the reactant minerals identified by petrographic observations.

Three sets of data were used in the geochemical investigation. First, records of chemical analyses of ground-water samples were obtained at the beginning of the NAWQA study from Federal, State, and local sources. These data were described in Parkhurst, Christenson, and Schlottmann (1989). Second,

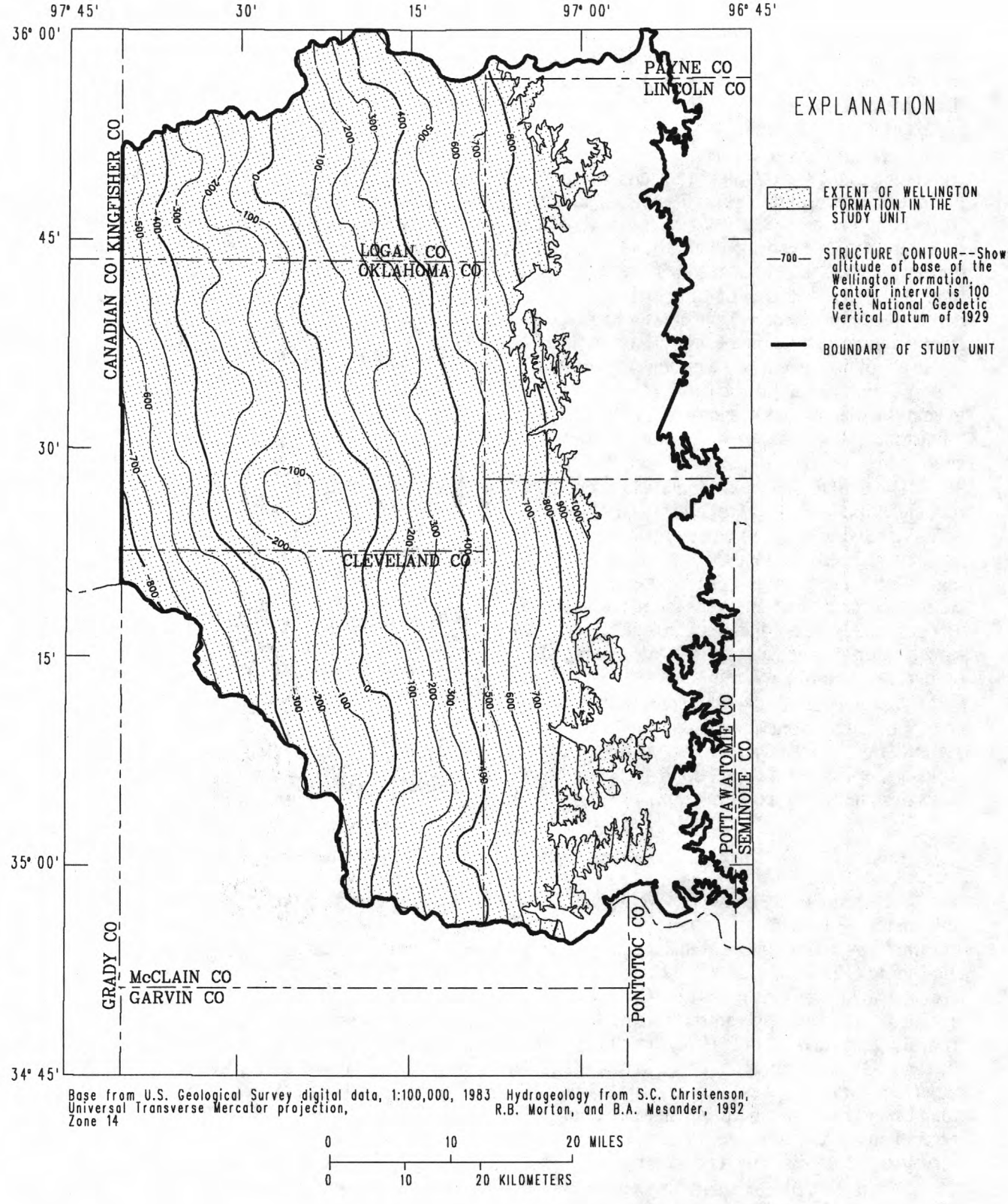

Figure 7. Altitude of the base of the Wellington Formation.

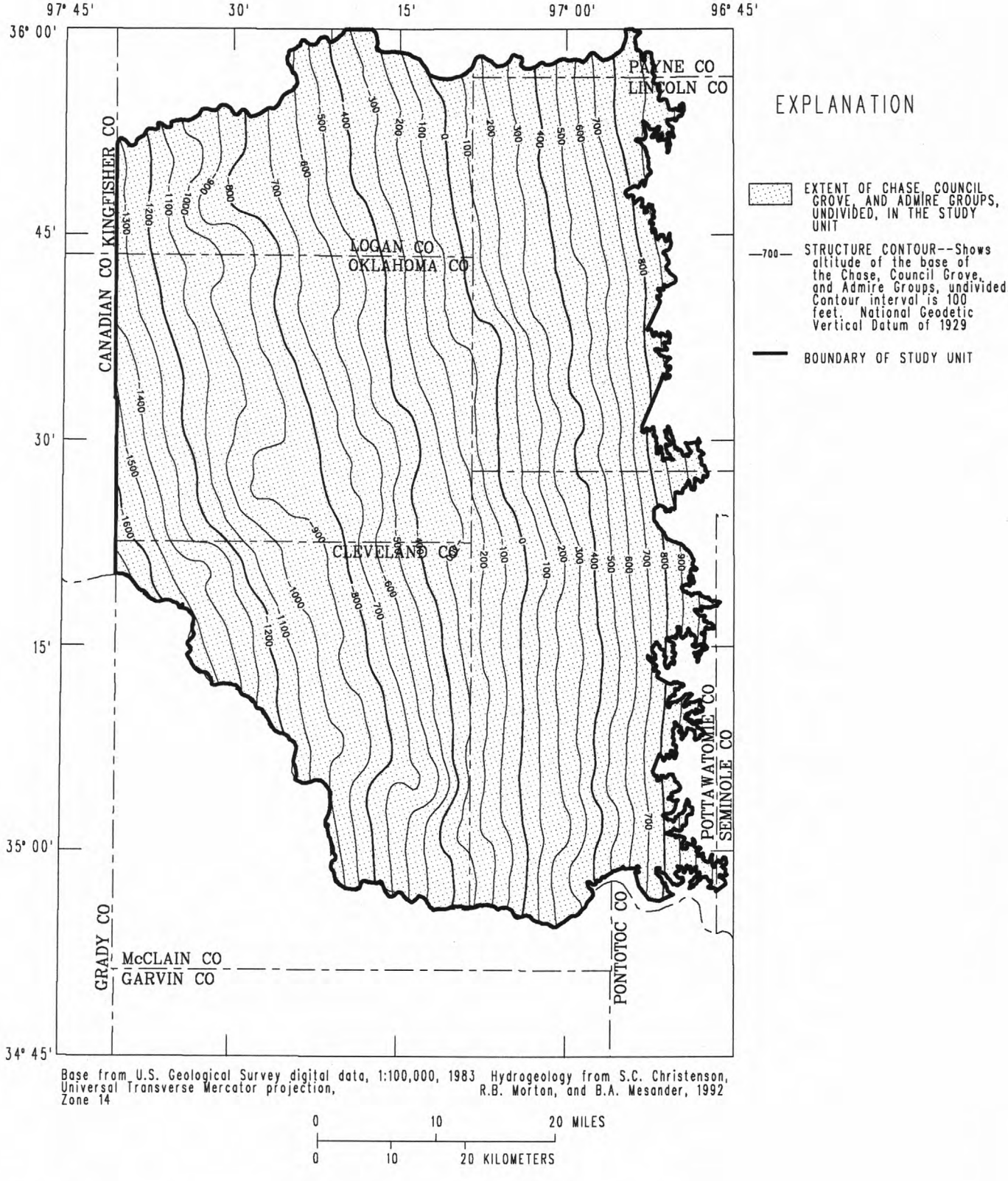

Figure 8. Altitude of the base of the Chase, Council Grove, and Admire Groups, undivided.

ground-water samples from wells in the study unit were collected and analyzed during the present study. These data were collected to provide spatial coverage of the entire study unit or of specific parts of the study unit. Finally, ground-water samples and core samples were collected from test holes drilled during the present study. Eight test holes at seven locations were drilled to investigate naturally occurring trace substances (NOTS) in ground water, specifically arsenic, chromium, selenium, uranium, and gross-alpha particle activity. The test holes are referred to as the NOTS test holes.

In this section, the geochemical reactions occurring in the Central Oklahoma aquifer are identified and quantified. First, general descriptions are presented of the chemical composition of ground water in the study unit. These descriptions are followed by an examination of the sources of water (recharge and residual brines) and the mineral reactants that are present in the system. Finally, mass-balance modeling uses these sources of water and reactant minerals to quantify geochemical reactions that account for the chemical and isotopic composition of ground water. The results of the mass-balance modeling are used with carbon-14 data to estimate ground-water ages.

Description of the Chemical Composition of Ground Water

Several methods are used to provide general descriptions of the chemical composition of ground water in the study unit. A statistical summary is presented to describe the distribution of chemical concentrations in the samples from the present study, exclusive of the test-hole samples. Maps show the geographic distribution of major elements in the shallow and deep parts of the study unit. Water-quality diagrams summarize the major-element concentrations in specific parts of the study unit. Only a brief discussion on the occurrence of trace elements is presented. Finally, the nature of the redox environment in the study unit is discussed in detail.

Summary Statistics

A statistical summary of the data collected in the present study is presented in table 1. The method of Helsel and Cohn (1988) was used to calculate percentiles for constituents that have censored data. The most recent sample from each sampling site, excluding test-hole sites, was included in the sample set used to calculate the summary statistics. Data from the test holes were excluded from the sample set because the drilling locations were not randomly chosen; the locations were chosen specifically to be near known water-quality problems. All other sites were selected to provide spatial coverage of the study unit.

Major-Element Chemistry

Reproduced here are two figures from Parkhurst, Christenson, and Schlottmann (1989) that show major ion concentrations in ground water from the shallow part (defined as depths less than 100 ft in that study) and the deep part (depths greater than 300 ft) of the study unit (figs. 9 and 10). All samples used in the construction of these two maps were from wells that were completed above the base of fresh ground water.

Ion concentrations are closely correlated with geologic units in the shallow part of the study unit (fig. 9). In ground water in the Garber Sandstone, Wellington Formation, and El Reno Group, calcium and magnesium are the dominant cations, and bicarbonate is the dominant anion. Ground water in the Hennessey, Chase, Council Grove, and Admire Groups has larger concentrations of sodium and, in parts of the groups, larger concentrations of sulfate and chloride. Samples from the deep parts of the Garber Sandstone and Wellington Formation were used to depict the major element chemistry of deep ground water (fig. 10). The map shows that the ground-water in the deep, unconfined part of the Garber Sandstone and Wellington Formation contains predominantly calcium magnesium bicarbonate water. However, ground water in the deep, confined part of these units contains larger concentrations of sodium.

Water-quality diagrams were generated by combining the data collected in the present study with the data of Parkhurst, Christenson, and Schlottmann (1989). Only data associated with individual wells of known depth were used from the study of Parkhurst, Christenson, and Schlottmann (1989). All data, except the data from the test holes, were used from the present study. Water-quality diagrams (fig. 11) were generated to distinguish variations in water composition that are apparent in figures 9 and 10. Water-quality diagrams were made by using samples from wells completed in seven distinct parts of the study unit: (1) The alluvium and terrace deposits; (2) the Hennessey Group; (3) the shallow, unconfined (depths less than or equal to 300 ft; note that this definition of shallow differs from the definition in fig. 9 and Parkhurst, Christenson, and Schlottmann, 1989), (4) the deep, unconfined (depths greater than 300 ft), (5) the shallow, confined, and (6) the deep, confined (depths greater than 300 ft) parts of the Garber Sandstone and Wellington Formation; and

Table 1. Summary statistics for chemical constituents using data from the present study, except for test-hole data

[These statistics were calculated using the most recent analysis for each constituent for each well. Constituents and properties: dis., dissolved; Specific cond., specific conductance; µS/cm, microsiemens per centimeter; °C, degrees Celsius; mg/L, milligrams per liter; µg/L, micrograms per liter; pCi/L, picocuries per liter; $\delta^{13}C$, carbon-13 relative to Peedee belemnite (PDB); δD, deuterium relative to SMOW (standard mean ocean water); $\delta^{18}O$, oxygen–18 relative to SMOW; $\delta^{34}S$, sulfur–34 relative to Canyon Diablo troilite (CDT). Method: 1, no censored data, ordinary percentile calculation; 2, censored data present, percentiles calculated using methods of Helsel and Cohn (1988); 3, no calculation, more than 95 percent of the data were censored. Largest MRL: largest minimum reporting level; percentiles less than this value were estimated using the methods of Helsel and Cohn (1988); percentiles greater than this value are the same as ordinary percentile calculation; --, no censored data for this constituent. Percentiles: --, indicates no statistic was calculated]

Constituents and properties	Method	Sample size	Minimum value	Largest MRL	Percentiles							Maximum value
					5	10	25	50	75	90	95	
Properties and major elements												
Specific cond. (µS/cm at 25°C)	1	202	91	--	270	353	482	669	1,040	1,807	2,358	6,440
Specific cond., lab (µS/cm at 25°C)	1	201	93	--	273	354	480	675	1,015	1,844	2,362	6,500
pH (standard units)	1	202	5.7	--	6.2	6.5	7.0	7.3	7.6	8.6	8.9	9.2
pH, laboratory (standard units)	1	202	5.9	--	6.5	6.8	7.2	7.5	7.8	8.6	8.9	9.1
Temperature, water (°C)	1	202	15.5	--	16	17	17	18	18	19	20	21
Oxygen, dis. (mg/L as O_2)	2	199	0	<0.1	.10	.20	2.2	4.7	7.1	8.6	9.2	13
Calcium, dis. (mg/L as Ca)	1	202	1	--	2.1	6.7	29	50	84	130	180	500
Magnesium, dis. (mg/L as Mg)	1	202	.33	--	.91	3.1	14	25	40	57	79	214
Sodium, dis. (mg/L as Na)	1	202	4.1	--	6.9	12	20	50	130	237	300	1,400
Potassium, dis. (mg/L as K)	2	202	<.1	<.1	.40	.50	.80	1.3	2.1	3.1	3.6	16
Alkalinity, total, field (mg/L as $CaCO_3$)	1	202	22	--	72	105	200	275	349	412	478	646
Alkalinity, total, laboratory (mg/L as $CaCO_3$)	1	171	20	--	70	109	196	272	344	406	483	637
Sulfate, dis. (mg/L as SO_4)	1	202	3.3	--	5.8	7.2	12	25	60	200	344	3,700
Chloride, dis. (mg/L as Cl)	1	202	2.4	--	5.9	7.9	11	24	66	200	288	1,820
Fluoride, dis. (mg/L as F)	2	202	<.1	<.1	.10	.10	.20	.30	.40	.77	1.2	3.9
Bromide, dis. (mg/L as Br)	1	202	0.02	--	0.03	0.04	0.07	0.15	0.27	0.57	0.98	7.7
Silica, dis. (mg/L as SiO_2)	1	202	8.7	--	9.5	10	14	17	21	25	29	36
Nutrients												
Nitrogen, nitrite, dis. (mg/L as N)	2	201	<.01	<0.05	.00	.00	.00	.00	.01	.01	.01	.02

Table 1. Summary statistics for chemical constituents using data from the present study, except for test-hole data—Continued

Constituents and properties	Method	Sample size	Minimum value	Largest MRL	Percentiles							Maximum value
					5	10	25	50	75	90	95	
Nitrogen, nitrite plus nitrate, dis. (mg/L as N)	2	202	<0.05	<0.1	0.04	0.07	0.24	0.65	3.3	8.6	12	85
Nitrogen, ammonia, dis. (mg/L as N)	2	201	<.01	<.05	.00	.00	.00	.01	.04	.11	.34	2.1
Phosphorus, dis. orthophosphate (mg/L as P)	2	201	<.01	<.01	.00	.00	.01	.01	.03	.06	.11	.20
Trace elements												
Aluminum, dis. (µg/L as Al)	2	198	<10	<10	.47	.69	1.3	2.8	5.7	10	20	70
Arsenic, dis. (µg/L as As)	2	202	<1	<1	.08	.14	.36	1.0	2.0	8.0	27	110
Barium, dis. (µg/L as Ba)	2	202	<5	<5	27	45	87	190	350	547	696	6,400
Beryllium, dis. (µg/L as Be)	2	202	<.5	<2.5	.00	.00	.01	.03	.12	.38	.76	2.4
Boron, dis. (µg/L as B)	1	200	10	--	30	41	70	160	540	1,590	3,481	9,600
Cadmium, dis. (µg/L as Cd)	2	202	<1	<5	.00	.01	.02	.07	.25	.75	1.5	10
Chromium, dis. (µg/L as Cr)	2	202	<1	<25	.06	.13	.40	1.4	5.1	16	36	100
Chromium, hexavalent (µg/L as Cr)	2	87	<1	<1	.09	.16	.43	1.0	2.0	14	35	93
Cobalt, dis. (µg/L as Co)	3	202	<3	<15	--	--	--	--	--	--	--	4.0
Copper, dis. (µg/L as Cu)	2	202	<10	<50	.34	.51	1.0	2.2	4.6	9.2	14	80
Iron, dis. (µg/L as Fe)	2	202	<3	<9	.24	.53	2.0	8.5	19	107	1,590	3,400
Lead, dis. (µg/L as Pb)	2	202	<10	<50	.36	.54	1.1	2.3	4.8	9.4	14	50
Lithium, dis. (µg/L as Li)	2	202	<4	<4	4.4	6.0	10	14	23	35	48	180
Manganese, dis. (µg/L as Mn)	2	202	<1	<3	.00	.01	.06	.59	5.3	92	359	1,300
Mercury, dis. (µg/L as Hg)	2	170	<.1	<.1	.00	.00	.00	.01	.05	.20	.34	.90
Molybdenum, dis. (µg/L as Mo)	2	202	<10	<50	.04	.07	.22	.74	2.5	7.5	15	80
Nickel, dis. (µg/L as Ni)	3	202	0	<50	--	--	--	--	--	--	--	40
Selenium, dis. (µg/L as Se)	2	202	<1	<1	.02	.04	.17	.79	2.3	20	50	190
Silver, dis. (µg/L as Ag)	2	202	<1	<3	.03	.05	.11	.26	.66	1.5	2.5	44
Strontium, dis. (µg/L as Sr)	1	202	17	--	48	77	150	350	993	2,070	3,570	10,000

Table 1. Summary statistics for chemical constituents using data from the present study, except for test-hole data—Continued

Constituents and properties	Method	Sample size	Minimum value	Largest MRL	Percentiles							Maximum value
					5	10	25	50	75	90	95	
Vanadium, dis. (µg/L as V)	2	202	<6	<30	0.29	0.56	1.7	6.0	21	91	229	560
Zinc, dis. (µg/L as Zn)	2	202	<3	<9	.78	1.3	3.1	8.3	21	41	92	1,300
Radionuclides												
Gross alpha, dis. (µg/L as U-natural)	2	164	<.4	<.4	.83	1.4	2.8	7.4	17	47	95	210
Gross beta, dis. (pCi/L as Cs–137)	2	164	<.4	<.4	1.1	1.7	3.0	6.3	12	23	49	110
Gross beta, dis. (pCi/L as Sr/Y–90)	2	164	<.4	<.4	.90	1.2	2.3	4.5	8.4	18	33	76
Carbon–14 (percent modern)	2	37	<.7	<.7	1.8	2.1	8.7	23.5	60.0	110.0	116.0	123.0
Radium–226, dis. (pCi/L)	1	37	.04	--	.04	.04	.09	.15	.28	.42	.64	.83
Radium–228, dis. (pCi/L)	2	36	<1	<2	.82	.94	1.2	2.0	2.0	2.0	3.0	3.0
Radon–222, total (pCi/L)	2	170	<80	<80	47	81	120	170	250	797	1,300	4,900
Tritium, total (pCi/L)	2	201	<.3	<.3	.02	.06	.34	3.7	30	47	60	92
Uranium–234, dis. (pCi/L)	2	196	.04	<.1	.12	.17	.70	3.1	7.9	22	31	65
Uranium–238, dis. (pCi/L)	2	196	.01	<.1	.04	.08	.26	1.0	3.5	13	23	73
Stable isotopes												
$\delta^{13}C$ (per mil)	1	36	–20.2	--	–18.2	–16.4	–13.6	–11.1	–10.3	–9.5	–8.9	–7.7
δD (per mil)	1	60	–44.0	--	–43.4	–41.5	–38.5	–36.0	–33.0	–30.6	–29.0	–27.5
$\delta^{18}O$ (per mil)	1	60	–7.05	--	–6.95	–6.85	–6.40	–6.13	–5.76	–5.46	–5.25	–4.00
$\delta^{34}S$ (per mil)	1	37	–26.8	--	–2.0	2.3	5.0	7.3	9.6	10.0	10.4	11.4
Organic carbon												
Carbon, organic dis. (mg/L as C)	1	159	.2	--	.40	.40	.60	.80	1.3	2.1	2.8	9.7

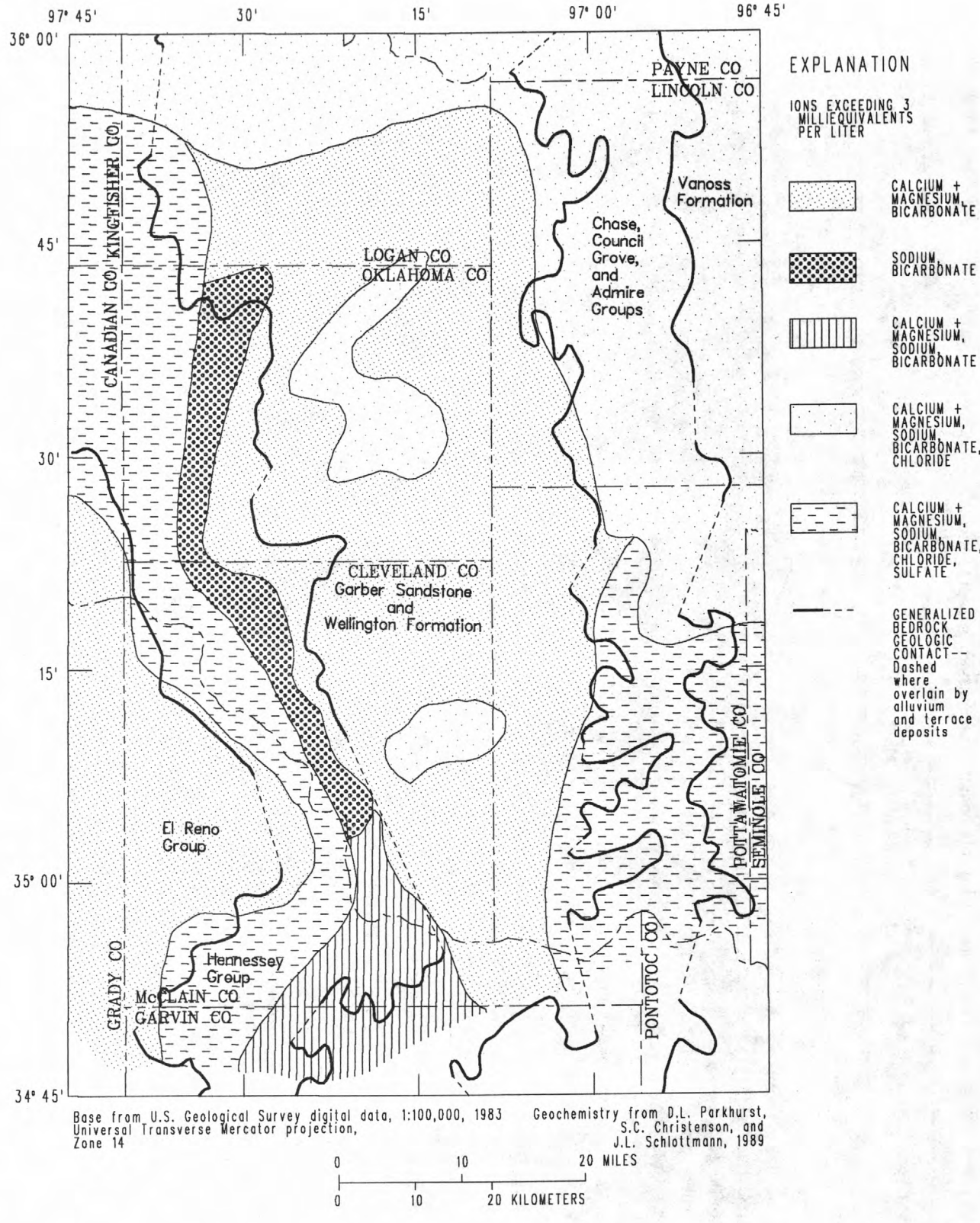

Figure 9. Major-element chemistry in the shallow part (depths less than 100 feet) of the study area.

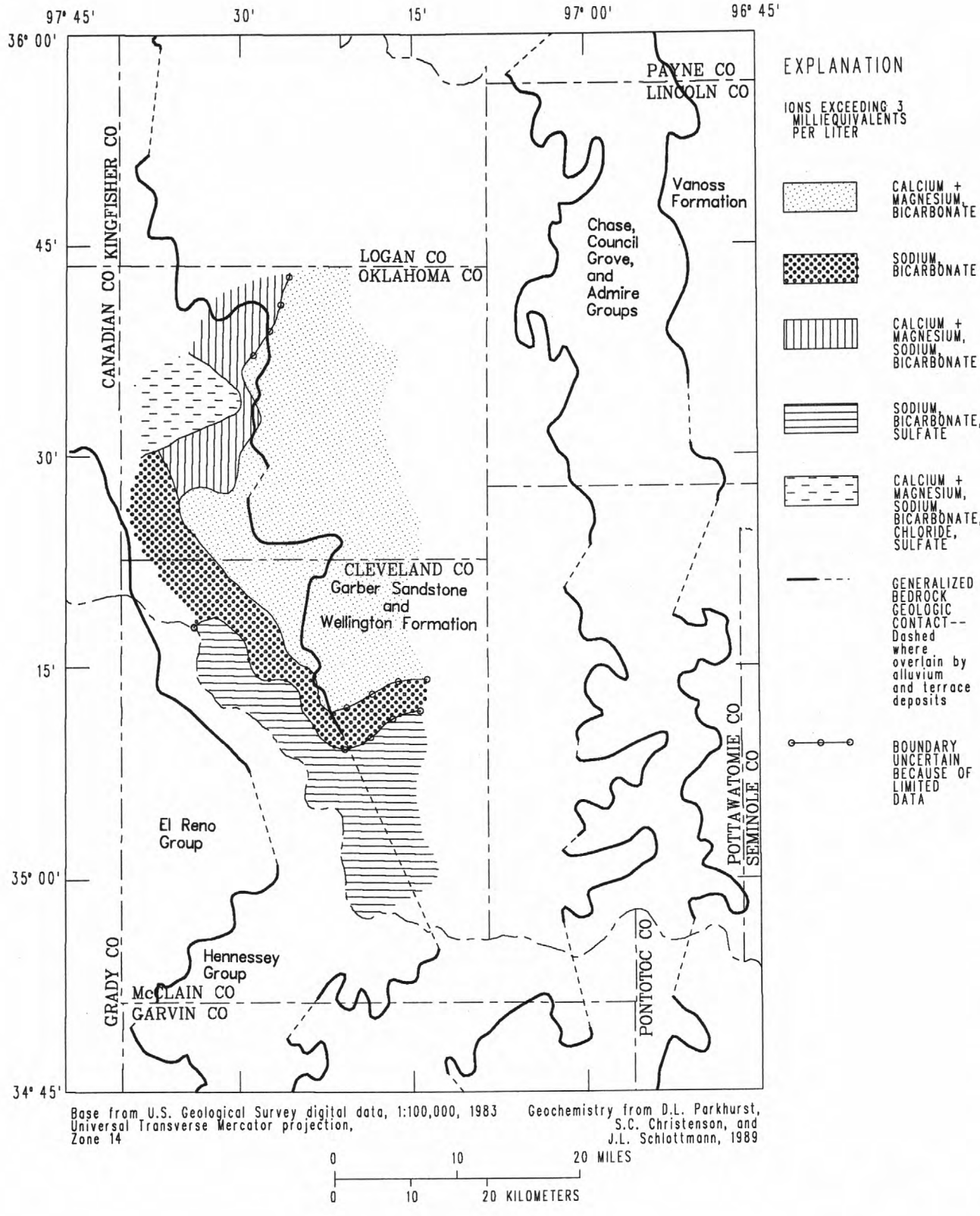

Figure 10. Major-element chemistry in the deep part (depths greater than 300 feet) of the Garber Sandstone and Wellington Formation.

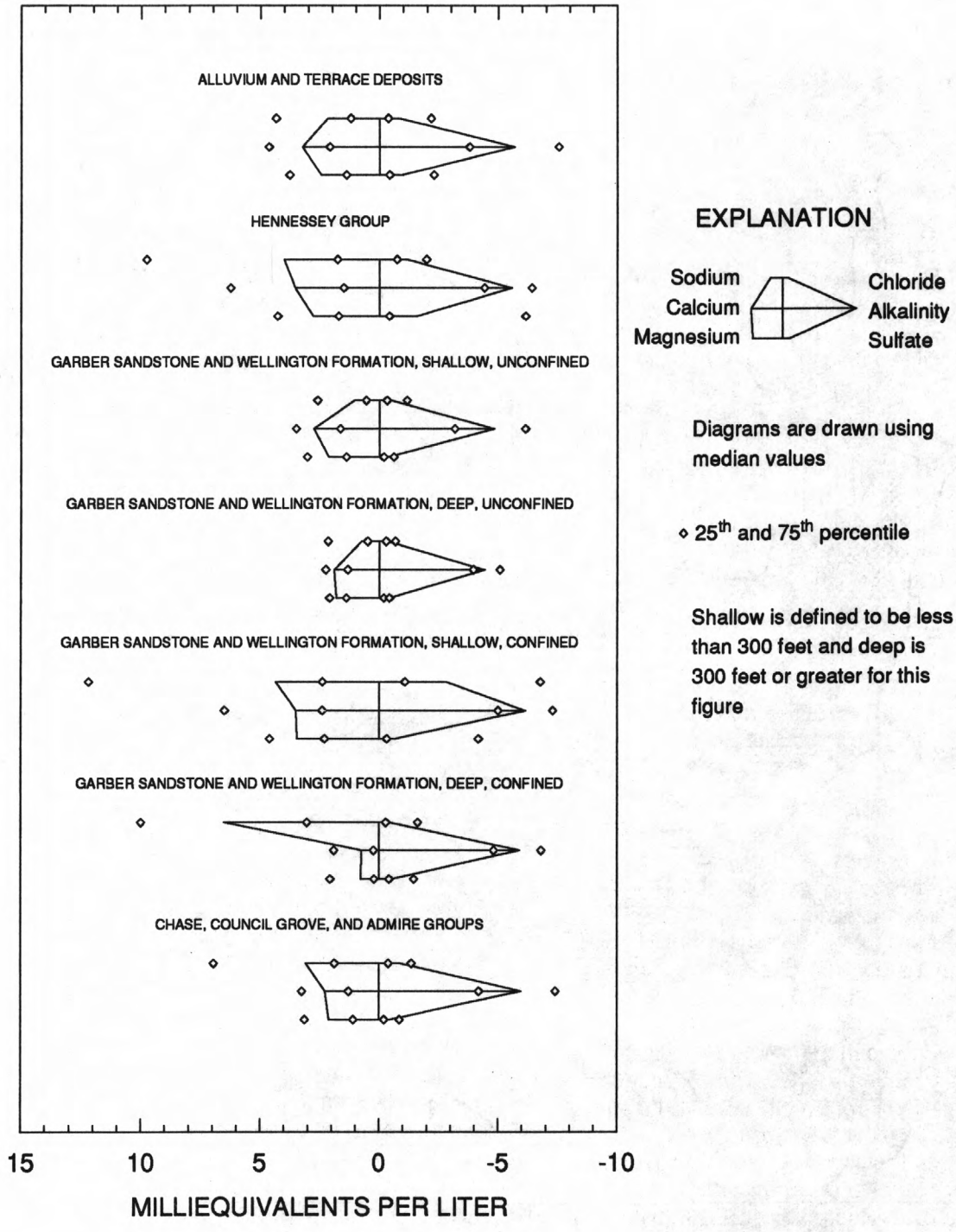

Figure 11. Median major-ion concentrations of water samples from hydrogeologic units within the Central Oklahoma aquifer.

(7) the Chase, Council Grove, and Admire Groups (undivided).

The water-quality diagrams show the median concentration in milliequivalents per liter of each major ion. Also shown are the 25th and 75th percentiles of each ion; 25 percent of the data are less than the 25th percentile, and 75 percent of the data are less than the 75th percentile. The percentiles are one measure of the range in concentrations that have been observed for each part of the study unit.

The following generalizations can be made from the maps of major ions and the water-quality diagrams. Calcium, magnesium, and bicarbonate are the dominant cations in the unconfined part of the Garber Sandstone and Wellington Formation. Sodium and bicarbonate are the dominant ions in the rest of the Permian geologic units, that is, the Hennessey Group, the confined part of the Garber Sandstone and Wellington Formation, and the Chase, Council Grove, and Admire Groups. All parts of the study unit have similar concentrations of bicarbonate. Concentrations of sulfate and chloride are relatively small in most parts of the study unit. The largest concentrations of chloride tend to occur in the shallow, confined part of the Garber Sandstone and Wellington Formation. The largest concentrations of sulfate tend to occur in the Hennessey Group and the southern part of the confined Garber Sandstone and Wellington Formation.

Trace-Element Chemistry

It is beyond the scope of this report to consider the geochemistry of trace elements in detail. Descriptive statistics for trace elements analyzed in the present study are presented in table 1. Relatively large concentrations of barium, boron, iron, and strontium are evident in some of the percentile statistics (table 1). Parkhurst, Christenson, and Schlottmann (1989) determined that, in the deep part of the Garber Sandstone and Wellington Formation, arsenic, chromium, and selenium concentrations commonly exceeded the primary water-quality standards set forth by the U.S. Environmental Protection Agency (1986). Concentrations of manganese greater than the secondary water-quality standards commonly occurred in the alluvium and terrace deposits (Parkhurst, Christenson, and Schlottmann, 1989). No standard exists for uranium, but large concentrations of uranium occur in most parts of the study unit (Parkhurst, Christenson, and Schlottmann, 1989). Large concentrations of uranium are most common in the Hennessey Group, at depths greater than 100 feet in the Garber Sandstone and Wellington Formation, and in the Chase, Council Grove, and Admire Groups (Parkhurst, Christenson, and Schlottmann, 1989). Implications of some trace-element concentrations with regard to the oxidation-reduction environment in the study unit are discussed in the following section.

Oxidation-Reduction Environment

Berner (1981) presents a classification of oxidation-reduction (redox) environments in sedimentary deposits that is equally applicable to ground-water systems. Berner classifies the redox environment on the basis of presence or absence of certain redox minerals and dissolved redox species. The environments in this classification are oxic, post-oxic, sulfidic, and methanic. The data from the NAWQA study are interpreted based on this classification and on the presence or absence of other redox-indicating species.

The sample set used in this discussion of redox environments includes one sample from each well that was sampled in this study. The sample set also includes one sample from each sampling depth of the test holes that were drilled during this study. The total number of samples in this set is 226, but some samples were not analyzed for all constituents.

In Berner's classification system, an oxic environment is defined by the presence of measurable dissolved-oxygen concentrations. Dissolved oxygen was measured in this study by a dissolved-oxygen electrode in a closed flow-through cell; however, the water was obtained through existing pumps and plumbing, which could allow air to be entrained in the sample. Therefore, a relatively large value of 1 mg/L was the criterion for measurability because of sampling uncertainties. Dissolved oxygen was greater than 1 mg/L in 179 of 225 samples analyzed; dissolved-oxygen concentrations were less than 1 mg/L only in 46 samples.

Environments lacking dissolved oxygen are termed anoxic and are subdivided into post-oxic, sulfidic, and methanic (Berner, 1981). Sulfidic environments have measurable concentrations of dissolved sulfide, and both sulfidic and methanic environments are characterized by the presence of sulfide minerals. Dissolved sulfide and sulfide minerals are rare or absent in the Central Oklahoma aquifer; thus, the anoxic samples are classified as post-oxic. The post-oxic environment is characterized by the successive reduction of nitrate, manganese, and iron (Berner, 1981). Some trace elements also may change redox states within a post-oxic environment.

The equilibrium distributions of redox states of redox-active elements are shown in figure 12 as a function of pe (negative log of the activity of the electron) for water compositions representative of two water types in the Central Oklahoma aquifer: a calcium mag-

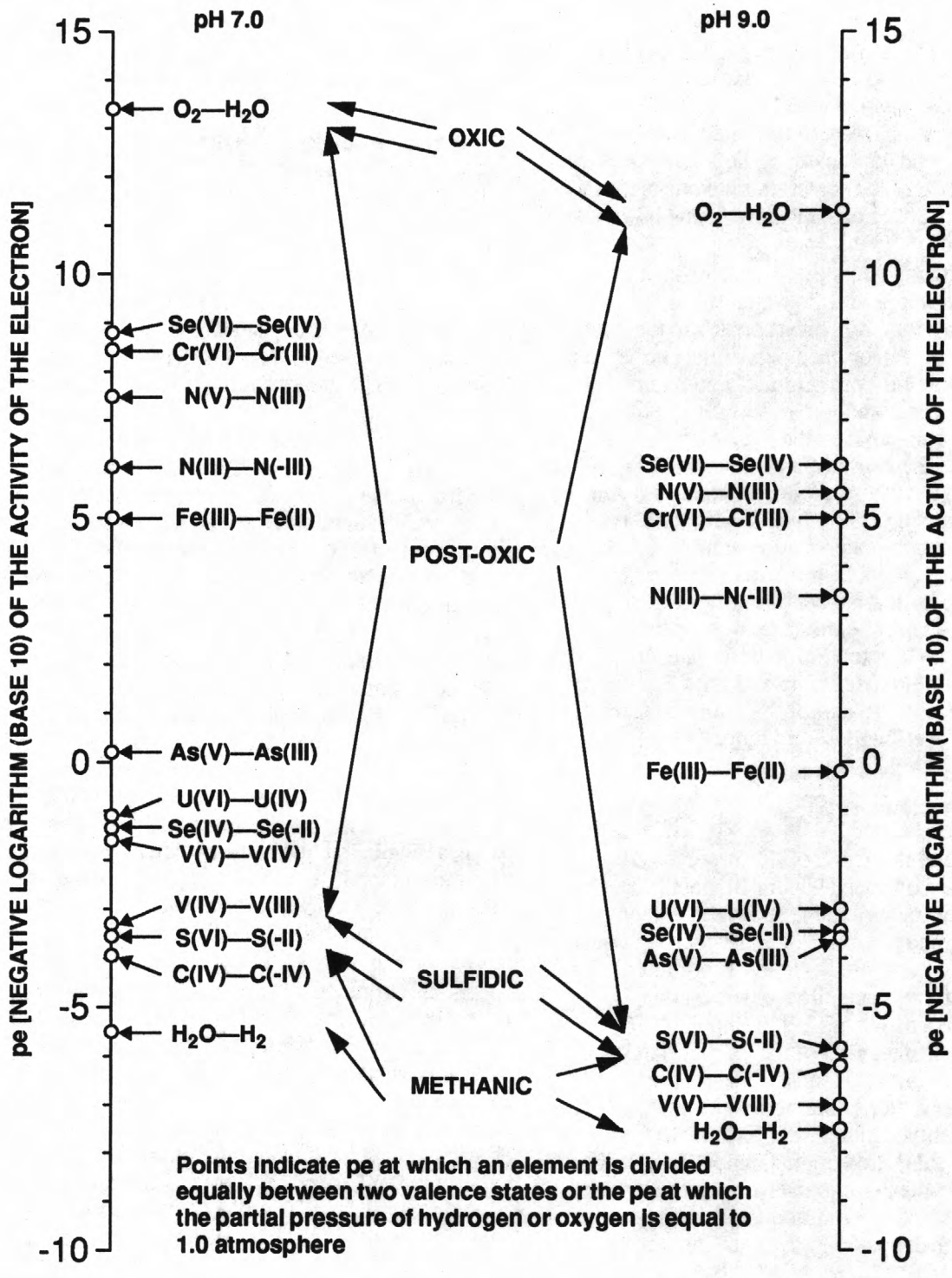

Figure 12. Valence-state transitions of redox-active elements as a function of pe [negative logarithm (base 10) of the activity of the electron] for two representative water compositions of the Central Oklahoma aquifer, a calcium magnesium bicarbonate water (pH 7.0) and a sodium bicarbonate water (pH 9.0).

nesium bicarbonate water (pH 7.0) and a sodium bicarbonate water (pH 9.0). Distributions were calculated with the equilibrium geochemical model PHREEQE (Parkhurst, Thorstenson, and Plummer, 1980) by using thermodynamic data from WATEQ4F (Ball and Nordstrom, 1990) for arsenic and selenium, MINTEQA1 (Brown and Allison, 1987) for chromium, Langmuir (1978) for uranium, and Wanty (1986) for vanadium. An arrow on the diagram points to the equilibrium pe at which half of the concentration of an element is in the more oxidized redox state and half is in the more reduced state. Although redox reactions are often non-equilibrium processes that are mediated by microorganisms, the presence and absence of the various oxidized or reduced states of elements are consistent with an oxic or post-oxic environment for the Central Oklahoma aquifer.

Nitrate [nitrogen(V)] plus nitrite [nitrogen(III)] concentrations were greater than the minimum reporting level (usually 0.1 mg/L as N) in 193 of 224 samples in the set. Nitrite concentrations were small relative to nitrate concentrations in all cases. The presence of nitrate indicates oxic or post-oxic redox conditions (fig. 12).

Ammonium [nitrogen(–III)] concentrations were greater than the minimum reporting level (usually 0.01 mg/L as N) in 111 of 222 samples. Seventy-five of these samples also had dissolved oxygen greater than 1 mg/L. The presence of ammonium (post-oxic) and dissolved oxygen (oxic) must be a disequilibrium phenomenon, as shown in figure 12. Nitrate plus nitrite and ammonium are both detectable in 88 samples. The simultaneous presence of these two redox states of nitrogen indicates that ammonium oxidation or nitrate reduction may control the redox environment in parts of the aquifer. In 23 samples, the absence of nitrate plus nitrite coupled with the presence of ammonium indicates post-oxic conditions that are more reducing than conditions where oxygen or nitrate are present.

Large iron concentrations at neutral or higher pH indicate the presence of iron(II) and post-oxic, which approaches sulfidic, redox conditions. In 178 of 226 samples, the iron concentrations were less than or equal to 30 µg/L. Only 15 of 226 samples had iron concentrations greater than 500 µg/L.

Analyses of other redox-active elements also indicate oxic or post-oxic conditions. Chromium(VI), the most oxidized form of chromium in natural waters, was analyzed in 110 of the ground-water samples. Chromium(VI) was less than the minimum reporting level (1 µg/L) in 36 samples; however, dissolved chromium also was less than its minimum reporting level (generally 5 µg/L) in all but two of these samples. In general, if chromium concentrations were measurable, chromium(VI) was the dominant form of chromium in solution. A limited number of samples were analyzed for multiple redox states of arsenic and selenium. The oxidized form of arsenic, arsenic(V), was the dominant form in all of the arsenic analyses. The oxidized form of selenium, selenium(VI), was the dominant form in all of the selenium analyses (Schlottmann and Funkhouser, 1991). The large concentrations of uranium (greater than 10 pCi/L) that are present in some samples indicate the presence of uranium(VI) because uranium(IV) phases are very insoluble. Similarly, large concentrations of vanadium (greater than 10 µg/L) indicate the presence of vanadium(V) because of the low solubility of vanadium(III) minerals. The oxidized form of all of these trace elements indicates oxic or post-oxic conditions (fig. 12).

The ground-water samples of this study were categorized as oxic or post-oxic and the locations of the sites with each redox environment were mapped in figure 13. Assuming sulfidic and methanic redox environments are absent in the Central Oklahoma aquifer, a ground-water sample was categorized as post-oxic if any one of three criteria were met: (1) Dissolved oxygen was less than 1 mg/L, (2) ammonium was greater than the minimum reporting level and nitrite plus nitrate less than the minimum reporting level, or (3) dissolved iron concentration was greater than 500 µg/L. All other samples were categorized as oxic because they contained oxygen concentrations greater than 1 mg/L. These criteria may underestimate the number of wells with post-oxic conditions if dissolved oxygen concentrations are greater than 1 mg/L because of sampling contamination.

A total of 53 samples from 49 sites indicated post-oxic conditions (fig. 13). The sites are distributed among the geologic units as follows: 23 sites have wells in the alluvium and terrace deposits; 12 sites have wells in or near the outcrop of the Chase, Council Grove, and Admire Groups; 6 sites have wells that penetrate the Hennessey Group to draw water from the Garber Sandstone; 6 sites have wells in the outcrop of the Garber Sandstone; and 2 sites have wells in the Hennessey Group. Two of the sites with wells in the outcrop of Garber Sandstone were test holes that were sampled at multiple depths. At these two sites, only the deepest samples had post-oxic redox conditions.

Petrographic data are consistent with the water-chemistry data, which indicate a predominantly oxic and post-oxic environment in the aquifer. Ferric-oxyhydroxide minerals, hematite and goethite, are ubiqui-

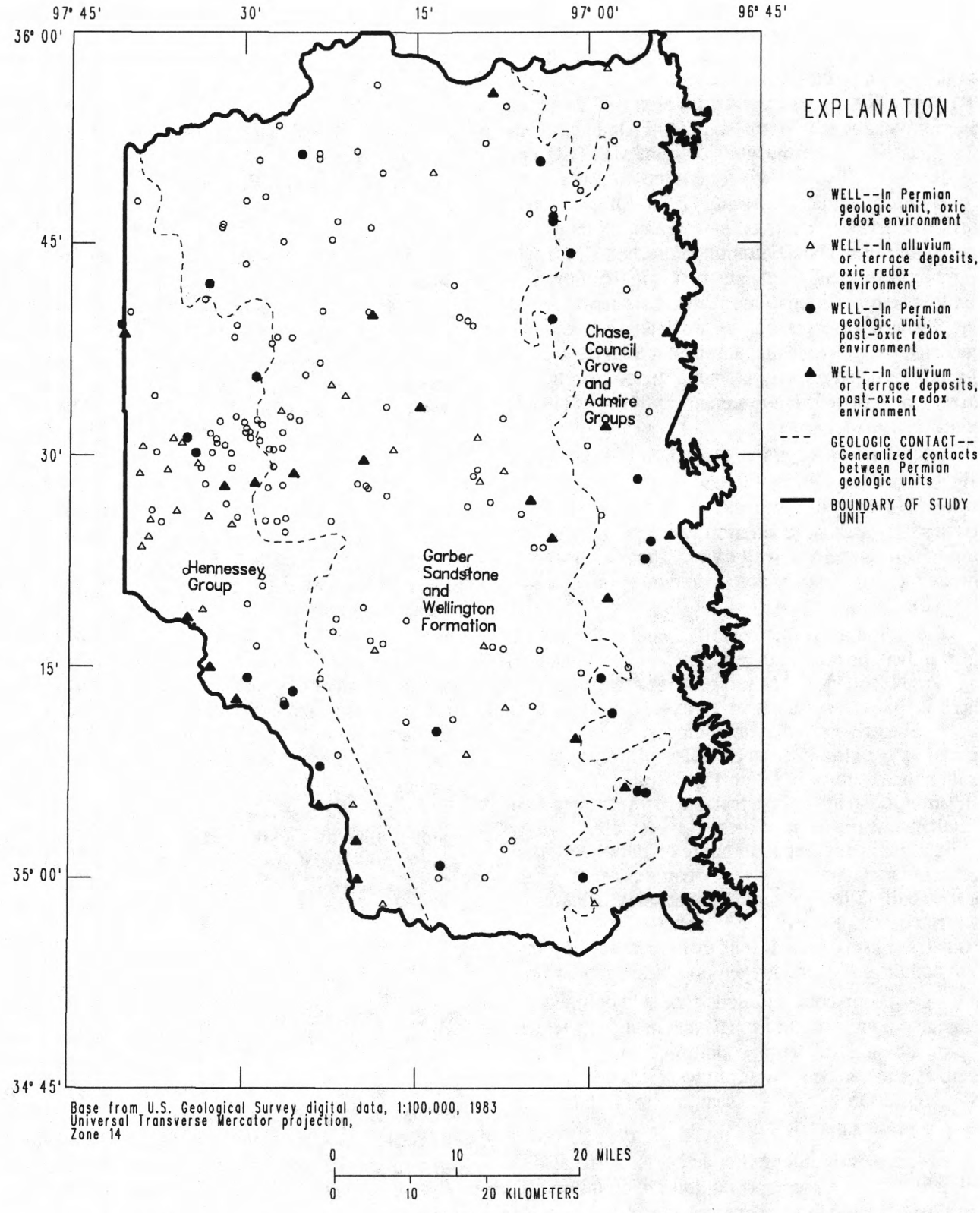

Figure 13. Locations of wells with samples that indicate oxic and post-oxic redox environments.

tous, and manganese oxides are common. Organic matter is almost completely absent from the core materials obtained from the aquifer. Pyrite is very rare, and the one pyrite grain that was identified was substantially oxidized to goethite. Some phases formed in reducing environments (sulfidic or methanic), for example selenium(-II) and vanadium(III) phases, have been identified. However, these phases persist in very small zones (less than 1.0 cm in diameter) and commonly are surrounded with minerals that are oxidation products of the reduced phases (see discussion in the section on geochemical reactants).

In summary, ground-water samples and petrographic data indicate the Central Oklahoma aquifer has an oxic or post-oxic redox environment. The most important redox-active species in the ground water are dissolved oxygen and nitrate. Most parts of the Central Oklahoma aquifer have oxic conditions. Post-oxic conditions are present most commonly in the alluvium and terrace deposits and in or near the Chase, Council Grove, and Admire Groups. Post-oxic conditions in the Garber Sandstone occur most commonly where the unit is confined by the Hennessey Group and in the deeper parts of the flow system where the unit is unconfined.

Sources of Water

The two major sources of the water in the aquifer are recharge from rainwater (see discussion in the Geohydrology section) and very ancient waters derived from seawater. Most of the water in the aquifer is derived from rainwater that recharges through the outcrop areas of the Garber Sandstone, Wellington Formation, and the Chase, Council Grove, and Admire Groups. However, below the base of fresh ground water are brines, and it is assumed that these brines once filled all of the geologic units that make up the study unit. Some water presently in the study unit may be derived from the flow or dispersion of these brines from depth. Some relict brines also may enter the flow system from fluid inclusions or dead-end pore spaces within the study unit.

Recharge

The source of most of the water in the Central Oklahoma aquifer is rainwater that recharges the aquifer through the outcrop areas. Evapotranspiration could concentrate the constituents of rainwater many fold before the water enters the saturated zone. To determine whether rainwater is a major source of the chemical constituents in ground water, the composition of rainwater and the estimated composition of rainwater after evapotranspiration were compared to the composition of recharge water.

Data on the chemical composition of rainwater were obtained from the National Atmospheric Deposition Program (NADP) (National Atmospheric Deposition Program, 1986, is a summary report for 1986.) for a site a few miles southwest of the study unit, Great Plains Apiaries (latitude 34°58′48″, longitude 97°31′16″, NADP site code 371740). The data included 92 samples that were collected from April 1983 through January 1987. The suite of constituents analyzed included calcium, magnesium, potassium, sodium, chloride, sulfate, ammonium, and nitrate. The volume-weighted concentrations (in milligrams per liter) of chemical constituents over the period of record are listed in table 2. A rough estimate of the potential concentration factor due to evapotranspiration was calculated by taking rainfall (about 30 to 35 in/yr), subtracting the runoff (about 4 to 5 in/yr) and dividing by the recharge (about 1 to 2 in/yr) (see "Evapotranspiration" section). These calculations give a range in concentration factor from 13 to 30. The concentration that would result from a twentyfold concentration of rainwater by evapotranspiration (assuming that water, but no solutes are removed by the evapotranspiration process) is listed in table 2.

The final column in table 2 is the median concentration of 32 water samples that are assumed to represent recent recharge. These 32 samples had tritium concentrations of 30 pCi/L or more, which indicates that these ground waters are less than about 40 years old. Thus, rainwater chemistry is being compared to ground water that is derived from recent rainwater but may have undergone geochemical reactions for about 40 years or less.

Concentrations of chemical constituents in rainwater are very small relative to concentrations in recharge water; thus, rainwater cannot be an important source of chemical constituents unless evapotranspiration concentrates the constituents. Concentrations after a twentyfold concentration indicate that rainwater could account for 70 percent or more of the median concentrations of potassium, sulfate, phosphate, and nitrogen species in recharge waters. However, rainwater could be a major source of these chemical constituents only if they were concentrated substantially by evapotranspiration, and were not removed by biological processes. If the effective concentration factor were fivefold instead of twentyfold, rainwater could not be an important source of any constituents except the nitrogen species. Alkalinity analyses are not included in the NADP data, but the relatively low pH

Table 2. Compositions of rainwater and recharge waters

[All data are in milligrams per liter. Samples assumed to be recharge waters were from wells completed in the Permian geologic units and had tritium concentrations greater than or equal to 30 picocuries per liter]

Constituent	Concentration in rainwater	Twentyfold concentration of rainwater	Median concentration of recharge waters
Calcium (as Ca)	0.384	7.68	60
Magnesium (as Mg)	.043	.87	25
Potassium (as K)	.036	.71	1.0
Sodium (as Na)	.141	2.82	35.5
Alkalinity (as $CaCO_3$)	(a)	(a)	231
Chloride (as Cl)	.236	4.74	33.5
Sulfate (as SO_4)	1.30	26.0	26.5
Phosphate (as P)	.0003	.006	.01
Ammonium (as N)	.208	4.16	.015
Nitrate (as N)	.237	4.74	2.9[b]

[a] Alkalinity data were not reported.

[b] Combined analysis of nitrite and nitrate species.

values of the samples (volume weighted pH is 4.8), indicate that alkalinity concentrations must be small even after concentration by evapotranspiration. The data (table 2) indicate that most of the calcium, magnesium, sodium, and chloride in recharge water is derived from sources other than rainwater. Rainwater is not a major source of these constituents even if the effective concentration factor is greater than twentyfold.

Evapotranspiration can be divided conceptually into two components, the physical process of evaporation and the biological processes associated with plants. The physical process of evaporation leaves a signature in the δD (deuterium measurement relative to standard mean ocean water, SMOW) and $\delta^{18}O$ (oxygen-18 measurement relative to SMOW) composition of a water mass. However, the effects of evaporation are not readily apparent in the δD and $\delta^{18}O$ data of this study (fig. 14). The isotopic composition of meteoric water is described by the equation $\delta D = 8\delta^{18}O + d$, where δD and $\delta^{18}O$ are in per mil and d is a constant. The mean global value for d is 10 per mil (Craig, 1961). The resistant line (a regression based on median rather than mean values) with slope 8 that best fits the data has a d value of 12.1 per mil. Several of the water samples with $\delta^{18}O$ concentrations greater than about -5.5 per mil are below this line, which is the tendency expected from evaporation or from mixing with water that has a different isotopic composition. Thus, the samples below the line may be an indication of evaporation affecting the isotopic composition. However, only a few of the data points are outside the range of scatter evident in samples that have $\delta^{18}O$ values less than -5.5 per mil. Of the six points that are farthest below the line, four were from test holes where there was potential contamination of samples by drilling fluid. It is concluded that most of the observations can be explained as water derived from a meteoric source with little alteration of the isotopic signature by evaporation.

In summary, the δD and $\delta^{18}O$ data indicate that rainwater that recharges the aquifer is not concentrated substantially by the physical process of evaporation. Evapotranspiration through biological processes could substantially concentrate solutes in recharge water. (To be consistent with the observations, these processes must not alter the isotopic signature of the recharge water.) Rainwater could be a major source of potassium, sulfate, phosphate, or nitrate species in recharge water only if evapotranspiration concentrates these species by about a factor of 10 greater than rainwater concentrations. Rainwater is not a major source of calcium, magnesium, sodium, alkalinity, and chloride in recharge water whether or not evapotranspiration concentrates these species.

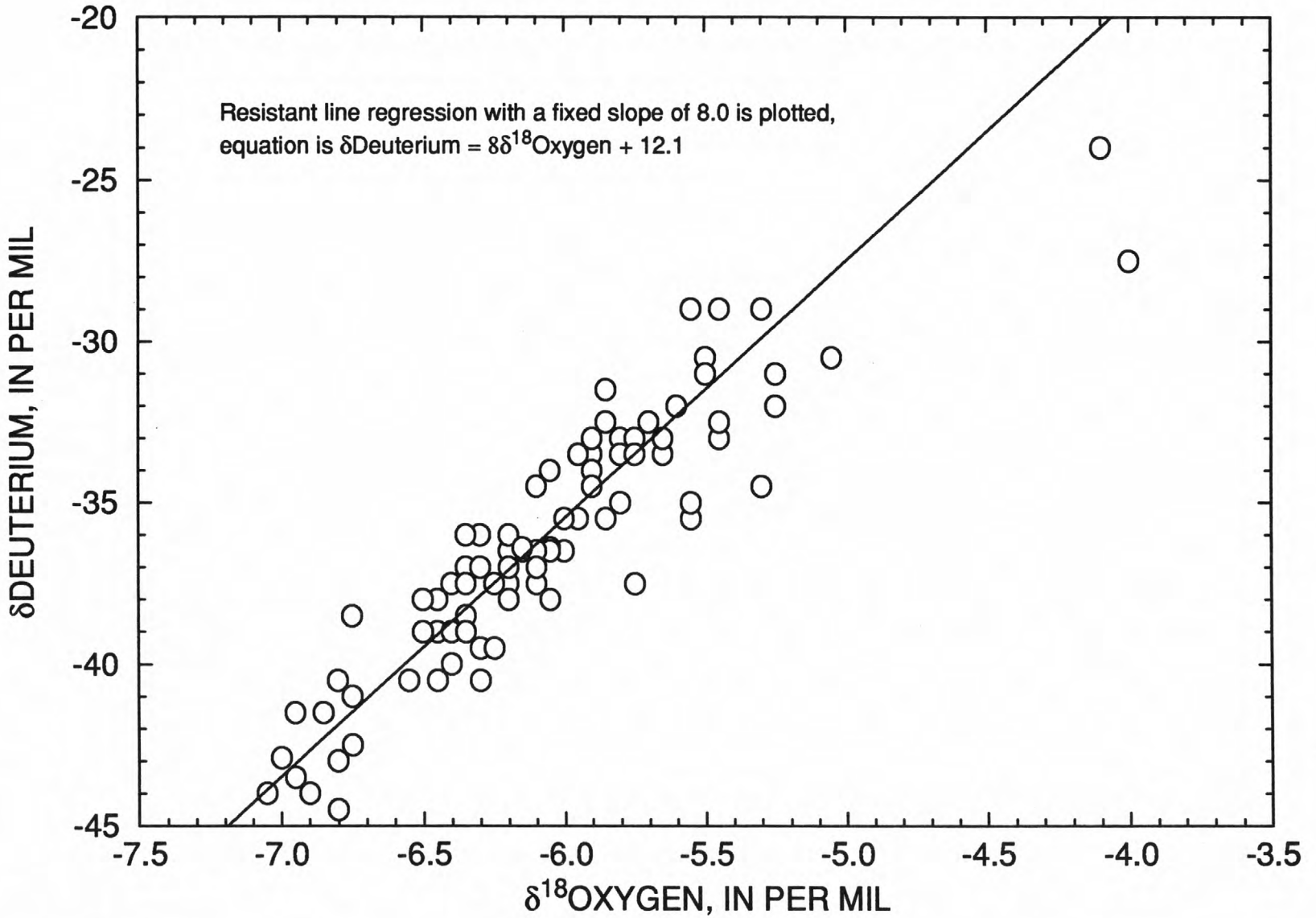

Figure 14. Relation between δDeuterium and δ^{18}Oxygen for water samples from the Central Oklahoma aquifer.

Brines

Chloride concentrations in the Central Oklahoma aquifer tend to be relatively small (median concentration 24 mg/L, table 1). However, underlying the base of the fresh ground water are sodium chloride brines that have chloride concentrations as large as 240,000 mg/L (Wright and others, 1957). These brines or remnants of these brines can affect the chemical composition of the freshwater. At the base of the freshwater flow system is a transition zone where freshwater and brines are mixed by diffusion or dispersion. In addition, some relict brines may be released slowly to ground water from dead-end pores or fluid inclusions within the freshwater flow system. This section examines brine compositions in the geologic units underlying the Central Oklahoma aquifer. Subsequently, the brines discussed here will be used in mass-balance modeling of the chemical evolution of ground-water within the aquifer.

Selected chemical analyses of brines from Wright and others (1957) and data from other sources were tabulated by Parkhurst and Christenson (1987). Analyses of 511 samples from wells completed in the study area were obtained from computer records of the Parkhurst and Christenson (1987) study. The analyses with chloride concentrations greater than 0.1 molar were sorted on chloride, smoothed with a 21-point running median, and plotted in figure 15. The smoothed data eliminate most of the scatter and show some basic trends in the brine data. Sodium is the dominant cation in these waters. At the largest chloride concentrations, calcium concentrations are about a factor of 10 less than sodium, and magnesium concentrations are about a factor of 3 less than calcium. Concentrations of sulfate and alkalinity are generally at least a factor of 20 smaller than chloride, for the data plotted. However, sulfate concentrations are extremely variable and range from less than 1 to more than 10 mmol/L throughout the entire range of chloride concentrations.

For each constituent, a dilution curve is plotted in figure 15. The dilution curves show the expected concentrations of species if a concentrated brine with the composition of the right-most points on the figure is diluted by a freshwater with the median recharge-water composition listed in table 2. Sodium concentrations are close to the concentrations expected from dilution. Calcium and magnesium concentrations tend to be slightly less than the dilution concentrations at chloride concentrations less than about 3 mol/L. The alkalinity data are variable but generally follow the dilution curve. Sulfate concentrations tend to be greater than the concentrations expected from dilution, which indicates an additional source of sulfate.

Saturation indices for halite and gypsum were calculated for the analyses with chloride concentrations greater than 0.1 mol/L using PHRQPITZ (Plummer and others, 1988). It is assumed that water in contact with halite or gypsum will quickly reach saturation or dissolve all of the available mineral. Halite is near saturation (saturation index of 0.0) only in a few of the most concentrated brines. The paucity of data near halite saturation indicates that halite is not present in the geologic units in sufficient quantities to maintain halite saturation. Gypsum is near saturation in some of the more concentrated brines and occasionally in the less concentrated brines. Thus, gypsum may exist in some geologic units below the Central Oklahoma aquifer.

The bromide to chloride ratio is an important clue to the origin of the brines underlying the aquifer. Brines evolving from seawater by evaporation (solid line on fig. 16) maintain a virtually constant bromide to chloride ratio up to the point of halite precipitation (at the change in slope of the solid line on fig. 16). During halite precipitation, the bromide concentrations increase more rapidly than chloride concentrations (Carpenter, 1978), which results in an increased bromide to chloride ratio. The composition of brines from below the Central Oklahoma aquifer are plotted in figure 16; some data from wells near but outside the study unit also are plotted. The brine data are near the path of seawater evaporation, and many data plot near the point where halite precipitation begins. Processes other than evaporation may have modified the brine compositions, but the data are close enough to the anticipated path to indicate that the brines have evolved from seawater.

Data from the freshwater flow system of the Central Oklahoma aquifer (all samples were from wells less than 1,000 ft deep) also are plotted in figure 16. The dashed line in figure 16 corresponds to the bromide to chloride ratio of seawater. Most samples with chloride concentrations less than 1,000 mg/L plot to the right of the dashed line, which indicates an excess of bromide and a larger bromide to chloride ratio than seawater. The most plausible explanation for the large bromide to chloride ratios is that the bromide and chloride concentrations in the aquifer are derived from a mixture of freshwater and a small quantity of brine that has a bromide to chloride ratio greater than seawater because halite has precipitated.

In summary, brines derived from seawater by evaporation and other processes are present in the geologic units below the Central Oklahoma aquifer. The evaporation proceeded to the point where halite precipitation occurred, which resulted in some bromide to chloride ratios that are greater than the seawater ratio.

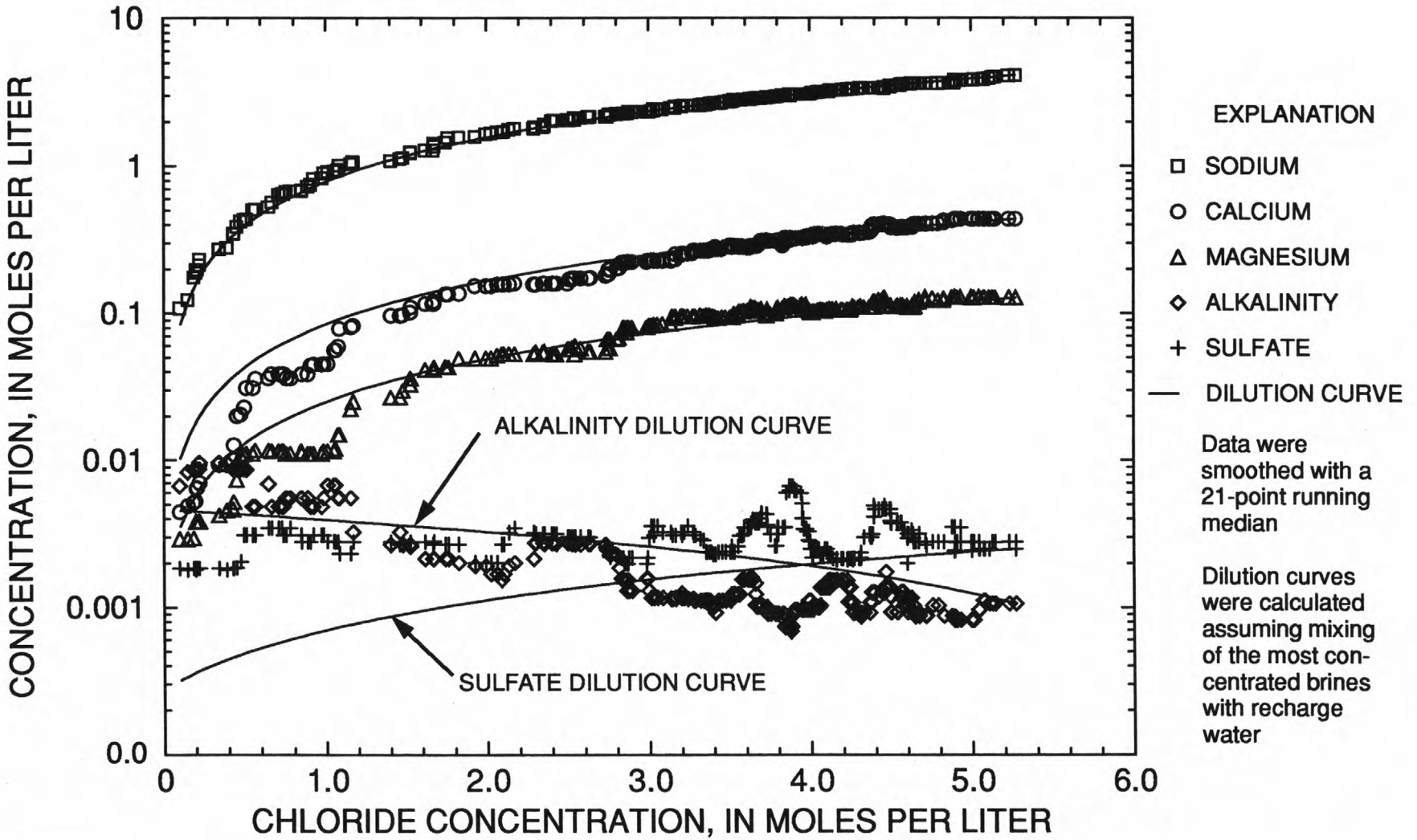

Figure 15. Concentrations of major ions relative to chloride in brines underlying the Central Oklahoma aquifer.

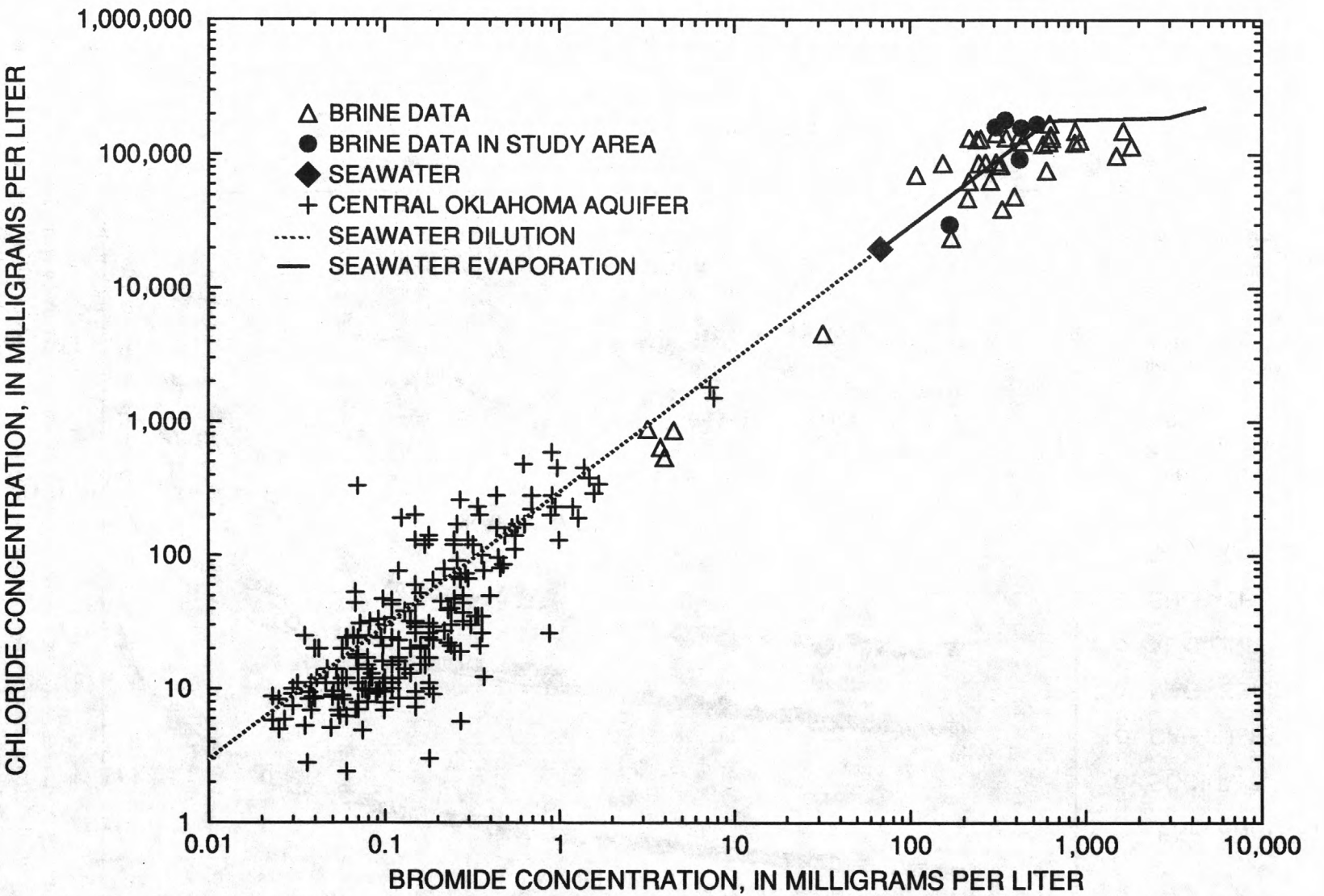

Figure 16. Relation between chloride and bromide in brine samples from geologic units in the vicinity of the Central Oklahoma aquifer and in water samples from the aquifer.

However, halite is not in contact with most of the brines, as indicated by halite saturation indices. Gypsum may be present in a few locations within these geologic units. Dispersive mixing of a freshwater with concentrated brines is sufficient to account for the trends in calcium, magnesium, sodium, chloride, and, perhaps, alkalinity concentrations in the samples from these geologic units below the Central Oklahoma aquifer. Other geochemical reactions, probably the dissolution of locally present gypsum, seem to control the sulfate concentrations in these geologic units. Above these units, in the Central Oklahoma aquifer, the bromide to chloride ratios are generally greater than or equal to the seawater ratio, which is consistent with a seawater-derived-brine source for these two elements within the aquifer.

Geochemical Reactants

Variations in the composition of ground water result from reactions with the minerals and gases that the water contacts. This section discusses the minerals present in the Central Oklahoma aquifer and identifies, where possible, whether these minerals are dissolving or precipitating. Several lines of evidence are used to identify the reactive minerals in the system, including: (1) petrographic and mineralogic observations of aquifer material obtained from cores, (2) stable isotope compositions of carbonate minerals, and (3) saturation indices calculated from the chemical compositions of ground-water samples. The information about the reactive minerals will be used to constrain mass-balance models that account for the evolution of water chemistry in the aquifer.

Rock samples from the aquifer were obtained from eight test holes that were cored as part of the NAWQA study (Schlottmann and Funkhouser, 1991). The widely spaced test holes (fig. 17) intersected the Hennessey Group (test hole 7), the Wellington Formation (test hole 4), the Garber Sandstone (test holes 1a, 3, 4, 6, and 7a), and the Chase, Council Grove, and Admire Groups (test holes 2 and 5). Samples from these cores have been analyzed chemically (Mosier and others, 1990) and mineralogically and petrographically (Breit and others, 1990).

Methods

Analytical methods used to identify and describe solid constituents of Permian rocks in the aquifer are listed in Breit and others (1990). The relative quantities of major rock-forming minerals were estimated by using semiquantitative X-ray diffraction. This technique compared the peak areas of samples with areas of standards composed of quartz, albite, illite, chlorite, calcite, dolomite, and hematite. Summary results of these analyses are presented in table 3. Additional compositional data were collected by point counting thin sections of aquifer sandstones for voids and major authigenic constituents (table 4). Optical microscopy and scanning electron microscopy (SEM) were used to define paragenesis, examine mineral surfaces, and evaluate textural variations.

The mineralogy of the clay-sized, <2 μm component was evaluated by X-ray diffraction of oriented mounts. The <0.5 μm fraction also was analyzed for some samples and was determined to contain the same minerals as the <2 μm fraction. The clay-sized fractions were physically separated by centrifugation, and selected samples were saturated with sodium, potassium, or magnesium prior to analysis; saturation with these ions aided in identification of mixed-layer clays. All <2 μm samples were scanned after saturation with ethylene glycol; a few also were scanned after they were treated with glycerol or heated to 425 °C. Cation-exchange capacities of untreated clay-sized separates were evaluated by treatment with 0.1 mol/L $SrCl_2$. The quantities of calcium, magnesium, potassium, and sodium exchanged from the clays was determined by atomic absorption spectrophotometry (table 6).

The $\delta^{13}C$ (carbon-13 measured relative to a standard, which was a belemnite taken from the Late Cretaceous Peedee Formation, referred to as Peedee belemnite or PDB) and $\delta^{18}O$ of petrographically characterized carbonate mineral cements, nodules, and clasts were analyzed according to the timed phosphoric-acid-dissolution procedure of Walters, Claypool and Chouquette (1972) (table 5). This technique separates CO_2 derived from calcite and dolomite by using the relative rates that these minerals react. Precisions for the analyses are estimated to be 0.1 per mil for $\delta^{13}C$ and 0.05 per mil for $\delta^{18}O$.

Saturation indices were calculated for all water samples collected during the study that were analyzed for a complete suite of major ions and pH. The program PHREEQE (Parkhurst, Thorstenson, and Plummer, 1980) was used to calculate the indices using the tabulation of Nordstrom and others (1990) as the primary source of thermodynamic data. Boxplots of saturation indices (fig. 18) were generated for the minerals of interest. In calculating the percentiles used in the boxplots, a single sample was selected to represent each well or each sampling depth of a well in the case of multiply-sampled test holes. The results are pre-

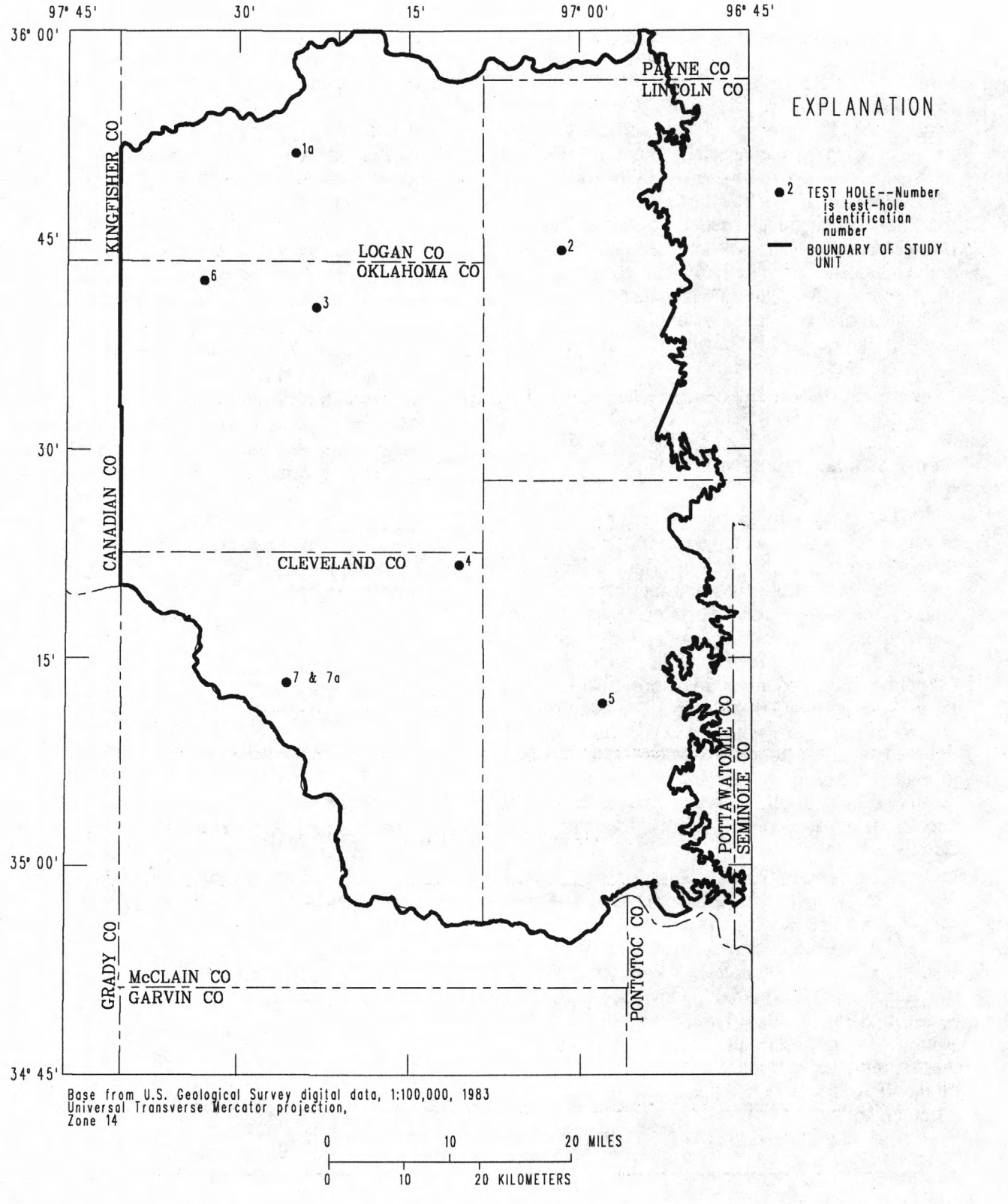

Figure 17. Locations of test holes from which core samples were collected to characterize the mineralogy and petrography of the Central Oklahoma aquifer.

Table 3. Average abundances of minerals in test-hole cores estimated by whole-rock X-ray diffraction

[All abundances are presented as weight percent. Samples in which the abundance of a constituent was less than the detection limit were assigned an abundance of 0 weight percent. All data includes sandstones, mudstones, siltstones, conglomerates, and lithologically mixed samples]

AVERAGE OF ALL DATA

Test hole	1a	2	3	4	5	6	7	7a
Quartz	57	46	55	63	49	71	41	69
Plagioclase	2	3	2	0	2	2	5	2
Dolomite	3	2	7	0	2	3	7	2
Calcite	0	0	0	0	0	2	0	0
Kaolinite	5	7	3	4	4	3	2	2
Hematite	4	5	1	6	5	3	2	3
Illite	28	35	30	27	42	18	41	24
Total	99	98	98	100	104	102	98	102
Number of samples	26	21	22	25	21	36	16	29

AVERAGE OF SANDSTONE SAMPLES

Test hole	1a	2	3	4	5	6	7	7a
Quartz	71	72	79	82	68	83	58	78
Plagioclase	3	4	3	0	4	2	8	2
Dolomite	4	1	3	0	1	3	7	2
Calcite	0	0	0	0	0	1	0	0
Kaolinite	5	6	3	4	5	2	2	2
Hematite	3	4	1	2	3	3	2	3
Illite	16	17	9	10	22	8	22	15
Total	102	104	98	98	103	102	99	102
Number of samples	17	8	11	15	11	25	4	21

AVERAGE OF MUDSTONE AND SILTSTONE SAMPLES

Test hole	1a	2	3	4	5	6	7	7a
Quartz	28	26	28	34	25	38	36	39
Plagioclase	1	0	2	0	1	2	4	2
Dolomite	2	1	7	0	1	4	4	2
Calcite	0	0	0	0	0	2	0	0
Kaolinite	4	7	2	4	3	3	1	2
Hematite	5	6	1	8	9	2	3	3
Illite	52	52	57	57	68	53	49	54
Total	92	92	97	102	107	104	97	100
Number of samples	7	9	9	9	7	7	11	5

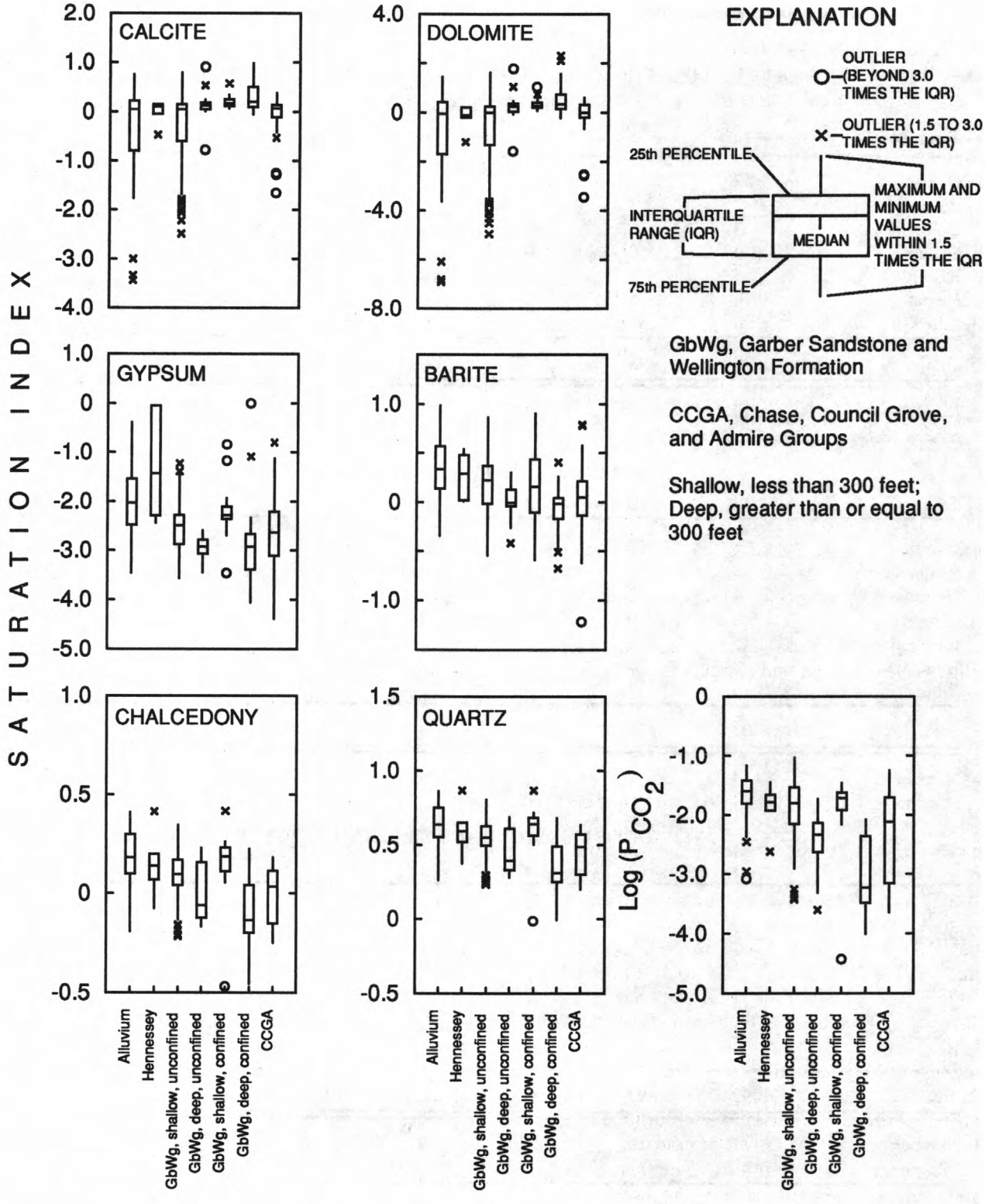

Figure 18. Boxplots of saturation indices for selected minerals calculated for water samples from hydrogeologic units within the Central Oklahoma aquifer study unit.

Table 4. Mean volume abundances of voids and major authigenic components of sandstones determined from point-count data

[Data are presented in volume percent. Values in parentheses are standard deviations, "--" indicates standard deviation not calculated because of insufficient data. No sandstone samples from test-hole 7 were point-counted]

Test-hole number	Voids	Hematite	Kaolinite	Dolomite	Calcite
1a	23 (8)	5 (6)	1 (1)	1 (3)	<1 (--)
2	17 (12)	4 (5)	<1 (--)	1 (2)	<1 (--)
3	22 (11)	5 (6)	<1 (--)	3 (6)	<1 (--)
4	23 (9)	3 (4)	1 (1)	<1 (--)	<1 (--)
5	20 (7)	2 (2)	1 (1)	2 (4)	<1 (--)
6	30 (10)	2 (3)	<1 (--)	5 (9)	1 (2)
7a	21 (13)	2 (3)	<1 (--)	5 (12)	<1 (--)

sented for seven distinct parts of the study unit: (1) Alluvium and terrace deposits; (2) the Hennessey Group; (3) shallow, confined (less than 300 ft), (4) deep, confined (greater than 300 ft), (5) shallow, unconfined (less than 300 ft), and (6) deep, unconfined (greater than 300 ft) parts of the Garber Sandstone and Wellington Formation; and (7) the Chase, Council Grove, and Admire Groups.

Results

Quartz and clay minerals are the major detrital constituents of Permian rocks within the aquifer. Illite-rich clays are the most abundant clay minerals and comprise about 30 percent of the rock sampled. Other detrital phases include minor quantities of plagioclase, potassium feldspar, muscovite, biotite, chlorite, dolostone, chert, metamorphic rock fragments, and trace quantities of heavy minerals. The rock-forming minerals of the Hennessey Group, the Garber Sandstone, the Wellington Formation, and the Chase, Council Grove and Admire Groups are similar, although the relative abundances of the minerals vary slightly among and within these rock units. Most notable among the compositional variations is the lack of chlorite, dolomite, and plagioclase in rocks from test hole 4.

Sandstones in the aquifer are very fine to medium grained and well to poorly sorted. According to the classification scheme of Folk (1980), these rocks are mainly sublitharenites with abundant clay matrix. Total porosity locally exceeds 30 percent, and most detrital grains contact adjacent grains at points or smooth edges, which is consistent with a shallow depth of maximum burial (< 1 mile; Johnson, 1989). The shapes of oversized pores and relict grain boundaries within some sandstones indicate the pores formed by dissolution of detrital and authigenic minerals (fig. 19A).

Recognized authigenic constituents of the aquifer include barite, calcite, dolomite, goethite, hematite, kaolinite, manganese oxides, and quartz overgrowths. These minerals form pore-filling cements and replace or thinly coat detrital grains. Estimates of the relative abundance of the most common authigenic constituents in sandstones are listed in table 4.

Illite, illite-smectite, chlorite, chlorite-smectite, kaolinite, smectite, hematite, and goethite were detected in the clay-sized fraction. No consistent variations in the clay mineralogy were detected between sandstones and mudstones. A few samples from test holes 2, 3, 4, and 5 were distinguished by the large quantities of smectite interlayers with illite (vermiculite/smectite of Breit and others, 1990) and the relatively small contents of chlorite and illitic material. These distinctive clay minerals most likely formed by weathering at the time these Permian sediments were deposited.

Within dispersed green zones in some otherwise red rocks are small accumulations of minerals that are rare within the aquifer. Among the minerals detected are clausthalite (PbSe), native selenium (Se), pyrite (FeS_2), haggite [$V_2O_4(OH)_3$], volborthite ($Cu_3VO_4 \cdot 3H_2O$), and metatyuyamunite [$Ca(UO_2)_2(VO_4)_2 \cdot H_2O$]. These local accumulations, referred to as reduction spots because of the low oxidation state of

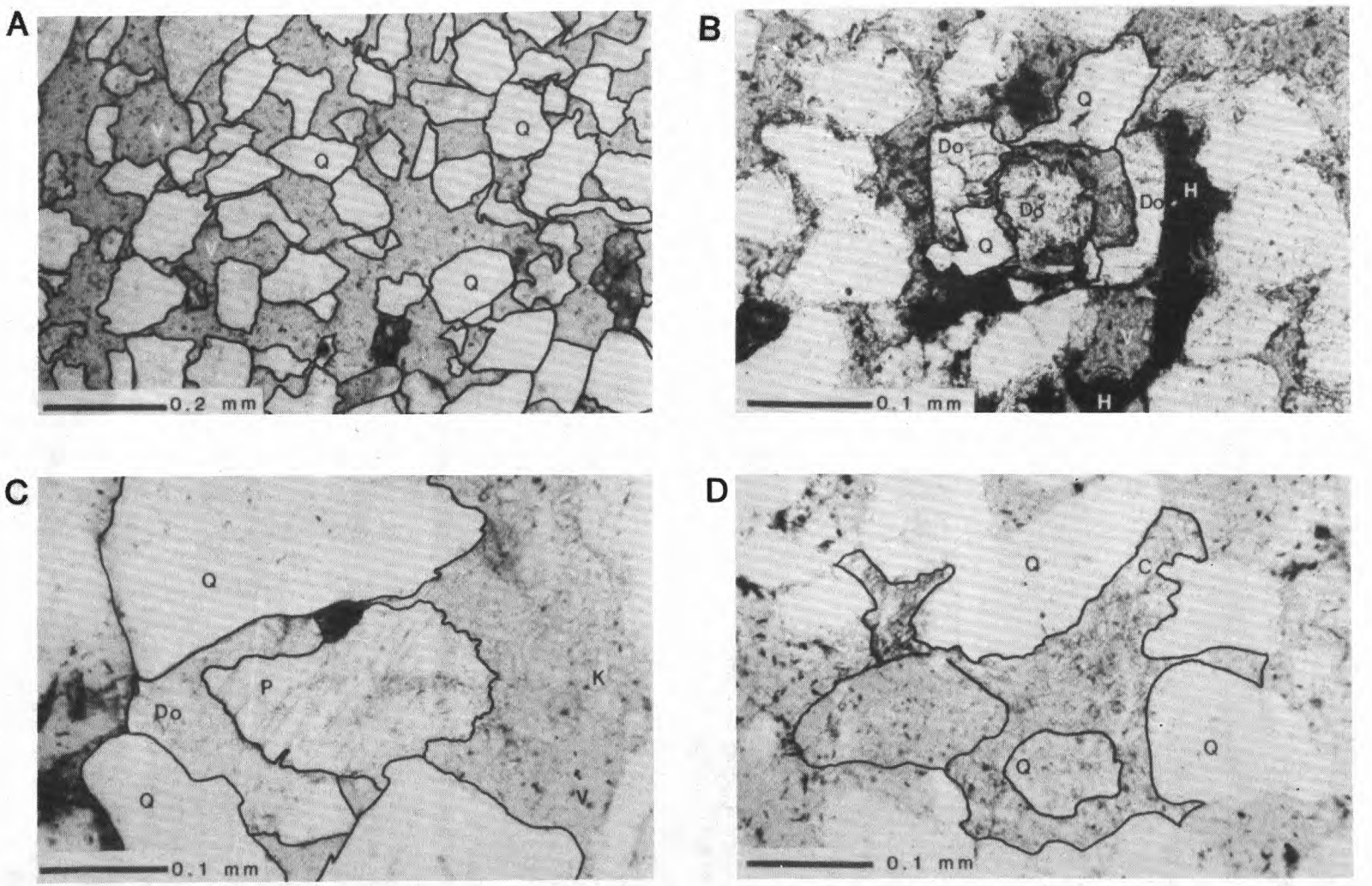

Figure 19. Photomicrographs illustrating textures of minerals in core materials collected from the Central Oklahoma aquifer: ***A.***—Porous sandstone (**Q**, quartz; **V**, void); ***B.***—Dissolution void (**V**) within sparry dolomite (**Do**) (**Q**, quartz; **H**, hematite); ***C.***—Partially dissolved plagioclase (**P**) along twin planes. Kaolinite (**K**) in vermicular books partially fills adjacent void. Dolomite (**Do**) also is partially dissolved (**Q**, quartz; **V** void); and ***D.***—Partially dissolved calcite (**C**) and chert (**Ch**) (**Q**, quartz).

the metals (Hofmann, 1990), were seen in core from most of the test holes.

The aquifer materials are discussed now with special emphasis on determining the reactant and product phases in the present geochemical environment.

Carbon dioxide

The log of the calculated partial pressure of carbon dioxide (pCO_2) ranges from -1.5 to -2.0 for shallow samples. This pCO_2 for ground waters is greater than atmospheric, which is -3.5, but is similar to the pCO_2 in unsaturated soil zones (Drever, 1982, p. 140). Therefore, the pCO_2 in the shallow ground water is consistent with an unsaturated-zone source of carbon dioxide. Values of pCO_2 tend to be -3.0 or less for the deep, confined Garber Sandstone and Wellington Formation and for the Chase, Council Grove and Admire Groups. Values of pCO_2 in the deep unconfined Garber Sandstone and Wellington Formation are intermediate, ranging from -2.0 to -3.0.

Dolomite

Dolomite occurs as micritic nodules and clasts, sparry cements, which are locally poikilotopic, and rare patches of micritic cement. The nodules are as large as 5 cm and typically occur in mudstones and siltstones. Local aggregates of reworked nodules form dolostone conglomerates. Sparry dolomite is common as a sandstone cement, although euhedral dolomite crystals were detected in some mudstones and siltstones. The $\delta^{18}O$ composition of all forms of dolomite are similar (table 5) and in the range expected if dolomite precipitated from seawater.

Textures characteristic of dissolution are typical of dolomite in most sandstones. Physically discontinuous areas of dolomite cement that are visible in thin section are optically continuous and indicate that the intervening voids once were filled with dolomite. Dolomite cement in some samples has well-formed rhombohedral outlines, others are irregular, indicative of embayment by dissolution (fig. 19 B,C; 20 A). Etch pits are detected by SEM on the surfaces of some dolomite cements, but similar cements in other samples have smooth surfaces. The distribution of these con-

Table 5. δ^{13}Carbon and δ^{18}Oxygen of carbonate minerals

[Data units are per mil: $\delta^{18}O$, oxygen-18 measurement relative to SMOW (Standard Mean Ocean Water); $\delta^{13}C$, carbon-13 measurement relative to Peedee belemnite (PDB); na, not analyzed]

Test-hole number	Depth (feet)	Sample description	Calcite		Dolomite	
			$\delta^{13}C$	$\delta^{18}O$	$\delta^{13}C$	$\delta^{18}O$
1a	161.5	Sparry calcite	–8.87	26.17	na	na
1a	211.7	Micritic dolomite nodule	na	na	–8.22	33.95
1a	211.7	Sparry dolomite from nodule	na	na	–9.51	30.95
1a	243.2	Sparry dolomite cement	na	na	–9.22	31.14
2	183.5	Sparry dolomite from clast	na	na	–11.37	31.81
2	240.5	Micritic dolomite clast	na	na	–8.81	31.98
3	113.9	Sparry calcite	–7.84	25.62	na	na
3	123.0	Sparry dolomite	na	na	–8.37	32.30
3	124.0	Sparry dolomite	na	na	–8.46	31.98
3	182.7	Micritic dolomite cement	na	na	–8.60	31.73
4	118.0	Sparry dolomite cement	na	na	–15.76	33.01
5	234.2	Micritic dolomite clasts	na	na	–9.05	31.06
6	124.8	Sparry dolomite and calcite	–8.53	29.62	–9.03	40.39
6	184.2	Sparry calcite cement	–8.14	26.11	na	na
6	494.8	Sparry dolomite cement	na	na	–9.12	31.27
6	560.6	Micritic dolomite clast	na	na	–8.67	31.86
7	59.0	Dolomite cement	na	na	–5.18	31.50
7	94.5	Dolomite cement	na	na	–4.72	31.32
7a	381.0	Sparry dolomite cement	na	na	–8.33	31.73
7a	598.0	Sparry calcite cement	–8.86	25.81	na	na

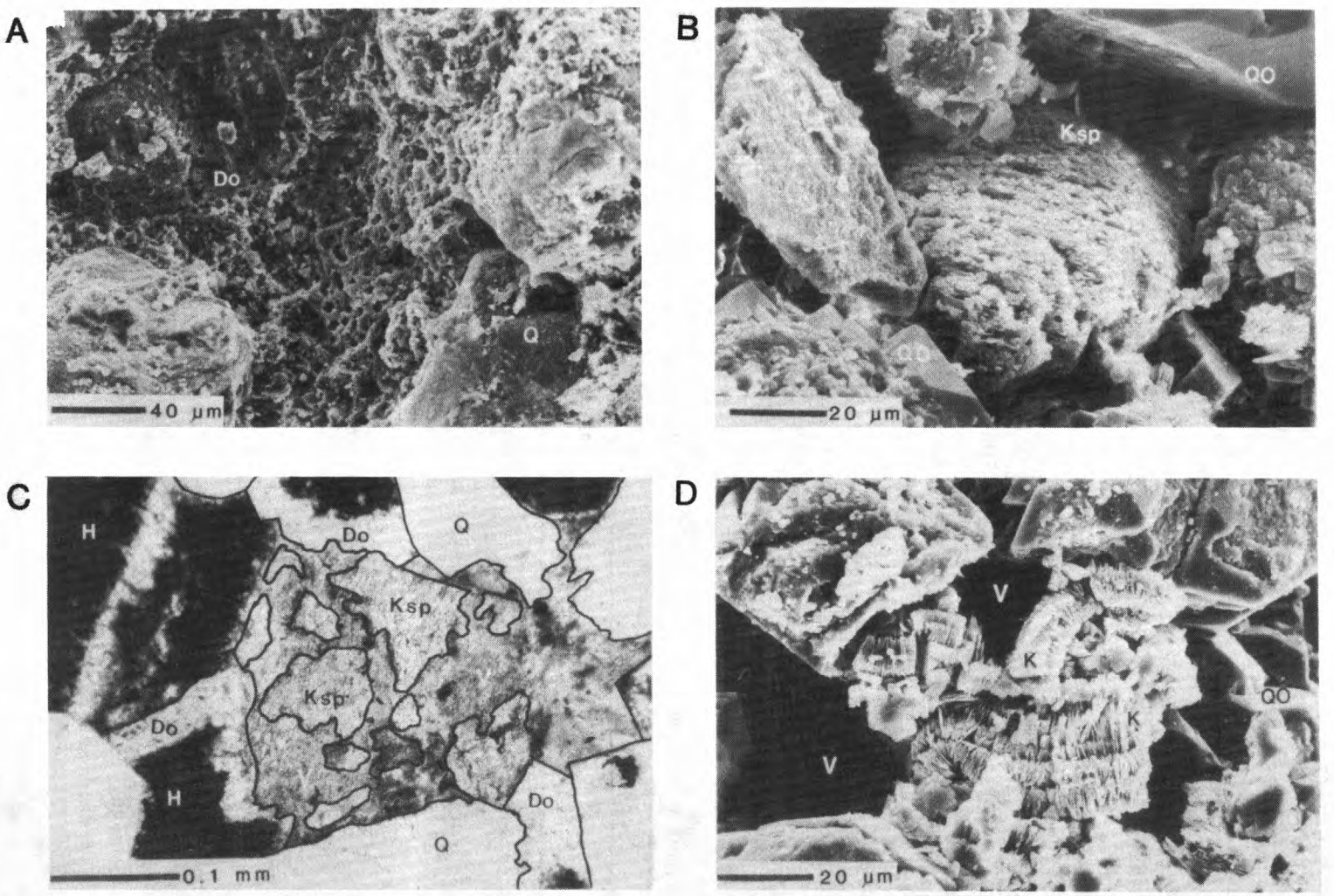

Figure 20. Scanning-electron-microscope micrographs and photomicrographs of dissolution and precipitation textures of minerals in core materials collected from the Central Oklahoma aquifer: ***A.***—Scanning-electron-microscope (SEM) micrograph of pitted and etched dolomite (**Do**) cement (**Q**, quartz); ***B.***—SEM micrograph of partially dissolved potassium feldspar (**Ksp**) (**QO**, quartz overgrowths); ***C.***—Photomicrograph of partially dissolved potassium feldspar (**Ksp**). Pore that contained the feldspar is surrounded by dolomite (**Do**) with inclusions of hematite (**H**); and ***D.***—SEM micrograph of vermicular books of kaolinite that bridge detrital grains (**QO**, quartz overgrowths).

trasting textures among the cores indicates dolomite has dissolved in most shallow samples and in some sandstones from deeper parts of the aquifer.

Saturation indices of dolomite are substantially less than zero in nearly half of the samples from wells in the alluvium and terrace deposits and shallow, unconfined Garber Sandstone and Wellington Formation. Saturation indices for dolomite generally are greater than or equal to zero for samples from the Hennessey Group, the Chase, Council Grove, and Admire Groups, and the deep and confined parts of the Garber Sandstone and Wellington Formation. For those samples that are supersaturated with dolomite, calculated supersaturations could be caused by degassing of carbon dioxide during the sampling process. Alternatively, dissolution of silicate minerals could produce supersaturation of dolomite by increasing pH or increasing the concentration of calcium or magnesium. At supersaturation, dolomite cannot dissolve. For those samples that are near saturation with dolomite, it is thermodynamically possible for dolomite to precipitate; however, precipitation is unlikely at the temperature, pressure, and chemical conditions that currently exist in the aquifer (Drever, 1982, p. 53). Thus, the petrographic data and saturation indices indicate that, in the shallow parts of the aquifer, dolomite is dissolving, but, in the deeper parts of the aquifer, dolomite is either stable or dissolving to a lesser extent.

Calcite

Calcite is a minor cement in sandstones and some mudstones. In sandstones, it fills pores and surrounds detrital sand grains as a poikilotopic cement. If large areas within sandstone are cemented with calcite, the cements have circular outlines in thin section and can contain as many as 50 adjacent detrital grains. Contacts between calcite and dolomite are smooth and do not clearly indicate dedolomitization. However, paragenetic relations with other minerals indicate that calcite formed after most authigenic phases. Calcite cement in shallow samples commonly is embayed and pitted, and optically continuous patches are interrupted by dissolution voids (fig. 19 D).

The $\delta^{13}C$ values of calcite are very similar to values measured for dolomite (table 5) and dissolved carbonate species in modern ground water (table 1). However, the $\delta^{18}O$ values of the calcite are substantially less than those measured for dolomite, which indicates that calcite formed from a water with an $\delta^{18}O$ value different from that from which dolomite formed. Based on the fractionation factor presented in Friedman and O'Neil (1977), the calcite formed from water in which $\delta^{18}O$ ranged from -3 to -4.5 per mil (assuming present temperatures in the aquifer, about 16°C). This value suggests that calcite is not in isotopic equilibrium with modern ground water and probably formed from a different meteoric water.

Saturation indices for calcite are very similar to those for dolomite. Undersaturation is observed commonly in the shallow parts of the study unit, and saturation or supersaturation is observed in the deep and confined parts of the aquifer. Both saturation indices and petrographic data indicate that calcite is dissolving in the shallow part of the aquifer. As with dolomite, supersaturations in the deep and confined parts of the aquifer could be the result of degassing of carbon dioxide as the samples were pumped to the land surface. Unlike dolomite, calcite precipitation in the aquifer is plausible; however textural evidence and isotopic data from the test-hole samples are inconsistent with precipitation. Given the possibility of supersaturations because of degassing of carbon dioxide during sampling, the textural and isotopic evidence indicating calcite is stable or dissolving in the deep and confined parts of the aquifer is considered to be more conclusive.

Authigenic iron oxides

Hematite and goethite are common authigenic minerals in sandstones and mudstones. Rocks stained and cemented by iron oxides have complex geometries and variations in color that resulted from redistribution of iron. These variations include dark purple rims of hematite that surround burrows, pseudo-rhombic aggregates of hematite within sparry dolomite, Liesegang bands, disseminated purple pore fillings, and dark red zones between the contacts of red and green rock. The textures are mainly the result of conditions during deposition and burial of the Permian rocks; however some textures may reflect modern alteration.

Hematite within the aquifer is present in a range of concentrations and grain sizes, which is consistent with the color variations of the aquifer material. It is absent in green sandstones and mudstones, but concentrations as large as 20 weight percent were detected in one conglomerate (Breit and others, 1990). The pervasive red color of sandstones and mudstones is the result of submicroscopic disseminated hematite. In contrast, dark purple rocks contain hematite plates tens of micrometers long that commonly form spherical aggregates. Intergrown plates as thick as several micrometers are particularly common adjacent to burrows and root traces.

Goethite is abundant locally, particularly in yellow-brown sandstones. Mudstone clasts in some con-

glomerates also are rimmed by yellow-brown iron oxides composed at least partly of goethite. Sandstones with large contents of yellow-brown iron oxides notably are void of carbonate cements. Several clay-sized separates contain detectable goethite in rocks that are pervasively red. This indicates that goethite is common but in such low concentrations that it is not readily visible within some red parts of the aquifer. Goethite in sandstones is one of the youngest authigenic minerals of the aquifer. It typically coats other authigenic minerals including kaolinite, and forms radiating acicular overgrowths on hematite. Saturation indices for goethite and hematite cannot be calculated because of the inability to determine the ferric iron concentrations from the available data. However, the relatively oxidizing conditions of the ground water and leaching of iron from altering silicate minerals are consistent with petrographic observations that indicate iron oxides are forming within the aquifer.

Manganese oxides

Manganese oxides form black, sooty, dendrites; pore-filling cement; and box-work relicts after dolomite. X-ray diffraction analysis identified todorokite and romanechite in manganese oxide cement from an outcrop siltstone; other manganese oxide minerals may be present in other samples. Some of the manganese oxides form by oxidation of manganese released during the dissolution of dolomite. Chemical analyses of dolomite nodules measured manganese concentrations of nearly 1 weight percent. The generally oxidizing conditions in the ground water are consistent with the precipitation of manganese oxides. Saturation indices for manganese oxides were not calculated because of the inability to define precisely the redox conditions at specific sample sites.

Barite

Barite was seen in three test-hole samples as elongate, clear prisms and pore-filling cement. Although rock in the aquifer is known for barite roses (Ham and Merritt, 1944), no massive barite cement, which is characteristic of the roses, was detected in the test-hole cores. Sulfur-isotope analyses of two barite roses collected from outcrop have $\delta^{34}S$ values that range from +12.8 to +16.9 per mil relative to a standard, which is an iron sulfide mineral from a meteorite, referred to as Canon Diablo troilite or CDT. These values are much larger than the $\delta^{34}S$ of dissolved sulfate in the ground water (table 1). Although barite saturation indices are consistently slightly greater than zero, indicating saturation or supersaturation, the sulfur isotope composition of exposed barite roses suggests they did not precipitate from modern ground water.

Gypsum

Gypsum was not detected by X-ray diffraction or optical microscopy in any of the samples. Although not detected within our sample set, beds of gypsum have been reported in the Hennessey Group within the study unit (D.D. Conway, written commun., 1991). Saturation indices indicate that gypsum is undersaturated in nearly all samples, which is consistent with the absence of gypsum in most of the aquifer. However, one sample in the deep, confined Garber Sandstone and Wellington Formation and two samples from the Hennessey Group are near saturation. Celestite ($SrSO_4$) saturation indices are similar to gypsum saturation indices.

Pyrite is another possible source of dissolved sulfate, but it is only a rare constituent of Permian rocks in the aquifer and does not appear to contribute a large quantity of sulfate. In reactions occurring in the saturated zone, the quantity of pyrite that can be oxidized to form sulfate is limited by the quantity of dissolved oxygen in ground water. If all of the oxygen in a typical ground water from the aquifer is used to oxidize pyrite, less than 15 mg/L of sulfate is produced before all of the oxygen is consumed. In addition, the sulfur isotopic composition of ground water is uniformly greater than 0 per mil, which is heavier than the composition that is expected from dissolution of sulfide minerals in most sedimentary rocks.

Feldspars

Detrital grains of sodic plagioclase, orthoclase, and microcline were detected in all test holes. Feldspars are best preserved in rocks with an abundant clay matrix. In contrast, feldspars in sandstones are partially to extensively dissolved (fig. 19 C; 20 B and C); only discontinuous relicts of the original grains remain. Dissolution of plagioclase is particularly notable in samples from test hole 4, which contain only skeletal remnants. A few grains of potassium feldspar are surrounded and embayed by dolomite. This texture indicates that some feldspar dissolution predates or is contemporaneous with precipitation of dolomite cement. Other feldspar grains dissolved subsequent to precipitation of carbonate and iron oxide cements. Saturation indices for feldspars and other aluminosilicates could not be evaluated because dissolved aluminum concentrations were rarely greater than the minimum

reporting levels. Multiple episodes of feldspar dissolution are indicated by the petrographic textures, some of which are consistent with modern dissolution.

Quartz

Approximately 60 percent of the framework grains in the aquifer are detrital quartz. Irregular grain outlines, consistent with replacement, are common to quartz grains surrounded by some hematite, manganese oxide, or dolomite cements. In contrast, small, incipient quartz overgrowths are locally common (fig. 20 B,D), although large overgrowths are rare. The overgrowths are common in sandstones with large areas of void space and on grains cemented with calcite. These overgrowths occlude plates of hematite and commonly occur beneath vermicular books of kaolinite. Faces and edges of the overgrowths are smooth and sharp. The saturation indices indicate quartz is supersaturated in nearly all water samples. The supersaturation and the euhedral outline of quartz overgrowths are consistent with precipitation of quartz within the aquifer.

Detrital grains of chert were detected in several samples. The grains have been partially dissolved, and only ghost remnants of the original grains remain. These relict grains typically are marked by cross cutting quartz veinlets and rims of quartz. Voids generated by the partial dissolution of chert grains have not been replaced by authigenic minerals, which indicates that some of the dissolution is recent. Saturation indices for chalcedony were used as an estimate of the stability of the chert. Chalcedony generally is supersaturated within the aquifer except in some deep ground-water samples. The chemical composition of the ground water and petrographic textures suggest that chert is dissolving within parts of the aquifer.

Kaolinite

Kaolinite occurs as large (>100 μm in width) vermicular books that cross voids (fig. 19 C; 20 D), as random, finer grained pore-filling aggregates, and intermixed with other clays in siltstones and mudstones. Kaolinite is a minor component of many mudstones and siltstones, which indicates that some kaolinite was detrital or formed soon after deposition of the Permian sediments. The delicate textures of kaolinite in sandstones indicate it is authigenic. Some sandstone voids that contain vermicular kaolinite have dust rims that suggest that the voids formed by dissolution of a detrital grain and that kaolinite is a replacement phase. Although kaolinite is common near dissolved feldspar grains, it rarely occurs within the original boundaries of those grains. Overgrowths of other clay minerals on kaolinite are absent. Angles and faces of the kaolinite in sandstones are clean and sharp (fig. 20 D). The euhedral shape of the vermicular kaolinite books and the association with quartz overgrowths indicate kaolinite is stable and may precipitate from modern ground water.

Chlorite

Delicate textures indicative of authigenic chlorite were not detected by SEM or optical microscopy. Therefore all chlorite in the aquifer is considered detrital. A few grains, as large as 200 μm, of metamorphic chlorite were detected, which suggests that some finer grained chlorite may be the result of abrasion. Chlorite is estimated to constitute 10 percent of the clay-sized fraction in most rocks. Precise estimates of the relative clay abundance were not possible because of interferences from other clay minerals in the X-ray diffraction results. Chlorite-smectite also was detected in several sample and may have formed by the alteration of chlorite.

Chlorite is absent in most samples from test hole 4 and in the upper portion of test hole 3. In test hole 4, the small quantities of chlorite and the apparent removal of plagioclase and dolomite is consistent with more extensive dissolution of these unstable constituents at this location relative to similar rocks elsewhere in the aquifer. Although the timing of the removal of these minerals is not tightly constrained, dissolution of these minerals is consistent with the compositions of water samples from these test holes.

Illite-smectite/illite

Most of the clay-sized fraction of the core material is composed of a mixture of illite, illite-smectite, and abraded muscovite. These minerals are grouped together because they are part of a continuum that has muscovite and smectite as the two end members. The quantity of smectite in most illite-smectite is approximately 30 percent as estimated by the techniques of Srodon (1984). This estimate of the amount smectite interlayers is approximate because of interferences from other clay minerals. All illite-smectite examined by SEM lacks delicate textures indicative of authigenesis. The stability of the clay could not be readily assessed on the basis of textures. However, the reported stability of illite (Reichenbach and Rich, 1975) in sedimentary rocks and weathering environments suggests that it is unreactive relative to other minerals in the aquifer.

Micas and rock fragments

Sand-sized grains of mica and rock fragments are minor detrital constituents of the aquifer, and all have been partially to extensively altered. Muscovite grains typically have frayed terminations that in a few samples have optical characteristics of vermiculite. Biotite typically has thick rims of iron oxides that obscure most of the grain. Metamorphic fragments of schist and phyllite have dissolved partially along foliations. Minor shale fragments typically are green in thin section and have thick iron oxide rims, analogous to those on biotite.

Cation-exchange capacity

The large quantity of expandable clays within the aquifer led to an assessment of the cation-exchange capacity of the rocks. Clay-sized separates were analyzed to determine the relative quantities of calcium, magnesium, potassium, and sodium that are bound in exchangeable sites. Most cation-exchange capacities (CEC) ranged from 20 to 50 meq/100 g (milliequivalents per 100 grams) of clay (table 6). The average abundance of clay in the test holes is about 30 percent, therefore the CEC for the aquifer ranges from about 6 to 20 meq/100 g of rock. The relative quantities of exchangeable calcium, sodium, and magnesium varies

Table 6. Results of cation-exchange determinations of clay-sized core material

[Element abundances are expressed as milliequivalents per 100 grams of sample. All samples <2 micrometers. Na, sodium; K, potassium; Ca, calcium, Mg, magnesium; Sr, strontium. Total is the sum of exchangeable ions. Strontium recovered refers to the quantity of strontium exchanged with other ions during the cation exchange procedure. The quantity of strontium recovered should approximately equal the total of the exchanged ions if ion exchange were the only source of measured sodium, potassium, magnesium, and calcium]

Test-hole Number	Depth (feet)	Lithology	Na	K	Ca	Mg	Total	Sr recovered
1a	33.4	Sandstone	0.2	2.0	23	14	39	36
1a	196.1-202	Mudstone	9.7	2.8	20	15	48	46
1a	212.9-234.5	Sandstone	2.4	1.3	21	7.0	32	25
1a	259.1-268	Sandstone	1.8	1.6	16	10	29	26
2	99.5-106.5	Sandstone	4.4	2.1	14	9.2	30	27
3	136.0-141	Mudstone	4.7	3.1	40	40	88	86
3	183.2-190.0	Sandstone	2.1	2.0	17	15	36	33
4	152.3-157.5	Sandstone	.1	2.3	19	19	40	33
4	227.8-240.3	Claystone	.1	2.3	18	16	37	37
5	21.9-23	Sandstone	.33	2.6	11	20	34	30
5	126.0-130	Mudstone	21.	2.0	14	8.0	44	38
5	189.0-194	Sandstone	.8	1.4	17	13	31	29
6	320.0-325	Sandstone	.3	1.0	19	15	35	33
6	573.0-585.7	Sandstone	2.8	1.1	17	6.8	27	28
7	52.7-54.5	Siltstone	3.6	1.4	19	16	40	29
7	170.0-179.9	Mudstone+siltstone	1.3	1.6	20	14	37	29
7a	381.1-394.6	Mudstone	4.5	1.8	16	11	33	35
7a	599.0-600.3	Sandstone	.3	1.6	12	7.6	22	29

among the samples analyzed. Calcium and magnesium combined are the dominant exchangeable cations in nearly all of the samples. Clay samples from mudstones had the largest concentrations of exchangeable sodium (4.5 to 21.0 meq/100 g), and sodium accounted for as much as 50 percent of the exchangeable cations in these samples. Clay samples from sandstones had smaller concentrations of exchangeable sodium (0.1 to 4.4 meq/100 g) than mudstones. Exchangeable sodium frequently was less than 1 percent of the exchangeable cations in sandstone samples from the shallow parts of the aquifer; exchangeable sodium tended to be greater in sandstone samples from the deeper parts of the aquifer. Concentrations of exchangeable potassium were relatively small and constant for the clay samples that were analyzed.

Conclusions

Etch pits, dissolution voids, variations in the relative abundances of minerals, and saturation indices indicate that dolomite, calcite, sodic plagioclase, potassium feldspars, chlorite, rock fragments, and micas are dissolving within parts of the aquifer. Euhedral, smooth-faced kaolinite and quartz overgrowths are consistent with the reprecipitation of aluminum and silica derived from dissolving aluminosilicate minerals. Although some water samples from deep within the aquifer have saturation indices that indicate dolomite and calcite should precipitate, precipitation does not seem to occur. Precipitation of dolomite from freshwater at low temperatures is rare, and textural and isotopic data are inconsistent with substantial calcite precipitation. As much as 30 percent of the aquifer material is clay minerals. The composition of exchangeable cations bound to clay minerals varies within the aquifer, which indicates that cation exchange reactions are occurring. Calcium and magnesium are the dominant exchangeable cations in the clay minerals. Exchangeable sodium is most abundant in mudstones. Sandstones from the deeper parts of the aquifer tend to have greater concentrations of exchangeable sodium than sandstones from the shallow parts of the aquifer. Although most water samples are saturated with barite, relatively little barite was detected during examination of the rocks. Gypsum is present locally within the study unit and may be the source of large concentrations of sulfate in some ground waters. Iron and manganese are being leached from unstable silicates and carbonates; the iron precipitates as goethite, and possibly hematite; and the manganese precipitates as manganese oxides.

Geochemical Modeling

Geochemical mass-balance and geochemical reaction-path modeling (henceforth referred to as mass-balance and reaction-path modeling) were used to determine geochemical reactions that account quantitatively for the observed water chemistry within the aquifer. A mass-balance model is a set of minerals that, when dissolved or precipitated in specified quantities, accounts for the change in composition between two ground waters. The quantities of minerals dissolved and precipitated are referred to as mass transfers. The primary assumptions of mass-balance modeling are that the two water compositions are representative of waters along a single flow path and that the final water composition evolved from the initial water composition. Plausible mass-balance models account for the chemical differences between the two waters; in addition, they must be consistent with petrographic and isotopic data and saturation indices. Reaction-path modeling was used to estimate the effects of reactions on the evolution of carbon isotopes. The purpose of the mass-balance and reaction-path modeling was to identify geochemical reactions that may be occurring in the aquifer and, in conjunction with carbon-14 data, to estimate ground-water ages.

The geochemical modeling is divided into three sections. First, a section describes the methods and data used in mass-balance and reaction-path modeling. Second, mass-balance models are developed for eight ground-water samples that represent recent recharge to the aquifer. It is advantageous to model these samples separately because dolomite can be identified as the predominant reactant for these ground waters. Also, it is possible to use these samples to investigate unsaturated-zone processes that affect the evolution of carbon-isotope compositions. Third, mass-balance models are developed and ground-water ages are calculated for the remaining samples, all of which are near saturation or supersaturated with dolomite and calcite. Reaction-path modeling and isotope-evolution equations are used to estimate the isotopic composition of the initial waters used in mass-balance modeling for these samples. The mass-balance models describe geochemical reactions and a range of ground-water ages for each sample.

Methods

This section describes the computer models used to make the mass-balance and reaction-path calculations, the set of reactants selected for inclusion in the mass-balance modeling, and the samples used for mass-balance and reaction-path modeling.

Computer models

An extensively modified version of the program BALANCE (Parkhurst, Plummer, and Thorstenson, 1982) was used for the mass-balance modeling. The modified program calculated mass-balance models that accounted for changes in concentrations of elements between initial and final water compositions. The required input for the program included (1) the stoichiometric compositions of reactants and products, (2) an initial water composition, and (3) a final water composition. The modified program allowed for uncertainty in the analytical data and for mineral reactants to be constrained to dissolve or precipitate (see Attachment at back of report). The modified program also used carbon-isotope data to calculate the isotopic evolution of $\delta^{13}C$ and carbon-14 and to estimate the carbon-14 age. Equations from Wigley, Plummer, and Pearson (1978, 1979), as implemented in the program NETPATH (Plummer, Prestemon, and Parkhurst, 1991), were used to calculate the effects of mass-balance models on the carbon-isotope composition.

The program PHREEQE (Parkhurst, Thorstenson, and Plummer, 1980) was used to make the reaction-path calculations. The thermodynamic data included in the revision of August 1990 were used for all calculations.

Reactants used in mass-balance modeling

Mass-balance modeling requires the definition of all of the potential reactants and products in the ground-water system. The section on geochemical reactants systematically evaluated the minerals and gases in the subsurface to determine whether each was reacting presently. The phases assumed to be reactive are listed with their stoichiometries in table 7. These reactants include carbon dioxide, calcite, dolomite, gypsum, kaolinite, silica, chlorite, potassium feldspar, sodic plagioclase, calcium/sodium exchange, and calcium-magnesium/sodium exchange. Sources and sinks for nitrate and ammonium also are included in table 7. The evaluation of bromide to chloride ratios in brines and freshwater indicated that brines could be the source of chloride and bromide in the aquifer, therefore, the list includes a brine typical of the most concentrated solutions shown in figure 15.

The evaluation of petrographic data and saturation indices determined the minerals that appeared to be dissolving and precipitating within the aquifer. The mass-balance models need to be consistent with these determinations. For example, a mass-balance model is not plausible if a phase precipitates in the model when the saturation index indicates undersaturation and dissolution textures are observed for this phase. Conclusions about dissolution and precipitation of phases were formulated into constraints on mass-balance models (table 7). A plus sign in the table indicates that a mineral must dissolve if it is included in a mass-balance model, and a minus sign indicates that a mineral must precipitate. With a few exceptions noted in the text, the mass-balance models are consistent with the constraints listed in the table.

To simplify the mass-balance modeling, idealized mineral compositions were used and some potential reactants discussed in the geochemical reactants section were excluded. To limit the number of models, chlorite was included as a silicate source of magnesium, whereas biotite was excluded in the modeling. If biotite were included in the list of reactants, additional models would indicate biotite dissolution instead of, or in addition to, chlorite dissolution. Thus, models that include chlorite represent additional models that include biotite. The effects of interchanging chlorite with biotite in mass-balance models are negligible in terms of the carbon-14 dating. Smectite was not included in mass-balance modeling because clearly authigenic smectite was not detected by petrographic study.

Iron and trace elements were not included in the modeling. Iron was excluded partly because of uncertainties in the quantity of iron present in various minerals. In addition, small iron concentrations in the ground waters of the Permian geologic units indicate that iron is conserved in the mineral phases; ferrous iron derived from dissolving silicate and carbonate minerals appears to be forming goethite and hematite. The quantity of ferrous-iron-bearing phases that react must be relatively small because dissolved oxygen persists in the water throughout most of the aquifer; large quantities of ferrous iron from dissolving minerals would consume the available oxygen. There is no mineralogical evidence for the formation of ferrous phases. Manganese was not included in the mass-balance modeling for reasons analogous to those described for iron. Other trace elements were excluded because their small concentrations in ground-water and rocks produce only small effects in the mass-balance modeling.

Ground-water samples used for geochemical modeling

Two water compositions are needed for mass-balance modeling, an initial and a final water composition. In this study, the final water compositions are the measured compositions of ground-water samples. The set of ground-water samples used in mass-balance modeling was restricted to 34 samples from wells in the Permian geologic units for which $\delta^{13}C$ and carbon-

Table 7. Geochemical reactants used in mass-balance modeling

[Units are millimoles per liter except where otherwise noted. Table lists the change in concentration in solution of each constituent for the dissolution of 1.0 millimole of each phase, except for the brine and ammonium phases. For the ammonium phase, the values are the change in concentration due to the oxidation of 1 millimole of dissolved ammonium. For the brine phase, the values are the change in concentration in solution for the addition of 1 milliliter of brine. Constraint: "+" means that this phase was allowed only to dissolve; "–" means that this phase was allowed only to precipitate; absence of any symbol means that the phase was allowed to dissolve or precipitate in the mass-balance models. Alkalinity: meq/L, milliequivalents per liter]

Reactant	Constraint	Calcium	Magnesium	Sodium	Potassium	Carbon	Chloride	Sulfate	Nitrate	Ammonium	Aluminum	Silica	Alkalinity (meq/L)
Carbon dioxide	+					1.0							
Calcite	+	1.0				1.0							2.0
Dolomite	+	1.0	1.0			2.0							4.0
Gypsum		1.0						1.0					
Kaolinite	–										2.0	2.0	6.0
SiO_2												1.0	
Chlorite	+		5.0								2.0	3.0	16.0
Potassium feldspar	+				1.0						1.0	3.0	4.0
Plagioclase	+	.33		0.67							1.33	2.67	5.32
Ca/Na exchange	+	–1.0		2.0									
Ca-Mg/Na exchange	+	–.5	–.5	2.0									
Nitrate									1.0				–1.0
Ammonium	+								1.0	–1.0			–2.0
Brine	+	.43	.19	4.99			6.23						

14 activity of dissolved inorganic carbon were analyzed. In addition, these samples were analyzed for major elements, some trace elements, tritium, δD and $\delta^{18}O$ of water, and $\delta^{34}S$ of sulfate (table 8). A complete listing of all data for these samples is included in Ferree and others (1992). The sampling locations for this set of samples are shown in figure 21, and information about the samples and wells is provided in table 9. Analyses of samples from two sites were omitted from this report because there were large discrepancies in tritium and major-element compositions in subsequent resampling. It was concluded that poor well construction precluded obtaining representative ground-water samples at these two sites.

Six of the first eight samples of table 8 are substantially undersaturated with dolomite and calcite. These samples were used in reaction-path modeling to estimate the mass transfer of dolomite and calcite necessary to obtain equilibrium and to estimate the effects of this mass transfer on the carbon isotopes.

Mass-Balance Modeling of Recharge Samples

The first eight samples of table 8 are considered to be representative of recharge because they either have large tritium concentrations and carbon-14 activities or are substantially undersaturated with dolomite (saturation index less than -1.0) and calcite (saturation index less than -0.5). The tritium concentrations were greater than 25 pCi/L in all but one of these samples; the single sample lacking measurable tritium had carbon-14 activity of 70 pmc (percent modern carbon). The large tritium concentrations indicate water that is less than about 40 years old, and carbon-14 activity of 70 pmc indicates a maximum age of about 3,000 years. The undersaturations with respect to dolomite and calcite indicate limited extents of geochemical reactions. All of these samples are from shallow wells; the maximum depth is 240 ft. These young, shallow ground waters are referred to as the recharge samples. The mass-balance modeling of these samples was designed to identify the geochemical reactions that occur from the time of infiltration of rainwater to the time water reaches a shallow well. Thus, both saturated- and unsaturated-zone processes are included in the mass-balance modeling.

Reactants and Initial Water for Recharge Samples

The most important feature of the unsaturated zone is that carbon dioxide gas is available for uptake by water as it moves through the unsaturated zone. This carbon dioxide, in turn, can cause dissolution of minerals in the aquifer material. In addition to carbon dioxide gas, all of the other reactants in table 7 were used in modeling the recharge samples.

The characteristics of the recharge samples make it possible to identify dolomite as the predominant reactant. Carbonates are expected to react more quickly and to a greater extent than silicate minerals. Of the two major carbonate minerals, dolomite and calcite, dolomite is much more abundant in the aquifer (tables 3 and 4). Calcite was sparse in the core samples examined by SEM, optical microscopy, and X-ray diffraction. Furthermore, six of the recharge samples are substantially undersaturated with both dolomite and calcite. For these samples, it can be assumed that neither dolomite nor calcite have precipitated, and it is likely that the ratios of the calcium and magnesium in solution are determined by the ratios of these elements in the mineral phases that are reacting. The concentrations of dissolved calcium are plotted against magnesium for all young ground waters that were undersaturated with dolomite and calcite (fig. 22). All samples from this study (not just the samples used for mass-balance modeling) were included in figure 22, provided they satisfied three criteria: (1) The saturation indices for dolomite and calcite were less than -0.5 and -0.25, respectively, which indicates undersaturation, (2) the tritium concentrations were greater than 10 pCi/L, which indicates ages less than about 40 years, and (3) the samples were from the Permian geologic units. The concentrations of calcium relative to magnesium are only slightly greater than the 1:1 ratio expected from dolomite dissolution (fig. 22). For other reactions to produce the results shown in figure 22, the relative rates of plagioclase or calcite (alternate calcium sources) and chlorite (alternate magnesium source) dissolution would have to be equal throughout the aquifer, which is unlikely. The lack of saturation with dolomite and calcite in the samples of the figure indicates that these waters are moving through parts of the aquifer in which dolomite and calcite are rare. The conclusion is that, even in carbonate-depleted parts of the aquifer, dolomite, rather than calcite or silicates, is the predominant reactant in recharge.

The initial water composition used for modeling the recharge samples is given in solution 1 of table 10. The composition was derived by tenfold concentration of the composition of rainwater presented in table 2. Although ammonium is a major component in rainwater, none of the recharge samples had substantial concentrations of ammonium. The dissolved ammonium in the initial water was assumed to be converted to dissolved nitrate by reaction with oxygen in the unsaturated zone. The mass-balance models calculated the additional gain or loss of nitrate that was necessary to

Table 8. Chemical and isotopic composition of samples used in mass-balance modeling

[Units of data are millimoles per liter unless otherwise noted; pH is in standard units; "--" indicates missing data. Sample number: locations of wells are shown in figure 21.Geologic unit: Hnss, Hennessey Group; GbWg, Garber Sandstone and Wellington Formation; CCGA, Chase, Council Grove, and Admire Groups; u, well completed in unconfined part of the unit; c, well completed in the confined part of the unit. Depth category: Shallow indicates wells less than 300 feet deep; Deep indicates wells greater than 300 feet deep. Dissolved oxygen: mg/L, milligrams per liter. Alkalinity: meq/L, milliequivalents per liter. δD, deuterium measurement in per mil relative to standard mean ocean water (SMOW). $\delta^{18}O$, oxygen–18 measurement in per mil relative to SMOW. $\delta^{34}S$, sulfur–34 measurement in per mil relative to Canyon Diablo troilite (CDT). $\delta^{13}C$, carbon–13 measurement in per mil relative to Peedee belemnite (PDB). Tritium: pCi/L, picocuries per liter. Carbon–14: pmc, percent modern carbon]

Sample number	Geologic unit	Depth category	pH	Dissolved oxygen (mg/L)	Calcium	Magnesium	Sodium	Potassium	Silica	Alkalinity (meq/L)	Carbon	Chloride	Sulfate	Nitrate plus nitrite	δD (per mil)	$\delta^{18}O$ (per mil)	$\delta^{34}S$ (per mil)	$\delta^{13}C$ (per mil)	Carbon–14 (pmc)	Tritium (pCi/L)	Saturation index: Calcite	Saturation index: Dolomite
Recharge samples																						
1	Hnss	Shallow	7.27	3.6	2.17	1.65	4.18	0.02	0.60	6.42	7.14	3.67	0.80	0.25	–30.5	–5.05	7.30	–10.0	92.5	29.0	0.15	0.22
2	GbWg,u	Shallow	6.65	4.7	.21	.21	2.83	.05	.37	2.32	3.52	.71	.23	.11	–33.0	–5.75	7.00	–17.8	70.1	<.3	–1.79	–3.54
3	GbWg,u	Shallow	6.34	4.5	.65	.53	.91	.08	.27	1.52	3.11	.68	.30	.42	–35.5	–6.00	4.10	–13.6	123.2	50.0	–1.79	–3.63
4	GbWg,u	Shallow	6.13	8.0	.90	.70	.65	.02	.37	1.72	4.67	.82	.23	.69	–36.0	–6.20	5.70	–20.2[a]	112.7	34.0	–1.83	–3.75
5	GbWg,u	Shallow	6.99	8.9	1.05	.82	1.09	.01	.35	3.40	4.20	.73	.24	.04	–27.5	–4.00	8.80	–16.1	109.3	30.0	–.64	–1.37
6	GbWg,u	Shallow	7.39	9.4	1.52	.78	1.31	.02	.32	4.88	5.32	.35	.28	<.01	–29.0	–5.55	4.60	–12.5	91.5	53.0	.06	–.14
7	CCGA	Shallow	6.52	6.5	.77	.66	1.96	.03	.28	3.18	5.39	.82	.30	.09	–37.0	–6.10	5.20	–14.2	115.4	44.0	–1.26	–2.57
8	CCGA	Shallow	6.77	7.4	.62	.62	1.48	.02	.27	2.04	2.83	.85	.51	.36	–32.0	–5.25	3.40	–15.6	91.5	66.0	–1.28	–2.54
Carbonate-saturated samples																						
9	GbWg,u	Shallow	8.56	3.1	.90	.91	14.81	.12	.35	4.20	4.05	12.71	.75	.02	–36.5	–6.20	8.69	–13.5	14.5	<.3	.81	1.67
10	GbWg,u	Shallow	7.46	--	.72	.66	1.96	.08	.18	4.46	4.79	.14	.11	<.01	–36.0	–6.30	–26.77	–13.1	8.8	1.2	–.17	–.31
11	GbWg,u	Shallow	7.32	6.5	1.50	1.52	.65	.06	.20	5.72	6.32	.40	.10	.04	–33.0	–5.45	5.60	–9.5[b]	44.9	.4	.04	.12
12	GbWg,u	Shallow	7.48	1.8	1.07	1.07	.52	.01	.15	4.24	4.55	.40	.05	.02	–34.5	–5.90	4.20	–17.0	23.5	<.3	–.05	–.08
13	GbWg,u	Shallow	7.55	2.0	1.05	.86	5.66	.06	.25	5.12	5.43	3.39	.49	.02	–36.5	–6.15	9.90	–14.1	44.8	1.5	.04	.00
14	GbWg,u	Deep	8.27	5.9	.19	.24	3.96	.04	.18	4.48	4.47	.08	.10	.01	–41.0	–6.75	6.40	–10.1	3.9	<.3	.04	.24
15	GbWg,u	Deep	9.00	13.2	.14	.12	10.88	.12	.18	5.44	5.07	5.65	.32	.03	–40.0	–6.40	10.30	–12.3	15.3	3.2	.53	1.04
16	GbWg,u	Deep	7.63	6.5	1.20	1.28	.70	.06	.25	4.28	4.48	1.13	.07	.05	–38.0	–6.05	2.40	–11.4	21.6	<.3	.16	.39
17	GbWg,u	Deep	7.61	5.4	1.10	.86	.26	.04	.18	3.76	3.95	.27	.05	.02	–37.5	–5.75	5.10	–13.4	29.6	<.3	.06	.04
18	GbWg,u	Deep	7.78	5.2	.75	.70	1.70	.06	.16	4.08	4.21	.31	.09	.03	–37.5[c]	–6.10	.70	–15.2	21.0	<.3	.10	.20
19	GbWg,u	Deep	7.57	4.0	1.05	.82	.52	.04	.23	3.80	4.02	.31	.08	.03	–33.5	–5.90	1.70	–13.8	32.0	<.3	.01	–.06
20	GbWg,u	Deep	7.68	6.2	.92	.86	2.13	.04	.33	5.00	5.21	.34	.11	<.01	–34.0	–5.90	7.80	–10.4	50.0	.4	.17	.35

Table 8. Chemical and isotopic composition of samples used in mass-balance modeling—Continued

Sample number	Geologic unit	Depth category	pH	Dissolved oxygen (mg/L)	Calcium	Magnesium	Sodium	Potassium	Silica	Alkalinity (meq/L)	Carbon	Chloride	Sulfate	Nitrate plus nitrite	δD (per mil)	$\delta^{18}O$ (per mil)	$\delta^{34}S$ (per mil)	$\delta^{13}C$ (per mil)	Carbon–14 (pmc)	Tritium (pCi/L)	Saturation index: Calcite	Saturation index: Dolomite
21	GbWg,c	Deep	8.80	5.7	0.04	0.03	10.45	0.02	0.14	8.36	7.96	0.34	0.86	0.02	–39.0	–6.45	9.80	–9.5	12.8	0.4	0.02	–0.04
22	GbWg,c	Deep	8.60	.2	.09	.06	13.06	.02	.17	7.92	7.67	.59	2.81	<.01	–41.5	–6.85	9.70	–7.7	<.7	<.3	.10	.08
23	GbWg,c	Deep	8.97	3.5	.03	.02	7.40	.01	.16	6.24	5.89	.31	.39	.03	–38.0	–6.45	9.80	–10.5	10.7	<.3	–.06	–.22
24	GbWg,c	Deep	8.86	5.0	.35	.54	4.35	.03	.22	5.90	5.56	.21	.14	.04	–38.5	–6.35	9.40	–10.8	12.3	<.3	.92	2.11
25	GbWg,c	Deep	8.87	3.5	.04	.04	6.09	.01	.18	5.64	5.38	.18	.15	.03	–40.5	–6.45	8.50	–11.2	7.2	<.3	.01	.03
26	GbWg,c	Deep	8.84	3.0	.11	.07	7.40	.01	.20	6.24	5.93	.37	.77	.02	–43.5	–6.95	9.60	–10.2	2.2	.4	.43	.73
27	GbWg,c	Deep	8.74	4.8	.21	.11	6.09	.01	.20	5.40	5.19	.25	.57	.02	–40.5	–6.80	9.90	–11.0	3.5	<.3	.56	.91
28	GbWg,c	Deep	8.63	2.1	.32	.40	8.27	.03	.22	5.24	5.06	3.67	.43	.01	–39.0	–6.50	11.40	–10.9	4.4	.6	.61	1.37
29	GbWg,c	Deep	7.53	5.7	2.07	1.19	6.97	.03	.27	4.72	4.99	.26	4.38	.02	–44.0	–7.05	10.30	–10.5	.7	.3	.19	.20
30	GbWg,c	Deep	7.52	9.1	.97	1.07	1.61	.04	.35	5.16	5.49	.28	.12	.04	–33.5	–5.75	4.90	–9.5	42.6	.6	.04	.17
31	GbWg,c	Deep	8.44	.2	11.04	4.14	48.12	.11	.15	.68	.62	6.52	38.74	<.01	–44.0	–6.90	9.70	–13.3[d]	8.5	<.3	.54	.72
32	GbWg,c	Deep	7.75	5.9	.62	.74	3.26	.01	.28	5.08	5.25	.19	.32	.03	–39.0	–6.40	7.70	–10.8	15.6	<.3	.07	.27
33	CCGA	Shallow	8.87	.1	.04	.02	10.88	.02	.16	6.96	6.59	.90	1.46	<.01	–39.5	–6.25	8.50	–11.1	1.5	.4	.02	–.18
34	CCGA	Deep	9.07	.6	.03	.02	8.27	.01	.16	7.68	7.16	.31	.14	.02	–36.5	–6.10	6.50	–10.7	25.1	<.3	.04	.01

[a] $\delta^{13}C$ analyzed as part of the carbon–14 analysis differed significantly, –17.7.
[b] $\delta^{13}C$ analyzed as part of the carbon–14 analysis differed significantly, –15.0.
[c] Duplicate analysis differed significantly, –32.5.
[d] $\delta^{13}C$ analyzed as part of the carbon–14 analysis differed significantly, –11.7.

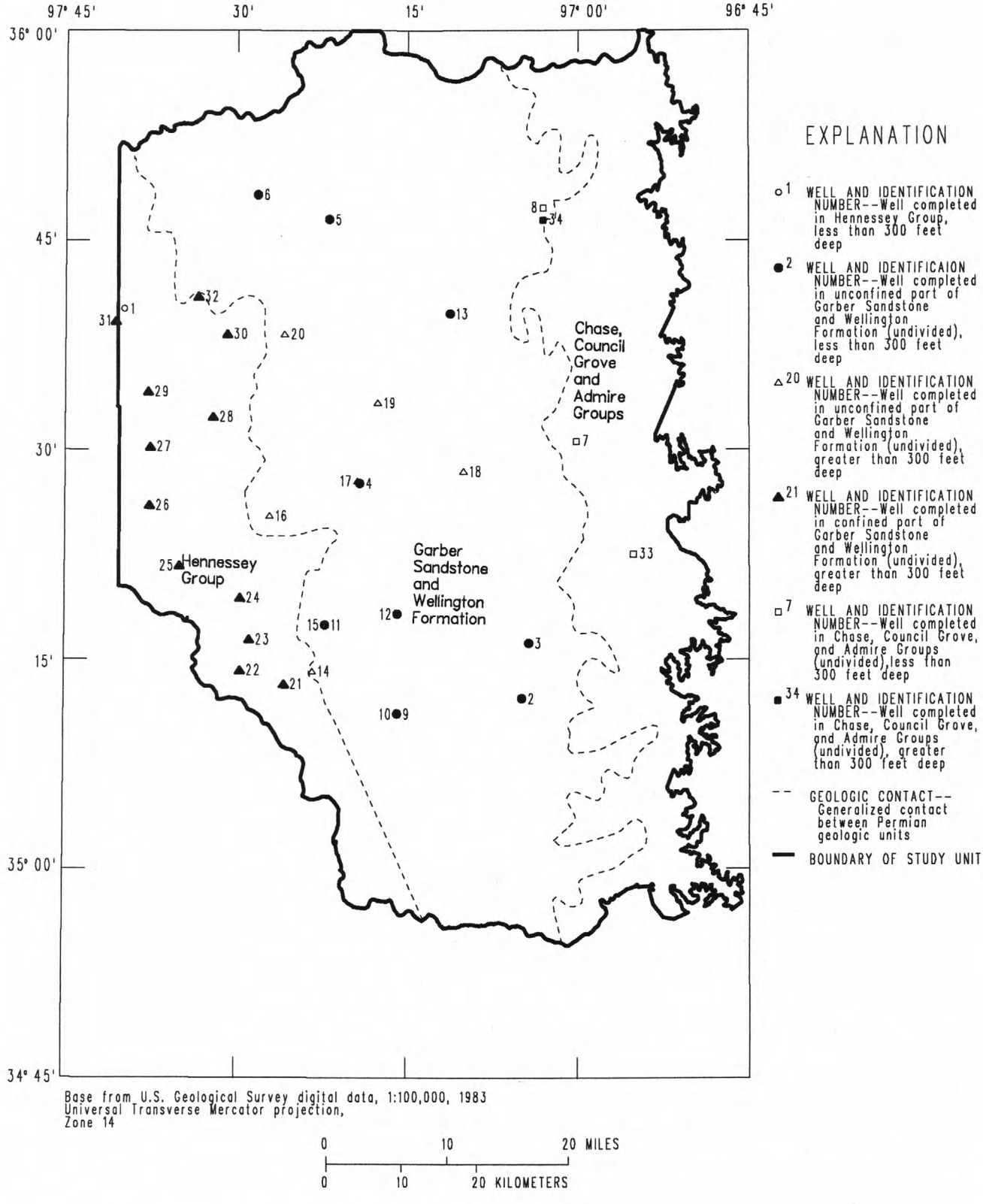

Figure 21. Locations of water samples from the Central Oklahoma aquifer used in the mass-balance modeling.

Table 9. Information about samples used in mass-balance modeling

[Sample number: locations of wells are shown in figure 21. Geologic unit: Hnss, Hennessey Group; GbWg, Garber Sandstone and Wellington Formation; CCGA, Chase, Council Grove, and Admire Groups; u, well completed in unconfined part of the unit; c, well completed in the confined part of the unit. Depth category: Shallow indicates wells less than 300 feet deep; Deep indicates wells greater than 300 feet deep]

Sample number	Geologic unit	Depth category	Site identification number	Latitude	Longitude	Well depth (feet)	Sampling	
							Date	Time
Recharge samples								
1	Hnss	Shallow	354007097395401	354007	973954	42.0	870831	1030
2	GbWg,u	Shallow	351212097045601	351212	970456	240.0	870903	1100
3	GbWg,u	Shallow	351611097042001	351611	970420	94.6	870908	1200
4	GbWg,u	Shallow	352738097191001	352738	971910	180.0	870917	1200
5	GbWg,u	Shallow	354631097215501	354631	972155	127.0	870921	1400
6	GbWg,u	Shallow	354817097281101	354817	972811	206.0	870819	1130
7	CCGA	Shallow	353040097000901	353040	970009	125.0	870915	1200
8	CCGA	Shallow	354725097030501	354725	970305	200.0	870923	1130
Carbonate-saturated samples								
9	GbWg,u	Shallow	351106097155201	351106	971552	280.0	871002	1300
10	GbWg,u	Shallow	351106097155202	351106	971552	154.0	870911	1500
11	GbWg,u	Shallow	351729097221301	351729	972213	178.0	871015	1300
12	GbWg,u	Shallow	351817097155201	351817	971552	170.0	871007	1200
13	GbWg,u	Shallow	353947097111501	353947	971115	178.0	870825	1100
14	GbWg,u	Deep	351409097231801	351409	972318	695.0	870729	1120
15	GbWg,u	Deep	351729097221302	351729	972213	795.0	871022	1600
16	GbWg,u	Deep	352518097270601	352518	972706	750.0	870810	1200
17	GbWg,u	Deep	352749097192301	352749	971923	658.0	870811	1000
18	GbWg,u	Deep	352830097100301	352830	971003	325.0	870824	1300
19	GbWg,u	Deep	353324097173701	353324	971737	460.0	870820	1100
20	GbWg,u	Deep	353819097254901	353819	972549	519.0	870817	1100
21	GbWg,c	Deep	351314097254701	351314	972547	643.0	870731	1030
22	GbWg,c	Deep	351414097293901	351414	972939	745.0	870803	1100
23	GbWg,c	Deep	351648097285101	351627	972851	674.0	870731	1530
24	GbWg,c	Deep	351926097293001	351926	972940	795.0	870804	1030
25	GbWg,c	Deep	352145097345901	352145	973459	900.0	870806	1400
26	GbWg,c	Deep	352605097375701	352604	973738	895.0	870806	1000
27	GbWg,c	Deep	353013097373301	353013	973733	822.0	870805	1415
28	GbWg,c	Deep	353223097320501	353223	973205	760.0	870727	1130
29	GbWg,c	Deep	353411097374501	353411	973745	635.0	870902	1000
30	GbWg,c	Deep	353819097305101	353819	973051	515.0	870814	1000
31	GbWg,c	Deep	353915097403901	353915	974039	600.0	870826	1000
32	GbWg,c	Deep	354105097332401	354100	973324	364.0	870925	1100
33	CCGA	Shallow	352236096551001	352236	965510	285.0	870827	1000
34	CCGA	Deep	354633097030801	354633	970308	401.0	870821	1200

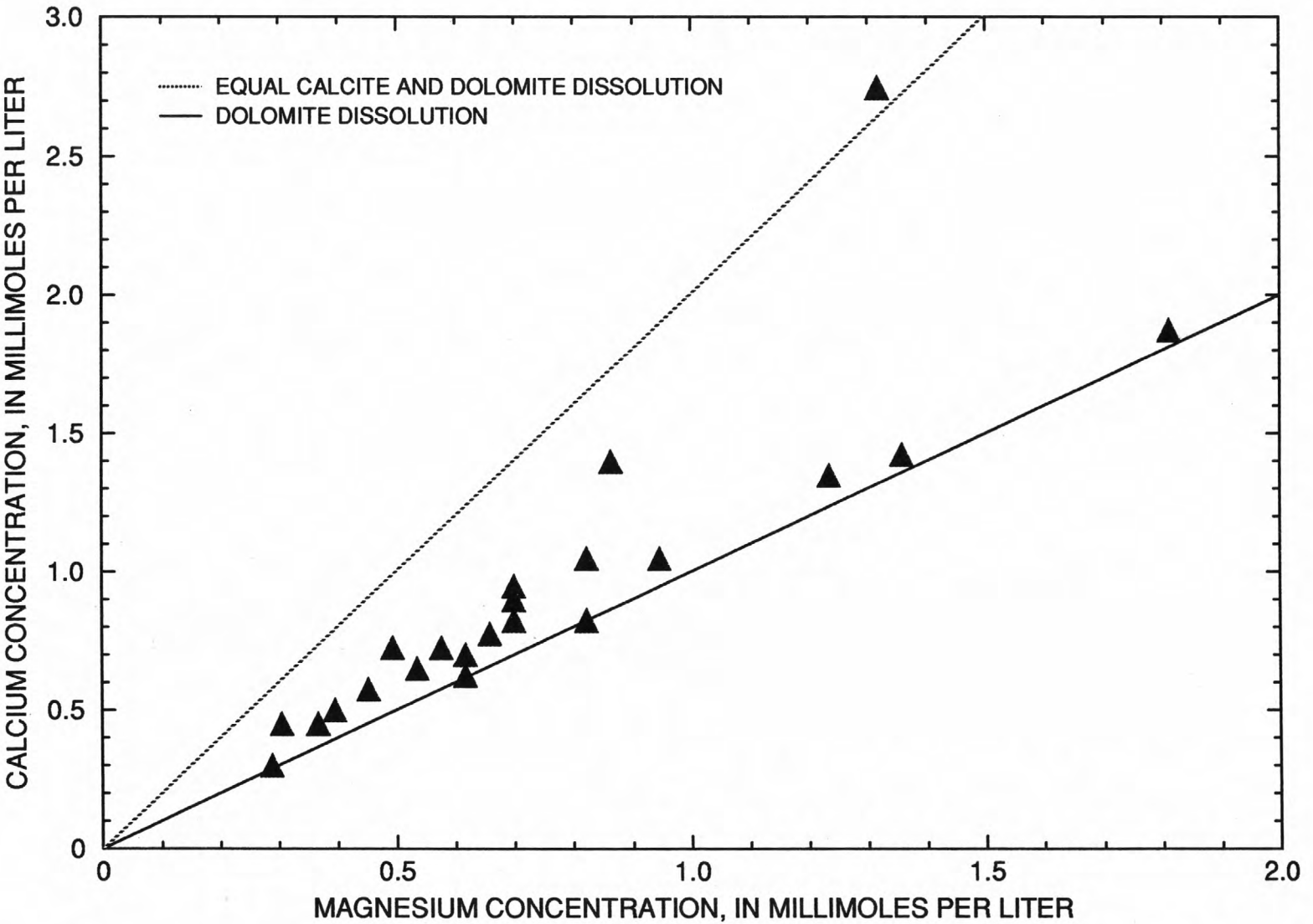

Figure 22. Relation between calcium and magnesium concentrations in recharge waters that are undersaturated with dolomite and calcite in the Central Oklahoma aquifer.

account for the nitrate concentrations in the recharge samples.

Mass-balance models

The conceptual model for the mass-balance modeling of the recharge samples is that rainwater is concentrated tenfold by evapotranspiration, dissolves carbon dioxide from the unsaturated zone, and reacts with dolomite and other minerals to produce the chemical composition of each of the samples. It has been shown that dolomite is the predominant reactant in recharge; thus dolomite was required to be included in each mass-balance model. For each of the eight recharge samples, the mass-balance modeling determined all combinations of minerals (that were minimal, see Attachment) that included dolomite, satisfied the constraints of table 7, and accounted for the difference in composition between the initial water and the recharge sample.

Multiple mass-balance models were found for all eight recharge samples (table 11). All samples had three or more models, and the maximum number of models for any sample was seven. It is important to realize that the models are a set of end members, and other models which combine one or more of the end members also are possible. For example, any two models for a ground-water sample can be combined by adding one half of the mass transfers of each model. The resulting model contains all of the phases that were in either model and satisfies all the constraints used in the mass-balance modeling. The reactants are now discussed individually in the order in which they are listed in table 11.

All mass-balance models indicate that a large quantity of carbon dioxide gas is taken up by water as it moves through the unsaturated zone. The mass transfer of carbon dioxide gas into solution is generally in the range from 2.0 to 4.5 mmol/L.

Dolomite was required to be in each model. Generally, the mass transfer of dolomite is in the range from 0.3 to 1.0 mmol/L and is the largest mass transfer of any phase except carbon dioxide gas. Some models have larger mass transfers of plagioclase than dolomite (models 5, 5, 5, 5, 3, and 7 of samples 1, 2, 3, 5, 6, and 7, respectively). These models are inconsistent with the previous conclusion that dolomite is the predominant reactant. Calcite is included in only five models. In each of these models, the mass transfer of dolomite is greater than that of calcite, which is consistent with figure 22.

Kaolinite precipitation is necessary in most of the mass-balance models. It was the only mineral containing aluminum that was not constrained to dissolve. Because dissolved aluminum concentrations are very small, these constraints required any aluminum derived from aluminosilicate dissolution to precipitate in kaolinite. Generally, the models precipitate from -0.05 to -0.2 mmol/L of kaolinite.

Two or more phases of varying stability may be represented by the reactant SiO_2. In table 11, SiO_2 dissolves in some models, precipitates in others, and does not react in the rest. In the models with positive mass transfers of SiO_2, SiO_2 is the predominant source of dissolved silica. However, both quartz and chalcedony are supersaturated in all of the recharge samples. Thus, the models with positive mass transfers of SiO_2 require dissolution of a relatively unstable phase—a phase less stable than chalcedony. It is unlikely that such an unstable phase has persisted for millions of years in the aquifer. It is more likely that dissolved silica is derived from dissolution of other aluminosilicates in the aquifer. The models that dissolve large quantities of plagioclase precipitate SiO_2. The saturation indices of quartz and chalcedony are consistent with the precipitation of either of these phases. However, these models are considered less plausible because dolomite is not the predominant reactant.

Chlorite has relatively small mass transfers, generally in the range from 0.02 to 0.1 mmol/L. However, with 5 millimoles of magnesium per millimole of chlorite (for the idealized chlorite composition used in the modeling), the quantity of magnesium derived from chlorite in these models is 0.1 to 0.5 mmol/L. Potassium-feldspar mass transfers are relatively small in all models (less than 0.1 mmol/L). Plagioclase mass transfers are generally in the range from 0.1 to 0.3 mmol/L. The models with large mass transfers of plagioclase (0.5 mmol/L or larger) are considered less plausible as previously discussed.

Measurements of exchangeable cations in clay samples have calcium to magnesium ratios that are about 1:1 to 2:1 (table 6), which indicates approximately equal exchange of calcium and magnesium for sodium. Models that contain calcium-magnesium/sodium exchange or both calcium-magnesium/sodium and calcium/sodium exchange are consistent with exchange reactions that have calcium to magnesium ratios between 1:1 and 2:1. Other models can be created that have similar ratios by combining a model that has calcium-magnesium/sodium exchange with a model that has calcium/sodium exchange.

The exchange reactions for all samples, except sample 4, were constrained to release sodium from the clays. With this constraint, sample 4 had only one mass-balance model, which dissolved a pure silica phase. Dissolution of a pure silica phase, as previously

Table 10. Chemical and isotopic composition of initial waters used in mass-balance modeling

[Units of data are millimoles per liter unless otherwise noted. Alkalinity: meq/L, milliequivalents per liter. Initial water 1 is the composition of rainwater concentrated tenfold. Initial waters 2 through 6 were generated from initial water 1 by eliminating the nitrogen species, adding 2.0 to 4.0 millimoles per liter of carbon dioxide gas to the solution, and equilibrating with dolomite and calcite using the program PHREEQE (Parkhurst, Thorstenson, and Plummer, 1980)]

Initial water number	Carbon dioxide added	pH (standard units)	Calcium	Magnesium	Sodium	Potassium	Silica	Alkalinity (meq/L)	Carbon	Chloride	Sulfate	Nitrate	Ammonium
1	—	4.80	0.10	0.02	0.06	0.01	0.0	0.0	0.0	0.07	0.13	0.17	0.15
2	2.0	7.63	.98	.96	.06	.01	.3	3.65	3.83	.07	.13	0	0
3	2.5	7.49	1.17	1.15	.06	.01	.3	4.39	4.70	.07	.13	0	0
4	3.0	7.38	1.34	1.32	.06	.01	.3	5.07	5.54	.07	.13	0	0
5	3.5	7.29	1.50	1.47	.06	.01	.3	5.70	6.36	.07	.13	0	0
6	4.0	7.21	1.65	1.62	.06	.01	.3	6.29	7.16	.07	.13	0	0

Table 11. Mass-balance models for recharge-water samples

[Units are millimoles per liter unless otherwise noted. "--" indicates that the mineral is not included in the mass-balance model. Geologic unit: Hnss, Hennessey Group; GbWg, Garber Sandstone and Wellington Formation; CCGA, Chase, Council Grove, and Admire Groups; u, well completed in unconfined part of the unit. Depth category: Shallow indicates wells less than 300 feet deep. Ca-Mg/Na exchange: cation-exchange reaction with equal quantities of calcium and magnesium going onto the exchanger and sodium being released. Ca/Na exchange: cation-exchange reaction with calcium going onto the exchanger and sodium being released. Brine: mL/L, milliliters per liter; this is the volume of the hypothesized brine phase that is added to the initial water to account for the chloride concentration of the final water. Each milliliter of brine contains 6.23 millimoles of chloride and other major ions (entire composition is listed in table 7)]

Sample number	Geologic unit	Depth category	Model number	Carbon dioxide	Calcite	Dolomite	Kaolinite	Silica	Chlorite	Potassium feldspar	Plagioclase	Ca-Mg/Na exchange	Ca/Na exchange	Gypsum	Brine (mL/L)	Nitrate
1	Hnss	Shallow	1	4.30	--	1.61	--	0.60	--	--	--	--	0.52	0.67	0.58	-0.07
			2	4.52	--	1.51	-0.30	--	--	--	0.45	--	.51	.67	.58	-.07
			3	4.61	--	1.46	-.08	.53	0.08	--	--	0.63	--	.67	.58	-.07
			4	4.99	--	1.27	-.35	--	.10	--	.37	.50	--	.67	.58	-.07
			5	6.48	--	.53	-1.45	-2.11	.20	--	1.88	--	--	.67	.58	-.07
2	GbWg,u	Shallow	1	2.44	--	.61	-.02	.29	--	0.04	--	.88	.22	.10	.11	-.21
			2	2.58	--	.54	-.16	--	--	.04	.22	.74	.29	.10	.11	-.21
			3	2.66	--	.50	-.06	.25	.04	.04	--	1.10	--	.10	.11	-.21
			4	2.83	--	.41	-.19	--	.05	.04	.18	1.04	--	.10	.11	-.21
			5	3.32	--	.17	-.90	-1.48	--	.04	1.32	--	.65	.10	.11	-.21
3	GbWg,u	Shallow	1	2.29	--	.48	-.03	.13	--	.07	--	--	.17	.18	.10	.11
			2	2.34	--	.45	-.10	--	--	.07	.10	--	.14	.18	.10	.11
			3	2.47	--	.39	-.07	.10	.04	.07	--	.17	--	.18	.10	.11
			4	2.54	--	.35	-.12	--	.04	.07	.07	.14	--	.18	.10	.11
			5	2.96	--	.14	-.43	-.60	.07	.07	.50	--	--	.18	.10	.11
4	GbWg,u	Shallow	1	3.73	--	.61	--	.37	--	--	--	--	--	.11	.12	.39
			2	3.91	--	.52	-.18	--	--	--	.27	-.23	.12	.11	.12	.39
			3	4.01	--	.47	-.19	--	.02	--	.26	-.11	--	.11	.12	.39
			4	4.10	--	.43	-.20	--	.04	--	.24	--	-.11	.11	.12	.39
5	GbWg,u	Shallow	1	2.57	--	.87	--	.35	--	--	--	.22	--	.12	.11	-.27
			2	2.57	0.22	.76	--	.35	--	--	--	--	.22	.12	.11	-.27
			3	2.72	--	.79	-.17	--	--	--	.26	--	.13	.12	.11	-.27
			4	2.72	--	.79	-.17	--	--	--	.26	.13	--	.12	.11	-.27
			5	3.23	--	.54	-.48	-.58	.04	--	.66	--	--	.12	.11	-.27
6	GbWg,u	Shallow	1	2.95	.49	.99	--	.31	--	--	--	.50	--	.16	.05	-.30
			2	3.11	.41	.95	-.16	--	--	--	.23	.43	--	.16	.05	-.30
			3	3.95	--	.74	-1.00	-1.70	--	--	1.51	--	--	.16	.05	-.30

Table 11. Mass-balance models for recharge-water samples—Continued

Sample number	Geologic unit	Depth category	Model number	Carbon dioxide	Calcite	Dolomite	Kaolinite	Silica	Chlorite	Potassium feldspar	Plagioclase	Ca-Mg/Na exchange	Ca/Na exchange	Gypsum	Brine (mL/L)	Nitrate
7	CCGA	Shallow	1	3.88	--	0.83	–0.01	0.25	--	0.02	--	0.45	0.18	0.18	0.12	–0.22
			2	3.88	0.45	.60	–.01	.25	--	.02	--	--	.63	.18	.12	–.22
			3	4.00	--	.77	–.13	--	--	.02	0.18	.33	.24	.18	.12	–.22
			4	4.00	.33	.60	–.13	--	--	.02	.18	--	.57	.18	.12	–.22
			5	4.06	--	.74	–.05	.21	0.04	.02	--	.63	--	.18	.12	–.22
			6	4.21	--	.66	–.15	--	.05	.02	.15	.58	--	.18	.12	–.22
			7	4.33	--	.60	–.46	–.66	--	.02	.67	--	.40	.18	.12	–.22
8	CCGA	Shallow	1	1.65	--	.58	--	.27	--	--	--	--	.46	.37	.12	.04
			2	1.93	--	.44	–.15	--	.03	--	.18	--	.37	.37	.12	.04
			3	2.13	--	.34	–.09	.17	.10	-	--	.43	--	.37	.12	.04
			4	2.25	--	.28	–.18	--	.10	--	.12	.39	--	.37	.12	.04

stated, seemed unlikely, and the only constraints that could reasonably be removed were those on the exchange reactions. Removing the constraints on the exchange reactions generated three more models for sample 3, all of which included reverse cation exchange, that is, sodium uptake by the clays. Reverse cation exchange is possible if the ratio of dissolved calcium and magnesium to dissolved sodium has changed because of a relative increase in sodium concentration or decrease in calcium and magnesium concentrations. Many sources of ground-water contamination are likely to have large sodium concentrations that could cause reverse cation exchange to occur. The large quantities of nitrate needed for the models of sample 4 are an indication of contamination at this site.

The initial water and gypsum are the only sources of sulfate in the modeling. All samples from the Garber Sandstone and Wellington Formation require less than 0.2 mmol/L gypsum to dissolve. The sample from the Hennessey Group and one from the Chase, Council Grove and Admire Groups require larger mass transfers of gypsum. The need for gypsum dissolution could be eliminated for the samples from the Garber Sandstone and Wellington Formation by increasing the concentration of sulfate in the initial water composition. Larger sulfate concentrations in the initial water could be caused by an evapotranspiration factor greater than 10 (which was used in the definition of the initial water composition).

The source of chloride in the ground-water samples is assumed to be a brine that is leaching from fluid inclusions or dead-end pores. The brine phase in table 11 refers to the composition of a brine near equilibrium with halite, calcite, and dolomite (brine composition is given in table 7). The mass-balance modeling calculates the number of milliliters of brine per liter of solution that are needed to account for the measured chloride in the ground-water sample. Each milliliter of brine contains 6.23 mmol of chloride and 4.99 mmol of sodium (table 7). All of the samples require about 0.1 mL of brine (0.6 mmol chloride) to account for chloride concentrations, except for the sample from the Hennessey Group. The concentrations of chloride in the recharge samples are larger than most of the samples from deeper in the aquifer (table 8). Because chloride is relatively conservative, chloride concentrations should stay constant or increase with depth in the aquifer rather than decrease. The larger concentrations in the shallow samples indicate that part of the chloride in these recharge samples is derived from contamination at the land surface. The brine phase may not be representative of the source of chloride contamination in these samples. However, a more plausible phase would require more detailed information about sources of chloride contamination than is available.

The concentrations of ammonium and nitrate in water that enters the saturated zone of the aquifer are uncertain because of variations in rainwater quantity and composition and because of uptake by biological processes in the unsaturated zone. For the mass-balance modeling, the initial water contained 10 times the quantity of nitrate (0.17 mmol/L) and ammonium (0.15 mmol/L) in recent rainwater. The ammonium concentrations in ground water in the study unit are negligible. All of the ammonium in evaporated rainwater was assumed to oxidize to nitrate by the reduction of oxygen in the unsaturated zone. This oxidation causes a decrease in alkalinity. Nitrate was assumed to be lost from solution to biological uptake or gained from some undetermined source. The loss or gain of nitrate was assumed to be accompanied by an increase or decrease in alkalinity to maintain electrical neutrality in the solution. Models for four samples have negative mass transfers of nitrate in the range from -0.2 to -0.3 mmol/L (table 11). The loss is approximately equal to the total quantity of nitrate and ammonium in the initial water. Under pristine conditions, it is expected that biological processes would consume most of the available ammonium and nitrate. The rest of the samples have small negative or positive mass transfers of nitrate relative to the initial water. These mass transfers indicate that more nitrate was available than could be consumed by biological processes. An additional source of nitrate is indicated for these samples; contamination by fertilizers or septic tanks is possible throughout the study area.

Carbon Isotopes

An important test of the mass-balance models is whether they are consistent with the $\delta^{13}C$ and carbon-14 measurements in the aquifer. For this study, carbon-isotope data are available for ground-water and carbonate-mineral samples. However, two essential types of information needed to understand carbon-isotope evolution in the unsaturated zone are missing—the isotopic composition of carbon dioxide gas throughout the unsaturated zone and the extent to which water in the unsaturated zone is in isotopic equilibrium with carbon dioxide gas. Given that the information on the carbon-isotope system is incomplete, the approach to interpreting $\delta^{13}C$ and carbon-14 data for the recharge samples is to (1) estimate a range of isotopic compositions for unsaturated-zone carbon dioxide gas from literature sources, (2) calculate the isotopic compositions of carbon dioxide gas that are consistent with the mass-balance models and the measured isotopic compositions

of the recharge samples, and (3) compare these two estimates of the isotopic composition of unsaturated-zone carbon dioxide gas for inconsistencies.

Estimated isotopic composition of carbon dioxide gas in the unsaturated zone

The $\delta^{13}C$ for plant-derived carbon dioxide gas is expected to be about -25 per mil (Mook, 1980, p. 60). Quade, Cerling, and Bowman (1989) estimate that diffusion can cause the $\delta^{13}C$ of carbon dioxide gas to be 4 per mil heavier than the plant material. Thorstenson and others (1983) measured the $\delta^{13}C$ of unsaturated-zone carbon dioxide gas at several sites in the western Great Plains and determined that the composition ranged from about -16 to -25 per mil for sites that did not have lignite in the unsaturated zone. This range from -16 to -25 per mil is the range that is expected for the carbon dioxide gas in the unsaturated zone of the Central Oklahoma aquifer because of the similarity of environments.

Carbon-14 activity in carbon dioxide gas is expected to have been 100 pmc at the top of the unsaturated zone before atmospheric nuclear testing introduced a large quantity of carbon-14 into the atmosphere in the early 1950's. The carbon-14 activity at the top of the unsaturated zone could have reached a maximum of about 180 pmc during a short period following the peak in atmospheric nuclear testing in the 1960's (Mook, 1980). Thorstenson and others (1983) observed carbon-14 activities of about 120 pmc in carbon dioxide gas samples from the top of the unsaturated zone; however these carbon-14 activities, which are typical of post-atmospheric nuclear testing, were not observed in the deep unsaturated zone, even though diffusion models predicted that it should be present. Thus, the unsaturated zone may not be uniform in the isotopic composition of carbon throughout its entire depth. For this report, the carbon-14 activities of carbon dioxide gas in the unsaturated zone are expected to have been less than or equal to 100 pmc before atmospheric nuclear testing. Activities are expected to have been greater than 100 pmc at the top of the unsaturated zone since atmospheric nuclear testing began.

Isotopic composition of carbon dioxide gas calculated from mass-balance models

To calculate the isotopic composition of the unsaturated-zone carbon dioxide gas that is consistent with the mass-balance models, it is necessary to know (1) the mass transfers of the carbon-containing phases, (2) the carbon-isotope compositions of dissolving dolomite and calcite, and (3) the extent of carbon-isotope fractionation between the aqueous phase and carbon dioxide gas. The mass transfers of the carbon-containing phases are precisely the results of the mass-balance modeling. The $\delta^{13}C$ of dolomite and calcite were measured for selected core samples from the test holes (table 6). A representative $\delta^{13}C$ was chosen to be -8.0 per mil for calcite and -9.0 per mil for dolomite. These $\delta^{13}C$ values were used in all isotopic calculations. Carbon-14 activities were assumed to be 0 pmc for calcite and dolomite.

The extent of isotopic fractionation between the aqueous and the gas phase is not known. However, the magnitude of fractionation effects can be estimated on the basis of two contrasting assumptions: (1) By assuming equilibrium isotopic fractionation occurs between the aqueous phase and carbon dioxide gas, and (2) by assuming that no isotopic fractionation occurs between the aqueous phase and carbon dioxide gas. Calculations made with these two assumptions should delimit the range of fractionation effects for carbon-isotope evolution.

The isotopic-equilibrium calculations assume that all carbonate dissolution occurs in the unsaturated zone while the aqueous phase is in isotopic equilibrium with carbon dioxide gas. For isotopic equilibrium, the isotopic composition of the dissolved inorganic carbon in the aqueous phase differs from the isotopic composition of carbon dioxide gas by an equilibrium fractionation factor. The fractionation factor between the gas and aqueous phase was calculated from the composition of the final water by using the equations of Thode and others (1965), Mook, Bommerson, and Staverman (1974), and Mook (1980). The equilibrium fractionation factor was added to the measured $\delta^{13}C$ of the final water to calculate the $\delta^{13}C$ of carbon dioxide gas. The fractionation effects on carbon-14 are theoretically twice as large as those for carbon-13; however, because carbon-14 activity is measured in percent and $\delta^{13}C$ is measured in per mil, in terms of percent, the fractionation effects on carbon-14 activity are negligibly small, about 1 pmc. For isotopic equilibrium, the calculated carbon-isotope composition of carbon dioxide gas is independent of mass-balance models because it depends only on the measured carbon-isotope composition of the final water and the equilibrium fractionation factor.

If isotopic fractionation does not occur, the carbon-14 activity and $\delta^{13}C$ of the carbon dioxide gas that enters the aqueous phase is the same as the gas-phase composition. For all of the recharge samples, all carbon phases dissolve. Therefore, a simple mass balance on the carbon isotopes is sufficient to calculate the iso-

topic composition of the carbon dioxide gas. In the absence of isotopic fractionation, the calculated isotopic composition of the carbon dioxide gas is different for each mass-balance model because each model has different mass-transfers of carbon phases.

The calculated carbon-isotope composition of carbon dioxide gas in the unsaturated zone is tabulated in table 12 for each sample for each of the two assumptions: equilibrium isotopic fractionation and no isotopic fractionation between the aqueous phase and carbon dioxide gas. For the assumption of equilibrium isotopic fractionation, there is only one set of equilibrium isotopic compositions of carbon dioxide gas for each sample. For the assumption of no isotopic fractionation, there is one set of calculated isotopic compositions of carbon dioxide gas for each mass-balance model. The differences among the models for a sample cause the calculated $\delta^{13}C$ of the carbon dioxide gas to differ only by 1 to 2 per mil. However, differences among the models for some samples cause the calculated carbon-14 activities to differ by as much as 40 pmc.

Comparison of literature estimates with calculated isotopic compositions of unsaturated-zone carbon dioxide gas

The calculated $\delta^{13}C$ of the carbon dioxide gas, assuming equilibrium fractionation, ranges from -17.2 to -23.1 per mil and, assuming no fractionation, ranges from -10.2 to -23.9 per mil (table 12). The calculated $\delta^{13}C$ for the carbon dioxide gas generally is heavier if no isotopic fractionation occurs than if equilibrium isotopic fractionation occurs. The equilibrium-fractionation $\delta^{13}C$ for each sample is within the range of compositions of unsaturated-zone carbon dioxide gas, -16 to -25 per mil, measured by Thorstenson and others (1983). If no fractionation occurs, the calculated $\delta^{13}C$ for most of the samples are within the expected range of isotopic compositions for unsaturated-zone carbon dioxide gas. However, the $\delta^{13}C$ for some samples are heavier than the expected range by 1 or 2 per mil, and sample 1 is more than 5 per mil heavier. Only equilibrium isotopic fractionation implies $\delta^{13}C$ values of unsaturated-zone carbon dioxide gas that are within the range -16 to -25 per mil for all of the recharge samples.

Assuming equilibrium isotopic fractionation, the calculated carbon-14 activity of carbon dioxide gas ranges from 70 to 123 pmc, which is within the range of carbon-14 activities of unsaturated-zone carbon dioxide gas measured by Thorstenson and others (1983) from 1979 through 1981. Assuming no isotopic fractionation, the calculated carbon-14 activity of carbon dioxide gas is between 10 and 70 pmc greater than for equilibrium fractionation for each sample. Most samples have some models with calculated carbon-14 activity of carbon dioxide gas that is greater than or equal to 150 pmc. Mook (1980) shows that concentrations greater than 150 pmc in plants could have persisted for only a few years in the 1960's and early 1970's. Thus both assumptions, equilibrium isotopic fractionation and no isotopic fractionation, are consistent with the measured carbon-14 data and the mass-balance models under certain conditions. Assuming equilibrium isotopic fractionation occurs, the measured carbon-14 activities of the samples can be explained by carbon-14 activities of carbon dioxide gas in the unsaturated zone that ranged from about 50 to 120 pmc while recharge occurred. This range is consistent with the measurements of Thorstenson and others (1983). Assuming no isotopic fractionation occurs, the measured carbon-14 activities of the samples can be explained by carbon-14 activities of carbon dioxide gas in the unsaturated zone that ranged from 120 to 180 pmc; this range of carbon-14 activities implies that recharge occurred in the late 1960's and early 1970's.

Discussion

Mass-balance models account quantitatively for the compositions of recharge samples (samples 1 through 8) by uptake of carbon dioxide gas from the unsaturated zone; dissolution of dolomite and, to lesser extents, plagioclase, potassium feldspar, chlorite, and biotite; and precipitation of kaolinite and, perhaps, a pure silica phase. Cation exchange accounts for most of the dissolved sodium. Gypsum dissolution or concentration of rainwater by evapotranspiration can account for sulfate concentrations in recharge samples. A sodium-chloride brine or other source of chloride is necessary to account for the chloride concentrations. The recharge samples have larger concentrations of chloride than samples from deeper in the aquifer, which indicates a recent source of chloride contamination. Some of the samples have large nitrate concentrations, which also is attributed to recent sources of contamination.

The mass-balance models for the recharge samples (table 11) are consistent with the petrographic observations and saturation indices. The petrographic observations indicate that dolomite, calcite, chlorite, plagioclase, potassium feldspar, and biotite are present and, if they are reactive, are dissolving. Saturation indices for carbonate minerals are consistent with dissolution. Six of eight recharge samples were undersaturated with dolomite and calcite. In the larger sample set of all samples of this study from Permian geologic units, 24 of 58 samples that had large tritium concentra-

Table 12. Calculated carbon-isotope composition of unsaturated-zone carbon dioxide gas

[The isotopic composition of carbon dioxide gas in the unsaturated zone was calculated from the measured isotopic data and the mass-balance models based on two different assumptions: (1) equilibrium isotopic fractionation between the aqueous solution and carbon dioxide gas and (2) no fractionation. Geologic unit: Hnss, Hennessey Group; GbWg, Garber Sandstone and Wellington Formation; CCGA, Chase, Council Grove, and Admire Groups; u, well completed in unconfined part of the unit; c, well completed in the confined part of the unit. Depth category: Shallow indicates wells less than 300 feet deep. $\delta^{13}C$, carbon–13 value relative to Peedee belemnite (PDB). C–14, carbon–14: pmc, percent modern carbon]

Sample number	Geologic unit	Depth category	Calculated isotopic composition of carbon dioxide gas				
			Equilibrium		No fractionation		
			$\delta^{13}C$ (per mil)	C–14 (pmc)	Model number	$\delta^{13}C$ (per mil)	C–14 (pmc)
1	Hnss	Shallow	–17.2	93	1	–10.8	162
					2	–10.7	154
					3	–10.6	151
					4	–10.5	140
					5	–10.2	108
2	GbWg,u	Shallow	–23.1	70	1	–22.2	105
					2	–21.4	99
					3	–21.1	96
					4	–20.4	91
					5	–18.7	77
3	GbWg,u	Shallow	–17.2	123	1	–15.5	175
					2	–15.4	171
					3	–15.0	162
					4	–14.9	157
					5	–14.0	135
4	GbWg,u	Shallow	–22.7	113	1	–23.9	150
					2	–23.2	143
					3	–22.8	139
					4	–22.5	136
5	GbWg,u	Shallow	–23.1	109	1	–20.9	183
					2	–21.0	183
					3	–20.2	173
					4	–20.2	173
					5	–18.5	146
6	GbWg,u	Shallow	–20.4	91	1	–15.6	168
					2	–15.2	160
					3	–13.8	126
7	CCGA	Shallow	–18.9	115	1	–16.4	165
					2	–16.5	165
					3	–16.2	160
					4	–16.3	160
					5	–16.1	157
					6	–15.8	152
					7	–15.6	148
8	CCGA	Shallow	–21.5	91	1	–20.2	156
					2	–18.6	133
					3	–17.7	121
					4	–17.2	114

tions were undersaturated with dolomite and calcite. Gypsum was not observed in any of the core samples, but saturation indices indicate it should dissolve if present.

The dominant reaction in recharge is uptake of carbon dioxide gas from the unsaturated zone and dissolution of dolomite. This reaction produces ground water with calcium and magnesium as the major cations and bicarbonate as the major anion. Recharge that is undersaturated with carbonate minerals has pH values that range from about 6.0 to 7.3; recharge that is in equilibrium with carbonate minerals has pH values that are about 7.5.

The mass-balance models are consistent with the available carbon-isotope data. Two processes for isotopic fractionation between the aqueous phase and carbon dioxide gas were tested—equilibrium fractionation and no fractionation. Only equilibrium isotopic fractionation is consistent for all of the recharge samples with the range of $\delta^{13}C$ of carbon dioxide gas in the unsaturated zone that was derived from the literature. Neither set of calculations for isotope-fractionation processes provides any specific contradictions by which mass-balance models could be rejected.

All recharge samples except sample 2 had tritium concentrations of 30 pCi/L or greater, which indicate ground water that is less than about 40 years old. The carbon-14 activity of sample 2 was 70 pmc, which could result from radioactive decay or dilution by low-activity carbon. If radioactive decay is responsible for the decrease in carbon-14 activity, the age of this ground water is about 3,000 years; if isotope dilution is responsible for the decrease in carbon-14 activity, the age is essentially modern but greater than 40 years old to account for the lack of tritium.

Mass-Balance Modeling of Carbonate-Saturated Samples

The recharge samples had large concentrations of tritium or were undersaturated with dolomite and calcite. All of the remaining samples (samples 9 through 34, table 8) have small concentrations of tritium and are saturated or supersaturated with dolomite and calcite. These samples will be referred to as the carbonate-saturated samples. For these samples, the mass-balance modeling assumes that recharge takes up carbon dioxide gas and then equilibrates with dolomite and calcite soon after it enters the saturated zone. The objective of mass-balance modeling is (1) to determine which additional geochemical reactions occur after ground water has attained equilibrium with dolomite and calcite and (2) to calculate ground-water ages for each sample. All of these samples have small concentrations of tritium and carbon-14 activities less than 50 pmc, which indicate older ground water than the recharge samples. The carbonate-saturated samples include all of the samples from deep wells (greater than 300 ft). The difficulty in mass-balance modeling these older and deeper samples is to determine the appropriate chemical and isotopic composition of the initial water to use with each sample.

Reactants and Initial Waters for Carbonate-Saturated Samples

The reactants and constraints of table 7 were used in mass-balance modeling the carbonate-saturated samples with a few modifications. The reactions that are modeled for the carbonate-saturated samples are defined to be those that occur in the saturated zone, and it is assumed that there is no additional input of carbon dioxide gas within this zone. Therefore, carbon dioxide gas was excluded as a reactant. The samples are all saturated or supersaturated with calcite, which indicates that calcite could precipitate; thus the constraint on calcite only to dissolve was removed. The constraints on cation-exchange reactions were removed for two samples as described in the text below. Ammonium and nitrate concentrations are negligible in all of the carbonate-saturated samples, and the initial waters for the mass-balance modeling contain no ammonium or nitrate. Therefore, sources and sinks for ammonium and nitrate were not needed in this mass-balance modeling.

The definition of initial water compositions for the carbonate-saturated samples is problematic. One modeling approach would be to equilibrate the recharge samples with carbonates, without allowing additional input of carbon dioxide, and use the resulting chemical compositions as initial waters for modeling the carbonate-saturated samples. Unfortunately, many of the recharge samples seem to be contaminated with nitrate and chloride, which complicates interpretation of the modeling results. It also is difficult to determine which, if any, of these samples are on flow paths that intersect the wells where the carbonate-saturated samples were obtained. Given the uncertainty in choosing an appropriate initial water composition from the limited number of recharge samples, a range of initial water compositions were used in modeling the carbonate-saturated samples. The initial waters were generated by PHREEQE by assuming equilibrium with dolomite and calcite. The appropriate isotopic composition for these initial waters was determined by interpretation of the isotopic compositions of the recharge samples.

Chemical compositions of initial waters

A ground water in equilibrium with calcite and dolomite was assumed to be an appropriate initial water for modeling the carbonate-saturated samples. However, there are many ground-water compositions that are in equilibrium with calcite and dolomite. Mass-balance models of the recharge samples indicated the predominant reaction in recharge is uptake of carbon dioxide and dissolution of dolomite. Thus, the primary factor determining the chemical composition of solutions in equilibrium with carbonates is the quantity of carbon dioxide gas that enters solution in the unsaturated zone. The more carbon dioxide gas that dissolves, the larger the calcium and magnesium concentrations that are necessary to produce equilibrium with dolomite and calcite.

PHREEQE was used to calculate five water compositions that are representative of the range of possible water compositions that would occur soon after water entered the saturated zone. The quantity of carbon dioxide in the mass-balance models for the recharge samples ranged from less than 2.0 to more than 4.0 mmol/L (table 11). The compositions of the initial waters were generated with PHREEQE by assuming that 2.0, 2.5, 3.0, 3.5, or 4.0 mmol/L carbon dioxide gas dissolved in rainwater, which was concentrated tenfold, and that dolomite and calcite reacted to equilibrium. The resulting solution compositions are listed in table 10 (solutions 2 through 6).

The magnitudes of mineral mass transfers in the mass-balance modeling of the carbonate-saturated waters depend largely on the calcium, magnesium, and carbon concentrations of the initial waters. The five simulated initial waters have a relatively large range in the concentrations of these elements. Silica concentrations were assumed to be 18 mg/L, the median concentration in recharge (32 samples described in the recharge section). The net decrease in silica concentrations is relatively small and has a small effect on the overall mineral mass transfers.

The sodium concentration in the initial waters was assumed to be 0.06 mmol/L, which is 10 times the concentration in rainwater (table 2). Many of the recharge samples have larger concentrations of sodium. In the mass-balance models for the recharge samples, the additional sodium is derived mostly from cation exchange. The initial water compositions are intended to incorporate all of the reactions that occur during recharge up to the point of carbonate equilibration in the saturated zone; thus the initial water compositions should include some sodium contribution from cation exchange. The quantity of cation exchange in mass-balance models for the recharge samples was variable, but generally was less than 1.0 mmol/L, which accounts for less than 2 mmol/L of sodium. By not including any of the cation exchange reactions in the initial water compositions, the quantity of cation exchange calculated in the mass-balance modeling may overestimate the quantity that occurs after carbonate equilibration, but only by about 1.0 mmol/L or less.

Carbon-isotope compositions of initial waters

The measured isotopic compositions of the recharge samples are not directly applicable to define the isotopic composition of the initial waters because six of the eight recharge samples are undersaturated with dolomite and calcite, whereas the initial waters are defined to be saturated with these carbonates. Furthermore, large tritium concentrations in seven of the recharge samples indicate contamination by carbon-14 from atmospheric nuclear testing. To use isotopic compositions of the carbonate-undersaturated recharge samples, first it is necessary to estimate what the isotopic composition would be after equilibration with dolomite and calcite. It also is necessary to make some adjustment for the effects of atmospheric nuclear testing on carbon-14 activities.

PHREEQE was used on the carbonate-undersaturated recharge samples (samples 2, 3, 4, 5, 7, and 8) to calculate the quantity of dolomite and calcite that would react to attain equilibrium in a system closed to carbon dioxide. Dolomite dissolution is the predominant reaction with mass transfers in the range from 0.3 to 1.1 mmol/L water (table 13). The calculations indicate only minor quantities of calcite dissolution or precipitation would occur. The mass transfers of dolomite that must dissolve to attain equilibrium (table 13) are similar to the mass transfers in the mass-balance models for these samples (table 11). Thus, for the recharge samples that are undersaturated with carbonate minerals, about half of the dolomite necessary for carbonate equilibrium would dissolve in the saturated zone, which is closed to carbon dioxide.

What is the effect of these carbonate-equilibration reactions on the $\delta^{13}C$ of the ground water? The $\delta^{13}C$ of the ground waters after carbonate equilibration can be calculated given the $\delta^{13}C$ of the ground-water samples, the $\delta^{13}C$ of the dissolving phases, and the mass transfers calculated from PHREEQE. The equations of Wigley, Plummer, and Pearson (1978, 1979) were used to calculate the $\delta^{13}C$ of the ground waters after carbonate equilibration. The calculated $\delta^{13}C$ values range from -12.2 to -16.6 per mil (table 13). The measured $\delta^{13}C$ of the other two recharge samples, which were not substantially undersaturated with car-

bonates, are -10.0 and -12.5 per mil. The $\delta^{13}C$ calculations for the carbonate-undersaturated samples and the measurements of $\delta^{13}C$ for the other two samples indicate that the initial solutions for mass-balance modeling should have $\delta^{13}C$ that range from -10.0 to -16.6 per mil.

All but one of the carbonate-undersaturated recharge samples have large tritium concentrations, which indicate that the carbon-14 activities are probably contaminated by carbon-14 produced during atmospheric nuclear testing. No method is available to determine what the carbon-14 activities would have been if no contamination were present in the samples. However, it can be assumed that the maximum carbon-14 activity before atmospheric nuclear testing began was 100 pmc. The effects of carbonate equilibration on carbon-14 activities were calculated using the measured carbon-14 activities or 100 pmc, whichever was smaller. The calculated carbon-14 activities after equilibration with dolomite and calcite range from 54 to 86 pmc.

Because these calculations do not indicate a specific carbon-14 activity that is appropriate for the initial waters, a range of carbon-14 activities was used to estimate ground-water ages for the carbonate-undersaturated samples. In one extreme, if carbonate-mineral equilibration occurs in the unsaturated zone at isotopic equilibrium with carbon dioxide gas, the carbon-14 activity in water entering the saturated zone could have an activity of 100 pmc. In the other extreme, if carbon dioxide gas entered solution in the unsaturated zone and carbonate-mineral equilibration occurred in the saturated zone (without additional input of carbon dioxide gas), the water in the saturated zone would have an activity of about 50 pmc before any radioactive decay occurred. Carbon-14 ages for the carbonate-undersaturated samples were calculated by assuming the initial waters had carbon-14 activities of 50 pmc and 100 pmc. The ages calculated with these two activities should span the range of possible ground-water ages caused by uncertainties in the carbon-14 activity in recharge.

Mass-balance models

The conceptual model for the evolution of the initial waters is that rainwater is concentrated tenfold; carbon dioxide from the unsaturated zone dissolves (2.0 to 4.0 mmol/L); and dolomite and calcite dissolve to equilibrium. The mass-balance modeling calculates the reactions necessary to produce the compositions of the carbonate-saturated samples from these initial waters. The reactions are assumed to occur in a system that is closed to carbon dioxide gas.

The calculations attempted to find mass-balance models for each of the carbonate-saturated samples by using each of the five simulated initial waters. Most samples had several models for each of two or more of the initial waters. A selection of mass-balance results for each sample are presented in table 14. Only one model is presented for each unique set of reactants and products. The petrographic data does not indicate that calcite is precipitating in the aquifer. Thus, models that

Table 13. Calculated mass transfers and carbon-isotope compositions that result from equilibration of carbonate-undersaturated samples with dolomite and calcite

[C–14, carbon–14 activity: pmc, percent modern carbon. $\delta^{13}C$, carbon–13 value relative to Peedee belemnite (PDB). Geologic unit: Hnss, Hennessey Group; GbWg, Garber Sandstone and Wellington Formation; CCGA, Chase, Council Grove, and Admire Groups; u, well completed in unconfined part of the unit. Depth category: Shallow indicates wells less than 300 feet deep. C–14 for calculation: if the measured carbon–14 activity was greater than 100 pmc, then 100 percent modern carbon was used in the calculations, otherwise the measured value was used. Mass transfer: mmol/L, millimoles per liter]

Sample number	Geologic unit	Depth category	Measured C–14 (pmc)	C–14 for calculation (pmc)	Mass transfer to attain equilibrium		Calculated after equilibration	
					Dolomite (mmol/L)	Calcite (mmol/L)	$\delta^{13}C$ (per mil)	C–14 (pmc)
2	GbWg,u	Shallow	70	70	0.47	0.07	–15.8	54
3	GbWg,u	Shallow	123	100	.65	.00	–12.2	71
4	GbWg,u	Shallow	113	100	1.10	–.10	–16.6	68
5	GbWg,u	Shallow	109	100	.34	–.18	–15.2	86
7	CCGA	Shallow	115	100	.76	–.04	–13.1	78
8	CCGA	Shallow	91	91	.30	.06	–14.3	74

precipitated calcite were considered to be less likely than other models. However, calcite precipitation is thermodynamically possible, and it is important to understand the sensitivity of the carbon-14 ages to this possibility. To simplify the table and eliminate less plausible models, a model that precipitated calcite was included in table 14 only if the carbon-14 age for the model was the youngest or oldest age for a sample. The reactants are now discussed individually in the order in which they are listed in table 14.

The initial solution number, corresponding to solutions in table 10 (solutions 2 through 6), is given for each model. All five initial waters were used in the mass-balance models, although four was the maximum number of initial waters used in modeling an individual sample.

Models that precipitate calcite generally were excluded from the table because the petrographic data did not indicate that calcite is precipitating in the aquifer. However, models that precipitate calcite can have ages as much as 4,500 years younger than models in which calcite dissolves or does not react. Generally, the ages for calcite-precipitation models are not more than 1,000 years older or younger than other models. All models for sample 31 precipitate calcite. This sample had the largest concentration of sulfate and it is likely that increased calcium concentrations due to dissolution of large quantities of gypsum caused precipitation of calcite from this ground water. For models that dissolve calcite, the mass transfer of calcite generally is less than about 1 mmol/L.

Dolomite dissolution is generally less than 1 mmol/L, except in models that precipitate calcite. Models that precipitate calcite have larger mass transfers of dolomite, but still less than 2 mmol/L. Some of the models for sample 31 (models 1 through 3) have large mass transfers of dolomite, but these models imply unrealistically light $\delta^{13}C$ of the initial solution and are not considered possible.

Kaolinite precipitation is small for most models, less than 0.1 mmol/L, unless there are large mass transfers of plagioclase or chlorite. All models for sample 31 require either plagioclase or chlorite dissolution, and kaolinite precipitation is as large as 1.68 mmol/L for this sample. Silica precipitates in all mass-balance models in which there is a mass transfer of silica. Chlorite mass transfers generally are small (less than 0.15 mmol/L), but potentially represent a substantial source of magnesium to solution because of the large stoichiometric coefficient of magnesium in the chlorite chemical formula. Mass transfers of potassium feldspar are small, less than 0.12 mmol/L in all models.

Plagioclase mass transfers are relatively large (greater than 0.3 mmol/L) in models for eight samples. Only one of these samples was from the unconfined Garber Sandstone and Wellington Formation (sample 11); seven of the samples were from the confined Garber Sandstone and Wellington Formation or from the Chase, Council Grove, and Admire Groups.

In general, cation-exchange reactions have the largest mass transfers in each mass-balance model. Only two models have no cation exchange. The quantities of exchange in the models range from a small quantity of reverse exchange to more than 22.0 mmol/L. No models were found for samples 16 and 17 unless the constraints on the cation-exchange reaction were removed. Removing these constraints allowed reverse cation exchange, which puts sodium onto clays and releases calcium and magnesium into solution. Sample 16 requires purely reverse cation exchange. Introduction of ground water with relatively larger sodium concentrations to a zone with clays that are equilibrated with relatively smaller sodium concentrations could cause reverse exchange. The well in question is a high-capacity municipal well, and it is possible that pumpage caused upconing of more saline water, which resulted in reverse cation exchange.

The quantities of cation exchange tend to be larger in models for samples from the Chase, Council Grove, and Admire Groups and the confined part of the Garber Sandstone and Wellington Formation (generally greater than 2.0 mmol/L) than for samples from the unconfined part of the Garber Sandstone and Wellington Formation (generally less than 2.0 mmol/L). All of the mass-balance models for the evolution of sodium bicarbonate waters require large quantities of cation exchange. No other reactants can account for water compositions with large sodium and bicarbonate concentrations and small calcium and magnesium concentrations.

Only four samples have mass transfers of more than 1 mmol/L gypsum (samples 22, 29, 31, and 33). Sample 31 has a mass transfer of almost 37.0 mmol/L. This is the only sample that has a saturation index for gypsum that indicates saturation. Most models require a small quantity of gypsum to dissolve (less than 1 mmol/L). Models for some of the samples have negative mass transfers of gypsum. The saturation indices indicate gypsum cannot be precipitating from any of these ground waters. The negative mass transfers are small and probably indicate the uncertainty in sulfate concentrations in the initial water. It is possible that precipitation of barite causes a decrease in sulfate concentrations. Barite saturation indices generally indicate saturation or supersaturation (fig. 18). Selective extractions indicate there is exchangeable barium in the clays, and this could be the source of barium for barite precipitation. No detailed models of this reaction were

Table 14. Selected mass-balance models for carbonate-saturated samples

[Units are millimoles per liter unless otherwise noted. "--" indicates that the mineral is not included in the mass-balance model. $\delta^{13}C$ is carbon–13 value relative to Peedee belemnite (PDB). Geologic unit: Hnss, Hennessey Group; GbWg, Garber Sandstone and Wellington Formation; CCGA, Chase, Council Grove, and Admire Groups; u, well completed in unconfined part of the unit; c, well completed in the confined part of the unit. Depth category: Shallow indicates wells less than 300 feet deep; Deep indicates wells greater than 300 feet deep. Ca-Mg/Na exchange: cation-exchange reaction with equal quantities of calcium and magnesium going onto the exchanger and sodium being released. Ca/Na exchange: cation-exchange reaction with calcium going onto the exchanger and sodium being released. Brine: mL/L, milliliters per liter; this is the volume of the hypothesized brine phase that is added to the initial water to account for the chloride concentration of the final water. Each milliliter of brine contains 6.23 millimoles of chloride and other major ions (entire composition is listed in table 7). Implied $\delta^{13}C$ of initial water is calculated to be consistent with the mass-balance model and the measured $\delta^{13}C$ of the ground-water sample. Minimum age is calculated by assuming carbon–14 activity in the initial water was 50 percent modern carbon; maximum age assumed 100 percent modern carbon]

Sample number	Geologic unit	Depth category	Model number	Solution number	Calcite	Dolomite	Kaolinite	Silica	Chlorite	Potassium feldspar	Plagioclase	Ca-Mg/Na exchange	Ca/Na exchange	Gypsum	Brine (mL/L)	Implied $\delta^{13}C$ of initial solution (per mil)	Age	
																	Minimum (years)	Maximum (years)
9	GbWg,u	Shallow	1	2	–1.12	0.68	–0.06	–0.17	--	0.11	--	2.25	--	0.60	2.04	–14.9	7,500	13,000
			2	2	--	.12	–.06	–.17	--	.11	--	1.13	1.12	.60	2.04	–13.7	9,500	15,500
			3	2	.24	--	–.06	–.17	--	.11	--	.89	1.36	.60	2.04	–13.8	9,500	15,500
			4	3	--	--	–.06	–.17	--	.11	--	1.27	1.12	.60	2.04	–13.5	10,000	16,000
10	GbWg,u	Shallow	1	3	--	--	–.04	–.26	--	.07	--	.93	--	–.02	.01	–13.1	14,500	20,000
11	GbWg,u	Shallow	1	4	--	.31	–.02	–.20	--	.05	--	.14	--	–.04	.05	–9.6	0	5,500
			2	4	.17	.22	–.02	–.20	--	.05	--	--	.14	–.04	.05	–9.6	0	5,500
			3	5	--	--	–.02	–.20	--	.05	--	.14	--	–.04	.05	–9.5	1,000	6,500
			4	5	--	--	–.02	–.20	--	.05	--	--	.14	–.04	.05	–9.5	1,000	6,500
			5	5	--	--	–.24	–.64	--	.05	0.33	--	--	–.04	.06	–9.5	1,000	6,500
12	GbWg,u	Shallow	1	3	--	--	--	–.14	--	--	--	.09	--	–.09	.05	–17.0	6,000	12,000
13	GbWg,u	Shallow	1	4	–.32	.18	–.02	–.15	--	.05	--	1.45	--	.35	.53	–14.4	500	6,000
			2	4	--	--	–.02	–.15	--	.05	--	1.09	.32	.35	.53	–14.1	1,000	6,500
			3	4	--	--	–.06	–.18	0.03	.05	--	1.50	--	.35	.53	–14.1	1,000	6,500
14	GbWg,u	Deep	1	2	--	.27	–.01	–.17	--	.03	--	1.96	--	–.02	--	–10.3	20,000	26,000
			2	2	.53	--	–.01	–.17	--	.03	--	1.42	.60	–.02	--	–10.4	20,000	26,000
			3	3	--	--	–.01	–.17	--	.03	--	1.92	--	–.03	--	–10.1	21,000	27,000
15	GbWg,u	Deep	1	3	–.40	.44	–.05	–.34	--	.11	--	3.26	--	.18	.89	–12.9	8,500	14,000
			2	3	--	.23	–.05	–.34	--	.11	--	2.85	.40	.18	.89	–12.6	9,000	14,500
			3	3	.47	--	–.05	–.34	--	.11	--	2.38	.87	.18	.89	–12.7	9,000	14,500
			4	3	--	.11	–.12	–.40	.06	.11	--	3.24	--	.18	.89	–12.5	9,500	15,000
			5	4	--	--	–.05	–.34	--	.11	--	2.72	.41	.18	.89	–12.3	10,000	15,500
			6	4	--	--	–.11	–.40	.06	.11	--	3.30	--	.18	.89	–12.3	10,000	15,500

Table 14. Selected mass-balance models for carbonate-saturated samples—Continued

Sample number	Geologic unit	Depth category	Model number	Solution number	Calcite	Dolomite	Kaolinite	Silica	Chlorite	Potassium feldspar	Plagioclase	Ca-Mg/Na exchange	Ca/Na exchange	Gypsum	Brine (mL/L)	Implied $\delta^{13}C$ of initial solution (per mil)	Age: Minimum (years)	Age: Maximum (years)
16	GbWg,u	Deep	1	3	--	0.01	–0.03	–0.16	--	0.05	--	--	–0.12	–0.07	0.17	–11.4	7,000	12,500
			2	3	--	--	–.03	–.16	--	.05	--	–0.12	--	–.07	.17	–11.4	7,000	12,500
			3	3	--	--	–.04	–.17	0.02	.05	--	--	–.12	–.07	.17	–11.4	7,000	12,500
17	GbWg,u	Deep	1	2	--	.05	–.01	–.17	--	.03	--	.31	–.30	–.08	.03	–13.5	4,000	10,000
			2	2	0.10	--	–.01	–.17	--	.03	--	.22	–.21	–.08	.03	–13.5	4,000	10,000
			3	3	–.39	--	–.02	–.18	--	.03	--	.62	–.62	–.08	.03	–13.3	4,500	10,000
18	GbWg,u	Deep	1	2	.23	--	–.02	–.24	--	.05	--	.53	.18	–.04	.04	–15.6	6,500	12,500
			2	2	--	.12	–.02	–.24	--	.05	--	.71	--	–.04	.04	–15.6	6,500	12,500
			3	2	.22	--	–.04	–.26	.02	.05	--	.71	--	–.04	.04	–15.6	6,500	12,500
			4	3	–.09	--	–.02	–.24	--	.05	--	.78	--	–.04	.04	–15.2	7,000	13,000
19	GbWg,u	Deep	1	2	.18	--	–.02	–.14	--	.04	--	.16	--	–.06	.04	–14.1	3,500	9,000
20	GbWg,u	Deep	1	3	--	.23	–.01	--	--	.02	--	.91	--	–.02	.04	–10.5	0	5,000
			2	3	.46	--	–.01	--	--	.02	--	.56	.35	–.02	.04	–10.6	0	5,000
			3	4	--	--	–.01	--	--	.02	--	.91	--	–.02	.04	–10.4	0	5,500
21	GbWg,c	Deep	1	5	–.79	1.12	–.01	–.19	--	.02	--	5.09	--	.73	.04	–9.6	8,500	14,500
			2	5	--	.73	–.01	–.19	--	.02	--	4.30	.79	.73	.04	–9.6	9,500	15,500
			3	5	1.45	--	–.01	–.19	--	.02	--	2.85	2.24	.73	.04	–9.8	9,500	15,500
			4	6	--	.33	–.14	–.32	.13	.02	--	5.18	--	.73	.04	–9.5	10,500	16,500
22	GbWg,c	Deep	1	5	–2.65	1.85	--	–.14	--	--	--	6.51	--	2.61	.08	–6.4	31,000	36,500
			2	5	--	.53	--	–.14	--	--	--	3.87	2.65	2.61	.08	–7.5	34,000	39,500
			3	6	.74	--	--	–.14	--	--	--	3.11	3.39	2.61	.08	–7.7	34,500	40,000
23	GbWg,c	Deep	1	3	–.32	.66	--	–.13	--	--	--	3.52	--	.26	.04	–10.9	10,500	16,500
			2	3	--	.50	--	–.13	--	--	--	3.20	.32	.26	.04	–10.8	11,000	17,000
			3	3	1.00	--	--	–.13	--	--	--	2.20	1.32	.26	.04	–11.0	11,000	17,000
			4	3	--	.44	–.05	–.18	.05	--	--	3.57	--	.26	.04	–10.8	11,500	17,000
			5	4	.17	--	–.10	–.23	.10	--	--	3.52	--	.26	.04	–10.6	12,500	18,000
			6	5	--	--	–.32	–.77	--	--	0.47	2.86	.48	.26	.04	–10.5	12,500	18,500
			7	5	--	--	–.07	–.20	.07	--	--	3.51	--	.26	.04	–10.5	12,500	18,500

Table 14. Selected mass-balance models for carbonate-saturated samples—Continued

Sample number	Geologic unit	Depth category	Model number	Solution number	Calcite	Dolomite	Kaolinite	Silica	Chlorite	Potassium feldspar	Plagioclase	Ca-Mg/Na exchange	Ca/Na exchange	Gypsum	Brine (mL/L)	Implied $\delta^{13}C$ of initial solution (per mil)	Age: Minimum (years)	Age: Maximum (years)
24	GbWg,c	Deep	1	3	–0.22	0.46	–0.01	–0.14	--	0.02	--	2.12	--	--	0.02	–11.1	10,000	16,000
			2	3	--	.35	–.01	–.14	--	.02	--	1.90	0.22	--	.02	–11.1	10,500	16,000
			3	3	.71	--	–.01	–.14	--	.02	--	1.19	.93	--	.02	–11.2	10,500	16,000
			4	3	--	.31	–.04	–.17	0.03	.02	--	2.12	--	--	.02	–11.0	10,500	16,500
			5	5	--	--	–.01	–.14	--	.02	--	1.83	.23	--	.02	–10.8	11,500	17,500
			6	4	--	--	–.38	–.89	--	.02	0.56	1.52	.41	--	.02	–10.8	11,500	17,500
			7	5	--	--	–.04	–.17	.03	.02	--	2.12	--	--	.02	–10.8	11,500	17,500
25	GbWg,c	Deep	1	3	--	.37	--	–.13	--	--	--	2.94	--	--	.02	–11.5	15,000	20,500
			2	3	.71	--	--	–.13	--	--	--	2.20	.75	--	.02	–11.7	15,000	20,500
			3	4	.16	--	–.04	–.17	.04	--	--	2.94	--	--	.02	–11.3	16,000	21,500
			4	4	--	--	–.36	–.86	--	--	.54	2.53	.23	--	.02	–11.2	16,000	22,000
			5	4	--	--	–.24	–.58	.03	--	.31	2.83	--	--	.02	–11.2	16,000	22,000
26	GbWg,c	Deep	1	3	–.62	.83	--	–.10	--	--	--	3.79	--	0.61	.05	–10.5	23,000	29,000
			2	3	--	.52	--	–.10	--	--	--	3.18	.62	.61	.05	–10.5	24,000	30,000
			3	3	1.03	--	--	–.10	--	--	--	2.14	1.65	.61	.05	–10.7	24,000	30,000
			4	4	--	.09	–.10	–.21	.10	--	--	3.69	--	.61	.05	–10.2	25,500	31,000
			5	5	--	--	–.20	–.52	--	--	.31	2.79	.73	.61	.05	–10.2	25,500	31,500
			6	5	--	--	–.08	–.18	.08	--	--	3.72	--	.57	.05	–10.2	25,500	31,500
27	GbWg,c	Deep	1	3	–.38	.46	--	–.10	--	--	--	2.99	--	.44	.03	–11.3	20,500	26,500
			2	3	--	.27	--	–.10	--	--	--	2.61	.38	.44	.03	–11.2	21,000	27,000
			3	3	.53	--	--	–.10	--	--	--	2.08	.91	.44	.03	–11.3	21,000	27,000
			4	3	--	.15	–.06	–.16	.06	--	--	2.96	--	.44	.03	–11.1	21,500	27,500
			5	4	--	--	--	–.10	--	--	--	2.41	.42	.44	.03	–11.0	22,000	28,000
			6	4	--	--	–.05	–.16	.05	--	--	2.96	--	.43	.03	–11.0	22,000	28,000
28	GbWg,c	Deep	1	3	–.53	.49	–.01	–.12	--	.02	--	2.68	--	.28	.58	–11.2	18,500	24,000
			2	3	--	.23	–.01	–.12	--	.02	--	2.15	.53	.28	.58	–11.1	19,500	25,000
			3	3	.45	--	–.01	–.12	--	.02	--	1.70	.98	.28	.58	–11.2	19,500	25,000
			4	4	--	--	–.01	–.12	--	.02	--	2.04	.53	.28	.58	–10.9	20,000	26,000
29	GbWg,c	Deep	1	3	–3.38	1.82	–.01	–.07	--	.02	--	3.50	--	4.22	.03	–10.6	29,000	34,500
			2	3	--	.13	–.01	–.07	--	.02	--	--	3.44	4.22	.03	–10.6	34,500	40,500
			3	3	.26	--	–.01	–.07	--	.02	--	--	3.53	4.22	.03	–10.6	34,500	40,500
			4	4	--	--	.00	–.05	--	.01	--	.20	3.18	4.06	.03	–10.5	35,000	41,000

Table 14. Selected mass-balance models for carbonate-saturated samples—Continued

Sample number	Geologic unit	Depth category	Model number	Solution number	Calcite	Dolomite	Kaolinite	Silica	Chlorite	Potassium feldspar	Plagioclase	Ca-Mg/Na exchange	Ca/Na exchange	Gypsum	Brine (mL/L)	Implied $\delta^{13}C$ of initial solution (per mil)	Age	
																	Minimum (years)	Maximum (years)
30	GbWg,c	Deep	1	3	--	0.25	–0.01	--	--	0.02	--	0.70	--	--	0.03	–9.6	500	6,000
			2	3	0.49	--	–.01	--	--	.02	--	.14	0.53	--	.03	–9.7	500	6,000
			3	4	--	--	–.02	--	--	.03	--	.66	--	--	.03	–9.5	1,500	7,000
31	GbWg,c	Deep	1	2	–31.05	13.95	–1.67	–3.63	--	.11	2.43	21.60	--	37.09	.99	<–99.9	–113,500	–108,000
			2	2	–28.61	12.73	–.38	–.69	0.33	.11	--	22.43	--	37.09	.99	<–99.9	–103,500	–98,000
			3	2	–9.45	3.15	–1.67	–3.63	--	.11	2.43	--	21.60	37.09	.99	<–99.9	–14,500	–9,000
			4	3	–5.68	.83	–.48	–.79	.43	.11	--	--	22.42	37.09	.99	–14.9	8,000	13,500
			5	6	–6.48	--	–.78	–1.09	.73	.11	--	2.26	20.18	37.14	.99	–11.1	14,500	20,500
			6	6	–6.48	--	–1.68	–3.13	.50	.11	1.69	--	21.87	37.14	.99	–11.1	14,500	20,500
			7	5	–5.38	--	–.62	–.93	.57	.11	--	--	22.15	37.04	.99	–11.6	14,500	20,500
32	GbWg,c	Deep	1	3	–.33	.36	--	--	--	--	--	1.53	--	.19	.02	–11.0	8,500	14,000
			2	3	--	.20	--	--	--	--	--	1.21	.33	.19	.02	–11.0	9,000	14,500
			3	3	.40	--	--	--	--	--	--	.80	.73	.19	.02	–11.0	9,000	14,500
			4	4	--	--	--	--	--	--	--	1.14	.39	.19	.02	–10.8	9,500	15,500
			5	4	--	--	–.04	–.06	.04	--	--	1.61	--	.17	.02	–10.8	9,500	15,500
33	CCGA	Shallow	1	4	–1.39	1.20	--	–.14	--	--	--	4.99	--	1.33	.14	–12.0	26,000	31,500
			2	4	--	.50	--	–.14	--	--	--	3.60	1.39	1.33	.14	–11.5	28,000	33,500
			3	4	1.01	--	--	–.14	--	--	--	2.59	2.40	1.33	.14	–11.7	28,000	33,500
			4	6	--	.08	–.01	–.16	--	.01	--	3.37	1.44	1.31	.14	–11.2	29,000	35,000
			5	6	.17	--	–.01	–.16	--	.01	--	3.20	1.61	1.31	.14	–11.2	29,000	35,000
			6	6	--	--	–.38	–.91	--	--	.57	3.20	1.60	1.33	.14	–11.1	29,500	35,000
			7	6	--	--	–.08	–.21	.08	--	--	3.96	1.03	1.33	.14	–11.1	29,500	35,000
34	CCGA	Deep	1	4	--	.74	--	–.14	--	--	--	4.01	--	--	.04	–11.2	3,500	9,500
			2	4	1.48	--	--	–.14	--	--	--	2.53	1.55	--	.04	–11.4	3,500	9,500
			3	6	.34	--	–.08	–.23	.08	--	--	3.96	--	--	.04	–10.8	5,500	11,000
			4	6	--	--	–.76	–1.68	--	--	1.15	3.12	.46	--	.04	–10.7	5,500	11,500
			5	6	--	--	–.52	–1.12	.06	--	.69	3.73	--	--	.04	–10.7	5,500	11,500

calculated because it has little effect on other mass transfers or the carbon-14 ages.

Most models have small mass transfers of brine (less than 0.06 mL/L or about 0.4 mmol/L chloride), which accounts for the chloride concentrations in the samples. Five samples have mass transfers of brine that are more than 0.5 mL/L (about 3.0 mmol/L chloride).

Carbon Isotopes

In the modeling process, an implied $\delta^{13}C$ of the initial water was calculated for each model (table 14). These implied $\delta^{13}C$ values were used to eliminate mass-balance models by comparing them to the expected range of -10.0 to -16.6 per mil (derived from the recharge samples and table 13). Except for one sample, the implied $\delta^{13}C$ values for the initial water for all models are in the range of -9.5 to -17.0 per mil (table 14), which is essentially the same as the expected range. Some models for sample 31 could be eliminated because they implied $\delta^{13}C$ values for the initial water that were less than -24.0 per mil, which is substantially outside the expected range.

Carbon-14 ages of the carbonate saturated samples range from modern to 40,000 years (table 14). Uncertainty in the ground-water ages is caused by uncertainty in the carbon-14 activity of the initial water and by differences among mass-balance models for a sample. Reasonable values for the initial water carbon-14 activity range from 50 pmc to 100 pmc. This range in the carbon-14 activity of the initial water introduces an uncertainty in the ground-water ages of about 6,000 years, or one half-life of carbon-14.

For most samples, the range in ages that results from differences among the mass-balance models is 2,000 years or less. Four samples have models that differ in carbon-14 age by more than 2,500 years. For each of these samples, the model with the youngest age (table 14) is a model that dissolves dolomite and precipitates calcite.

The calculated carbon-14 ages could be too old if recrystallization or solid-liquid isotopic exchange occurs between carbonate minerals and ground water. The amount of isotopic exchange that is consistent with the $\delta^{13}C$ data could not be quantified because many of the ground-water $\delta^{13}C$ measurements are close to isotopic equilibrium with dolomite and calcite. Thus, a large quantity of isotopic exchange would produce little or no change in the $\delta^{13}C$ of the ground water. The occurrence of solid-liquid isotopic exchange has been discounted because of the limited quantity of calcite in the aquifer and because there is no petrographic evidence of calcite recrystallization or dedolomitization. Other processes that could make the calculated carbon-14 ages too old are diffusion of carbon-14 into dead-end pores, the presence of very slow-moving zones of the flow system (Sudicky and Frind, 1981), or sorption of carbon-14 on the surfaces of aquifer material. There is no way to evaluate the importance of these processes with the available data.

The ground-water ages can be corroborated qualitatively by examining the δD measurements of the ground-water samples. δD values are expected to have been lighter in the past because of a cooler climate during the last glaciation. δD is plotted against the minimum ages of table 14 (fig. 23); recharge samples also are plotted. The curve shown is a smooth of the data (method 3RSSH, P-STAT, Inc., 1989). The minimum ages of table 14 were used because these ages produced the youngest ages for the plateau of minimum δD values, which should correspond with the glacial maximum. The age of the glacial maximum is qualitatively consistent with the results for ground water in New Mexico (Phillips, Peeters, and Tansey, 1986), European ground waters (Rozanski, 1985), and, by assuming $\delta^{18}O$ is directly proportional to δD, coral reefs in the Caribbean Sea (Fairbanks, 1989) and Antarctic ice cores (Lorius and others, 1985). All of these records demonstrate a transition from the glacial to the present interglacial period. The records show (or imply in $\delta^{18}O$ records) δD that is 10 to 30 per mil lighter than modern values until the transition to heavier, modern values that began from 15,000 to 5,000 years ago.

Discussion

The mass-balance models indicate that the predominant reaction that occurs in the aquifer after equilibration with carbonate minerals is cation exchange. The mass-balance models also indicate dissolution of minor quantities of dolomite, plagioclase, potassium feldspar, chlorite, and biotite and precipitation of kaolinite and, perhaps, a pure silica phase. Gypsum dissolution can account for increases in sulfate concentrations. Chloride concentrations can be accounted for by mass transfers of brine; variations in brine mass transfers among the samples indicate that introduction of brines into ground water occurs under specific local conditions within the aquifer.

Quantities of cation exchange in the unconfined part of the Garber Sandstone and Wellington Formation are relatively small (generally less than about 2 mmol/L) and are similar to the mass transfers for the recharge samples. Sodium generally is not the domi-

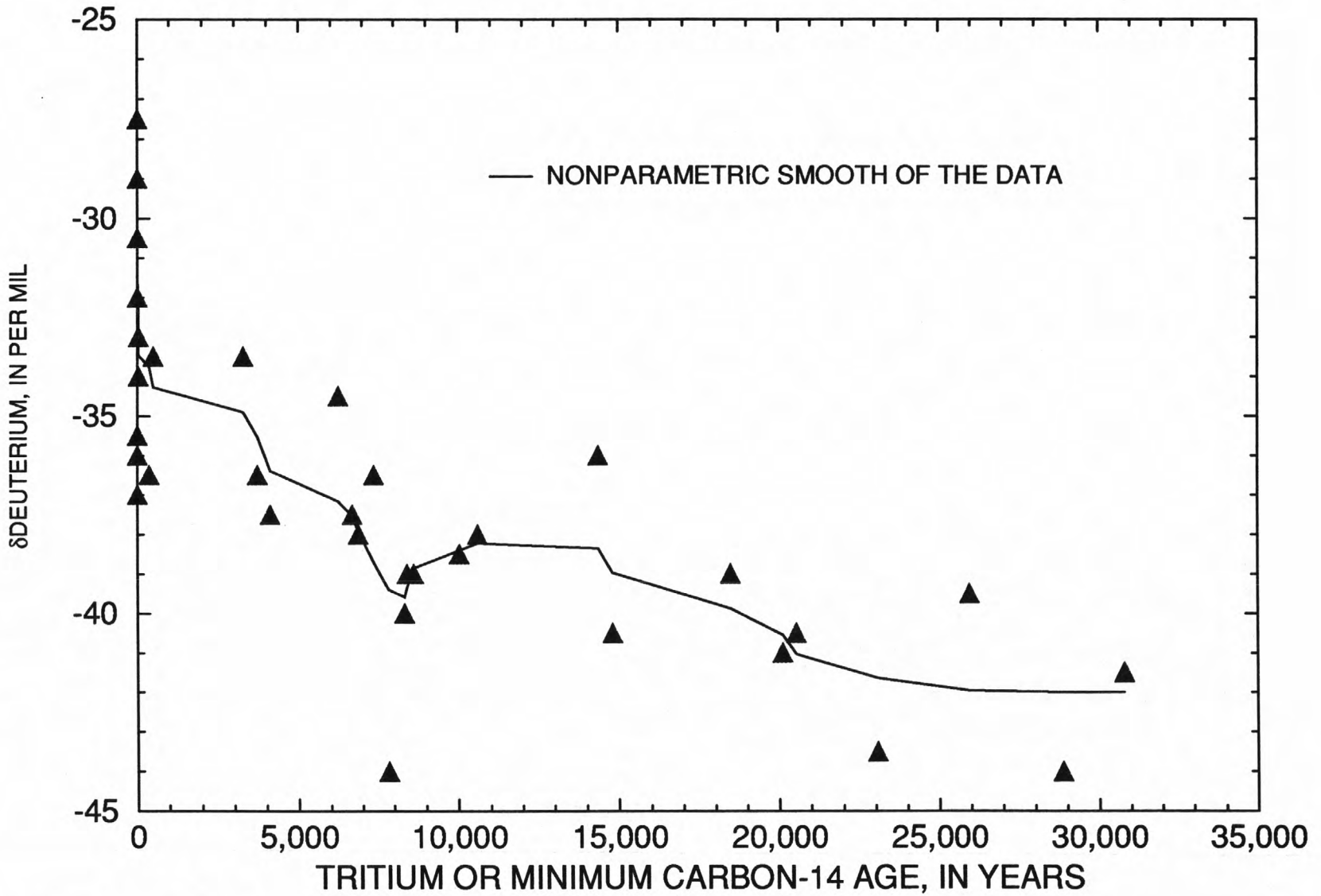

Figure 23. Relation between δDeuterium and tritium or minimum carbon–14 age in water samples from the Central Oklahoma aquifer.

nant cation in water from this part of the aquifer; the major ions here are calcium, magnesium, and bicarbonate, and pH values generally are in the range from 7.3 to 7.8. Mass transfers of cation exchange in the confined part of the Garber Sandstone and Wellington Formation and in the Chase, Council Grove and Admire Groups are larger (generally greater than 2 mmol/L). Cation exchange causes sodium generally to be the dominant cation in these parts of the aquifer; bicarbonate is the dominant anion; and pH values generally are 8.6 to 9.1.

The cation-exchange reaction puts calcium and magnesium onto the clays and releases sodium into solution. The cation-exchange measurements on clay samples are consistent with this cation-exchange reaction. Clay minerals with sufficient cation-exchange capacity and with large concentrations of exchangeable sodium have been identified in core samples (table 6). The loss of calcium and magnesium from solution due to the exchange reaction should cause some dissolution of carbonate minerals to maintain equilibrium. Reaction-path modeling indicates that less than 0.5 mmol/L of dolomite dissolves to maintain equilibrium in response to several millimoles of cation exchange. This quantity of dolomite dissolution is similar to the quantities in many of the mass-balance models. The dolomite dissolution produces equilibrium primarily by raising the pH, which increases the concentration of the carbonate ion. The large pH values for many of the samples from the confined Garber Sandstone and Wellington Formation and the Chase, Council Grove, and Admire Groups are attributed, in part, to dissolution of small quantities of dolomite. Dissolution of biotite, chlorite, plagioclase, and potassium feldspar also tend to increase the pH. Dissolution of these aluminosilicate minerals is consistent with the mass-balance models and the petrographic information. Large supersaturations of dolomite and calcite in some samples precludes dolomite or calcite dissolution. These supersaturations indicate dissolution of one or more of the aluminosilicate minerals.

Three of the four samples with mass transfers of gypsum greater than 1 mmol/L were from wells in the westernmost part of the aquifer. The western part of the aquifer is confined by the Hennessey Group, which has large concentrations of sulfate in its ground water (figs. 9 and 11). The large gypsum mass transfers in the three samples may indicate leakage of sulfate-rich ground water from the Hennessey Group. The other sample with mass transfer of gypsum greater than 1 mmol/L (and sulfate concentration greater than 1 mmol/L) was from the Chase, Council Grove, and Admire Groups. Samples from test hole 5, drilled in the Chase, Council Grove, and Admire Groups, also had large concentrations of sulfate. These large concentrations of sulfate may indicate gypsum is present locally within Chase, Council Grove, and Admire Groups.

The mass-balance models were tested to determine whether they implied initial water $\delta^{13}C$ within the range from -10.0 to -16.6 that was estimated from an analysis of the recharge samples. Except for some models for one sample, all of the models implied $\delta^{13}C$ (table 14) near the expected range, which indicates that the models are consistent with the available $\delta^{13}C$ data.

The carbon-14 ages for the carbonate-saturated samples are thousands to tens of thousands of years. Samples from the unconfined Garber Sandstone and Wellington Formation have minimum ages that generally are less than 10,000 years (table 14). Samples from the confined Garber Sandstone and Wellington Formation have minimum ages that generally are greater than 10,000 years. All of the ages have uncertainties of about 6,000 years because the appropriate carbon-14 activity in the unsaturated and shallow, saturated zone is not known. Differences among mass-balance models can cause the carbon-14 ages to differ by several thousand years for a sample, but generally the differences in ages from this cause are less than 2,000 years. The decrease in δD values with calculated carbon-14 age (fig. 23) is qualitatively consistent with other investigations, which corroborates the carbon-14 ages. Solid-liquid isotopic exchange and other processes that could cause the carbon-14 ages to be too old were assumed not to occur in the aquifer. If any of these processes do occur, the ground-water ages could be substantially younger.

GEOHYDROLOGY

The purpose of the geohydrologic investigation is to describe the major elements of the geohydrology of the Central Oklahoma aquifer. These elements include the geometry, stratigraphy, lithology, and hydraulic properties of the aquifer's geohydrologic units, the distribution of hydraulic head, and the rate of recharge and discharge. As part of the investigation a conceptual model of the aquifer was developed, which, in turn, was used to develop a numerical flow model. The numerical flow model was used with a particle-tracking model to determine flowlines and times of travel within the aquifer. The flow model was calibrated to be consistent with hydraulic heads measured in the aquifer, as well as ground-water ages (that is, the residence time since recharge) and sulfate concentrations determined as part of the geochemical investigation.

A description of the geometry, stratigraphy, and lithology of the aquifer's geohydrologic units was presented in a previous section of this report. It was necessary to present this description prior to the discussion of geochemistry. However, the rest of the discussion of geohydrology follows the discussion of geochemistry because ground-water ages, used to develop the discussion of the geohydrology, were presented in the geochemistry section.

Potentiometric Surface

A potentiometric surface is a surface that represents static head, where head is defined by the level to which water will rise in a tightly cased well. A map, called a potentiometric-surface map, can be constructed by contouring measurements of static head in wells. Where most of the flow is horizontal, a potentiometric-surface map can be used to infer the direction of ground-water flow. However, in an aquifer with substantial vertical flow, different heads will be observed in wells at a particular location but completed at different depths, and no single potentiometric surface can be mapped to represent the three-dimensional distribution of head. Thus, it is difficult to infer the direction of ground-water flow. In the Central Oklahoma aquifer head changes with depth in much of the aquifer, and vertical flow is considered to be substantial.

No attempt was made to construct a potentiometric-surface map for the deep parts of the Central Oklahoma aquifer. In wells drilled for water supplies in the Central Oklahoma aquifer, wells frequently are constructed by gravel packing over long intervals and perforating, slotting, or screening in more than one sandstone layer, each layer having a different head. In wells with this type of construction, the head measured in the well is between the highest and lowest head in the sandstone layers intercepted by the well. Because most of the deep wells in the Central Oklahoma aquifer are constructed with long gravel packs and multiple open intervals (open intervals are those zones in the well that are screened, slotted, or perforated), no potentiometric-surface map could be constructed for the deep zones of the aquifer.

A potentiometric surface was determined for the shallow parts of the Central Oklahoma aquifer by measuring water levels in shallow water wells. Water levels were measured from December 22, 1986, through April 24, 1987, from the shallowest wells that could be located, regardless of the geologic unit in which the wells were completed (fig. 24). The potentiometric surface defined by the water levels in these wells approximates the upper limit of the zone of saturation, sometimes referred to as the water table.

Examination of the water-table map reveals a great deal about the basic geohydrology of the Central Oklahoma aquifer. The most obvious feature is the general west-to-east trend of the slope of the water table. This slope of the water table is interpreted to mean that the regional trend in shallow ground-water flow is from west to east. This trend extends to the western and eastern limits of the Central Oklahoma aquifer study area, indicating that some volume of shallow ground water is entering the study unit from the west and some is discharging to the east.

Although the general trend of the water table is to slope from west to east, there is considerable local variation. Much of the local variation is caused by ground water discharging to perennial streams. The most obvious example is the water table in the vicinity of the Deep Fork in Oklahoma County. The water table slopes steeply toward this stream, and the potentiometric contours "V" pointing upstream, indicating that the Deep Fork is a major drain for the ground-water flow system.

The potentiometric contours do not "V" substantially in the vicinity of the North Canadian River, which indicates that there is little exchange of water between the aquifer and the North Canadian River. The North Canadian River is one of the larger streams in the study area based on the size of its drainage basin, and is much larger than the Deep Fork, which is a tributary to the North Canadian River. In many hydrologic systems, the main stream would be the principal discharge for the ground-water flow system, because the main stream is at a lower altitude than the tributary, and thus is the drain with the lowest head. In central Oklahoma, the situation is reversed, with the Deep Fork about 100 ft lower in altitude where the two streams are close together. Thus, the Deep Fork is thought to be the major drain for the regional ground-water flow system in the northern half of the study unit.

The water-table map shows that there are no streams that are major sources of water to the ground-water flow system. For streams that are sources of water to the ground-water flow system, the potentiometric contours "V" downstream where they intersect the streams. This configuration is not evident to any substantial degree in figure 24.

Another notable feature of the water-table map is the lack of large cones of depression from ground-water withdrawals. Although ground-water withdrawals from the Central Oklahoma aquifer are substantial (over 5 billion gallons per year every year since 1968), no large cone of depression is observed. Most large-capacity wells withdraw water from deep in the aquifer,

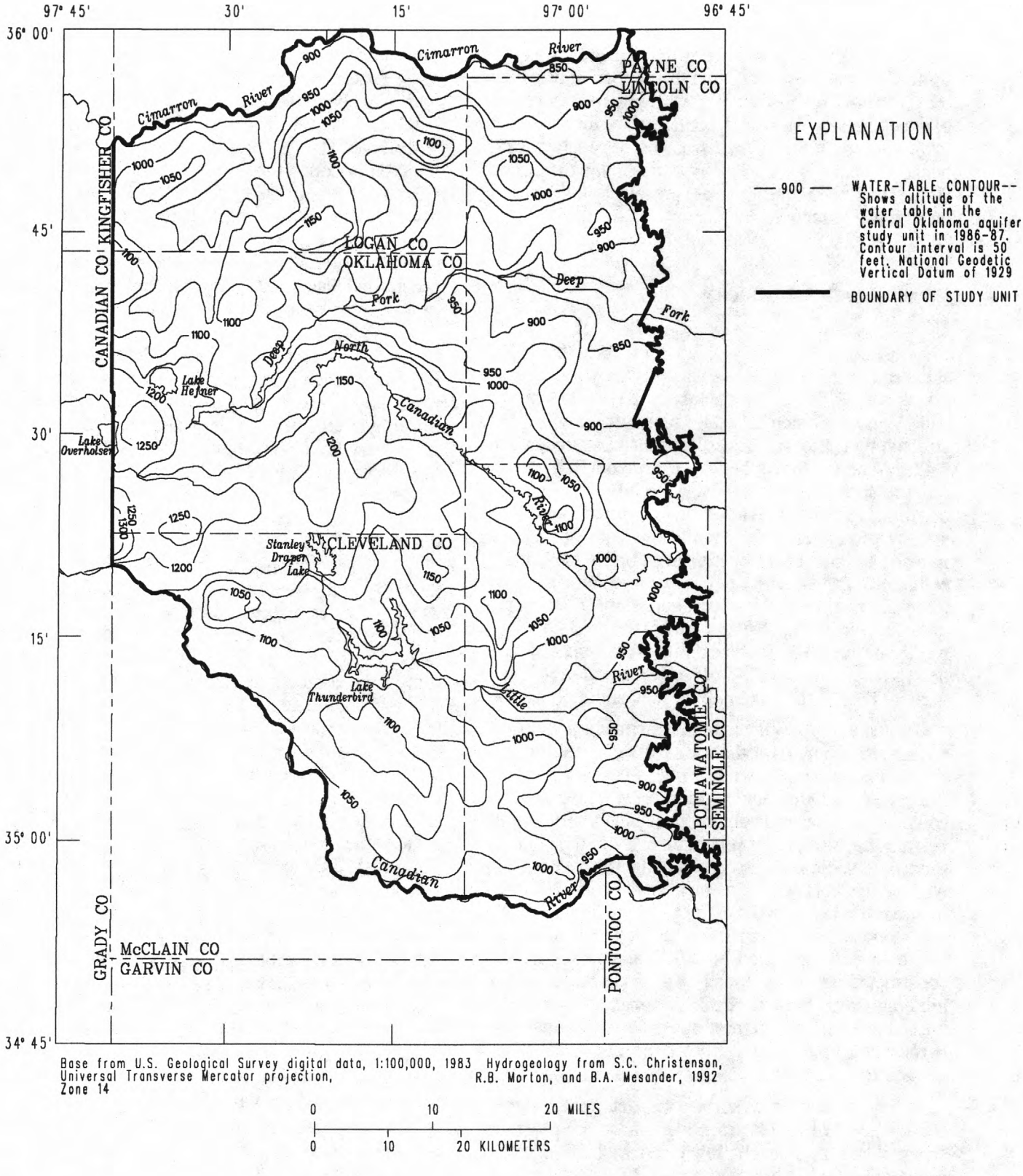

Figure 24. Altitude of the water table in the Central Oklahoma aquifer study unit, 1986–87.

and Havens (1989) documents the presence of some cones of depression at depth in the Garber Sandstone. However, the withdrawals from deep in the aquifer had not caused drawdowns in the water table when the water table map was prepared in 1987.

Hydraulic Properties

Data concerning the hydraulic properties for Permian geologic units of the Central Oklahoma aquifer were available from Wood and Burton (1968), the U.S. Geological Survey's National Water Information System (NWIS) data base, Gates, Marsh, and Fryberger (1983), drillers' logs supplied by the Oklahoma Water Resources Board, and some limited testing done as part of the Central Oklahoma aquifer NAWQA project. Because the Central Oklahoma aquifer NAWQA project is primarily concerned with the quality of the water in the Central Oklahoma aquifer, and because data were available from other sources, very little testing of hydraulic properties was done as part of the project.

Specific Capacity

The ability of a well to yield water is measured by its specific capacity. Specific capacity is computed by dividing well yield by drawdown. In the United States, yield commonly is measured in gallons per minute and drawdown commonly is measured in feet, so the units of specific capacity are gallons per minute per foot of drawdown [(gal/min)/ft]. Specific capacity is a function of the hydraulic characteristics of the well and the geohydrologic units in which the well is completed. In general, larger diameter wells will have a greater specific capacity than smaller diameter wells of equal depth in the same aquifer. Conversely, assuming the wells are constructed in a similar manner, a well with a greater specific capacity indicates a greater transmissivity than a well with a lesser specific capacity.

Specific-capacity data from all sources are summarized in table 15. Wood and Burton (1968) considered data from 51 municipal wells, most of which were 700 to 800 ft deep and were located in the central Oklahoma urban corridor along the western boundary of the study area from Norman to Edmond (fig. 2). All wells were completed in the Garber Sandstone and Wellington Formation. Specific capacities calculated from these data ranged from 0.63 to 3.3 (gal/min)/ft, and had a median specific capacity of 1.3 (gal/min)/ft.

Specific capacities available from the U.S. Geological Survey's NWIS data base also are summarized in table 15. The NWIS data base had entries for 63 wells, all completed in the Garber Sandstone, Wellington Formation, or both, for which specific capacities had been computed. The wells are a mixture of domestic and municipal wells, and ranged in depth from 20 to 1,090 ft. Specific capacities ranged from 0.16 to 15 (gal/min)/ft, and had a median of 1.1 (gal/min)/ft. Specific capacities from Gates, Marsh, and Fryberger (1983) were available from 28 wells, all of which were high-capacity municipal wells in the urban corridor along the western boundary of the study area from Norman to Edmond. Specific capacities ranged from 0.57 to 4.3 (gal/min)/ft, and had a median of 1.3 (gal/min)/ft (table 15).

The last source of specific-capacity data was drillers' logs received from the Oklahoma Water Resources Board. A total of 2,806 drillers' logs were received from the Board for Cleveland, Lincoln, Logan, Oklahoma, and Pottawatomie Counties. Of these wells, 297 had sufficient information to calculate specific capacity. Of the 297 wells, 203 were domestic wells, 59 were municipal wells, 19 were industrial wells, and 16 were for various other uses. Of the 297 wells, 252 wells were completed in the Garber Sandstone, Wellington Formation, or both, 14 wells were completed in the Chase, Council Grove, and Admire Groups, 13 wells in alluvium and terrace deposits, 7 wells in the Hennessey Group, and 11 wells in the El Reno Group or Vanoss Formation. The wells were areally distributed throughout the entire study unit, as opposed to the restricted distribution of the other sources of specific-capacity data. To compare specific capacities from drillers' logs to the other specific-capacity data for municipal wells, specific capacities were calculated first for municipal wells greater than 500 ft deep completed in either the Garber Sandstone, the Wellington Formation, or both. For the 32 deep municipal wells, specific capacities ranged from 0.58 to 3.5 (gal/min)/ft, and had a median of 1.8 (gal/min)/ft (table 15). For all 252 wells completed in the Garber Sandstone and Wellington Formation having drillers' logs with sufficient information to calculate specific capacities, specific capacities ranged from 0.050 to 5.0 (gal/min)/ft, and had a median of 0.45 (gal/min)/ft. Specific capacities in the Chase, Council Grove, and Admire Groups ranged from 0.025 to 2.4 (gal/min)/ft, and had a median of 0.36 (gal/min)/ft.

Transmissivity

Transmissivity is the rate at which water of the prevailing kinematic viscosity is transmitted through a unit width of the aquifer under a unit hydraulic gradient (Lohman, 1972). The transmissivity of the Central

Table 15. Summary statistics of specific-capacity, transmissivity, and hydraulic-conductivity data for wells completed in the Central Oklahoma aquifer

[Source of data: NWIS, U.S. Geological Survey's National Water Information System data base; WB, Wood and Burton (1968); GMF, Gates, Marsh, and Fryberger (1983); DM, drillers' logs from municipal wells greater than 500 feet deep; D, drillers' logs. Geologic unit: GbWg, Garber Sandstone and Wellington Formation, undivided; CCGA, Chase, Council Grove, and Admire Groups, undivided; d, day; ft, feet; gal, gallons; min, minute]

Hydraulic property	Source of data	Geologic unit	Sample size	Minimum	25th percentile	Median	75th percentile	Maximum
Specific capacity [(gal/min)/ft]	WB	GbWg	51	0.63	0.91	1.3	1.9	3.3
	NWIS	GbWg	63	.16	.86	1.1	1.8	15
	GMF	GbWg	28	.57	1.0	1.3	2.0	4.3
	DM	GbWg	32	.58	1.1	1.8	2.1	3.5
	D	GbWg	252	.050	.21	.45	1.1	5.0
	D	CCGA	14	.025	.080	.36	.99	2.4
Transmissivity (ft^2/d)	WB	GbWg	51	150	220	290	460	800
	NWIS	GbWg	63	39	210	260	430	3,600
	GMF	GbWg	28	22	230	350	500	940
	DM	GbWg	32	140	270	450	520	850
Geohydrologic-unit hydraulic conductivity (ft/d)	WB	GbWg	51	.51	.64	.93	1.3	4.8
	GMF	GbWg	18	.48	1.6	2.2	2.8	4.8
	DM	GbWg	32	.30	1.3	1.5	1.9	7.1
	D	GbWg	251	.090	1.5	3.0	5.5	60
	D	CCGA	14	.29	.62	1.3	4.9	29
Sandstone hydraulic conductivity (ft/d)	D	GbWg	160	.16	2.5	4.5	9.7	120

Oklahoma aquifer was estimated from two types of information, aquifer tests and specific-capacity data.

Gates, Marsh, and Fryberger (1983) report transmissivities calculated from aquifer tests. The aquifer-test transmissivities were from high-capacity municipal wells in the urban corridor along the western boundary of the study area. Transmissivities ranged from 22 to 940 ft^2/day (square feet per day), and had a median of 350 ft^2/d.

Transmissivity was calculated from the specific-capacity data in Wood and Burton (1968), the U.S. Geological Survey's NWIS data base, and the drillers' log data. Transmissivities were calculated from specific-capacity data from drillers' logs only for municipal wells greater than 500 ft deep because these wells intercept a large percentage of the total aquifer thickness. Because the base of the Central Oklahoma aquifer is the base of fresh ground water, wells are completed some distance above the base of the aquifer to avoid the upconing of saline water into the well. Thus, all the calculated transmissivities are somewhat less that the actual transmissivity because transmissivity, by definition, is for the entire aquifer thickness.

Transmissivity was calculated from specific-capacity data by using a method described in Heath (1982). The Theis nonequilibrium equation (Theis, Brown, and Meyer, 1954) can be arranged in a form convenient for deriving transmissivity from specific capacity:

$$T = \frac{W(u)}{4\pi} \times \frac{Q}{s} \qquad (1)$$

where T is transmissivity, Q/s is specific capacity, Q is the discharge of the well, and s is the drawdown in the well. $W(u)$ is the well function of u where u is equal to:

$$u = \frac{r^2 S}{4Tt} \qquad (2)$$

where r is the effective radius of the well, S is the aquifer storage coefficient, and t is the length of the pumping period preceding the determination of specific capacity.

For convenience in using equation 1, $W(u)/4\pi$ is expressed as a constant. To do so, it is first necessary to determine values for u and, by using a table of values of u and $W(u)$, determine the corresponding values for $W(u)$.

Values for u are determined by substituting in equation 2 values of T, S, r, and t that are representative of conditions in the study unit. T and S were taken as the medians of the aquifer-test data in Gates, Marsh, and Fryberger (1983), and t and r were taken to be the medians of the municipal wells that are greater than 500 ft deep for which specific-capacity data were available from drillers' logs. Only municipal wells deeper than 500 ft were used because these are the type of wells described in Gates, Marsh, and Fryberger (1983). The aquifer parameters substituted into equation 2 were $T = 350$ ft^2/d, $S = 2.0 \times 10^{-4}$, $r = 8.75$ in, and $t =$ 24 hours.

Converting to consistent units and substituting into equation 2, u equals 7.60×10^{-8}. From a table of $W(u)$ for u (Heath, 1982), $W(u)$ is equal to 15.81. Substituting into equation 1, $T = 1.26\ Q/s$ in consistent units. Transmissivity frequently is reported in units of gallons per day per foot [(gal/day)/ft] or square feet per day (ft^2/d), while specific capacity is reported in units of gallons per minute per foot of drawdown [(gal/min)/ft]. Applying the appropriate conversion factors to derive transmissivity in gallons per day per foot, $T = 1{,}810\ Q/s$; to derive transmissivity in square feet per day, $T = 242\ Q/s$.

The transmissivities derived from the specific capacities are summarized in table 15. Transmissivities calculated from the specific capacities in Wood and Burton (1968) ranged from 150 to 800 ft^2/d, and had a median of 290 ft^2/d. Transmissivities calculated from the specific capacities in the U.S. Geological Survey's NWIS data base ranged from 39 to 3,600 ft^2/d, with a median of 260 ft^2/d. The NWIS data has a relatively small interquartile range (from 210 to 430 ft^2/d), but the difference between the smallest and largest transmissivity is quite large. The largest transmissivity is an outlier and is not considered to be representative of the Garber Sandstone and Wellington Formation. Transmissivities calculated from specific capacities from drillers' logs for municipal wells deeper than 500 ft completed in the Garber Sandstone and Wellington Formation ranged from 140 to 850 ft^2/d, and had a median of 450 ft^2/d.

Hydraulic Conductivity

Under ideal conditions, transmissivity is calculated for a well that fully penetrates the entire thickness of a homogeneous aquifer, and hydraulic conductivity is calculated by dividing transmissivity by the aquifer thickness. Data from the available sources were less than ideal, because most wells do not penetrate the entire Central Oklahoma aquifer, and the aquifer is not homogeneous. Wells do not fully penetrate the aquifer because the deeper zones in the aquifer contain brines, and wells are completed above the brines to avoid upconing of brines into the freshwater zone. The Permian geologic units of the Central Oklahoma aquifer are not homogeneous, consisting of interbedded sandstones, siltstones, and mudstones, and these different lithologic units have many different hydraulic conductivities. Most of the water withdrawn from wells completed in the Permian geologic units is derived from the most transmissive units, the sandstones. One method of calculating hydraulic conductivity is to divide the transmissivity by the combined thickness of all sandstone units intercepted. Hydraulic conductivity calculated in this manner is the weighted mean hydraulic conductivity of the sandstone geologic units and is referred to as "sandstone hydraulic conductivity" in this report. An alternative method is to divide transmissivity by the open (screened, slotted, or perforated) interval in the well. Hydraulic conductivity calculated in this manner is a weighted mean for all geohydrologic units along the entire open interval and is referred to as "geohydrologic-unit hydraulic conductivity" in this report. In wells open only to sandstones, sandstone hydraulic conductivity is equal to geohydrologic-unit hydraulic conductivity. However, many wells completed in the Central Oklahoma aquifer are open over long intervals that include siltstones and mudstones in addition to sandstones, and many wells are not open to all available sandstones. For these wells, sandstone and geohydrologic unit hydraulic conductivity are not equal. Both sandstone and geohydrologic hydraulic conductivity were calculated, where possible, and the results are summarized in table 15.

The data from Wood and Burton (1968) only included the top and bottom of the open interval in the wells tested, so it was possible to compute only geohydrologic-unit hydraulic conductivity. These geohydrologic-unit hydraulic conductivities ranged from 0.51 to 4.8 ft/d (feet per day), and had a median of 0.93 ft/d. The data from the U.S. Geological Survey's NWIS data base could not be used to calculate hydraulic conductivity because no information was available for the open interval in the well. Hydraulic conductivity was already calculated in Gates, Marsh, and Fryberger (1983), but they include no information about open

intervals or the total quantity of sandstone penetrated. Because of the limited data included with their report, it is not possible to tell if this is geohydrologic-unit or sandstone hydraulic conductivity. The data from Gates, Marsh, and Fryberger (1983) are listed in table 15 as geohydrologic-unit hydraulic conductivity because the range of data is similar to the Wood and Burton (1968) geohydrologic-unit hydraulic conductivity data.

Geohydrologic-unit hydraulic conductivities were calculated from specific-capacity data on drillers' logs for 251 wells completed in the Garber Sandstone and Wellington Formation. Geohydrologic-unit hydraulic conductivity ranged from 0.090 to 60 ft/d, and had a median of 3.0 ft/d. Geohydrologic-unit hydraulic conductivity for 32 municipal wells completed in the Garber Sandstone and Wellington Formation deeper than 500 ft ranged from 0.30 to 7.1 ft/d and had a median of 1.5 ft/d. Geohydrologic-unit hydraulic conductivity for 14 wells completed in the undivided Chase, Council Grove, and Admire Groups ranged from 0.29 to 29 ft/d, and had a median of 1.3 ft/d. Because many of the wells used to calculate hydraulic conductivity from the drillers' log data are less than 300 ft deep, the wells do not penetrate a large fraction of the total aquifer thickness. Thus, the calculated hydraulic conductivity is representative of only that fraction of the geologic unit penetrated, instead of the entire unit.

The drillers' logs included data concerning open intervals and lithologic descriptions of the geology penetrated during drilling. However, the lithologic descriptions were very general, and the lithology was described in very simple terms. Both geohydrologic-unit and sandstone hydraulic conductivities were calculated after applying some quality-assurance checks to the lithologies reported on the drillers' logs (drillers' logs were eliminated if the lithologic data were not sufficiently specific). After quality-assurance checking of the lithologic data, the only category with sufficient data to calculate sandstone hydraulic conductivity was wells of all uses completed in the Garber Sandstone and Wellington Formation. Sandstone hydraulic conductivity for 160 wells ranged from 0.16 to 120 ft/d, and had a median of 4.5 ft/d. Plotting geohydrologic-unit and sandstone hydraulic conductivity on a map showed no obvious trends or patterns.

The median geohydrologic-unit hydraulic conductivity from drillers' log data of the Chase, Council Grove, and Admire Groups is 43 percent of the median geohydrologic-unit hydraulic conductivity of the Garber Sandstone and Wellington Formation. The median sandstone percentage of the Chase, Council Grove, and Admire Groups is 43 percent of the median sandstone percentage of the Garber Sandstone and Wellington Formation. It is possible that the sandstone hydraulic conductivities of both geohydrologic units are approximately equal and that the geohydrologic-unit hydraulic conductivity is smaller in the Chase, Council Grove, and Admire Groups because there is less sandstone.

No estimates for the vertical hydraulic conductivity of the Central Oklahoma aquifer could be found in the literature, and no measurements of vertical hydraulic conductivity were made during this investigation. Vertical hydraulic conductivity commonly is expressed as a ratio of horizontal to vertical hydraulic conductivity, and the term "k_h/k_v" is used in this report. The literature contains a large range for this ratio. Weeks (1969) determined k_h/k_v to be 2 in glacial outwash deposits, while Williamson, Grubb, and Weiss (1990) determined k_h/k_v to be as large as 210,000 for coastal-plain sediments. A range of k_h/k_v for the Central Oklahoma aquifer of 100 to 10,000 was established by using a numerical flow model (see the "Flow Simulations" section of this report).

Storage Coefficient and Porosity

Data for the storage coefficient of the Central Oklahoma aquifer were available from aquifer tests described in Gates, Marsh, and Fryberger (1983). They calculate storage coefficients for six aquifer tests, which ranged from 0.0001 to 0.0004 and had a median of 0.0002. Storage coefficients in this range for an aquifer of the thickness of the Central Oklahoma aquifer are reasonable based on the elasticity of water and the aquifer material (Jorgensen, 1980).

Porosity was determined by point counts for the sandstone strata in cores from seven test holes in the Central Oklahoma aquifer (Breit and others, 1990). Porosity ranged from 0.17 to 0.30, and had a median of 0.22. Breit and others (1990) do not list porosity data for nonsandstone strata.

Biases

All the sources of data used for calculating hydraulic properties had some inherent biases, caused by well construction or location. The wells used in Wood and Burton (1968) were all high-capacity municipal wells, which biases the hydraulic properties toward larger numbers, as compared to domestic wells. Domestic wells have smaller specific capacities because the wells are smaller diameter, do not penetrate the aquifer completely, and have short open intervals. However, when compared to other municipal wells, the hydraulic properties calculated from Wood and Bur-

ton's data are thought to be systematically biased toward small numbers because of the well-completion practices commonly in use at the time. Wells described in Wood and Burton (1968) probably were completed by gun-perforating or slotting the casing instead of using well screens. Perforated wells completed in the Garber Sandstone and Wellington Formation typically have specific capacities two to three times smaller than screened wells (Carr and Marcher, 1977). Wells with smaller specific capacities have smaller calculated transmissivities and hydraulic conductivities.

Hydraulic properties calculated from the NWIS data base are thought to be biased toward smaller numbers because many of the wells are older slotted or gun-perforated municipal wells and domestic wells. Because only the hydraulic properties and not the original data were available from Gates, Marsh, and Fryberger (1983), it was not possible to evaluate their data for well-construction biases. Most of the drillers' log wells were domestic wells, which biases these data toward smaller hydraulic properties. However, many of the drillers' log wells were newer wells and were screened instead of perforated, which results in larger hydraulic properties than those computed from older, perforated wells.

The wells from Wood and Burton (1968), Gates, Marsh, and Fryberger (1983), and from driller's logs for municipal wells were located in the central Oklahoma urban corridor, and thus contain a spatial bias. The aquifer is thickest in the urban corridor, so the hydraulic properties are biased toward larger numbers. The hydraulic conductivities calculated from drillers' logs are thought to be the least biased, because the sample size is largest and the wells have the widest spatial distribution of all the data sources examined in this report.

Recharge

For this study, recharge is defined to be the addition of water to the saturated ground-water flow system at the upper limit of the zone of saturation. Two processes probably account for all of the recharge to the Central Oklahoma aquifer system, infiltration of surface water through stream channels or lake beds and infiltration of precipitation through the unsaturated zone. The infiltration of surface water is thought to account for only a small volume of the total recharge because the water-table map (fig. 24) does not indicate large areas where streams are losing water to the aquifer.

The infiltration of precipitation is thought to account for most of the recharge to the Central Oklahoma aquifer. The term "recharge rate" is used to express recharge from precipitation as the equivalent thickness of a layer of water that infiltrates through the unsaturated zone in a given time. The units are length per time; this report uses inches per year (in/yr). Factors that affect quantity of recharge at any location include the amount and rate of precipitation, the vertical hydraulic conductivity and moisture capacity of the unsaturated zone, slope of the land surface, and numerous other factors. The recharge rate is difficult to quantify because it varies substantially across the aquifer and it is difficult to measure directly. The recharge rate at a site can be inferred from measurements of moisture content in the unsaturated zone using soil tensiometers, electrical resistance cells, neutron probes, or other devices. However, no site-specific measurements of recharge for the Central Oklahoma aquifer were found in the literature and none were done for this study.

Another technique for measuring recharge is to measure discharge from the aquifer in areas where the aquifer is in, or nearly in, a steady-state condition. Where an aquifer is in a steady-state condition, discharge is equal to recharge. Discharge from the aquifer consists of transpiration by plants, withdrawals by wells, and natural discharge to streams. Transpiration is minimal during the winter months, when plants are dormant. There are small drainage basins in rural areas of the Central Oklahoma aquifer where withdrawals are very small, consisting of only a few domestic wells. In these small drainage basins, during the winter months, the aquifer was assumed to be in a steady-state condition and the stream discharge was considered to be equal to recharge.

The streams that were selected for measurement (fig. 25) had drainage basins entirely within the Central Oklahoma aquifer, were not regulated, did not have withdrawals of surface water, did not have discharges from sewage-treatment plants, and did not have substantial ground-water withdrawals within the drainage basin. All large streams were eliminated as candidates for measurement, because these conditions were not met. Measurements were made in the winter, when vegetation was dormant and transpiration was minimal, and after surface-water runoff from storm events had dissipated, so the entire flow in the stream channels was inferred to be ground-water discharge. Discharge measurements made during such conditions are described as "base-flow" discharge measurements. The base-flow discharge measurements are listed in table 16.

Recharge rates were calculated from the stream-flow discharge measurements by dividing the discharge by the area of the drainage basin. Recharge rates range from 0.19 in/yr for one measurement at Pond Creek to 4.05 in/yr for one measurement at Wildhorse Creek. The median recharge rate for each measurement site ranges from 0.60 in/yr on the unnamed tributary to Deer Creek to 3.77 in/yr on Wildhorse Creek. The median of the median recharge rates at all sites is 1.61 in/yr.

Pettyjohn and Miller (1982) estimated recharge in central Oklahoma by using hydrograph-separation methods with stream-discharge data from U.S. Geological Survey gages (fig. 25) to separate surface-water runoff from ground-water discharge to streams. They assumed that ground-water discharge was equal to recharge, and thus concluded that for the "Garber-Wellington aquifer" the average recharge rate was about 2.11 in/yr. Examination of their results for streams and gages that are entirely or mostly within the

Table 16. Base-flow discharge measurements and calculated recharge rates from selected small streams in central Oklahoma

Site identifier	Stream	Drainage area (square miles)	Discharge (cubic feet per second)	Date	Recharge rate (inches per year)
07229320	Little Buckhead Creek	2.40	0.19	12–10–1987	1.08
			.37	02–25–1988	2.11
			.00	09–01–1988	--
07229325	Buckhead Creek	19.20	1.77	12–10–1987	1.25
			4.48	02–25–1988	3.17
			.39	09–01–1988	--
			.74	12–05–1988	.52
			2.78	03–16–1989	1.97
07229360	Pond Creek	10.70	.64	12–10–1987	.81
			1.43	02–25–1988	1.82
			.05	09–01–1988	--
07229365	Pond Creek	27.60	2.05	12–10–1987	1.01
			4.14	02–25–1988	2.04
			.15	09–01–1988	--
			.72	12–05–1988	.35
			.39	03–16–1989	.19
07230200	Pecan Creek	15.50	1.15	12–10–1987	1.01
			2.55	02–25–1988	2.23
			.00	09–01–1988	--
07230205	Pecan Creek	37.40	3.17	12–10–1987	1.15
			5.60	02–25–1988	2.03
			.39	09–01–1988	--
			1.86	12–05–1988	.68
			5.78	03–16–1989	2.10

Table 16. Base-flow discharge measurements and calculated recharge rates from selected small streams in central Oklahoma—Continued

Site identifier	Stream	Drainage area (square miles)	Discharge (cubic feet per second)	Date	Recharge rate (inches per year)
07230300	Jim Creek	7.46	0.83	12–10–1987	1.51
			1.47	02–25–1988	2.67
			.09	09–01–1988	--
07230302	Jim Creek	11.20	1.11	12–10–1987	1.35
			1.81	02–25–1988	2.20
			.18	09–01–1988	--
			.67	12–05–1988	.81
			2.09	03–16–1989	2.53
07241570	Deer Creek	15.30	.22	12–10–1987	.20
			1.36	02–25–1988	1.21
			.00	09–01–1988	--
07241580	Unnamed tributary to Deer Creek	8.70	.16	12–10–1987	.25
			.60	02–25–1988	.94
			.00	09–01–1988	--
07241590	Deer Creek	40.40	.85	12–10–1987	.29
			4.96	02–25–1988	1.67
			.00	09–01–1988	--
			.73	12–05–1988	.25
			4.87	03–16–1989	1.64
07242368	Wildhorse Creek	9.50	2.44	12–10–1987	3.49
			2.83	02–25–1988	4.05
			.72	09–01–1988	--
07242371	Wildhorse Creek	18.20	3.07	12–10–1987	2.29
			4.06	02–25–1988	3.03
			.86	09–01–1988	--
			2.89	12–05–1988	2.16
			3.82	03–16–1989	2.85
07242375	West Captain Creek	28.60	4.66	12–10–1987	2.21
			7.06	02–25–1988	3.35
			1.16	09–01–1988	--
07242376	West Captain Creek	34.80	4.71	12–10–1987	1.84
			8.27	02–25–1988	3.23
			.98	09–01–1988	--
07242377	East Captain Creek	12.40	.66	12–10–1987	.72
			1.82	02–25–1988	1.99
			.11	09–01–1988	--

Table 16. Base-flow discharge measurements and calculated recharge rates from selected small streams in central Oklahoma—Continued

Site identifier	Stream	Drainage area (square miles)	Discharge (cubic feet per second)	Date	Recharge rate (inches per year)
07242378	Captain Creek	57.90	7.09	12–10–1987	1.66
			10.90	02–25–1988	2.56
			1.13	09–01–1988	--
			6.11	12–05–1988	1.43
			11.40	03–16–1989	2.67

Central Oklahoma study unit indicates large variance for different streams, for different hydrograph-separation methods, and for different years (table 17). Recharge ranged from a minimum of 0.03 in/yr on Little River in 1978 and 1979 to a maximum of 8.33 in/yr on the Deep Fork in 1979.

Total recharge to the Central Oklahoma aquifer was estimated by multiplying the recharge rate by the area of the unconfined part of the aquifer, which includes the outcrops of the Garber Sandstone, Wellington Formation, the Chase, Council Grove, and Admire Groups, and alluvium and terrace deposits. The area of the unconfined part of the aquifer is about 2,600 mi^2. Assuming a recharge rate of 1.61 in/yr, the total recharge is about 300 ft^3/sec.

There are limitations to estimating recharge from stream discharge. The small drainage basins in which discharge measurements were made have both Permian geologic units and alluvium with the basin boundaries. The recharge rate to the alluvium probably is greater than to the Permian geologic units, because the alluvium is unconsolidated and contains a large amount of sand and some gravel. Thus, the calculated recharge rate probably represents a rate between the recharge rate to the alluvium and the rate to the Permian geologic units.

Another limitation to using stream discharge to estimate recharge is the presence of regional and local flow systems. Toth (1963) describes how topography can create local and regional flow systems within an aquifer. The local flow system is the ground water that discharges to the nearest stream in the drainage basin, and the regional flow system is ground water that flows under drainage basins to discharge to streams at lower altitude. When calculating recharge by dividing stream discharge by the area of the drainage basin, the assumption is all the recharge in a drainage basin is discharging to the local flow system.

A regional flow system is inferred to exist in the Central Oklahoma aquifer; some drainage basins on the aquifer are thought to function either as sources or sinks to the regional flow system. Ground-water discharge to a stream will be less than or greater than the total recharge to the basin, depending on whether the local flow system is losing or gaining ground water from the regional flow system, and the recharge rate inferred from ground-water discharge will be either less than or greater than the actual recharge rate. For example, the Deep Fork and its tributaries are at lower altitudes than other, nearby streams and consistently have recharge rates greater than the median recharge rate. The Deep Fork is inferred to function as a drain for the regional ground-water flow system.

Ground-Water Discharge

Ground-water discharge from the Central Oklahoma aquifer can be classified into three different categories: (1) Discharge to streams, (2) evapotranspiration, and (3) withdrawals.

Discharge to Streams

At the present time (1992), measuring total ground-water discharge to streams is complicated by the presence of reservoirs, sewage discharges, interbasin transfers of water (Oklahoma City imports large volumes of water from drainage basins outside the Central Oklahoma aquifer study unit), and numerous other factors. As discussed in the "Recharge" section of this report, some discharge measurements were made for small streams, but none were made for large streams in the study unit. Determining the total ground-water discharge to streams was outside the scope of this investigation. However, prior to the development of ground-

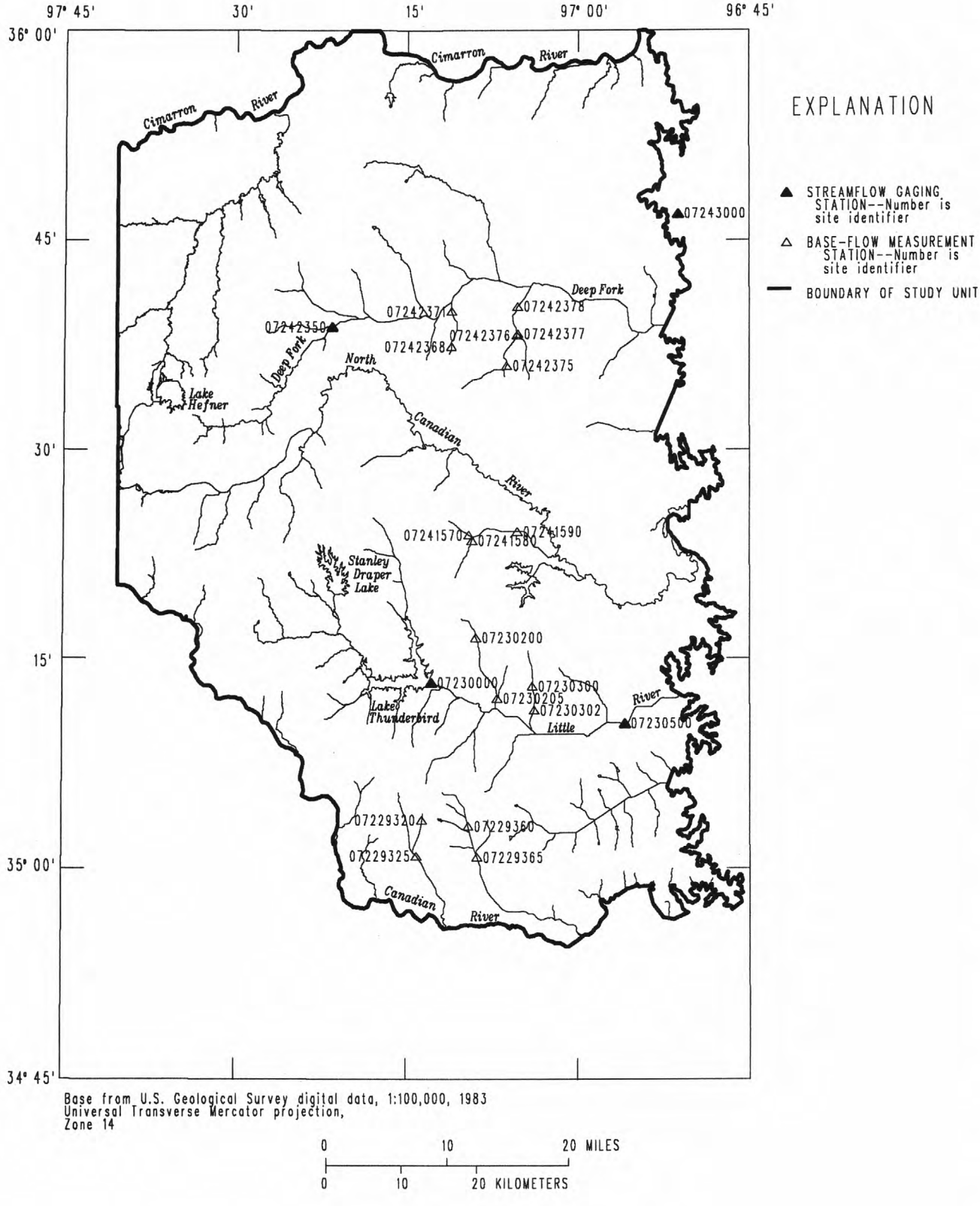

Figure 25. Locations of streamflow-measurement sites used for calculating recharge.

Table 17. Recharge rates estimated by hydrograph separation (from Pettyjohn and Miller, 1982)

[Method: 1, fixed interval; 2, sliding interval; 3, local minima]

Site identifier	Stream	Method	Recharge rate (inches per year)			
			1973	1976	1978	1979
07230000	Little River	1	1.23	0.05	0.03	0.28
		2	1.39	.05	.03	.29
		3	.59	.05	.03	.03
07230500	Little River	1	2.90	.33	.18	1.54
		2	3.03	.33	.17	1.25
		3	2.65	.32	.13	.70
07242350	Deep Fork	1	5.11	3.51	3.29	8.33
		2	5.12	3.50	3.30	8.32
		3	4.75	3.48	3.20	5.40
07243000	Dry Creek	1	1.32	.98	.17	1.38
		2	1.32	.096	.16	1.41
		3	1.25	.90	.15	.26

water withdrawals, the total ground-water discharge probably was close to the estimated total recharge of 300 ft^3/sec. Ground-water withdrawals probably have decreased ground-water discharge to streams, but the magnitude of this decrease is not known.

Evapotranspiration

Evapotranspiration takes place both from the unsaturated soil zone throughout the entire Central Oklahoma aquifer as well as where the depth to ground water is shallow and plant roots penetrate to the zone of saturation, generally along streams. Precipitation that infiltrates the soil zone and is evapotranspired before reaching the saturated zone is not considered to be discharge from the Central Oklahoma aquifer because the water never becomes part of the saturated ground-water flow system. This type of evapotranspiration can be estimated by subtracting surface-water runoff and ground-water recharge from total precipitation at a site. Pettyjohn, White, and Dunn (1983) estimate at the western limit of the Central Oklahoma aquifer study area, for 1970–79, precipitation averaged 30 in/yr, runoff averaged 4 in/yr, and recharge averaged 1 in/yr (all numbers are rounded to one significant figure). Thus, evapotranspiration from the soil zone averaged 25 in/yr. Similarly, at the eastern limit of the study area, precipitation averaged 36 in/yr, runoff averaged 5 in/yr, and recharge averaged 2 in/yr, thus yielding an estimated evapotranspiration of 29 in/yr.

Evapotranspiration occurring along streams is considered to be discharge from the Central Oklahoma aquifer. Ground water that is flowing to a stream is intercepted by plant roots and is transpired or is evaporated through the soil as the ground water approaches the stream. This type of evapotranspiration generally occurs close to streams in the Central Oklahoma aquifer because only near streams is the saturated ground-water flow system close enough to the land surface for evapotranspiration to be substantial. Evapotranspiration near streams can be quite substantial in summer months, when plants transpire large volumes of water, but transpiration is considered to be insignificant during winter months when many plants are dormant. Summer and winter base-flow stream discharge measurements are shown in table 16. Although there is natural variability in base-flow stream discharge, the large differences between summer and winter measurements are attributable mainly to evapotranspiration.

Determining total or seasonal evapotranspiration was considered to be outside the scope of this investigation. However, it is evident from the stream-discharge data in table 16 that during the summer months evapotranspiration is capable of taking up all or nearly all the ground water that is discharging to the small streams in the study unit. Numerous streams listed in table 16 had no flow during the summer measurement, and in many

other streams the summer flow decreased by greater than an order of magnitude as compared to winter flow.

Withdrawals

At the present time (1992), withdrawals from the Central Oklahoma aquifer are major sources of water for public supply, industry, irrigation, domestic supply, stock watering, and other uses (the term "withdrawal" is preferred to the term "water use" in this report, because it is the withdrawal of ground water that is significant from a geohydrologic point of view, as opposed to the use of the water). To estimate total withdrawals from the aquifer, two separate sources of information were considered. The Oklahoma Water Resources Board collects reported water-use data in Oklahoma, for surface and ground water (the Board compiles data concerning "reported water use;" data concerning reported water use listed as having a ground-water source are treated as ground-water withdrawals in this report). Domestic withdrawals from the Central Oklahoma aquifer were estimated from population census information. Withdrawal of ground water for stock use was not estimated.

All users of water other than domestic and stock users are required to report water use to the Oklahoma Water Resource Board on an annual basis. Water use is reported to the Board for the following categories: irrigation; public supply; industrial; power; mining; commercial; recreation, fish, and wildlife; nonirrigated agriculture; and "other" uses. However, compliance with the requirement to report water use is not complete, and the State of Oklahoma does not require metering of water use, so some reported uses are estimates. For this study, data for reported water use from ground-water sources for Cleveland, Lincoln, Logan, Oklahoma, and Pottawatomie Counties (fig. 2) were provided by the Board. Wells not withdrawing water from the Central Oklahoma aquifer were eliminated, based on the legal description of the locations of the wells and knowledge of the geohydrology of the aquifer. Ground-water withdrawals, excluding domestic and stock use, from wells completed in the Central Oklahoma aquifer are summa-

Table 18. Reported ground-water withdrawals from the Central Oklahoma aquifer

[Source of data: Oklahoma Water Resources Board; --, reported water use less than 0.5 million gallons per year or no data]

	Reported water use, in millions of gallons per year									
Year	Agri-culture	Com-mercial	Indus-trial	Irri-gation	Mining	Other	Power	Public supply	Recreation, fish, and wildlife	Total
1967	10	827	435	300	342	--	199	2,356	16	4,485
1968	--	818	438	300	433	--	202	3,658	--	5,849
1969	--	833	416	--	234	--	356	4,140	41	6,019
1970	--	897	513	--	125	--	558	3,833	52	5,976
1971	10	973	847	--	112	--	430	3,366	8	5,747
1972	--	--	--	--	--	--	--	--	--	--
1973	10	925	798	--	23	--	407	4,920	40	7,123
1974	10	915	497	2	14	--	230	4,998	41	6,707
1975	9	881	825	9	59	--	52	6,045	--	7,881
1976	10	887	706	20	52	--	53	5,062	8	6,799
1977	10	1,120	842	19	120	--	--	7,297	15	9,423
1978	10	932	616	5	224	--	63	8,436	15	10,301
1979	--	813	115	9	404	--	76	7,374	19	8,810
1980	4	864	622	954	617	--	70	8,413	--	11,544
1981	6	821	699	408	351	--	64	7,030	--	9,378
1982	4	2,445	245	657	278	77	67	8,580	15	12,367
1983	25	2,220	588	782	269	108	60	9,225	3	13,280
1984	10	483	209	711	286	102	90	9,703	--	11,595
1985	37	2,088	478	871	1,294	81	68	8,956	26	13,900
1986	38	2,141	465	1,109	167	45	167	7,635	48	11,815
1987	61	2,153	501	808	284	41	170	8,016	54	12,087
1988	74	595	572	1,149	282	3	117	6,157	82	9,032
1989	62	1,754	161	1,062	270	--	65	4,401	85	7,860

rized in table 18 and shown on figure 26. No attempt was made to correct for differences in compliance with the State's requirement for reporting water use. Ground-water withdrawals in 1972 are omitted from table 18 and figure 26 because records are incomplete for that year.

The general trend in total withdrawals was a gradual increase from 4,485 million gallons per year in 1967, the first year data were available, to a peak use of 13,900 million gallons per year in 1985. As a fraction of total reported use, public supply was by far the largest use, increasing from 53 percent of the total withdrawals in 1967 to a maximum of 84 percent in 1979 and 1984. A decline in total withdrawals began in 1986, caused entirely by a dramatic decline in withdrawals for public supplies. The decline in public-supply withdrawals was caused by some of the municipalities in central Oklahoma, notably the cities of Edmond, Midwest City, and Del City, shifting sources of water from the Central Oklahoma aquifer to surface-water supplies. In 1989, the last year for which data were available, withdrawals for public supplies had declined to 4,401 million gallons per year, or 45 percent of the peak of 9,703 million gallons per year in 1984.

Although domestic use is not reported to the Oklahoma Water Resources Board, it is a significant component of total withdrawals. Most homes outside the major urban areas are supplied by domestic wells, and there are areas within the city limits of the major metropolitan areas where homes are supplied by domestic wells. Because there is no requirement to report domestic water use, domestic use was inferred from population census information. Domestic withdrawals were estimated by first determining the number of housing units overlying the Central Oklahoma aquifer that are supplied by domestic wells, estimating the number of occupants per household, and multiplying by the per capita use obtained from the literature. Total domestic withdrawals were calculated from these data.

Since the 1960 census, the type of water supply used in homes has been one of the data elements collected by the Bureau of the Census (U.S. Department of Commerce, 1960, 1970, and 1980). The total number of housing units overlying the Central Oklahoma aquifer and supplied by domestic wells was compiled from Bureau of the Census data. Lincoln, Logan, and Pottawatomie Counties have areas that do not overly the aquifer, and the number of domestic wells in those counties was multiplied by the ratio of the population living over the aquifer, based on census tracts, to the total population of the county. It was assumed that the ratio of homes with domestic wells to the total number of homes is the same in that part of the county overlying the Central Oklahoma aquifer as in the entire county. The domestic-well data has two limitations: in 1960, information was not collected on the source of water supply for areas of population greater than 50,000, so wells in such areas were not counted; and no domestic wells completed in the Central Oklahoma aquifer in Payne County are included because only a small, sparsely populated part of Payne County overlies the aquifer. The number of domestic wells and the number of occupied housing units are listed in table 19.

The number of occupants per home was estimated from Bureau of the Census data. For each of the five counties with a large area underlain by the Central Oklahoma aquifer (excluding Payne County), the population in census tracts overlying the aquifer was divided by the number of occupied housing units in the same census tracts. It was assumed that the mean number of occupants per home is the same regardless of whether the home is supplied by a domestic well or by other types of water supplies. Finally, per capita water use was estimated by Stoner (1984) to be 56 gallons per day per capita for self-supplied domestic use in Oklahoma in 1980. Applying this estimate of per capita water use, estimated domestic water use for the Central Oklahoma aquifer for 1960, 1970, and 1980 is shown in table 19. Adding domestic withdrawals to reported ground-water withdrawals from the Water Resources Board indicates that total ground-water withdrawals were 7,017 million gallons per year in 1970, of which domestic use was 15 percent of the total, and 13,229 million gallons per year in 1980, of which domestic use was 13 percent of the total.

Underflow

Underflow is ground water that is added to or removed from the Central Oklahoma aquifer by flowing across the aquifer boundaries. Underflow differs from recharge or ground-water discharge, as defined in previous sections of this report, in that recharge and discharge occur within the boundaries of the aquifer. Underflow includes ground water flowing (1) into or out of the Central Oklahoma aquifer through the Hennessey Group and Vanoss Formation; (2) into or out of the aquifer under the Cimarron or Canadian Rivers; (3) and into or out of the aquifer through alluvium and terrace deposits at the boundaries of the study unit. Underflow through the Hennessey Group and Vanoss Formation is thought to be small because these units are less transmissive than the Central Oklahoma aquifer. As discussed in the section "Definition of the Central Oklahoma aquifer," little ground water flows under

Table 19. Estimated domestic ground-water withdrawals from the Central Oklahoma aquifer

[All figures adjusted to the area overlying the Central Oklahoma aquifer; Mgal/yr, million gallons per year]

Year	County	Domestic wells	Occupied housing units	Population	Ground-water withdrawal (Mgal/yr)
1960	Cleveland	2,328	13,025	47,600	174
	Lincoln	2,382	4,340	13,058	146
	Logan	1,955	5,655	17,249	122
	Oklahoma	8,183	139,844	439,506	526
	Pottawatomie	3,698	13,529	41,143	230
	Total	18,546	176,393	558,556	1,198
1970	Cleveland	3,484	24,246	81,839	240
	Lincoln	2,202	4,446	12,720	129
	Logan	1,872	5,827	17,681	116
	Oklahoma	5,303	175,914	526,805	325
	Pottawatomie	3,827	13,942	41,189	231
	Total	16,688	224,375	680,234	1,041
1980	Cleveland	7,209	45,776	133,173	429
	Lincoln	3,553	6,754	18,624	200
	Logan	3,525	8,670	24,767	206
	Oklahoma	8,744	220,580	568,933	461
	Pottawatomie	6,915	20,062	55,239	389
	Total	29,946	301,842	800,736	1,685

the Cimarron and Canadian Rivers because the aquifer is less transmissive beyond these rivers and the rivers are hydrologic barriers to underflow. Some water flows into or out of the Central Oklahoma aquifer through alluvium and terrace deposits, but this volume also is thought to be small because of the small cross-sectional area of the alluvium and terrace deposits (relative to the entire aquifer thickness) and because the largest component of ground-water flow through the alluvium and terrace is toward streams. Thus, total underflow into or out of the Central Oklahoma aquifer is thought to be small.

Ground-Water Models

Three models were used to describe the ground-water flow system in the Central Oklahoma aquifer: (1) A conceptual model, (2) a numerical flow model, and (3) a particle-tracking model. The conceptual model can be considered to be the theory that describes the ground-water flow system in the Central Oklahoma aquifer. This conceptual model was translated into boundary conditions and model parameters that were used to develop numerical flow and particle-tracking models. The numerical flow and particle-tracking models are computer models that simulate certain aspects of the ground-water flow system. The computer models were used to quantify fluxes and flow velocities within the aquifer and to aid the visualization of the ground-water flow system.

Conceptual Model

The information regarding the lithology and geometry of the geohydrologic units, the water-table map, the hydraulic properties of the aquifer, and the recharge and discharge of the aquifer were combined with basic principles of geohydrology to define a conceptual model of the Central Oklahoma aquifer, which is stated here:

> The conceptual model of ground-water flow within the Central Oklahoma aquifer is based primarily on the transmissivities of the geologic units that make up the aquifer. The most transmissive geologic units are the Garber Sandstone and Wellington Formation and the alluvium and terrace deposits; the Chase, Council Grove, and Admire Groups appear to be less transmissive

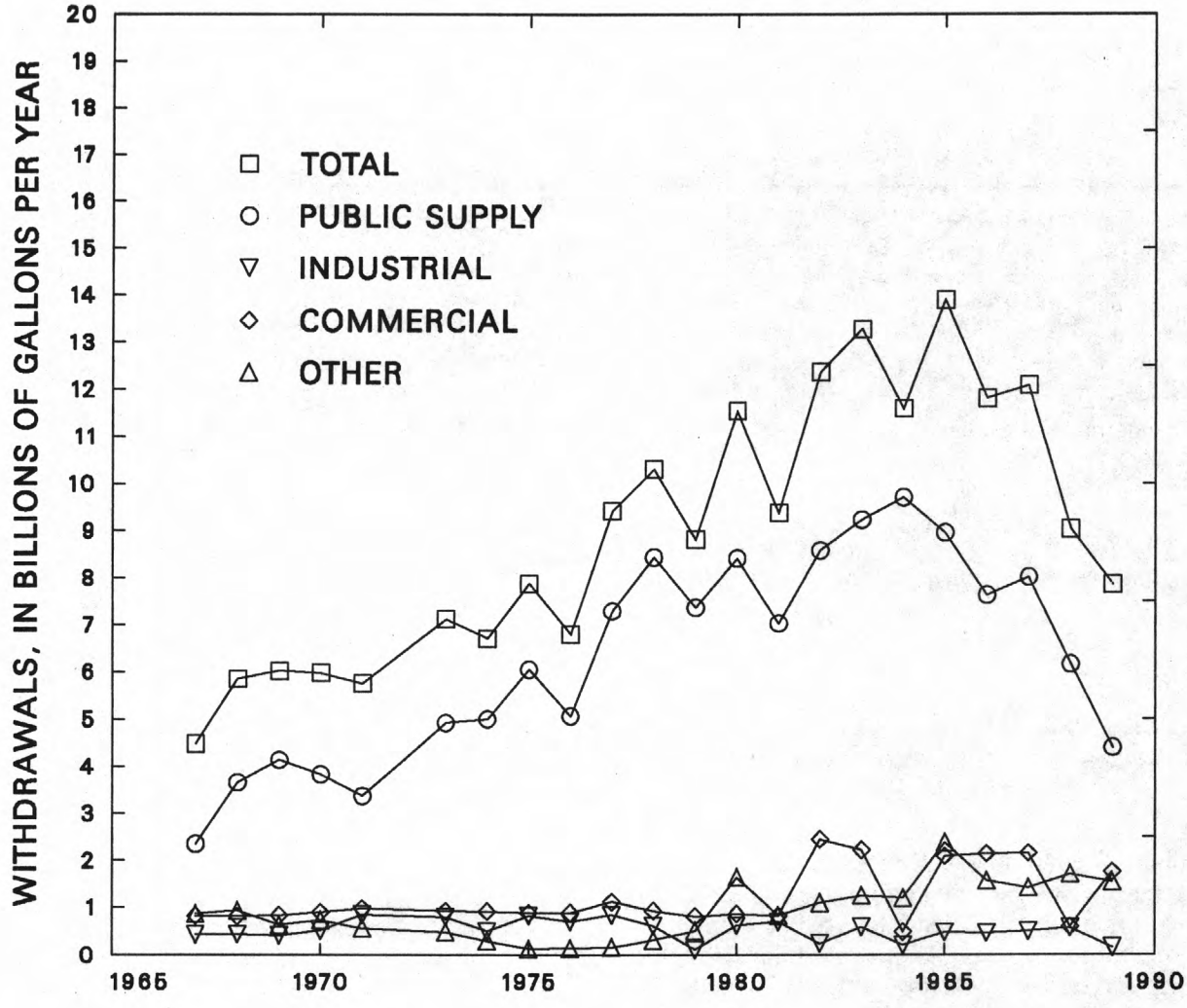

Figure 26. Reported ground-water withdrawals from the Central Oklahoma aquifer, 1967-89 (Source of data: Oklahoma Water Resources Board).

based on the available specific-capacity data. The transmissivities of the Permian geologic units depend largely on the percentage of sandstone. The percentage of sandstone is greatest in the central part of the aquifer, and decreases in all directions. The Hennessey Group and Vanoss Formation are primarily siltstones and mudstones, and therefore were considered to be confining units above and below the aquifer.

The Cimarron River was defined to be the northern boundary of the aquifer because the transmissivities in the Permian geologic units decrease to the point that no high-capacity wells are completed north of the river; the Canadian River was defined to be the southern boundary for similar reasons. Ground-water underflow beneath these rivers was assumed to be negligible. Thus, the rivers are no-flow boundaries to the aquifer. The eastern boundary of the aquifer is the eastern limit of the outcrop of the Chase, Council Grove, and Admire Groups. The western boundary of the aquifer is considered to be where freshwater circulation in the aquifer becomes negligible, which is indicated by an increase in dissolved-solids concentrations to greater than 5,000 mg/L.

Similarly, the base of the aquifer is considered to be where freshwater circulation becomes negligible, marked by an increase in dissolved solids to greater than 5,000 mg/L.

The water-table map indicates regional ground-water flow is west to east; the Deep Fork is a major discharge area for the regional flow system. The water-table map also indicates local flow systems are present within the unconfined part of the aquifer. Most streams are gaining streams, and very few losing streams are evident.

Most of the recharge to the study unit is infiltration of precipitation through the outcrops of the Garber Sandstone, Wellington Formation, the Chase, Council Grove, and Admire Groups, and the alluvium and terrace deposits. Most recharge in the outcrop area flows through local flow systems and discharges to nearby streams. Some recharge enters a regional flow system and discharges to streams at lower altitudes, especially the Deep Fork. Small volumes of water recharge the aquifer through the Hennessey Group and discharge from the aquifer to the Vanoss Formation.

Numerical Flow Model

A numerical flow model was used to test the validity of the conceptual model. A numerical flow model combines a mathematical model of ground-water flow with a conceptual model of the aquifer and computes response variables. These response variables then are compared to field measurements of the same properties. When the simulated response variables from the numerical flow model approximate the measured response variables, the numerical flow model is considered to be a reasonable approximation of the modeled aspects of the flow system, and by extension that the conceptual model of the aquifer is reasonable. Of course, good agreement can be achieved between the response variables and field measurements by specifying unrealistic or erroneous aquifer properties or boundary conditions. The uses, limitations, and misuses of numerical flow models are well documented in references such as Mercer and Faust (1981).

The Central Oklahoma aquifer was modeled only as a steady-state system without withdrawals. Because the water table does not indicate substantial effects from withdrawals (see the discussion in "Potentiometric Surface"), no transient conditions were simulated.

The numerical flow model used to simulate the Central Oklahoma aquifer was the U.S. Geological Survey's modular ground-water flow model (McDonald and Harbaugh, 1988). This model uses a block-centered, finite-difference approach to simulate flow in three dimensions. The Central Oklahoma aquifer simulations contained 40 columns, 60 rows, and, because vertical flow is substantial, 12 layers (figs. 27 and 28). In the horizontal dimensions, cells are 6,562 ft (2,000 meters) on a side, and cell spacing is constant for the region of simulation. All layers are 100 ft thick. Unlike many flow models, the model layers do not correspond to particular geologic units. Instead, the layers are horizontal, and each cell is assigned properties that represent the geohydrologic unit that is the thickest within the cell (fig. 28). For this report, the term "stack" is used to mean the cells in all layers at a particular row and column in the finite-difference grid.

The uppermost active cell in a stack is the cell in which the water table occurs, and the lowermost active cell is the cell containing the base of fresh ground water (fig. 28). The number of active cells in each stack ranges from 1 to 11. A few stacks around the edge of the aquifer, where the aquifer is thinnest, contain only a single active cell. In no stack were all 12 layers active because the highest altitude of the water table was not at the same location as the lowest altitude of the base of fresh ground water.

Boundary conditions were established to represent as closely as possible the conceptual model of the flow system. Lakes and perennial streams were simulated as head-dependent flux boundaries, and flow between the lake or stream and the aquifer was dependent on the difference in head between the lake or stream and the aquifer. Stacks of cells corresponding to the aquifer at the Cimarron and Canadian Rivers contained one or more active cells, but no active cells were included north of the Cimarron River or south of the Canadian River. This arrangement of active and inactive cells produced no-flow boundaries for the model, which precluded any underflow at these two rivers.

The western boundary of the model was established as a no-flow boundary at the freshwater/brine interface, which is assumed to mark the limit of freshwater circulation in the aquifer. For steady-state conditions without withdrawals (the conditions simulated here), the interface was considered to be stable, and simulating this interface as a no-flow boundary seemed to be a valid assumption. To simulate the small amount of underflow into the study unit through the Hennessey Group, the uppermost active cell in the stacks at the western boundary were made into constant-head cells. These constant-head cells served as sources or sinks for

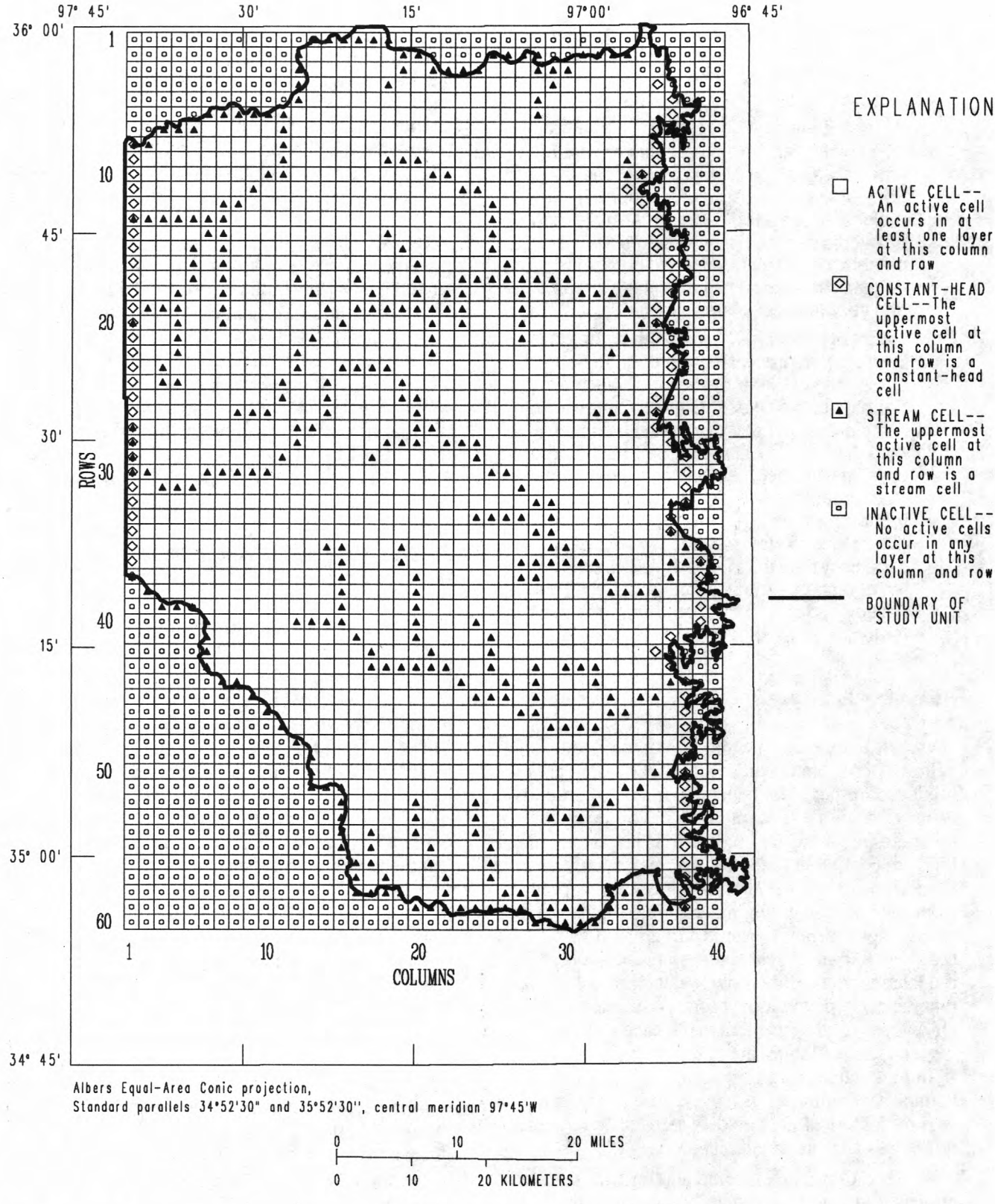

Figure 27. Finite-difference grid used for simulating the Central Oklahoma aquifer ground-water flow system.

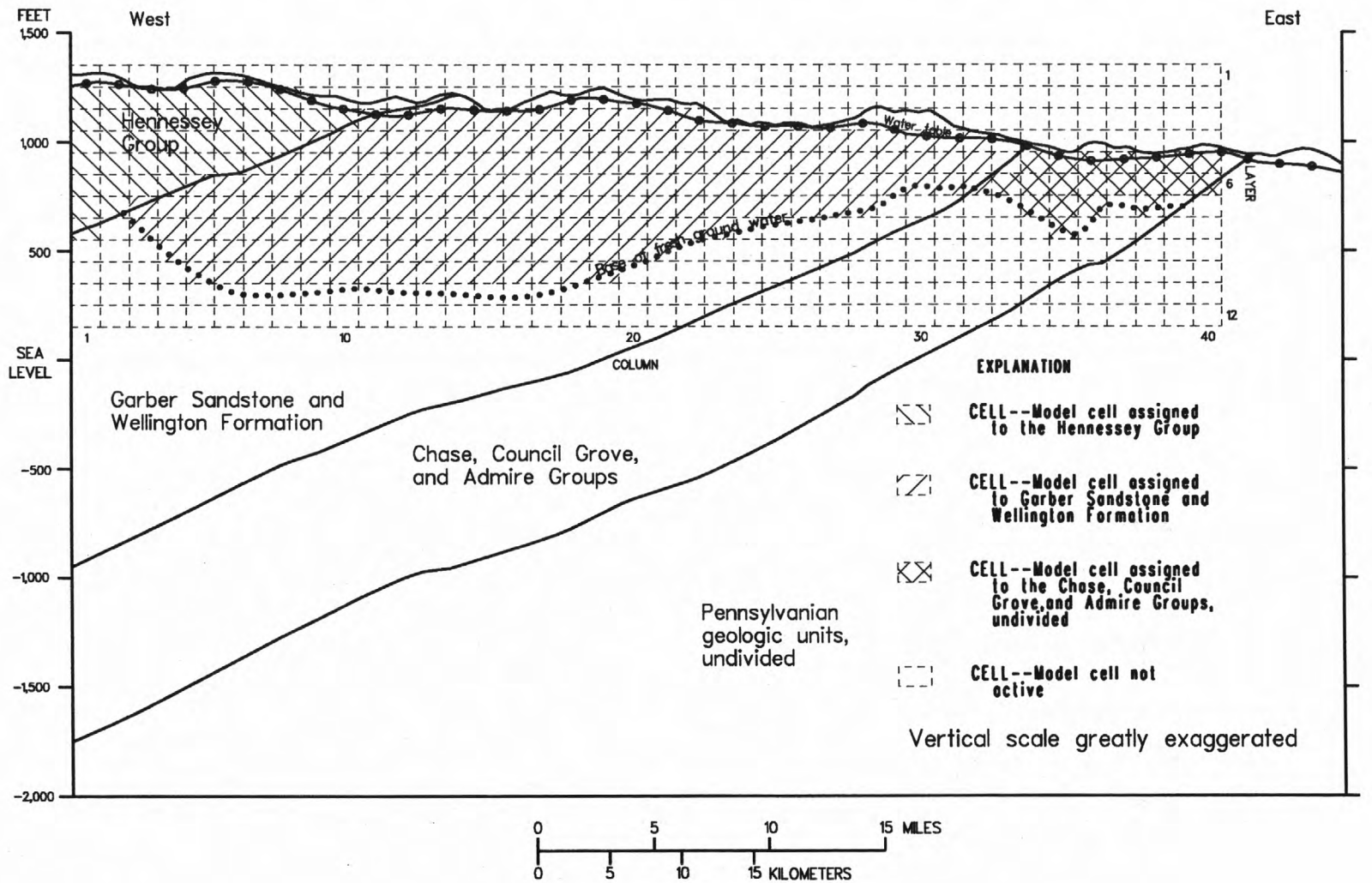

Figure 28. Example of discretization of layers in the ground-water flow model.

whatever quantity of water was needed to maintain the hydraulic head at a constant altitude. Because the magnitude of the boundary flux into the study unit through the Hennessey Group is unknown (but thought to be small), the hydraulic conductivity of these rocks is unknown (and also thought to be small), and the model was used only to simulate steady-state conditions, the use of constant-head cells was considered to be an acceptable approach to simulate the ground-water flux across the western boundary. Similarly, a no-flow boundary simulated the eastern boundary of the study unit, where the Chase, Council Grove, and Admire Groups have been removed by erosion. As at the western boundary, constant-head cells were used in the uppermost active cell in the stack at the eastern boundary to simulate the small flux of water flowing out of the Central Oklahoma aquifer as underflow through the Vanoss Formation. The lower boundary of the aquifer (the base of fresh ground water) was simulated as a no-flow boundary.

Spatial data for the Central Oklahoma aquifer model were stored in a geographic information system (GIS). At the beginning of each simulation, data were retrieved from the GIS to define the position of the base of fresh ground water, water table, tops and bottoms of geohydrologic units, and the positions of streams and lakes. The data were transferred to a Fortran program that formulated input data for the numerical flow model. Saturated thickness was calculated as the difference between the altitude of the water table and the base of fresh ground water. A model cell was set to active if the cell had a positive saturated thickness. The maximum saturated thickness was 100 ft, the total thickness of the cell. If the cell had a positive saturated thickness, the Fortran program determined the predominant (thickest) geologic unit in each cell and assigned that geologic unit to the cell. The same sandstone hydraulic conductivity was assigned to every cell representing a particular geologic unit. Transmissivity was calculated as the product of the saturated thickness within the cell, the sandstone hydraulic conductivity, and the sandstone percentage. The sandstone percentage was determined from geophysical and drillers' logs (R.A. Funkhouser, U.S. Geological Survey, written commun., 1990) and assigned to every cell in the stack. Finally, recharge was assigned to the uppermost cell in each stack based on the predominant geologic unit in the uppermost cell in the stack, corresponding to the geologic unit at the land surface. The same recharge rate was assigned to every cell of the same geologic unit. The Fortran program generated input files in the format required by the numerical flow model.

The numerical flow model computes heads at every cell and volumetric fluxes, both between active cells and through boundaries. The volumetric fluxes were used to calculate ground-water ages (see the "Particle-Tracking Model" section of this report). The response variables, simulated heads and ground-water ages, should be similar to the measured heads and ages, but rarely does this occur based on the initial estimates of aquifer properties. After the initial simulation, the parameters in the model that represent aquifer properties are adjusted to produce better agreement between response variables and measured properties. This process is known as calibration and is discussed in the section entitled "Calibration."

Particle-Tracking Model

A particle-tracking model was used in conjunction with the numerical flow model to calibrate the flow model, assist in visualizing flowlines in the flow system, and integrate the results of the flow model simulations with the analysis of the geochemistry of the Central Oklahoma aquifer. The particle-tracking model generates pathlines, which are the paths of hypothetical "particles" of water moving through the aquifer as simulated by the numerical flow model. The pathlines correspond to flowlines in the Central Oklahoma aquifer. Flowlines can be inferred from potentiometric-surface maps, but such inferences are difficult in aquifers with complex flow systems such as the Central Oklahoma aquifer. The particle-tracking model is especially useful in conjunction with geochemical studies. Many geochemical studies require knowledge of the locations of flowlines in aquifer systems, but in most such studies the locations of the flowlines are known only approximately.

A particle-tracking model, MODPATH, developed by Pollock (1989) and designed to be used with the U.S. Geological Survey's modular ground-water flow model, was used to compute pathlines. In addition to calculating the position of pathlines, the particle-tracking model was used to compute the time of travel of water along the pathlines. In general terms, MODPATH takes the cell-by-cell flow terms (volumetric fluxes) computed by the flow model and computes the pathlines through each model cell. MODPATH assumes that each directional velocity component varies linearly with each grid cell. Particles can be placed anywhere in the model flow field and tracked forward or backward, and travel times can be computed. One of the limitations of this particular particle-tracking model is that it works only for steady-state flow models.

Calibration

Calibration is the process by which the parameters in the flow model that represent aquifer properties are adjusted to produce agreement between model response variables and measured properties. Calibration is needed because of uncertainties in formulating the conceptual model of the aquifer and because of measurement uncertainties associated with the determinations of the aquifer properties. Calibration reconciles these uncertainties, providing the model parameters are adjusted within reasonable ranges. Some aquifer properties are known with more precision than other properties, and during calibration those aquifer properties with small uncertainties are adjusted less, or not at all. For example, the altitudes of the geologic units in the aquifer have small uncertainties and were not adjusted during calibration, whereas the recharge rate, which is inferred from stream discharge measurements and has a larger uncertainty, was adjusted as part of the calibration process.

For the Central Oklahoma aquifer numerical flow model, the calibration process consisted of adjusting the recharge rate and the vertical hydraulic conductivity of each geologic unit to match measured and simulated heads, and then matching ground-water ages computed by the particle-tracking model against ages determined by carbon-14 and tritium age dating. The calibration then was tested by comparing pathlines to sulfate concentrations in wells and by comparing particle-tracking ages against ground-water ages inferred from tritium concentration (these processes are discussed in detail later). The base of fresh ground water, the positions of streams, and the tops and bottoms of geologic units were not adjusted during calibration because these properties were thought to be reasonably well defined.

A decision was made early in the process of modeling the Central Oklahoma aquifer to hold the horizontal hydraulic conductivity constant (vertical hydraulic conductivity will be discussed later) and to vary recharge to produce a good fit between measured and simulated response variables. Recharge and hydraulic conductivity are directly proportional, and either recharge or hydraulic conductivity can be fixed and the other quantity adjusted to produce a simulated head distribution that matches the observed head distribution. The horizontal hydraulic conductivity was held constant and recharge adjusted, for several reasons: (1) Recharge varies in space and time but hydraulic conductivity varies only spatially; (2) the methods used to estimate recharge to the Central Oklahoma aquifer are thought to overestimate recharge to the Permian geologic units (see the "Recharge" section of this report); and (3) the quantity of recharge necessary to calibrate a numerical flow model frequently is smaller than the measured recharge rate. The smaller modeled recharge generally is attributed to the discretization process in the model (Jorgensen, Signor, and Imes, 1989). In many aquifers some recharge occurs at locations where the ground water discharges within a short distance from the point it enters the aquifer, which results in a short flowline. If the flowline is contained entirely within a model cell, the model does not account for this volume because the model only simulates flow between cells, not flow within cells. The net recharge to any cell in the model should be the total recharge minus the recharge that is discharged within the cell. Rather than attempt to calculate the net recharge rate most appropriate for each cell in the Central Oklahoma aquifer numerical flow model, the recharge rate to each geologic unit was adjusted to produce agreement between measured and simulated heads when the hydraulic conductivity was fixed.

Horizontal hydraulic conductivity in cells that correspond to the Garber Sandstone and Wellington Formation and the Chase, Council Grove, and Admire Groups was set to the median sandstone hydraulic conductivity calculated from specific-capacity data, 4.5 ft/d. Transmissivity was calculated as the product of the saturated thickness within the cell, the sandstone hydraulic conductivity, and the sandstone percentage. Because the sandstone percentage is smaller in the Chase, Council Grove, and Admire Groups than in the Garber Sandstone and Wellington Formation, the transmissivity in the Chase, Council Grove, and Admire Groups was smaller than in the Garber Sandstone and Wellington Formation.

No data are available for either horizontal hydraulic conductivity or recharge for the Hennessey Group. Because the Hennessey Group does not yield large quantities of water to wells, hydraulic conductivity was set to a fraction of 0.001 of the sandstone hydraulic conductivity used for the Garber Sandstone and Wellington Formation. This fraction was selected somewhat arbitrarily, based on a hydraulic conductivity that might be expected for a geologic unit with the lithology of the Hennessey Group (Freeze and Cherry, 1979). Similarly, no data are available for either hydraulic conductivity or recharge for the Vanoss Formation. Sandstone hydraulic conductivity in the Vanoss Formation was set to a fraction of 0.01 of the sandstone hydraulic conductivity of the Garber Sandstone and Wellington Formation, based on lithology.

As discussed in the "Hydraulic Conductivity" section of this report, no measurements of vertical hydraulic conductivity were found in the literature for any of the modeled geologic units. A uniform anisotropy, expressed as the ratio of horizontal to vertical

hydraulic conductivity (k_h/k_v), was used for each geologic unit in the flow model. Ratios that ranged from 10 to 100,000 were tried in the Central Oklahoma aquifer flow model, and the effects of the different ratios are discussed below.

In each simulation, the flow model simulated hydraulic heads and volumetric fluxes of water based on a set of parameters representing aquifer properties. The model transferred these simulated heads to a data management and statistical program, which compared the simulated head in the uppermost active cell (the simulated altitude of the water table) to the measured altitudes of the water table. The goodness of fit was measured by the mean head difference (MHD) between measured and simulated heads and the mean of the absolute value of head difference (MAVHD) between measured and simulated heads. The MHD was computed by summing the difference between measured and simulated head at each node and dividing by the total number of nodes. Ideally, the MHD should be reduced nearly to zero during the process of calibrating the model. A near-zero MHD indicates that deviation between measured and simulated heads is, on the average, nearly zero, and that positive differences are balanced by negative differences. The MAVHD was computed by summing the absolute value of the difference between measured and simulated heads at each node and dividing by the number of nodes. During the modeling process, the MAVHD should be minimized, which indicates that the absolute difference between measured and simulated head is small. For different k_h/k_v's, recharge was adjusted for each type of geologic unit to produce a small MHD for cells corresponding to the water table. For all values of k_h/k_v, when the MHD was reduced to nearly zero, the MAVHD was acceptably small.

After the numerical flow model was adjusted to produce a reasonable match between simulated and measured heads, the particle-tracking model was used to compute the time needed for particles to flow to wells for which carbon-14 and tritium ages were available from the geochemical investigation (see the discussion in the "Geochemistry" section of this report). In the particle-tracking model, particles were placed at locations that corresponded to these wells. The particles were placed at 1-foot intervals between the depths corresponding to the top and bottom of the open interval in the well, or, if the open interval was not known, between the water table and the bottom of the well. The particles then were tracked back to their recharge locations, and the distribution of particle ages was computed. The distribution of particle ages was compared to the carbon-14 and tritium ages, and the numerical flow model was adjusted to produce a better fit between particle-age distributions and carbon-14 and tritium ages.

At each well, particle ages and carbon-14 and tritium ages are described by ranges of ages. For particle ages, the range is from the youngest to oldest particle. For the carbon-14 and tritium ages, the range is the youngest and oldest ages calculated for a sample, which includes the effects of different mass-balance models and different choices of initial-water carbon-14 activities. The particle ages were compared to carbon-14 and tritium ages by counting the number of wells for which the ranges of ages overlapped. Good agreement between particle ages and carbon-14 and tritium ages consisted of a majority of wells with overlapping ranges and approximately equal numbers of wells with particle ages older and younger than the carbon-14 and tritium ages.

Particle ages were especially sensitive to k_h/k_v. Initially, a k_h/k_v of 100 was used in the flow model, and reasonable agreement between simulated and measured heads was achieved (that is, the MHD was nearly zero and the MAVHD was small). However, at a majority of wells, the particle ages tended to be much younger than carbon-14 and tritium ages, so k_h/k_v was increased. The best agreement between particle ages and carbon-14 and tritium ages was achieved with k_h/k_v equal to 10,000. At k_h/k_v equal to 10,000, of the 31 wells used to compare particle to carbon-14 and tritium ages, ages at 21 wells overlapped, 6 wells had all particle ages older than the carbon-14 and tritium ages, and 4 wells had all particle ages younger than the carbon-14 and tritium ages. A comparison between particle and carbon-14 ages for the model with k_h/k_v of 10,000 is summarized in table 20. Particle ages could not be calculated for 3 of the 34 wells shown in table 20 because the wells were outside the boundary of the numerical flow model.

The simulated heads in the uppermost active cells (which correspond to the water table) were not particularly sensitive to k_h/k_v. Large changes in the ratio produced relatively small changes in simulated heads. Increasing k_h/k_v increased simulated heads, but the MHD could be reduced nearly to zero by decreasing recharge. The total MAVHD decreased slightly as k_h/k_v increased in excess of 10,000, but the particle ages became older than the carbon-14 and tritium ages at many wells, so k_h/k_v was set at 10,000.

The recharge, MHD, and MAVHD of the calibrated model with k_h/k_v equal to 10,000 are listed below:

Geologic unit	Recharge (in/yr)	MHD (ft)	MAVHD (ft)
Hennessey Group	0.00113	0.0342	21.6
Garber Sandstone and Wellington Formation	0.279	0.0469	22.8
Chase, Council Grove, and Admire Groups	0.0198	–0.00962	17.7
All geologic units, combined	--	0.0332	21.6

The model computed volumetric fluxes are listed below:

Volume in (ft^3/s)		Volume out (ft^3/s)	
Constant head =	1.0775	Constant head =	0.81581
Recharge =	38.684	Recharge =	0.00000
Stream leakage =	0.94717	Stream leakage =	39.971
Total =	40.709	Total =	40.787
		In – Out =	–0.077896 ft^3/s
		Percent discrepancy =	–0.19

The major fluxes to and from the ground-water flow system are recharge added to the aquifer and stream discharge (referred to as "stream leakage" in the preceding table) removed from the aquifer. The values of recharge and stream discharge are less than the values discussed in the "Recharge" and "Discharge to Streams" sections of this report because the recharge and stream discharge simulated by the model are only those fluxes that flow between model cells. Ground water that enters the flow system and discharges within a single cell is not simulated by the numerical flow model (Jorgensen, Signor, and Imes, 1989). The flow model computes a small influx of ground water from stream leakage, which corresponds to water from losing streams. Small volumes of water flow in and out of the flow system through constant-head cells, which corresponds to underflow in the Hennessey Group and Vanoss Formation.

A test of the calibration of the model was a comparison of the sulfate concentration in wells to pathlines. Some deep wells in the western part of the study unit produce water with a substantial sulfate concentration (in excess of 1 mmol/L), which is assumed to be derived from the Hennessey Group (see the "Geochemistry" section of this report). Particles were placed at locations corresponding to deep wells in the urban corridor and tracked back to their recharge locations. The geologic units in which the particles originated were tabulated and compared to sulfate concentrations. At k_h/k_v equal to 10,000, all wells with substantial sulfate concentrations had some pathlines that originated in the Hennessey Group, and all wells without substantial sulfate concentrations had no pathlines that originated in the Hennessey Group. At k_h/k_v less than 10,000, some wells without substantial sulfate concentration had particles that originated in the Hennessey Group.

Another test of the calibration of the flow model was made by comparing the range of particle ages to the presence or absence of detectable tritium in other wells sampled during the NAWQA study. The wells for which tritium concentration was determined were in sampling networks that were part of the Central Oklahoma aquifer NAWQA program and are describe in Ferree and others (1992). These wells are less than 300 ft deep, are completed in Permian geologic units, and had tritium concentrations determined but not carbon-14 ages. The particle-tracking model was used to determine the time needed for water to arrive at these wells. In the simulation, particles were placed along the well bore at 1-foot intervals, tracked backwards to their recharge locations, and particle ages were computed.

Particle ages were compared to tritium ages by using a contingency table analysis (for a discussion of contingency tables, see Iman and Conover, 1983). Contingency tables are used to compare categorical variables. The particle ages were converted to a categorical

Table 20. Tritium or carbon-14 ages and particle-tracking ages

["--" indicates no estimate of the quantity was made. Particle-tracking ages: percentiles are calculated from the distribution of ages for particles placed at one-foot intervals through the open interval of the well. Tritium or carbon-14 age: Minimum and Maximum refer to the youngest and oldest age from any mass-balance model, including the effects of the choice of carbon-14 value for the initial solution]

Sample number	Particle-tracking age Percentiles			Tritium or carbon-14 age	
	1	50	99	Minimum	Maximum
1[a]	0	0	23,200	0	40
2	1,500	2,300	4,200	0	3,000
3[a]	--	--	--	0	40
4[a]	0	800	1,100	0	40
5[a]	0	200	400	0	40
6[a]	700	2,700	7,300	0	40
7[a]	600	700	800	0	40
8[a]	300	800	1,200	0	40
9	4,500	4,800	5,100	7,500	16,000
10	600	1,200	2,200	14,500	20,000
11	500	1,000	2,600	0	6,500
12	0	1,500	3,900	6,000	12,000
13	13,000	17,700	42,700	500	6,500
14	3,700	43,900	210,900	20,000	27,000
15	79,300	82,700	86,600	8,500	15,500
16	400	3,900	17,300	7,000	12,500
17	2,200	5,100	11,500	4,000	10,000
18	2,400	3,500	4,900	6,500	13,000
19	100	2,100	6,600	3,500	9,000
20	3,400	17,100	36,800	0	5,500
21	51,500	66,700	1,137,600	8,500	16,500
22	34,300	59,200	1,449,700	31,000	40,000
23	10,300	20,000	442,200	10,500	18,500
24	7,400	16,400	46,900	10,000	17,500
25	17,100	23,800	42,600	15,000	22,000
26	25,700	41,700	143,000	23,000	31,500
27	18,500	33,600	52,600	20,500	28,000
28	11,700	22,600	49,900	18,500	26,000
29	16,900	170,200	1,240,300	29,000	41,000
30	1,000	6,700	34,000	500	7,000
31	--	--	--	14,500	20,500
32	1,100	8,300	21,600	8,500	15,500
33	--	--	--	26,000	35,000
34	2,700	4,100	5,600	3,500	11,500

[a] Ground-water age in this well was inferred to be modern from tritium concentration, which was greater than 25 picocuries per liter.

variable by determining if any particle age at a particular well was younger than 40 years, or all particle ages were older than 40 years. Tritium concentration also was treated as a categorical variable. If the water sample from the well contained detectable tritium, the well was categorized as containing water younger than 40 years. If the sample contained no detectable tritium, the water in the well was categorized as having no water younger than 40 years. The contingency table analysis tests the independence of the two variables. The null hypothesis is that the proportion of wells with detectable tritium is the same regardless of particle age. The alternate hypothesis is that there are differences in the proportions of wells with detectable tritium based on particle age. If the model is calibrated properly and is simulating the time required for ground water to travel to wells, there should be differences in the proportion of wells with detectable tritium based on particle age, and the null hypothesis should be rejected. For a contingency table analysis, the attained significance level, called the *p*-value, is calculated and used to determine whether to accept or reject the null hypothesis. For this investigation, a significance level of 0.05 was chosen, meaning that a *p*-value less than 0.05 resulted in rejecting the null hypothesis and accepting the alternate hypothesis.

The contingency table analysis was done on calibrated numerical flow models (calibrated in that the MHD was nearly zero and the MAVHD was minimized for all geologic units) with k_h/k_v in all geologic units of 10,000, 1,000, 100, and 10. The first model tested was the simulation with k_h/k_v equal to 10,000, because this model produced the best agreement between the model and carbon-14 ages and sulfate concentrations. The *p*-value of 0.077, larger than the 0.05 significance level, indicated that the null hypothesis was accepted. However, it should be noted that the calculated *p*-value was only slightly above the 0.05 significance level.

Decreasing k_h/k_v decreased the *p*-value. The *p*-value for the model with k_h/k_v of 1,000 was 0.049. The models with k_h/k_v of 100 and 10 produced identical *p*-values of 0.014. Because the *p*-values for the models with k_h/k_v of 1,000, 100, and 10 were less than 0.05, the null hypothesis was rejected and the alternate hypothesis was accepted. Thus, the models with k_h/k_v of 1,000, 100, and 10 were better for simulating flow to wells less than 300 ft deep than the model with k_h/k_v equal to 10,000. Of the three models, a model with k_h/k_v equal to 100 is considered to be best, because it has the lowest *p*-value and this ratio fits in the range of k_h/k_v commonly cited in the literature.

As discussed previously, particle ages do not compare favorably to carbon-14 and tritium ages in the model with k_h/k_v equal to 100. For that model, particle ages are young compared to carbon-14 ages. In addition, sulfate concentrations compared poorly. Wells with no substantial sulfate concentration had particles that originated in the Hennessey Group. Thus, two different sets of simulated aquifer properties were needed to reconcile the numerical flow and particle-tracking models with carbon-14 and tritium ages and sulfate and tritium concentrations. The best fit between the flow model and carbon-14 and tritium ages and sulfate concentrations (measured in deep wells) required k_h/k_v equal to 10,000, and the best fit between the flow model and tritium concentrations (measured in shallow wells) required a k_h/k_v of 100. Possible explanations include:

1. Because the Central Oklahoma aquifer consists of interlayered sandstones, siltstones, and mudstones, water must pass through more siltstone and mudstone layers in order to arrive at the well screens of deep wells. Thus, the vertical hydraulic conductivity needed to simulate flow to deep wells needs to be smaller. Because the lower hydraulic conductivity siltstones and mudstones are not modeled discretely in any of the Central Oklahoma aquifer models, the only method to reduce vertical flow is to increase k_h/k_v.

2. Hydraulic conductivity decreases with increasing depth, because the weight of overlying sediments increases (Jorgensen, Helgesen, and Imes, in press). The difference between the two models could be accounted for if vertical hydraulic conductivity decreases with depth at a greater rate than horizontal hydraulic conductivity. Another possibility is that vertical fractures, which tend to increase vertical hydraulic conductivity, become sealed off at depth due to compaction of the sediments as the weight of overburden increases. A numerical flow model that incorporated a function that increased k_h/k_v with depth might account for all the measured data. However, the nature of this function is not known, and the uncertainties associated with the data are large, so this function has not been incorporated into the Central Oklahoma aquifer numerical flow model.

3. Modeling particle ages may be a scale-dependent phenomenon, such as the dispersivity coefficient used in solute-transport models (Mercer and Faust, 1981). Longer flowlines may require a larger k_h/k_v, much as longer flowlines in solute-transport models require a larger dispersivity coefficient. The dispersivity coefficient is considered to be a measure of the scale of heterogeneity that is not included in the model; the larger the area, the larger the dispersion (Mercer and Faust, 1981). Possibly, k_h/k_v is a measure of the scale of heterogeneity of the aquifer.

The above reasons are related to physical processes in the aquifer or the process of modeling ground-water flow in general. For this specific investigation, the scale of discretization used to simulate flow in the Central Oklahoma aquifer is better suited to analyzing deep, regional flow than shallow, local flow of ground water. At the scale of discretization of the Central Oklahoma aquifer numerical flow model, particles must travel through many cells to arrive at the simulated well screens of deep wells, but may travel through as few as one cell to arrive at the simulated well screens of shallow wells. The particle-tracking model computes pathlines at a scale within a single cell, but the numerical flow model upon which the particle-tracking model is based does not simulate flow inside a single cell.

Another consideration in comparing the applicability of the two models for this investigation is that the *p*-value calculated from the contingency table analysis of particle ages versus tritium concentration for k_h/k_v equal to 10,000 was 0.077, which was only slightly larger than 0.05. Because there is other compelling evidence (the comparisons of model results to carbon-14 ages and sulfate concentrations) indicating that the model with k_h/k_v equal to 10,000 is the better model, it was decided that this model would be used to simulate the flow of ground water in the Central Oklahoma aquifer, and all subsequent discussion in this report refers to that model.

Discussion

The numerical flow and particle-tracking models were able to simulate hydraulic heads, sulfate concentrations, and ages of ground water. Simulated heads always could be brought into reasonable agreement with measured heads by adjusting recharge and the ratio of horizontal to vertical hydraulic conductivity. Simulated heads for the uppermost active nodes for the Central Oklahoma aquifer flow model are shown in figure 29. Comparing the simulated head map, which corresponds to the water table, to the measured water table in figure 24, shows differences and similarities. As is typical of numerical flow models with generalized aquifer parameters, the simulated water table is less complex than the measured water table, and many of the smaller features of the water table are not reproduced. However, the major features of the water table are reproduced by the model.

A calibrated numerical flow model can be used to study aspects of the aquifer flow system that are difficult to observe without a flow model. In particular, combining the particle-tracking model with the numerical flow model shows flowlines directly instead of inferring them from a potentiometric-surface map. The flowlines in the confined part of the Central Oklahoma aquifer could not be determined from field measurements of hydraulic head, because hydraulic gradients under the confining layer are so small they are difficult to measure. Visualizing flowlines was still difficult with only hydraulic heads computed by the flow model because of the many layers in the model and the small hydraulic gradients in the confined part of the aquifer. The particle-tracking model makes visualizing flowlines relatively easy, assuming the numerical flow model has been calibrated properly.

Pathlines generated by placing one particle at the top-center of the uppermost cell in every stack of cells corresponding to the unconfined part of the Central Oklahoma aquifer are shown in figure 30. Because of the large number of cells representing the unconfined part of the aquifer (and thus the large number of pathlines) and pathlines that cross due to flow moving in different directions at different depth in the same location, figure 30 is complicated. Figure 31 shows selected pathlines from figure 30 and includes arrowheads to show the direction of flow, thus making the pathlines easier to visualize. In both figures, the pathlines represent flowlines of ground water flowing through the aquifer from recharge to discharge locations. Many pathlines in the unconfined part of the aquifer are relatively short, and transit times (the time required for ground water to flow from recharge to discharge) are relatively rapid, as particles travel from their recharge locations to nearby streams. These relatively short pathlines correspond to water in local flow systems. Longer pathlines, with longer transit times, also are observed in the unconfined part of the aquifer. Some of the longer pathlines show flow under streams. These longer pathlines represent the deep, regional flow system.

As can be observed in figures 30 and 31, many pathlines that enter the western, confined part of the

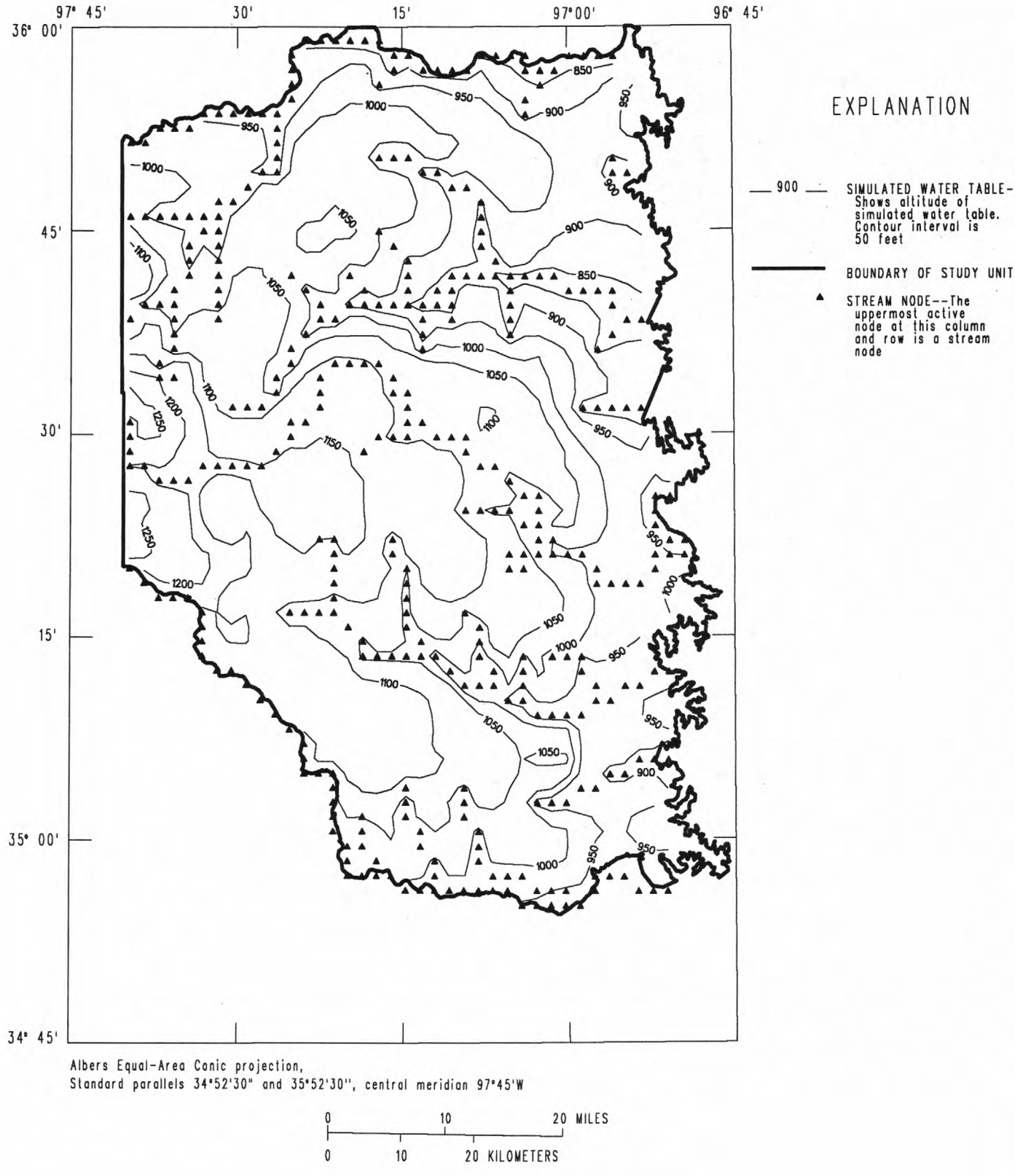

Figure 29. Altitude of the simulated water table in the Central Oklahoma aquifer.

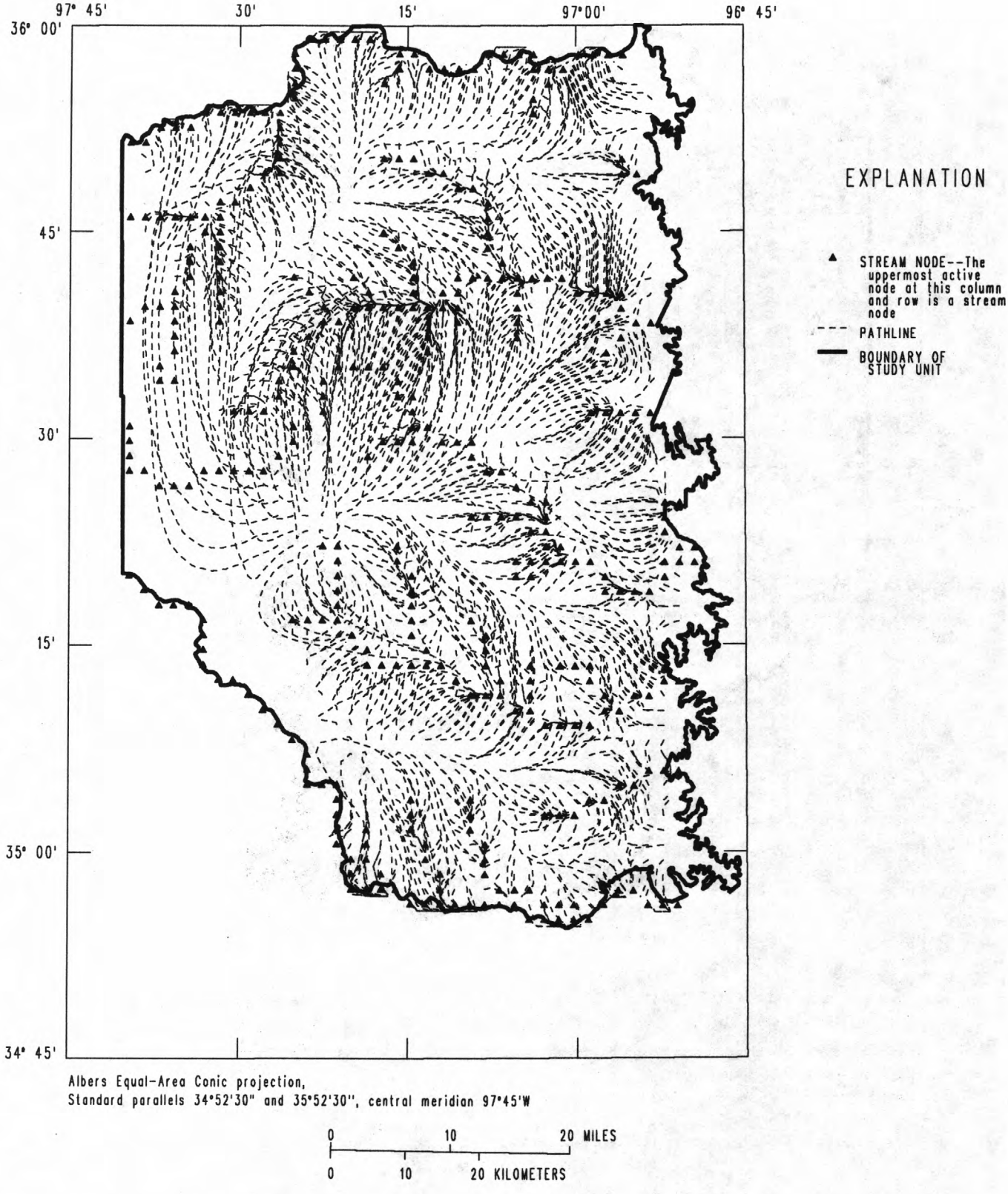

Figure 30. Pathlines generated by the particle-tracking model by placing a particle at the center of cells that correspond to the unconfined part of the Central Oklahoma aquifer.

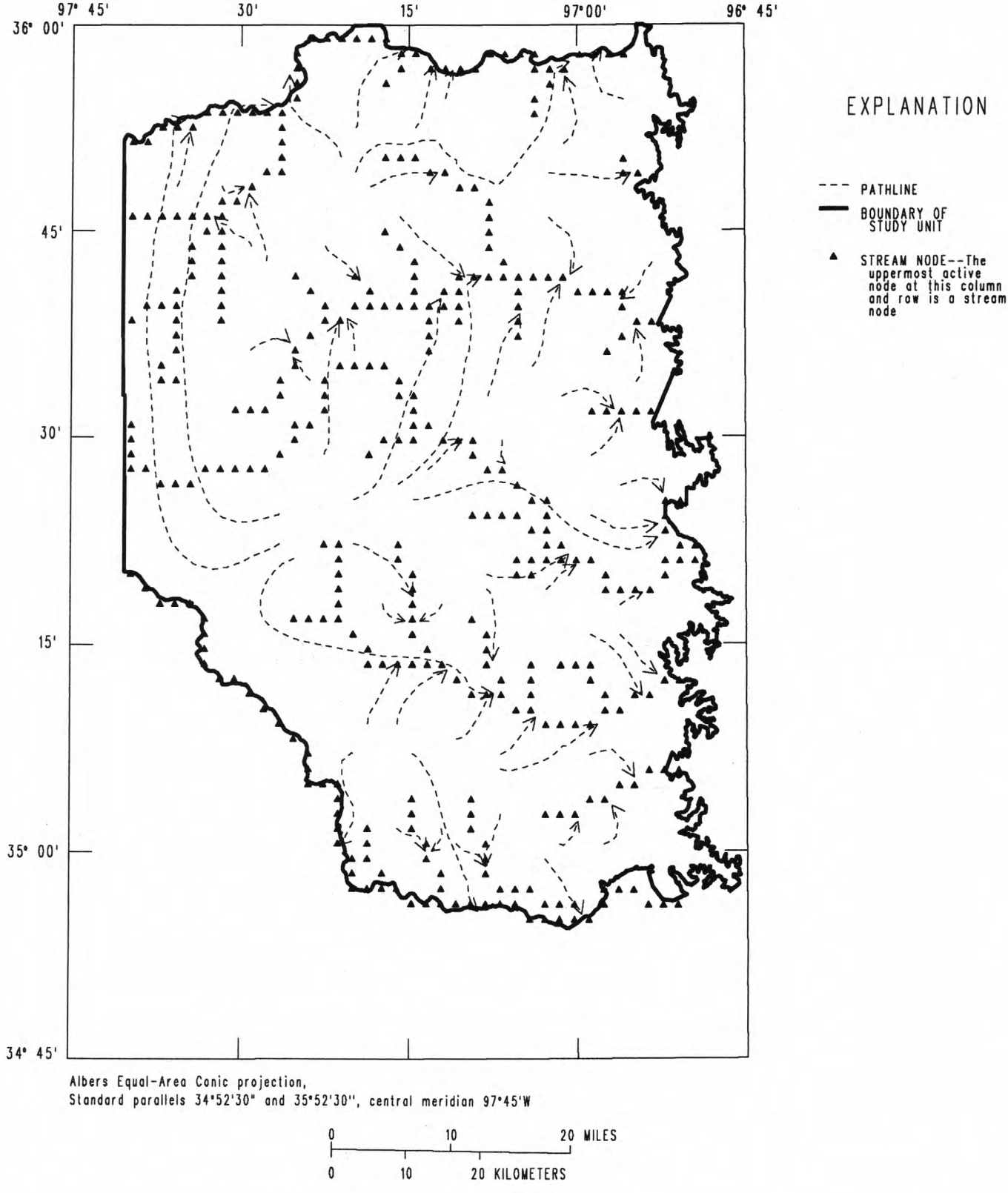

Figure 31. Selected pathlines generated by the particle-tracking model by placing a particle at the center of selected cells that correspond to the unconfined part of the Central Oklahoma aquifer.

aquifer originate in a relatively small area on the outcrop of the Garber Sandstone, in the unconfined part of the aquifer at about latitude 35° 23′, longitude 97° 23′. This location corresponds to a mound in the water table in south-central Oklahoma County, which is shown with the 1,200-ft contour on the water-table map (fig. 24). A more detailed view of the movement of water originating in the water-table mound is shown in figure 32. Pathlines were generated for figure 32 by placing 4 particles on the top of the uppermost active cell (one in the center of each quadrant) in columns 10 through 17 and rows 28 through 36. These cells correspond to the water-table mound in the unconfined part of the aquifer. Particles on the west side of the water-table mound flow westward into the confined part of the aquifer, then turn north to discharge to streams as far away as the Cimarron River. The pathlines under the confining unit are long, as much as 50 miles. These long pathlines are characteristic of the deep, regional flow system in the confined part of the aquifer.

Visible in figure 32 are pathlines representing water recharging the flow system on the north side of the water-table mound in the unconfined part of the aquifer, flowing under the North Canadian River, and discharging to the Deep Fork. This phenomenon was predicted from the water-table map and base-flow measurements, and is corroborated by the numerical flow and particle-tracking models. Ground water flowing under streams to discharge at other streams at lower altitudes is characteristic of the deep, regional flow system.

Another method that uses the particle-tracking model to visualize the complex ground-water flow system in the Central Oklahoma aquifer is mapping of ground-water transit time. A map of transit time was generated by placing one particle at the top-center of all the uppermost-active cells in each stack, tracking particles to their discharge points, plotting (at the recharge point) the time required for the particles to discharge, and generating lines of equal transit time (fig. 33). Transit times for local flow systems are relatively short, on the order of a few years to tens of years. Flow along ground-water divides in the unconfined part of the aquifer are longer and transit times can be longer than 5,000 years. Transit times for recharge from the water-table mound in south-central Oklahoma County are large, on the order of tens of thousands of years. Long transit times are characteristic of the deep, regional flow system. Transit times for recharge to the Hennessey Group are very long, on the order of many thousands of years, because water takes a long time to flow downward through the Hennessey Group. The absolute age of the water flowing through the Hennessey Group cannot be estimated accurately, because hydraulic conductivity and recharge rate are not known for the Hennessey Group.

The results of the numerical flow model combined with the geochemical and petrographic data provide a consistent description of the hydrogeochemical processes that are occurring in the aquifer. In the shallow, local flow systems, ground water recharges the aquifer and discharges to nearby streams. Flow-model and tritium ages indicate that the rate of flow and the flux of water is greatest in these local flow systems. Continuous geochemical reactions associated with the large ground-water flux have been sufficient to deplete dolomite, calcite, unstable aluminosilicate minerals, and exchangeable sodium in many of the local flow systems. The depletion of the carbonate minerals is demonstrated by large numbers of samples from shallow wells that are undersaturated with dolomite and calcite and by extensive dissolution textures visible in these minerals in core material. Petrographic evidence (as discussed in the "Geochemical reactants" section of this report) indicates that, in addition to carbonate minerals, chlorite and feldspars have been largely removed in some parts of the aquifer that have rapid, local flow systems. The small mass transfers of cation exchange in mass-balance models for recharge samples indicate that exchangeable sodium has been largely removed by exchange of calcium and magnesium (derived from dissolution of carbonates) for sodium. Concentrations of exchangeable sodium in clays tend to be smallest in the shallow parts of the aquifer, which indicates exchangeable sodium has been removed.

Flow-model results and carbon-14 and tritium ages indicate that flow is slower and flowlines are longer in the deep, regional flow system of the unconfined Garber Sandstone and Wellington Formation than in the shallow, local flow systems. In this regional flow system, ground water flows under nearby streams to discharge primarily to the Deep Fork and Little River. The flux of ground water through this regional flow system has not been sufficient to remove carbonate minerals. All ground-water samples from the deeper parts of the unconfined Garber Sandstone and Wellington Formation are saturated with dolomite, which indicates that this mineral is present and reactive. However, small mass-transfers of cation exchange in the mass-balance models for samples from the deeper parts of the unconfined Garber Sandstone and Wellington Formation indicate exchangeable sodium has been largely removed.

Flow-model results and carbon-14 ages indicate that flow is slowest in the confined part of the Garber Sandstone and Wellington Formation and in the less transmissive parts of the unconfined flow system, including parts of the Chase, Council Grove, and

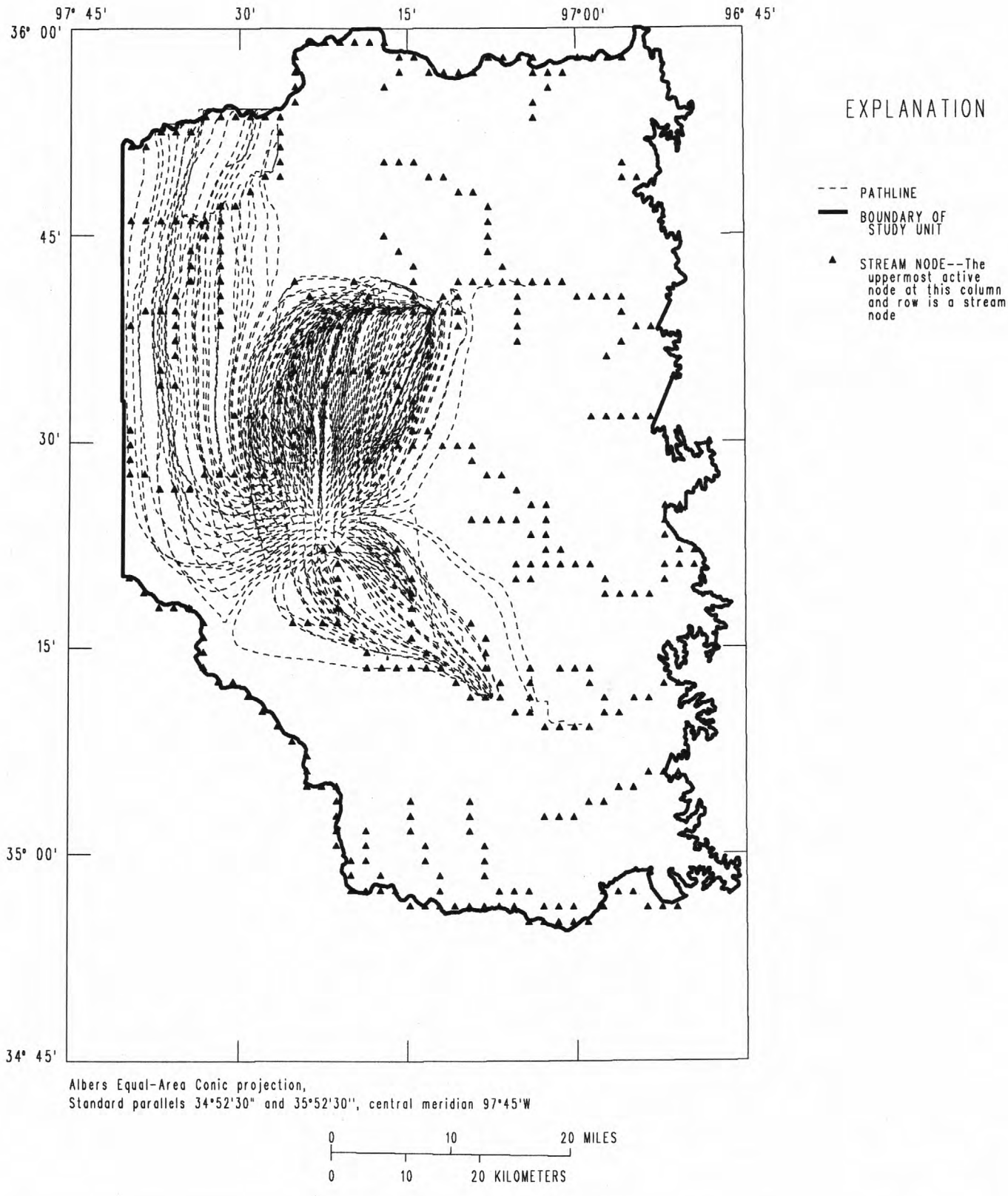

Figure 32. Pathlines generated by the particle-tracking model by placing four particles in the uppermost-active cell in columns 10 through 17 and rows 28 through 36.

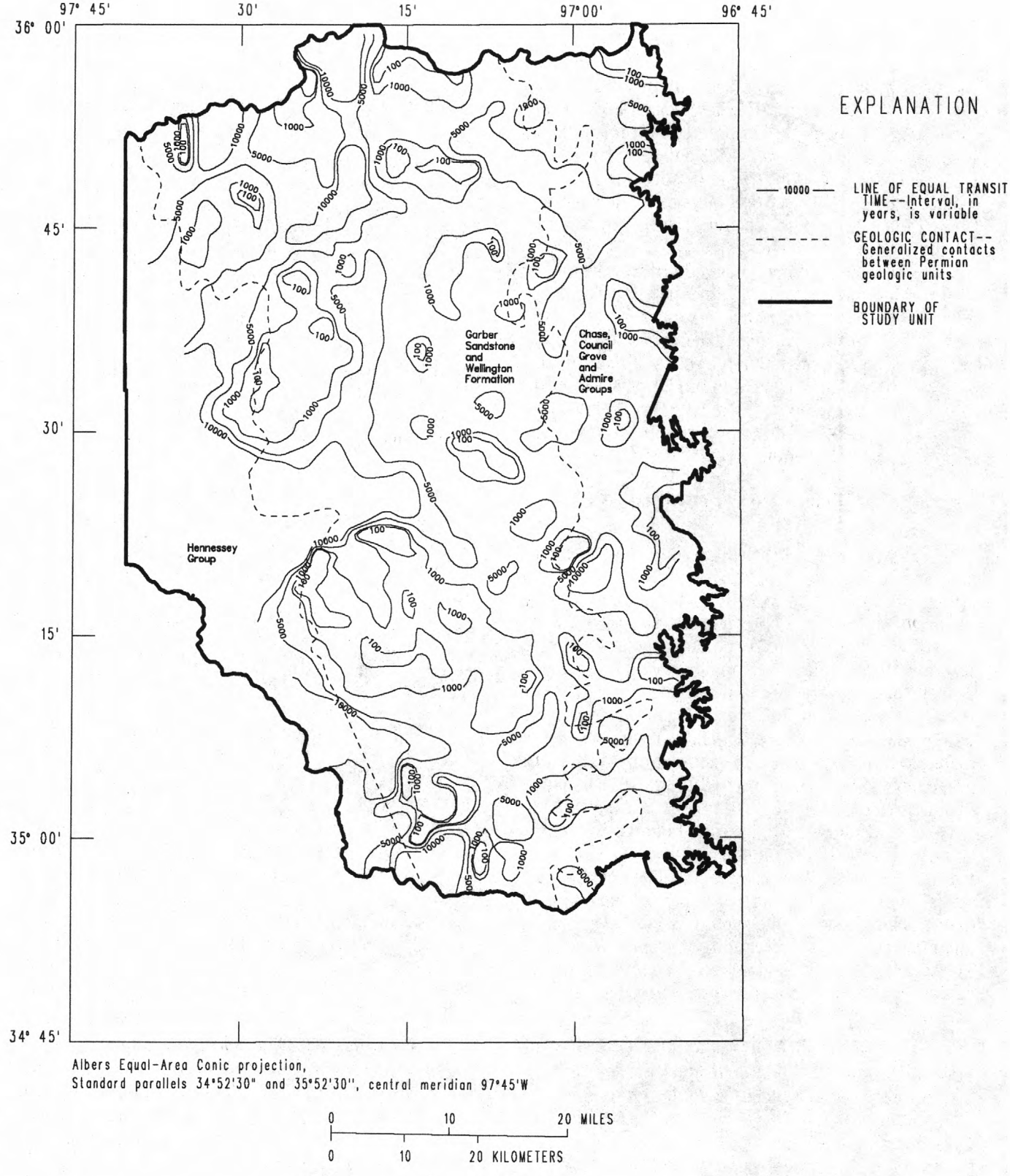

Figure 33. Model-calculated transit time required for ground water to flow through the Central Oklahoma aquifer.

Admire Groups. In the confined aquifer, ground water recharges from a small area of the unconfined part of the aquifer, transits long flowlines, and discharges to the Deep Fork, Little River, and Cimarron River drainage basins. The flux of ground water through the confined part of the aquifer has not been sufficient to remove carbonate minerals (although petrographic data indicate carbonate minerals are dissolving) or exchangeable sodium. Mass-balance models for samples from these parts of the aquifer have large mass-transfers of cation exchange, and the composition of the ground water generally has sodium as the dominant cation. Cation-exchange data indicate that exchangeable sodium is most abundant in mudstones; the large quantities of cation exchange that occur in the confined part of the aquifer and the large ratios of horizontal to vertical conductivity needed to model ground-water flow in the confined part of the aquifer may indicate a substantial amount of flow through mudstones in the confined part of the aquifer.

SUMMARY AND CONCLUSIONS

This report describes the results of geochemical and geohydrologic investigations of the Central Oklahoma aquifer. The geochemical investigation examined core material and chemical and isotopic analyses of ground water to identify the major geochemical reactions in the aquifer and to develop mass-balance models that quantify the extent to which these reactions occur. In addition, the mass-balance models were used with measurements of tritium and carbon-14 to estimate ground-water ages. The geohydrologic investigation examined geologic and hydrologic data to define the geometry, stratigraphy, lithology, and hydraulic properties of the aquifer, the distribution of hydraulic head, and the rate of recharge and discharge. These aquifer properties were used to develop a conceptual model, which was the basis of numerical flow and particle-tracking models; these models then were used to quantify the rates and directions of ground-water flow. The two investigations yield a consistent explanation of the long-term hydrogeochemical processes that are occurring in the aquifer.

The Central Oklahoma aquifer underlies about 3,000 mi^2 of central Oklahoma and includes parts of the Permian Garber Sandstone, Wellington Formation, and Chase, Council Grove, and Admire Groups and Quaternary alluvium and terrace deposits. The eastern two thirds of the aquifer is unconfined, and the western one third is confined by the Hennessey Group. Calcium, magnesium, and bicarbonate are the dominant ions in ground water from the unconfined parts of the Garber Sandstone and Wellington Formation and the alluvium and terrace deposits. Sodium and bicarbonate are the dominant ions in the other Permian geologic units, that is, in the Hennessey Group, the confined part of the Garber Sandstone and Wellington Formation, and the Chase, Council Grove, and Admire Groups.

Nearly all of the Central Oklahoma aquifer has an oxic or post-oxic environment as indicated by the large dissolved concentrations of oxygen, nitrate, arsenic(V), chromium(VI), selenium(VI), vanadium, and uranium. Post-oxic environments, where the ground water lacks measurable dissolved oxygen, were most common in the alluvium and terrace deposits, the Chase, Council Grove, and Admire Groups, and in the confined and deep, unconfined parts of the Garber Sandstone and Wellington Formation. Sulfidic and methanic environments are virtually absent, and minerals with elements in reduced oxidation states are restricted to very small zones (less than 1 cm in diameter), which are being oxidized at their margins.

The predominant source of recharge to the aquifer is rainfall. A comparison of the concentrations of major elements in rainwater to those in shallow ground water indicates that rainwater cannot be an important source of chemical constituents unless evapotranspiration concentrates the constituents. Most of the rainfall that enters the unsaturated zone of the study unit is returned to the atmosphere through evapotranspiration. If evapotranspiration concentrates the chemical constituents of rainwater tenfold or more, rainwater can be a major source of potassium, sulfate, phosphate, and nitrogen species in ground water. Rainwater is not a major source of calcium, magnesium, sodium, alkalinity, or chloride in ground water.

A minor source of water in the aquifer is brines that enter the aquifer from dispersion, fluid inclusions, or dead-end pores. The brines most likely are derived from seawater by evaporation and other diagenetic processes. The bromide to chloride ratios of the brines indicate that evaporation of seawater proceeded to the point at which halite precipitation occurred. The bromide to chloride ratios generally are consistent with a brine source for bromide and chloride in the Central Oklahoma aquifer.

Petrographic observations and saturation indices indicate that several minerals may be reacting in most parts of the aquifer. Etch pits, dissolution voids, and variations in mineral abundances indicate that dolomite, calcite, sodic plagioclase, potassium feldspars, chlorite, rock fragments, and micas are dissolving. The presence of euhedral, smooth-faced kaolinite and quartz overgrowths is consistent with the precipitation of these minerals as a result of dissolution of aluminosilicate minerals. Clay minerals constitute as much as

30 percent of the aquifer material; the largest percentages of these minerals are in the mudstones. The dominant exchangeable cations in most clay samples are calcium and magnesium. Sodium can account for as much as 50 percent of the exchangeable cations in some mudstone samples. Exchangeable sodium tends to be greater in clays in sandstones from the deep part of the aquifer than in sandstones from the shallow part of the aquifer. Variations in the quantity of exchangeable sodium in clays indicate that cation exchange is occurring within the aquifer. Although most water samples are saturated with barite, relatively little barite was found in core samples. Gypsum may be present locally within the aquifer, as indicated by water that contains large concentrations of sulfate, but it was not found in core samples. Saturation indices indicate gypsum should dissolve, if present. Iron and manganese oxides are present as alteration products derived from unstable silicate and carbonate minerals.

Mass-balance models quantitatively account for the geochemical evolution of recharge by the following chemical reactions: uptake of carbon dioxide from the unsaturated zone (about 2.0 to 4.0 mmol/L); dissolution of dolomite (about 0.3 to 1.0 mmol/L), and to lesser extents, biotite, chlorite, plagioclase, and potassium feldspar; and precipitation of kaolinite and, perhaps, a pure silica phase. Cation exchange of calcium and magnesium for sodium occurs to a limited extent locally (usually less than 1.0 mmol/L). Small quantities of sulfate are derived from rainwater or dissolution of gypsum. Large concentrations of nitrate and chloride in some recharge samples indicate recent sources of contamination.

The reactants and products in the mass-balance models for the recharge samples are consistent with the results of petrographic studies of aquifer material and saturation indices. The mass-balance models also are consistent with the available carbon-isotope data. The models imply reasonable isotopic compositions for carbon dioxide gas in the unsaturated zone (-16.0 to -25.0 per mil). The assumption of equilibrium isotopic fractionation between the aqueous phase and unsaturated-zone carbon dioxide gas fits the data better than the assumption of no isotopic fractionation.

Bicarbonate is the dominant anion and equimolar calcium and magnesium are the dominant cations in recharge waters. Saturation indices indicate that dolomite and calcite are undersaturated in about half of the recharge waters. Recharge that is undersaturated with carbonate minerals has pH values that range from 6.0 to 7.3, and, in the absence of cation exchange, recharge that is in equilibrium with carbonate minerals has pH values that are about 7.5. By the time recharge enters the deeper parts of the flow system, all water is saturated or supersaturated with dolomite and calcite.

Mass-balance modeling of carbonate-saturated samples, which include all of the samples from wells more than 300 ft deep, indicates that, after carbonate-mineral equilibration has occurred, cation exchange of calcium and magnesium for sodium is the dominant geochemical reaction. The model results also indicate other reactions are occurring, including: dissolution of minor quantities of dolomite and aluminosilicate minerals and precipitation of kaolinite and a silica phase. Gypsum dissolution or leakage of sulfate-rich water from the Hennessey Group can account for sulfate concentrations, and introduction of sodium chloride brines can account for chloride concentrations. Except for some models for one sample, all of the mass-balance models were consistent with the available $\delta^{13}C$ data.

Cation exchange occurs to a substantial extent only in parts of the aquifer. Mass transfers of cation exchange tend to be less than 2.0 mmol/L in the unconfined part of the Garber Sandstone and Wellington Formation, and ground water in this part of the aquifer has calcium, magnesium, and bicarbonate as dominant ions. Mass transfers of more than 2.0 mmol/L cation exchange occur in the confined part of the Garber Sandstone and Wellington Formation and in less transmissive parts of aquifer, including the Chase, Council Grove, and Admire Groups. This cation-exchange reaction accounts for the transition from calcium-magnesium-bicarbonate to sodium-bicarbonate water compositions. Model results also indicate the dissolution of small quantities of dolomite, calcite, biotite, chlorite, plagioclase, and potassium feldspar were consistent with the water compositions in these parts of the aquifer. Dissolution of these carbonate and aluminosilicate minerals tends to increase the pH of ground water. Ground water in the confined Garber Sandstone and Wellington Formation and parts of the Chase, Council Grove, and Admire Groups commonly has pH values that range from 8.6 to 9.1.

Carbon-14 ages of ground water in the unconfined part of the Central Oklahoma aquifer generally are less than 10,000 years. Carbon-14 ages of ground water in the confined part of the aquifer range from about 10,000 to 30,000 years or older. These ages produce a time trend in δD values that is qualitatively consistent with the timing of the transition from the last glacial maximum to the present interglacial period.

A conceptual model of the flow system in the Central Oklahoma aquifer was developed from information about the lithology and geometry of the geohydrologic units, the water table, the hydraulic properties of the aquifer, and recharge and discharge. The conceptual model is based primarily on the transmissivities

of the geologic units. The most transmissive units are the Garber Sandstone and Wellington Formation and the alluvium and terrace deposits; the Chase, Council Grove, and Admire Groups are less transmissive based on the available specific-capacity data. The transmissivities of the Permian geologic units depend largely on the percentage of sandstone. The percentage of sandstone is greatest in the central part of the aquifer, and decreases in all directions. Because of large mudstone and siltstone contents, the Hennessey Group and the Vanoss Formation are assumed to be confining units above and below the aquifer.

The Cimarron and Canadian Rivers are defined to be the northern and southern extent of the aquifer because of decreases in transmissivity beyond the rivers and because there is no indication of ground-water underflow at these rivers. The eastern boundary of the aquifer is the limit of the outcrop of the Chase, Council Grove, and Admire Groups. The presence of brines in the western part of the study unit and below the aquifer indicate the extent of the freshwater flow system in these directions.

The water-table map indicates regional ground-water flow is west to east; the Deep Fork is a major discharge area for the regional flow system. The water-table map also indicates local flow systems are present within the unconfined part of the study unit. Most streams are gaining streams, and very few losing streams are evident.

Aquifer properties were evaluated using data collected as part of this study and data from other sources. Estimates of transmissivity for the Garber Sandstone and Wellington Formation ranged from 22 to 3,600 ft^2/d, and median values (depending on the source of data) ranged from 260 to 450 ft^2/d. Estimates of the horizontal hydraulic conductivity of sandstone in the study unit ranged from 0.16 to 120 ft/d, and had a median of 4.5 ft/d. The median porosity of sandstones in the Permian geologic units was determined from point counts of thin sections to be 0.22. The median storage coefficient calculated from data from six aquifer tests in the Garber Sandstone and Wellington Formation was 0.0002. The median recharge rate estimated from measurements of base flow to streams was 1.6 in/yr. The ratio of horizontal to vertical hydraulic conductivity was estimated to be 10,000:1.

The aquifer is a major source of water for public and domestic supply, industry, irrigation, and stock use. Total reported withdrawals reached a maximum of 13,900 million gallons in 1985, but decreased to 7,860 million gallons by 1989. The decrease was caused by the shifting of sources of public supply from ground water to surface water by some of the municipalities in central Oklahoma, notably the cities of Edmond, Midwest City, and Del City. Domestic withdrawals are not reported, but were estimated to be approximately 1,685 million gallons in 1980. The withdrawals have not produced any major cones of depression that are observable in the water table, which was mapped on the basis of measurements obtained from December 22, 1986, to April 24, 1987.

The flow system in the aquifer can be considered to have three major components: (1) A shallow, local flow system in the unconfined part of the aquifer, (2) a deep, regional flow system in the unconfined part of the aquifer, and (3) a deep, regional flow system in the confined part of the aquifer. In the shallow, local flow system, water flows relatively quickly along short flowlines from the point of recharge to the point of discharge at the nearest stream. Many water samples from shallow wells contain large concentrations of tritium, which indicate ground-water ages of less than 40 years. In the deep, regional flow system in the unconfined part of the aquifer, water takes more time to flow along longer flowlines than in the shallow, local flow system. Much of the water in this flow system is recharged along ridges that correspond to ground-water divides between drainage basins. Transit times for water recharging the aquifer along ridges is greater than 5,000 years, computed using a numerical flow model in conjunction with a particle-tracking model. The models also indicate water in the deep, regional flow system in the unconfined part of the aquifer flows under some streams, such as the North Canadian River, to discharge at other streams at lower elevations. The deep, regional flow system in the confined part of the Garber Sandstone and Wellington Formation is recharged from a small part of the outcrop area of the Garber Sandstone. From the recharge area, water flows west under the confining unit to discharge to streams as far away as the Cimarron River. Flowpaths are relatively long, as much as 50 miles. The transit times in this flow system range from thousands to tens of thousands of years. The pathlines for some wells in the confined part of the aquifer indicate some flow through the Hennessey Group. Large sulfate concentrations in water samples from these wells are consistent with a small flux of sulfate-rich water from the Hennessey Group.

The geochemical and geohydrologic investigations demonstrate that the long-term hydrogeochemical process occurring in the Central Oklahoma aquifer is removal of unstable minerals, including dolomite, calcite, biotite, chlorite, and feldspars, and the replacement of exchangeable sodium on clays with calcium and magnesium as a result of chemical reaction and ground-water flow. Saturation indices, abundances and dissolution textures of minerals, cation-exchange measurements, quantitative mass-balance models, and

ground-water ages as calculated by tritium, carbon-14, and ground-water flow modeling are consistent with this hydrogeochemical process.

Over geologic time, the rapid flux of water through the shallow, local flow systems has been sufficient to remove most of the dolomite, calcite, and exchangeable sodium. In places, most chlorite and feldspars also have been removed. In the deep, regional flow system of the unconfined part of the Garber Sandstone and Wellington Formation, the flux of water has been sufficient to remove most of the exchangeable sodium, but sufficient carbonate minerals remain to maintain dolomite and calcite equilibrium. In the confined part of the Garber Sandstone and Wellington Formation and in the less transmissive parts of the unconfined aquifer, including the Chase, Council Grove, and Admire Groups, ground-water flow is slowest, and the flux of water and extent of reaction have been insufficient to remove either the carbonate minerals or the exchangeable sodium on clays.

REFERENCES

Ball, J.W. and Nordstrom, D.K., 1990, WATEQ4F—User's manual with revised thermodynamic data base and test cases for calculating speciation of major, trace and redox elements in natural waters: U.S. Geological Survey Open-File Report 90–129, 185 p.

Berner, R.A., 1981, A new geochemical classification of sedimentary environments: Journal of Sedimentary Petrology, v. 51, p. 359–365.

Bingham, R.H., and Moore, R.L., 1975, Reconnaissance of the water resources of the Oklahoma City quadrangle, central Oklahoma: Oklahoma Geological Survey Hydrologic Atlas 4, scale 1:250,000, 4 sheets.

Breit, G.N., Rice, Cyndi, Esposito, Ken, and Schlottmann, J.L., 1990, Mineralogy and petrography of Permian rocks in the Central Oklahoma aquifer: U.S. Geological Survey Open-File Report 90–678, 50 p.

Brown, D.S. and Allison, J.D., 1987, MINTEQA1, An equilibrium metal speciation model—user's manual: Environmental Research Laboratory, Office of Research and Development, U.S. Environmental Protection Agency, Athens, Georgia, National Technical Information Service number PB88–144167.

Carpenter, A.B., 1978, Origin and chemical evolution of brines in sedimentary basins: Thirteenth Annual Forum on the Geology of Industrial Minerals, eds. Johnson, K.S. and Russell, J.A., Oklahoma Geological Survey Circular 79, p. 60–77.

Carr, J.E., and Marcher, M.V., 1977, A preliminary appraisal of the Garber-Wellington aquifer, southern Logan and northern Oklahoma counties, Oklahoma: U.S. Geological Survey Open-File Report 77–278, 23 p.

Case, H.L., 1973, An approach for the evaluation of environmental impact: Unpublished master's thesis, Oklahoma State University, 97 p.

Christenson, S.C., 1983, Numerical simulation of the alluvium and terrace aquifer along the North Canadian River from Canton Lake to Lake Overholser, central Oklahoma: U.S. Geological Survey Water-Resources Investigations Report 83–4076, 36 p.

Christenson, S.C., Morton, R.B., and Mesander, B.A., 1992, Hydrogeologic maps of the Central Oklahoma aquifer, Oklahoma: U.S. Geological Survey Hydrologic Investigations Atlas HA–724, 3 sheets.

Christenson, S.C., and Parkhurst, D.L., 1987, Ground-water quality assessment of the Central Oklahoma aquifer, Oklahoma: Project description: U.S. Geological Survey Open-File Report 87–235, 30 p.

Craig, Harmon, 1961, Standard for reporting concentrations of deuterium and oxygen–18 in natural water: Science, v. 133, p. 1702–1703.

Drever, J.I., 1982, The geochemistry of natural waters: Englewood Cliffs, N.J., Prentice-Hall, 388 p.

Fairbanks, R.G., 1989, A 17,000–year glacio-eustatic sea level record—influence of glacial melting rates on the Younger Dryas event and deep-ocean circulation: Nature, v. 342, p. 637–642.

Ferree, D.M., Christenson, Scott, Rea, A.H., and Mesander, B.A., 1992, Ground-water-quality assessment of the Central Oklahoma aquifer, Oklahoma: Hydrologic, water-quality, and quality-assurance data, 1987–90: U.S. Geological Survey Open-File Report 92-641, 193 p.

Folk, R.L., 1980, Petrology of Sedimentary Rocks: Hemphill Publishing Company, Austin, Tex., 185 p.

Freeze, R.A., and Cherry, J.A., 1979, Groundwater: Prentice-Hall, Inc., Englewood Cliffs, N.J., 604 p.

Friedman, Irving, and O'Neil, J.R., 1977, Data of Geochemistry, Chapter KK. Compilation of stable isotope fractionation factors of geochemical interest: U.S. Geological Survey Professional Paper 440–KK, 48 p.

Gates, M.M., Marsh, J.H., and Fryberger, J.S., 1983, Technical considerations for the development plan of the Garber-Wellington aquifer: Norman, Oklahoma, Engineering Enterprises, Inc., 2 vols.

Ham, W.E., and Merritt, C.A., 1944, Barite in Oklahoma: Oklahoma Geological Survey Circular 23, 42 p.

Hart, D.L., Jr., 1966, Base of fresh ground water in southern Oklahoma: U.S. Geological Survey Hydrologic Atlas HA–223, scale 1:250,000, 2 sheets.

———1974, Reconnaissance of the water resources of the Ardmore and Sherman quadrangles, southern Oklahoma: Oklahoma Geological Survey Hydrologic Atlas 3, scale 1:250,000, 4 sheets.

Havens, J.S., 1989, Geohydrology of the alluvial and terrace deposits of the North Canadian River from Oklahoma City to Eufaula Lake, central Oklahoma: U.S. Geological Survey Water-Resources Investigations Report 88–4234, 32 p.

Heath, R.C., 1982, Basic ground-water hydrology: U.S. Geological Survey Water-Supply Paper 2220, 84 p.

Helsel, D.R., and Cohn, T.A., 1988, Estimation of descriptive statistics for multiply censored water quality data: Water Resources Research, v. 24, no. 12, p. 1997–2004.

Hirsch, R.M., Alley, W.M., and Wilber, W.G., 1988, Concepts for a National Water-Quality Assessment Program: U.S. Geological Survey Circular 1021, 42 p.

Hofmann, B.A., 1990, Reduction spheroids from northern Switzerland: Mineralogy, geochemistry and genetic models: Chemical Geology, v. 81, p. 55–81.

Iman, R.L., and Conover, W.J., 1983, A modern approach to statistics: New York, John Wiley and Sons, 497 p.

Johnson, K.S., 1989, Geologic evolution of the Anadarko basin, *in* Johnson, K.S., ed., Anadarko Basin Symposium 1988, Oklahoma Geological Survey Circular 90, p. 3–12.

Jorgensen, D.G., 1980, Relationships between basic soils-engineering equations and basic ground-water flow equations: U.S. Geological Survey Water-Supply Paper 2064, 40 p.

Jorgensen, D.G., Helgesen, J.O., and Imes, J.L., in press, Geohydrologic framework of aquifer systems underlying Kansas, Nebraska, and parts of Oklahoma, Missouri, Colorado, Arkansas, Texas, Wyoming, South Dakota, and New Mexico: U.S. Geological Survey Professional Paper 1414–B.

Jorgensen, D.G., Signor, D.C., and Imes, J.L., 1989, Accounting for intracell flow in models with emphasis on water table recharge and stream-aquifer interaction: 1. Problems and concept: Water Resources Research, v. 25, no. 4, p. 669–676.

Langmuir, Donald, 1978, Uranium solution-mineral equilibria at low temperatures with applications to sedimentary ore deposits: Geochimica et Cosmochimica Acta, v. 42, 547–569.

Lindberg, F.A., ed., 1987, Correlation of stratigraphic units of North America (COSUNA) project, Texas-Oklahoma tectonic region: American Association of Petroleum Geologists, 1 sheet.

Lohman, S.W., 1972, Definitions of selected ground-water terms—Revisions and conceptual refinements: U.S. Geological Survey Water-Supply Paper 1988, 21 p.

Lorius, C., Jouzel, J., Ritz, C., Merlivat, L., Barkov, N.I., Korotkevich, Y.S., and Kotlyakov, V.M., 1985, A 150,000–year climatic record from Antarctic ice: Nature, v. 316, p. 591–596.

McDonald, M.G., and Harbaugh, A.W., 1988, A modular three-dimensional finite-difference ground-water flow model: Techniques of Water-Resources Investigations of the U.S. Geological Survey, Book 6, Chapter A1, 586 p.

Mercer, J.W., and Faust, C.R., 1981, Ground-water modeling: National Water Well Association, 60 p.

Mook, W.G., 1980, Carbon–14 in hydrogeological studies, A, Fritz, P. and Fontes, J.Ch., eds., *in* Handbook of Environmental Isotope Geochemistry, volume 1, the terrestrial environment, New York, Elsevier Scientific Publishing Company, p. 49–74.

Mook, W.G., Bommerson, J.C., and Staverman, W.H., 1974, Carbon isotope fractionation between dissolved bicarbonate and gaseous carbon dioxide: Earth and Planetary Science Letters, v. 22, p. 169–176.

Mosier, E.L., Briggs, P.H., Crock, J.G., Kennedy, D.R., McKown, D.M., Vaughn, R.B., and Welsch, E.P., 1990, Analyses of subsurface Permian rock samples from the Central Oklahoma aquifer: U.S. Geological Survey Open-File Report 90–456, 65 p.

National Atmospheric Deposition Program, 1986, NADP/NTN Annual data summary— precipitation chemistry in the United States, 1986: Fort Collins, Colo., NADP/NTN Coordinator's Office, Natural Resource Ecology Laboratory, Colorado State University.

Nordstrom, D.K., Plummer, L.N., Langmuir, Donald, Busenberg, Eurybiades, May, H.M., Jones, B.F., and Parkhurst, D.L., 1990, Revised chemical equilibrium data for major water-mineral reactions and their limitations, *in* Bassett, R.L. and Melchior, D. eds., Chemical modeling in aqueous systems II: Washington D.C., American Chemical Society Symposium Series 416, Chapter 31, p 398–413.

Parkhurst, D.L., Christenson, S.C., and Schlottmann, J.L., 1989, Ground-water-quality assessment of the Central Oklahoma aquifer, Oklahoma—Analysis of available water-quality data through 1987: U.S. Geological Survey Open-File Report 88–728, 80 p.

Parkhurst, D.L., Plummer, L.N., and Thorstenson, D.C., 1982, BALANCE—A computer program for calculating mass transfer for geochemical reactions in ground water: U.S. Geological Survey Water-Resources Investigations Report 82–14, 29 p.

Parkhurst, D.L., Thorstenson, D.C., and Plummer, L.N., 1980, PHREEQE—A computer program for geochemical calculations: U.S. Geological Survey

Water-Resources Investigations Report 80–96, 210 p., revised August 1990.

Parkhurst, R.S., and Christenson, S.C., 1987, Selected chemical analyses of water from formations of Mesozoic and Paleozoic age in parts of Oklahoma, northern Texas, and Union County, New Mexico: U.S. Geological Survey Water-Resources Investigations Report 86–4355, 222 p.

Pettyjohn, W.A., and Miller, Andrew, 1982, Preliminary estimate of effective ground-water recharge rates in central Oklahoma: Final Report to the Oklahoma Water Resources Board, Department of Geology, Oklahoma State University, Stillwater, Okla., 32 p.

Pettyjohn, W.A., White, Hal, and Dunn, Shari, 1983, Water atlas of Oklahoma: University Center for Water Research, Oklahoma State University, Stillwater, Okla., 72 p.

Phillips, F.M., Peeters, L.A., and Tansey, M.K., 1986, Paleoclimatic inferences from an isotopic investigation of groundwater in the central San Juan Basin, New Mexico: Quaternary Research, v. 26, p. 179–193.

Plummer, L.N., Parkhurst, D.L., Fleming, G.W., and Dunkle, S.A., 1988, A computer program incorporating Pitzer's equations for calculation of geochemical reactions in brines: U.S. Geological Survey Water-Resources Investigations Report 88–4153, 310 p.

Plummer, L.N., Prestemon, E.C., and Parkhurst, D.L., 1991, An interactive code (NETPATH) for modeling net geochemical reactions along a flow path: U.S. Geological Survey Water-Resources Investigations Report 91–4087, 227 p.

Pollock, D.W., 1989, Documentation of computer programs to compute and display pathlines using results from the U.S. Geological Survey modular three-dimensional finite-difference ground-water flow model: U.S. Geological Survey Open-File Report 89–381, 188 p.

P–STAT, Inc., 1989, P–STAT user's manual, Princeton, N.J., vol. 2, p. 38.17–38.20.

Quade, Jay, Cerling, T.E., and Bowman, J.R., 1989, Systematic variations in the carbon and oxygen isotopic composition of pedogenic carbonate along elevation transects in the southern Great Basin, United States: Geological Society of America Bulletin, v. 101, p. 464–475.

Reichenbach, H.G. v., and Rich, C.I., 1975, Fine–grained micas in soils, *in* Gieseking, J.E., ed., Soil Components, volume 2, Inorganic Components: New York, Springer Verlag, p. 59–95.

Rozanski, K., 1985, Deuterium and oxygen–18 in European groundwaters—links to atmospheric circulation in the past: Chemical Geology (Isotope Geoscience Section), v. 52, p. 349–363.

Schlottmann, J.L. and Funkhouser, R.A., 1991, Chemical analyses of water samples and geophysical logs from cored test holes drilled in the Central Oklahoma aquifer, Oklahoma: U.S. Geological Survey Open-File Report 91–464, 58 p.

Srodon, Jan, 1984, X-ray powder diffraction identification of illitic materials: Clays and Clay Minerals, v. 32, p. 337–349.

Stoner, J.D., 1984, Estimate of self-supplied domestic water use in Oklahoma during 1980: U.S. Geological Survey Water-Resources Investigations Report 83–4223, 20 p.

Sudicky, E.A. and Frind, E.O., 1981, Carbon^{14} dating of groundwater in confined aquifers—implications of aquitard diffusion: Water Resources Research, v. 17, no. 4, p. 1060–1064.

Theis, C.V., Brown, R.H., and Meyer, R.R., 1954, Estimating transmissibility from specific capacity: U.S. Geological Survey Open-File Report, 11 p.

Thode, H.G., Shima, M., Rees, C.E., and Krishnamurty, K.V., 1965, Carbon–13 isotope effects in systems containing carbon dioxide, bicarbonate, carbonate, and metal ions: Canadian Journal of Chemistry, v. 43, p. 582–595.

Thorstenson, D.C., Weeks, E.P., Haas, Herbert, and Fisher, D.W., 1983, Distribution of gaseous $^{12}CO_2$, $^{13}CO_2$, and $^{14}CO_2$ in the sub-soil unsaturated zone of the western U.S. Great Plains: Radiocarbon, v. 25, p. 315–346.

Toth, J., 1963, A theoretical analysis of ground-water flow in small drainage basins: Journal of Geophysical Research, v. 68, no. 16, p. 4795–4812.

U.S. Department of Commerce, 1960, Census of population: Bureau of the Census.

———1970, Census of population: Bureau of the Census.

———1980, Census of population: Bureau of the Census.

U.S. Environmental Protection Agency, 1986, Maximum contaminant levels (subpart B of part 141, National interim primary drinking-water regulations): U.S. Code of Federal Regulations, Title 40, Parts 100–149, revised as of July 1, 1986, p. 374.

Walters, L.J., Claypool, G.E., and Chouquette, P.W., 1972, Reaction rates and $\delta^{18}O$ variation for the carbonate-phosphoric acid preparation method: Geochimica et Cosmochimica Acta, v. 36, p. 129–140.

Wanty, R.B., 1986, Geochemistry of vanadium in an epigenetic sandstone-hosted vanadium-uranium deposit, Henry Basin, Utah: Ph.D. Thesis, Colorado School of Mines, 198 p.

Weeks, E.P., 1969, Determining the ratio of horizontal to vertical permeability by aquifer test analysis: Water Resources Research, v. 5, no. 1, p. 196–214.

Wigley, T.M.L., Plummer, L.N., and Pearson, F.J. Jr., 1978, Mass transfer and carbon isotope evolution in natural water systems, Geochimica and Cosmochimica Acta, v. 42, p. 1117–1139.

———1979, Errata, Geochimica and Cosmochimica Acta, v. 43, p. 1395.

Williamson, A.K., Grubb, H.F., and Weiss, J.S, 1990, Ground-water flow in the Gulf Coast aquifer systems, south-central United States—A preliminary analysis: U.S. Geological Survey Water-Resources Investigations Report 89–4071, 124 p.

Wood, P.R., and Burton, L.C., 1968, Ground-water resources in Cleveland and Oklahoma Counties, Oklahoma: Oklahoma Geological Survey Circular 71, 75 p.

Wright, Jack, Pearson, Cynthia, Kurt, Effie, and Watkins, J.W., 1957, Analyses of brines from oil-productive formations in Oklahoma: U.S. Bureau of Mines Report of Investigations 5326, 71 p.

ATTACHMENT

An extensively modified version of the program BALANCE (Parkhurst, Plummer, and Thorstenson, 1982) was used to make the mass-balance calculations. BALANCE accepted as input a set of mineral compositions and the total elemental concentrations of two ground waters, the initial water and the final water. The number of minerals had to equal the number of elemental concentrations. The program then solved a set of linear equations of the form:

$$\Delta C_i = \sum_j b_{i,j}\alpha_j , \qquad \text{(A1)}$$

where ΔC_i is the concentration difference between the two waters for element i, $b_{i,j}$ is the stoichiometric coefficient of element i in mineral j, and α_j is the mass transfer of mineral j (positive for dissolution, negative for precipitation). The unknowns in the equations are the α_j, which are the mass transfers of minerals needed to account for the differences in concentrations between the initial and final waters.

The modified version of BALANCE used a linear programming formulation of the problem. Uncertainties were assigned to the analytical data from which uncertainties in ΔC_i were derived. The new formulation used inequality constraints of the form:

$$\Delta C_i - \varepsilon_{l_i} \le \sum_j b_{i,j}\alpha_j \le \Delta C_i + \varepsilon_{u_i} \qquad \text{(A2)}$$

where ε_{l_i} and ε_{u_i} are the lower and upper bounds of the uncertainty. BALANCE implicitly assumed charge balance in the mass-balance models it produced. With uncertainties in the analytical data, charge balance had to be considered explicitly in the modified version of the program. An alkalinity equation of the form of equation A2 (alkalinity is a combination of charge-balance and mass-balance equations) was used for this purpose (the coefficients $b_{alkalinity,j}$ are given for the minerals used in this report in table 7). It also was necessary to include a mass-balance equation for each valence state of each redox element to account properly for alkalinity produced or consumed by redox processes. The linear programming approach made it possible to constrain the α_j to be positive or negative. Thus, a mineral could be constrained only to dissolve or precipitate, if there were geochemical evidence that the mineral reacted only in one way. The number of minerals was allowed to exceed the number of elemental concentrations, and an exhaustive search procedure was implemented to find all mass-balance models that had a minimal number nonzero mass transfers of minerals. A mass-balance model, which satisfied the constraints and had K minerals with nonzero mass transfer, had a minimal number of nonzero mass transfers if no model could be found with any subset of those K minerals that also satisfied the constraints.

An uncertainty of plus or minus 5 percent was used for alkalinity and all of the elemental concentrations, except for carbon. Uncertainties in total carbon concentrations were calculated by Monte-Carlo simulations that used the uncertainties in alkalinity, pH, and all of the other elements. The uncertainty in pH usually was assumed to be 0.1 unit. Large saturation indices for calcite could indicate high pH values due to degassing of carbon dioxide. If the calcite saturation index was greater than 0.05, then larger uncertainties in pH values were used. The uncertainty was adjusted so that the range in pH values included a pH that would produce calcite saturation.

★U.S GOVERNMENT PRINTING OFFICE 1993-770-084/